

Mechanisms of Cigarette Smoke-Induced Mitochondrial Dysfunction in Striated Muscle and
Aorta

A Dissertation Presented
by
STEPHEN T DECKER

Submitted to the Graduate School of the
University of Massachusetts Amherst in partial fulfillment
of the requirements for the degree of

DOCTOR OF PHILOSOPHY

Department of Kinesiology
School of Public Health and Health Sciences

(c) by Stephen Decker 2023

All Rights Reserved

**MECHANISMS OF CIGARETTE SMOKE-INDUCED MITOCHONDRIAL
DYSFUNCTION IN STRIATED MUSCLE AND AORTA**

A Dissertation Presented

by

STEPHEN T. DECKER

Approved as to style and content by:

DocuSigned by:



A7CECA4BF005400...

Dr. Gwenael Layec, Chair

DocuSigned by:



8DD63332AE0B409

Dr. Jane A Kent, Member

DocuSigned by:



60FD0A15A9CE401

Dr. Edward Debold, Member

DocuSigned by:



D8952C5A67B8471

Dr. David J Marcinek, Member

DocuSigned by:



3EB0DB06FD00E416...

Dr. Richard Van Emmerik, Department Chair
Department of Kinesiology

DEDICATION

To my parents, who have always been in the stands cheering me on; and to my kids, as proof that
resilience trumps any obstacle.

ACKNOWLEDGEMENTS

I want to thank my mentor, Gwenael Layec, for his many years of unwavering patience, guidance, and support. Thanks are also due to my labmates: Jyotika Vallurupalli, Alexs Matias, Jack Madden, Sean Bannon, Cory Serviente, and Enes Erol. Their assistance, support, and guidance through my years at UMass are truly invaluable. Likewise, I extend my gratitude to my close colleagues Liam Fitzgerald, Miles Bartlett, Rajakumar Nagarajan, Elena Bliss, Oh-Sung Kwon, Taylor Thurston, and Steve Ratchford for their lasting friendship and collaboration. I would also like to thank the members of my committee, Drs. Jane Kent, Ned Debold, and David Marcinek, for their helpful comments, suggestions, and guidance throughout this project.

I want to thank Ernie Cuadra, Karine Fenelon, Nadia, Alexandrou-Majaj, and David Moorman for allowing me to use their lab resources used in this project.

I would like to acknowledge the many individuals who have stuck with me through all of the years, despite the many cross-country relocations and the grueling days – specifically my parents, Mark and Kristina, my friends Johnathan and Jenny Hubbard, Richard Haifley, Perla and Jesse Garcia, Jill Fusco, Lauretta Minor, Vaughn Chung, Uma Phadnis, Alex Ondary, and Shana Timmermann – without whom my completion of this project would have been, quite literally, impossible. Lastly, I would like to give a special thank you to Rachel Decker, Alice-May, and Kyra, who continue to celebrate my achievements and tolerate my daily antics and shortcomings better than anybody else I know.

ABSTRACT

MECHANISMS OF CIGARETTE SMOKE-INDUCED MITOCHONDRIAL DYSFUNCTION IN STRIATED MUSCLE AND AORTA

FEBRUARY 2023

STEPHEN DECKER, B.S., STEPHEN F. AUSTIN STATE UNIVERSITY
M.S., STEPHEN F. AUSTIN STATE UNIVERSITY
Ph.D., UNIVERSITY OF MASSACHUSETTS AMHERST

Directed by: Professor Gwenael Layec

Cigarette Smoke is a significant cause of morbidity and mortality in the United States, accounting for over 480,000 annual deaths. Of these deaths, the most common cause of mortality in chronic smokers is cardiometabolic diseases. Likewise, a significant portion of smokers experience some form of cardiac, vascular, or metabolic dysfunction throughout their lifetime. More specifically, smoking is shown to induce mitochondrial dysfunction in these tissues, causing an increase in oxidative damage and poor overall health. However, despite the advances in the health outcomes related to cigarette smoke exposure, the mechanisms underlying mitochondrial dysfunction in striated muscle and the vasculature remain largely unexplained. Particularly, no investigations have been conducted to (1) characterize the acute inhibitory effects of cigarette smoke to the mitochondria in these tissues, (2) assess the changes in mitochondrial substrate oxidation with exposure to cigarette smoke, or (3) identify the mechanisms by which cigarette smoke induces deleterious effects on the mitochondrial electron transport chain. Therefore, the purpose of this dissertation is to use high-resolution respirometry to characterize the toxicity of cigarette smoke in the mitochondria of the aorta, heart, and two types of skeletal muscle, determine

the capacity for cigarette smoke to induce a shift in mitochondrial carbohydrate- or fatty acid-stimulated mitochondrial respiration, and further investigate the mechanisms by which cigarette smoke impairs the mitochondrial electron transport chain.

Herein, we first demonstrate that cigarette smoke-induced inhibition of mitochondrial respiration is tissue-specific and depends on the intrinsic qualities of the mitochondria in each tissue (e.g. morphology) as well as the tissue-specific mitochondrial content. Second, we show that mitochondrial pyruvate oxidation, not fatty acid oxidation, is a primary mechanism for cigarette smoke-induced mitochondrial dysfunction. Third, we further support the hypothesis that mitochondrial complex I is a primary site of smoke-induced mitochondrial dysfunction. However, we also identify the ADP/ATP transporter, ANT, as another site of smoke-induced mitochondrial impairment. Lastly, we discuss the clinical implications of each of these findings as well as future research directions.

TABLE OF CONTENTS

	Page
ACKNOWLEDGEMENTS.....	v
ABSTRACT.....	vi
LIST OF TABLES.....	xvi
LIST OF FIGURES.....	xvii
 CHAPTER	
1– INTRODUCTION.....	1
<i>1.1. Adverse health outcomes from cigarette smoke exposure: extra-pulmonary manifestations</i>	
	2
1.1.1. Cardiovascular function	2
1.1.2. Skeletal muscle function	3
<i>1.2. Pathways and cellular mechanisms for cardiovascular and skeletal muscle dysfunction induced cigarette smoke</i>	
	4
1.2.1. Tissue-specific susceptibility to cigarette smoke-induced mitochondrial damage	5
1.2.2. Direct effects of cigarette smoke on mitochondrial function: <i>in vitro</i> findings	7
1.2.3. Direct effects of cigarette smoke on mitochondrial function: muscle cells and fibers ..	9
1.2.4. Effects of cigarette smoke on substrate oxidation.....	10
<i>1.3. Statement of the Problem</i>	
	12
<i>1.4. Purpose & Aims</i>	
	13

2 – LITERATURE REVIEW	15
<i>2.1. Peripheral Manifestations of Cigarette Smoke Exposure.....</i>	<i>18</i>
2.1.1. Cigarette Smoke Exposure Impairs Skeletal Muscle Function	20
2.1.2. Cigarette Smoke Exposure Impairs Vascular Function	23
<i>2.2. ROS are a Result of Cigarette Smoke Exposure</i>	<i>25</i>
2.2.1. Mitochondria are Major Sources of ROS	26
2.2.2. ROS Scavenging.....	29
2.2.3. Other Endogenous Sources of ROS	31
<i>2.3. Cigarette Smoke Disrupts Mitochondrial Bioenergetics</i>	<i>32</i>
2.3.1. Cigarette Smoke Constituents Inhibit the Mitochondrial Electron Transport Chain ..	32
2.3.2. Cigarette Smoke Increases Proton Leak Through ANT	33
<i>2.4. Tissue-Specific Susceptibility to Cigarette Smoke</i>	<i>35</i>
2.4.1. Tissue-Specific Variation of Cigarette Smoke-Induced ROS Production	35
2.4.2. Tissue-Specific Variation of Cigarette Smoke-Induced Membrane Potential	36
<i>2.5. Cigarette Smoke-Induced Shifts in Mitochondrial Substrate Utilization.....</i>	<i>39</i>
2.5.1. Whole-body Observations of Shifts in Substrate Utilization	39
2.5.2. In vitro Evidence of Altered Mitochondrial Substrate Preference	41
<i>2.6. Purpose</i>	<i>41</i>
2.6.1. Purpose Statement	43
<i>2.7. Aims.....</i>	<i>43</i>

2.7.2. Aim 1 – Acute Effects of Cigarette Smoke Condensate on Mitochondrial Respiration	43
2.7.3. Aim 2 – Effects of Cigarette Smoke Exposure on Mitochondrial Substrate Utilization	44
2.7.3. Aim 3 – Mechanisms of Cigarette Smoke-Induced Mitochondrial Dysfunction.....	44
3 – METHODS.....	45
<i>3.1. Animal Care and Ethics Approval</i>	45
3.1.1. Animal Selection and Care.....	45
3.1.2. Euthanasia	46
3.1.3. Tissue Harvesting	46
<i>3.2. Chemical and Tissue Preparations</i>	47
3.2.1. Tissue Preservation Solution (BIOPS)	47
3.2.2. Mitochondrial Respiration Medium (MiR-05).....	50
3.2.3. Tissue Permeabilization	53
<i>3.3. Equipment</i>	56
3.3.1. Mitochondrial Respiration: Oroboros O2k-FluroRespirometer	56
<i>3.4. Acute Effects of Cigarette Smoke Condensate on Mitochondrial Respiration (Aim 1)</i>	59
3.4.1. Mitochondrial Respiration Protocols and Measurements	59
3.4.2. Citrate Synthase Activity.....	61

3.4.3. Data Analysis & Sample Size Estimates	63
<i>3.5. Effects of Cigarette Smoke Exposure on Mitochondrial Substrate Utilization (Aim 2)</i>	
	64
3.5.1. Preparation and Incubation of Tissues	65
3.5.2. Mitochondrial Respiration and Measurements.....	65
3.5.3. Data Analysis & Sample Size Estimates.....	70
<i>3.6. Mechanisms of Cigarette Smoke-Induced Mitochondrial Dysfunction (Aim 3)</i>	72
3.6.1. Preparation and Incubation of Tissues	72
3.6.2. Mitochondrial Respiration Measurements	72
3.6.3. Citrate Synthase Activity.....	75
3.6.6. Data Analysis	77
4 – ADDENDA TO THE PROPOSAL & PILOT STUDIES	81
5 – AIM I RESULTS AND DISCUSSION	84
<i>5.2. Abstract</i>	85
<i>5.3. New & Noteworthy.....</i>	87
<i>5.4 Introduction.....</i>	88
<i>5.5 Methods</i>	91
5.5.1 Animals and Experimental Design.....	91
5.5.2. Cigarette Smoke Condensate Preparation	91

5.5.3 Preparation of Permeabilized Muscle Fibers & Mitochondrial Respiration Measurements.....	91
5.5.4. Citrate Synthase (CS) Activity	93
5.5.5. Data Analysis	93
<i>5.6. Results</i>	95
5.6.1. Effects of CSC on Absolute Rates of Mitochondrial Respiration.....	95
5.6.3. Effects of CSC on Mitochondrial Respiration Normalized to CS Activity.....	97
<i>5.7. Discussion</i>	102
5.7.1. Cigarette Smoke Condensate Directly Impairs Mitochondrial Respiration.....	103
5.7.2. Aorta is Intrinsically Less Susceptible and Sensitive to CSC Than Gastrocnemius, Soleus, or Heart	105
5.7.3. Sensitivity to CSC in Striated Muscle is Dependent on Mitochondrial Content	106
<i>5.8. Conclusions</i>	109
6 – AIM II RESULTS AND DISCUSSION.....	110
<i>6.1. Effects of Cigarette Smoke on In Situ Mitochondrial Substrate Oxidation of Slow- and Fast-Twitch Skeletal Muscles.....</i>	<i>110</i>
<i>6.2. Abstract</i>	<i>111</i>
<i>6.3. New & Noteworthy</i>	<i>113</i>
<i>6.4. Introduction</i>	<i>114</i>
<i>6.5. Methods</i>	<i>117</i>

6.5.1. Animals and Experimental Design.....	117
6.5.2. Preparation of Permeabilized Muscle Fibers.....	117
6.5.3. Protocol 1: Pyruvate-Stimulated Respiration	118
6.5.4. Protocol 2: Palmitoylcarnitine-Stimulated Respiration and Pyruvate-Palmitoylcarnitine Respiration Interaction.....	119
6.5.5. Data Analysis	119
<i>6.6. Results</i>	121
6.6.1. Effects of CSC on Mitochondrial Respiration supported by Pyruvate Oxidation	121
6.6.2. Effect of CSC on Mitochondrial Respiration supported by Palmitoylcarnitine Oxidation	122
6.6.3. Effect of CSC on Mitochondrial Respiration with concurrent addition of Pyruvate and Palmitoylcarnitine	124
6.6.4. Specific Effect of CSC on Palmitoylcarnitine induced inhibition of Pyruvate supported respiration	125
<i>6.7. Discussion</i>	127
6.7.1. CSC Impairs Skeletal Muscle Mitochondrial Respiration Supported by Pyruvate....	128
6.7.2. Skeletal Muscle Mitochondrial Respiration Supported by Fatty Acids is Unaffected by CSC	129
6.7.3. CSC Alters Skeletal Muscle Mitochondrial Respiration with Competing Substrates	130
6.7.4. Clinical Perspectives	132
<i>6.8. Conclusion</i>	134

7 – AIM III RESULTS AND DISCUSSION	135
<i>7.2. Abstract</i>	<i>136</i>
<i>7.3. New & Noteworthy.....</i>	<i>137</i>
<i>7.4. Introduction.....</i>	<i>138</i>
<i>7.5. Methods</i>	<i>141</i>
7.5.1. Animals and Experimental Design.....	141
7.5.2. Preparation of Permeabilized Muscle Fibers.....	141
7.5.4. Measurement of Mitochondrial Respiration.....	142
7.5.5. Data Analysis	144
<i>7.6. Results</i>	<i>147</i>
7.6.1. Effects of CSC on Components of the Mitochondrial Respiratory System	147
7.6.2. Effects of CSC on Complex I/II and ANT Contributions and Mitochondrial Quality	150
7.6.3. Effects of CSC on ETS Activity.....	152
7.6.4. Effects of CSC on ADP Kinetics	153
7.6.3. Effects of CSC on ANT-dependent Mitochondrial Respiration.....	155
<i>7.7. Discussion</i>	<i>158</i>
7.7.1. Complex I is a Primary Site of CSC-Induced Mitochondrial Impairments in Gastrocnemius but not soleus.....	159

7.7.3. Cigarette Smoke-Induced Blockade of Nucleotide Exchange Across the Mitochondrial Membrane.....	163
7.7.4. Mitochondrial Quality is Impaired with CSC Exposure	166
7.7.5. Clinical Perspectives	168
<i>7.8. Conclusion.....</i>	<i>170</i>
8 – CONCLUSION	172
<i>8.1. Overview of Main Findings.....</i>	<i>173</i>
8.1.1. Summary of Aim 1	173
8.1.2. Summary of Aim 2	174
8.1.3. Summary of Aim 3	175
<i>8.2. Experimental Considerations.....</i>	<i>175</i>
<i>8.3. Future Directions</i>	<i>181</i>
APPENDIX	
A. Data collection Sheets.....	182
B. Sample size estimates.....	184
BIBLIOGRAPHY	185

LIST OF TABLES

Table	Page
3-1. Comparison of three commonly used different tissue preservation solutions.....	49
3-2. Comparisons of commonly-used mitochondrial respiration media for in situ mitochondrial respiration experiments.....	52
3-3. Experimental protocol for Aim 1.....	62
3-4. Experimental protocol for aim 2, part 1.....	67
3-5. Experimental protocol for aim 2, part 2.....	69
3-6 Experimental protocol for Aim 3.....	76
7-1 Mean Mitochondrial Respiration Rates.....	174

LIST OF FIGURES

Figure	Page
2-1. Estimated number of annual deaths due to smoking-related diseases.....	17
2-2. The coordination of active muscle and blood vessels during exercise.....	20
2-3. Common shifts in muscle size, strength, and metabolism in patients with COPD.	21
2-4. The Role of cigarette smoke-induced ROS formation in cells.....	25
2-5. A representative schematic of the Electron Transport Chain (ETC).....	27
2-6. A representative schematic of cigarette smoke-induced mitochondrial superoxide (O_2^-) generation.....	28
2-7. Tissue-specific changes in ROS levels induced by 4 days of nose-only cigarette smoke exposure.....	35
2-8. Cigarette smoke-induced changes to $\Delta\Psi_{mt}$ in human primary bronchial endothelial cells and isolated liver mitochondria, as well as changes to ATP in human primary bronchial endothelial cells and isolated liver mitochondria.....	37
2-9. Percentage of $\Delta\Psi_{mt}$ collapse induced by cigarette smoke extract in mitochondria isolated from the mouse eye, fetus, kidney, liver, and skin.	38
2-10. Whole-body palmitate rate of appearance, oxidation, and incorporation into IMTG in nonsmokers and smoker.....	39
3-1. Overview of the 3 aims proposed for this project.	45
3-2. Cartoon image of tissues used in this study.....	47
3-3. General workflow of the protocols used to permeabilize the tissues for this project.....	53
3-4. Diagram illustrating the chemical process of saponin permeabilization.....	54

3-5. Screenshot taken from the DatLab Software output created by Oroboros Instruments.	58
3-6. Overview of Aim 1.....	59
3-7. Overview of Aim 2	64
3-8. Overview of Aim 3.....	72
3-9. Results of a pilot experiment demonstrating kinetics of CAT, including IC ₅₀ and the I _{max} ..	74
3-10. Diagram illustrating the conversion of the Michaelis-Menten curve to a Lineweaver-Burke Plot.....	78
5-1. Absolute Respiration Rates for the heart, soleus, gastrocnemius, and aorta.....	95
5-2. Absolute Respiration Rates for gastrocnemius, soleus, the heart, and aorta	96
5-3. Results of the piecewise linear regression in absolute rates of mitochondrial respiration....	97
5-4. Citrate synthase activity for the heart, soleus, gastrocnemius, and aorta	98
5-5. Respiration rates normalized to CS activity for the heart, soleus, gastrocnemius, and aorta	99
5-6. Respiration rates normalized for CS activity for gastrocnemius, soleus, the heart, and aorta.	
.....	100
5-7. Results of the piecewise linear regression in mitochondrial respiration rates normalized to CS activity.....	101
5-8. Summary of findings from Aim 1	109
6-1. Dose-response curve for Pyruvate-stimulated mitochondrial respiration in the Gastrocnemius and Soleus, and the mean estimates for the apparent K _m and V _{max} of mitochondrial respiration to pyruvate for both control and CSC-exposed fibers.....	121
6-2. Dose-response curve for palmitoylcarnitine-stimulated mitochondrial respiration in the Gastrocnemius and Soleus, and the mean estimates for the apparent K _m and V _{max} of	

mitochondrial respiration to palmitoylcarnitine (PC) for both control and cigarette smoke condensate-exposed fibers.	123
6-3. Dose-response curve for Pyruvate-stimulated mitochondrial respiration in the presence of 0.04 mM PC for the Gastrocnemius and Soleus, and the mean estimates for the apparent K_m and V_{max} of mitochondrial respiration to pyruvate for both control and cigarette smoke condensate-exposed fibers.	125
6-4. Change in the K_m and V_{max} of mitochondrial pyruvate oxidation in the presence of saturating (0.04 mM) concentration of palmitoylcarnitine relative to mitochondrial pyruvate oxidation without palmitoylcarnitine in control and cigarette smoke condensate-exposed white gastrocnemius and soleus fiber bundles.....	126
6-5. Schematic outlining the hypothesized mechanisms by which cigarette smoke induces skeletal muscle mitochondrial dysfunction and the downstream effects.....	133
7-1. Respiration rates (JO_2) of permeabilized gastrocnemius and soleus skeletal muscle fibers, and their respective CSC-exposed counterparts normalized to the wet weight of the sample. Also shown are the contribution of complex II, ratio of GMDS to CAT _{5.0} , Respiratory Control Ratio, and thermodynamic coupling.....	148
7-2. The relative differences in uncoupled (FCCP _{Peak}) respiration and the CSC-induced inhibition of ANT between the control and CSC-exposed fibers for the gastrocnemius and soleus muscle fibers.	151
7-3. Dose-response kinetic curves for ADP-stimulated respiration in the gastrocnemius and soleus and their respective CSC-exposed counterparts; and mean estimates for the apparent K_m and V_{max}	154

7-4. Dose-response kinetic curves for carboxyatractyloside-inhibited respiration (A) in the gastrocnemius and soleus and their respective CSC-exposed counterparts. Mean estimates for the initial rate, apparent IC ₅₀ , I _{max} , and the inhibitory effect of CAT relative to the initial rate.....	157
7-5. Summary of the findings in aim 3.	168
8-1. Conceptual framework and summary of the main findings in the present work.....	174
8-2. Schematic showing the differences in sample preparation between striated muscles and the aorta, as used in aim 1.....	177
8-3. Citrate synthase activities of control and CSC-exposed tissues	179

CHAPTER 1

INTRODUCTION

Cigarette smoke exposure is estimated to cause more than 480,000 deaths annually in the United States and is a primary contributor to developing several cancers, respiratory, cardiovascular, and chronic metabolic diseases (United States Department of Health and Human Services, 2014). For example, cigarette smoke exposure is the most significant predictor of developing Chronic Obstructive Pulmonary Disease (COPD), a condition in which prolonged airway inflammation irreversibly damages alveolar structures, leading to emphysema and airflow limitation (Mannino & Buist, 2007). In addition to lung damage, cigarette smoke exposure impairs the function of numerous organs and tissues of the body (Larsson & Örlander, 1984; Messner & Bernhard, 2014; A. Meyer et al., 2013; Örlander et al., 1979), increases the risk for frailty (Ambrosino & Strambi, 2004; Caram et al., 2016; De Tarso Muller et al., 2019; Papathanasiou et al., 2007a), and ultimately decreases healthspan and lifespan (Sakata et al., 2012; United States Department of Health and Human Services, 2014). With vaping and cannabis smoke growing in popularity as new forms of smoking, exposure to smoke is currently and will continue to be a significant public health concern worldwide. Knowledge of the biological mechanisms underlying the pathogenic effects of cigarette smoke on health is therefore of great importance, and, accordingly, the adverse effects of cigarette smoking on lung structure and function have been well characterized. In stark contrast, the extra-pulmonary manifestations of cigarette smoke exposure, which also significantly contribute to poor health outcomes and increased mortality, are still poorly understood.

1.1. Adverse health outcomes from cigarette smoke exposure: extra-pulmonary manifestations

While cigarette smoke exposure has been implicated in the altered function of multiple organs, the present work will focus on the effects of cigarette smoke on the cardiovascular and skeletal muscles systems, given the scarcity of the literature on those organs, their crucial role on the quality of life and mortality, and their therapeutic potential. Considering the increased odds ratios in various muscular (e.g., sarcopenia and diabetes) and vascular diseases (e.g., peripheral artery disease and stroke) with exposure to cigarette smoke, it is imperative that we increase the understanding of the causal mechanisms underlying the increased risk of these diseases (Jo et al., 2019; Lee & Choi, 2019; Maddatu et al., 2017a; Münzel et al., 2020).

1.1.1. Cardiovascular function

Epidemiological studies have consistently demonstrated a strong association between cigarette smoke and the risk for cardiovascular diseases (CVD) such as stroke, peripheral artery disease, and aortic aneurism (United States Department of Health and Human Services, 2014). The contribution of cigarette smoke to cardiovascular morbidity is complex and involves several intertwined pathophysiological mechanisms, including autonomic dysregulation, atherosclerosis, endothelial dysfunction, and a shift in blood characteristics toward a pro-coagulant state (Messner & Bernhard, 2014). In a landmark study on the clinical effects of cigarette smoke, (Celermajer et al., 1993) demonstrated a dose-response relationship between smoking exposure (pack-years smoked) and flow-mediated dilation in conduit arteries of healthy young adults. The deleterious effects of cigarette smoke on flow-mediated dilation in conduit arteries were subsequently confirmed in a large clinical trial, the Gutenberg Health Study (Hahad et al., 2021), which also

revealed a dose-dependent effect of cigarette smoke on conduit arteries stiffness and microvascular function. Combined with other studies (Amato et al., 2013; Doonan et al., 2010; Graham Barr et al., 2007; Siasos et al., 2014), there is robust evidence that atherosclerosis and endothelial dysfunction are hallmarks of chronic exposure to cigarette smoke.

1.1.2. Skeletal muscle function

Epidemiological data demonstrated that cigarette smoking predicts frailty status amongst adults (Kojima et al., 2015). Consistent with this observational study, chronic cigarette smoking has been associated with detrimental effects on physical function such as quadriceps weakness (Degens et al., 2015; Seymour et al., 2010) and greater susceptibility to exercise-induced fatigue (Wüst et al., 2008). Also, mice chronically exposed to cigarette smoke developed skeletal muscle abnormalities. For instance, Nogueira et al. (Nogueira et al., 2018) showed slower calcium reuptake into the sarcoplasmic reticulum of mice exposed to cigarette smoke. Furthermore, cigarette smoke oxidizes several proteins related to contractile function and aerobic metabolism, decreasing their functionality and exacerbating muscular fatigue (Barreiro et al., 2010, 2012; Gosker et al., 2009).

Aerobic metabolism appears to be particularly affected by cigarette smoke exposure. Several studies demonstrated that smokers presented with slower whole-body oxygen uptake ($\dot{V}O_2$) onset kinetics (Chevalier et al., 1963; Krumholz et al., 1964), and lower maximal $\dot{V}O_2$ ($\dot{V}O_{2\max}$) (Cooper et al., 1968; Morton & Holmik, 1985). The impairments in aerobic metabolism in humans were also evident with acute exposure to cigarette smoke (Hirsch et al., 1985; Morton & Holmik, 1985), indicating both rapid and long-lasting effects of cigarette smoke exposure on

whole-body aerobic capacity. Although limited O₂ availability caused by altered vascular function may play a role in these findings, mechanisms intrinsic to skeletal muscles are also involved.

It is noteworthy that chronic exposure to cigarette smoke induces muscle atrophy (Marques et al., 2020; Montes De Oca et al., 2008b; Sadaka et al., 2021), and disproportionately impact oxidative type I fibers (Kapchinsky et al., 2018; Montes De Oca et al., 2008b) thus translating metabolically in a shift toward non-oxidative metabolism (Montes De Oca et al., 2008b). Accordingly, the skeletal muscle of mice exposed to cigarette smoke exhibited lower activities of enzymes involved in aerobic metabolism (Gosker et al., 2009). Notably, the extent of these metabolic alterations is such that it can compromise skeletal muscle energy status and result in a lower concentration of ATP at rest (Pérez-Rial et al., 2020; van der Toorn et al., 2007, 2009). However, such a mechanism would not explain the acute impairments in aerobic metabolism in response to acute cigarette smoke exposure (Hirsch et al., 1985; Morton & Holmik, 1985).

1.2. Pathways and cellular mechanisms for cardiovascular and skeletal muscle dysfunction induced cigarette smoke

While the epidemiological evidence for the deleterious effects of cigarette smoke on the cardiovascular and skeletal muscle systems are no longer disputed (Tong & Glantz, 2007), the cellular mechanisms that initiate those dysfunctions are still under investigation. Among those, perturbed mitochondrial function appears to play a pivotal role.

Cigarette smoke is composed of approximately 4,800 different chemicals (Rodgman & Green, 2016), including reactive oxygen species (ROS) and several well-known toxicants such as nicotine, carbon monoxide (CO), and cyanide. Some of these compounds can diffuse through the alveolar-capillary barrier in the lungs, be carried in the bloodstream, and reach peripheral tissues.

Other compounds can augment endogenous sources of free radicals by altering the function of enzymes involved in the redox balance, such as NADPH oxidase (NOX) (Chang et al., 2017), NO synthase (NOS) (Abdelghany et al., 2018; Satoh et al., 2005), xanthine oxidase (XO) (Kim et al., 2013), or altering mitochondrial-derived ROS production (van der Toorn et al., 2009). Mitochondria are a well-known source of cellular ROS production, and the compromised function of these organelles can have crippling implications for cells far beyond changes in bioenergetic status (Murphy, 2009). Indeed, it is now recognized that mitochondria also play a critical role in cell signaling, calcium homeostasis, and apoptosis. Recent *in vitro* evidence suggests that mitochondrial dynamics and respiration are affected by exposure to cigarette smoke (Agarwal et al., 2012; Ahmad et al., 2015; Hara et al., 2013). Given the ubiquity of these organelles in the cells of the human body, identifying the mechanisms by which cigarette smoke affects mitochondrial function has important implications for understanding the systemic effects of cigarette smoke exposure.

1.2.1. Tissue-specific susceptibility to cigarette smoke-induced mitochondrial damage

Cigarette smoke alters the function of nearly every organ in the body. However, the organs' susceptibility to the detrimental effects of cigarette smoke varies greatly, as illustrated by the greater relative risks for cancer of some tissues relative to others (Gandini et al., 2008). Although the literature is scarce on this topic, the degree of dysfunction inflicted on the mitochondria appears to be tissue-dependent. For example, IC₅₀ values, the concentration at which an inhibitor decreases the activity of an enzyme by 50%, for succinate dehydrogenase activity in cigarette smoke extract-exposed mitochondria isolated from rat eye, kidney, skin, and liver tissues range from 3% to 46% of the final solution concentration (Naserzadeh et al., 2015; Naserzadeh & Pourahmad, 2013),

highlighting the large variability in the degree of tissue susceptibility to cigarette smoke-induced damage. Furthermore, the degree of ROS production, mitochondrial swelling, cytochrome C release, and mitochondrial membrane potential collapse in response to cigarette smoke exposure all differed between eye, kidney, skin, and liver mitochondria (Naserzadeh et al., 2015). Using a mouse model of nose-only cigarette smoke exposure, Raza et al. (Raza et al., 2013) showed distinct ROS levels and lipid peroxidation in liver, kidney, heart, and lungs in response to cigarette smoke exposure. Furthermore, cigarette smoke-induced inhibition of mitochondrial complex I and IV enzymatic activities in the liver, kidney, heart, and lung was tissue-dependent, with cardiac tissues being more resistant to the effects of cigarette smoke. Lastly, Haji et al. (Haji et al., 2020) showed that, unlike the quadriceps muscle, which was similar between groups, complex I and V protein expression in isolated mitochondria from lung tissues of ex-smokers were downregulated compared to age-matched healthy controls, suggesting that skeletal muscle may have a greater resistance to cigarette smoke-induced toxicity than airway tissues. However, considering the likely variability in the levels of toxicant exposure between *in situ* cigarette smoke exposure and the exposure experienced in the human condition, it is challenging to compare the direct toxicity of cigarette smoke exposure to ROS production and mitochondrial function between tissues.

Collectively, these studies point towards variable tissue-dependent effects of cigarette smoke on mitochondrial function. However, an important caveat in these studies is the use of isolated or homogenized tissue, which may produce a selection bias favoring more robust mitochondria and disrupt mitochondrial functional characteristics (Picard et al., 2010), unlike permeabilized fiber bundles (Kuznetsov et al., 2008b). In line with these observations, recent advancements in 3-dimensional electron microscopy have elegantly shown that mitochondria form

dense networks within tissues (especially skeletal muscle), which may comprise an interconnected network spanning large distances across a given tissue (Glancy et al., 2015). Effectively, his vast reticulum of mitochondria allows for a greater ability to maintain the chemiosmotic gradient across the mitochondrial network, as the phosphorylation potential can then be spread across the whole mitochondria (Glancy et al., 2017). Therefore, in intact tissues, localized disruptions in the electron transport chain are compensated for by the activity in other areas of the mitochondria. However, in isolated mitochondria, the structural network of the mitochondrial reticulum is likely compromised, thereby exacerbating deficits in mitochondrial function. In addition, the activities of a limited selection of enzymes do not fully reflect oxidative phosphorylation *in vivo*. Therefore, it remains unclear whether the sensitivity of mitochondrial respiration to cigarette smoke differs across tissue types under physiological conditions, especially in tissues critical to the development of cardiometabolic disease, which includes the heart, skeletal muscle, and arteries. This is indeed a necessary piece of information to determine the relevant dose of cigarette smoke that can elicit mitochondrial dysfunction, which will help better understand the greater susceptibility of some organs to the adverse effects of cigarette smoke.

*1.2.2. Direct effects of cigarette smoke on mitochondrial function: *in vitro* findings*

In airway epithelial cells, cigarette smoke exposure resulted in mitochondrial fragmentation and branching, lower protein expression of respiratory complexes, and mitophagy (Agarwal et al., 2012; Ahmad et al., 2015; Hara et al., 2013). Functional changes accompanied these alterations in mitochondrial dynamics and morphology. Specifically, incubation of epithelial cells in cigarette smoke extract (CSE) induced a dose-dependent decrease in mitochondrial membrane potential ($\Delta\Psi_m$), greater ROS production, which ultimately resulted in lower ATP

levels in the cells (van der Toorn et al., 2009). CSE incubation inhibited mitochondrial complex I and II activities of epithelial cells (van der Toorn et al., 2007) and increased proton leakage caused by adenylate translocase activation (ANT), a key mitochondrial ADP/ATP carrier involved in the regulation of the $\Delta\Psi_m$ (Wu et al., 2020). Together, these *in vitro* findings suggest that CSE incubation can de-energize mitochondria by decreasing both the supply of reducing equivalents through complex I and II and/or increasing proton leakage, ultimately resulting in bioenergetic failure. Importantly, similar findings were documented in airway smooth muscle cells from humans (Aravamudan et al., 2014, 2017), thus suggesting that circulating factors, such as lung-derived ceramides (Thatcher et al., 2014) or lipid-soluble constituents of cigarette smoke (van der Toorn et al., 2009), derived from cigarette smoke could elicit mitochondrial defects in other cell types.

In cardiac, skeletal, and vascular smooth muscles, mitochondrial energy production through the process of oxidative phosphorylation is essential for sustaining muscle contractions, myogenic tones, and cellular transport involved in maintaining the structural integrity of the cells (Larson-Meyer et al., 2000, 2001; Zhang & Gao, 2021). Interestingly, in recent years, there has been a growing recognition that mitochondrial-derived ROS is also an important signaling pathway involved in the maintenance of vascular and skeletal muscle homeostasis (Ashok & Ali, 1999; Cui et al., 2012; Moylan & Reid, 2007; Weseler & Bast, 2010). Importantly, acute exposure to cigarette smoke has been related to excessive mitochondrial-derived free radical levels and attenuated endothelial-dependent vasodilation in response to acetylcholine in mice aorta (Csiszar et al., 2008; Dikalov et al., 2019), thus implicating mitochondria as both a target and a contributor to cigarette-smoke induced vascular dysfunction. However, a limitation in these studies was that

mitochondrial respiration was not measured. Therefore, it is unclear whether the elevated levels of mitochondrial-derived ROS stemmed from a lower antioxidant capacity within the mitochondrial matrix, e.g., manganese superoxide dismutase, or from perturbed oxidative phosphorylation through the respiratory complexes.

1.2.3. Direct effects of cigarette smoke on mitochondrial function: muscle cells and fibers

While *in vitro* studies in isolated mitochondria from epithelial cells have improved our fundamental understanding of the mechanisms of action of cigarette smoke on mitochondrial function (van der Toorn et al., 2009), whether those mechanisms are involved in mitochondrial dysfunction under physiologically relevant conditions for other organs and tissues remains unclear. Recent studies by Khattri et al. (Khattri et al., 2022) showed that an acute (~10 minutes) CSE incubation with mitochondria isolated from mouse skeletal muscles directly inhibited mitochondrial respiration state III respiration. Furthermore, the loss of mitochondrial respiration was attributed to the direct inhibition of complex I-driven respiration via the presence of nicotine and o-cresol. However, while these findings show the direct cause of CSE-induced loss of mitochondrial respiration, these studies homogenized several muscle fiber types to produce their isolated mitochondria preparation and did not identify if muscle fiber types (i.e. oxidative or glycolytic muscles) are differentially impacted by CSE. Therefore, it remains to be determined if the CSE-induced inhibition of mitochondrial respiration is the same in muscles with different fiber compositions.

Furthermore, in C2C12 muscle cells conditioned in media from smoke-exposed lung cells and smoke-exposed mice, (Thatcher et al., 2014) reported impaired muscle respiratory capacity using substrates replicating the Krebs cycle (glutamate, malate, succinate). Interestingly, in another

set of experiments with mice chronically exposed to cigarette smoke, the authors also demonstrated impaired whole-body glucose tolerance and ceramide accumulation, a fatty acid of the sphingolipid family that accumulates in response to an imbalance between fatty acid supply and oxidation (Watt et al., 2012). In addition, inhibition of ceramide formation by myriocin injection resulted in higher *in situ* respiratory capacity from both cardiac and skeletal muscle permeabilized fibers. The authors interpreted this result as evidence that ceramide accumulation caused by cigarette smoke inhibited mitochondrial respiration in both tissues. However, a caveat to this study was that both mice chronically exposed to cigarette smoke and their corresponding time-control demonstrated improvement in mitochondrial respiration with ceramide inhibition. In addition, the sensitivity and capacity of the mitochondria to oxidize fatty acids were not assessed. Therefore, it is still unclear whether ceramide accumulation *caused* mitochondrial dysfunction or was *secondary* to a shift in substrate preference and/or altered capacity for fatty acid oxidation with cigarette smoke exposure.

1.2.4. Effects of cigarette smoke on substrate oxidation

Despite the study by Thatcher implicating mitochondrial dysfunction in the metabolic disruption induced by cigarette smoke, the effects of cigarette smoke on energy metabolism and substrate oxidation have predominantly focused on whole-body metabolism. For instance, whole-body fatty acid oxidation has been reported to increase in smokers (Bergman et al., 2009; Jensen et al., 1995). Moreover, Jensen et al. (1995) reported that the increase in fatty acid oxidation was proportional to the concentration of urine cotinine, a metabolite of nicotine, indicating a greater ability to oxidize fatty acids following smoke exposure. This shift in substrate preference, specifically the greater incorporation and oxidation of fatty acids observed by Bergman et al.

(Bergman et al., 2009) in smokers acutely undergoing a cigarette smoking session, is also linked to a decrease in insulin sensitivity and the development of type II diabetes. However, while 1-2 weeks of smoking cessation was able to reverse the loss of insulin resistance in smokers, palmitate rate of appearance and the percentage of saturated triglycerides and diglycerides remained elevated relative to control subjects, indicating that smoking cessation may only partially restore the metabolic perturbations associated with cigarette smoke (Bergman et al., 2012).

In contrast, several reports have documented higher serum triglycerides and fatty acids in smokers (Muscat et al., 1991a). There is a dose-response relationship between the number of cigarettes smoked per day and serum cholesterol levels (Muscat et al., 1991a). Specifically, cigarette smoking was documented to acutely increase free fatty acid (FFA) and glycerol fluxes as well as circulating FFA secondary to nicotine-induced stimulation of lipolysis (Hellerstein et al., 1994). Cigarette smoking increased delivery of FFA to the liver, increased hepatic reesterification, and augmented very low-density cholesterol production (Hellerstein et al., 1994). However, despite the increase in lipolysis, cigarette smoking did not increase the rate of whole-body lipid oxidation, and these smoke-induced changes were not reversed after one week of smoking cessation (Neese et al., 1994). Data from the CARDIA study showed that while smokers have less subcutaneous adipose tissue than never or former smokers, intramuscular adipose tissue (IMAT) volume was increased (as was IMAT/lean tissue ratio) in current smokers (Terry et al., 2020), indicating greater storage and less fatty acid oxidation of lipids in skeletal muscle of smokers per volume of lean mass.

These findings are indicative of larger deposits of fatty acids in the skeletal muscle of smokers, which may be due to incomplete fatty acid oxidation. There is, therefore, an apparent

conundrum in the literature as whole-body studies demonstrate an increased reliance on fatty acid metabolism, whereas recent experiments in mice chronically exposed to cigarette smoke indicate a build-up of toxic lipids such as ceramides perhaps secondary to impaired (decreased capacity) or incomplete (change in substrate preference) fatty acid oxidation. However, no studies have directly measured whether cigarette smoke directly alters substrate preference or the capacity for mitochondrial fatty acid oxidation.

1.3. Statement of the Problem

Therefore, considering the critical role that the mitochondria play in cellular energy metabolism and redox homeostasis and the damaging consequences that cigarette smoke may inflict upon the mitochondria, it is imperative that we better understand the causal mechanisms underlying cigarette smoke-induced mitochondrial dysfunction in order to identify possible therapeutic targets to mitigate these dysfunctions. Specifically, it is critical to understand the mitochondrial damage that cigarette smoke can cause in skeletal and cardiac muscle and vascular tissues, as these are the primary tissues involved in developing cardiometabolic diseases, which amount to the most significant cause of smoking-related deaths. However, there are currently several gaps in the literature that require reconciliation.

First, while it is apparent that tissue susceptibility to cigarette smoke-mitochondrial dysfunction is variable across organs, the sensitivities of skeletal and cardiac muscles and vascular tissues have not been characterized in the literature. Therefore, it is unknown if the mitochondria in the arteries, cardiac muscle, or type I and type II skeletal muscle fibers have different sensitivities to cigarette smoke, an essential piece of information in identifying which tissues are most susceptible to cigarette smoke-induced damage and more likely to be the targets of therapies.

Second, cigarette smoke alters the metabolism of many energy-generating substrates, especially fatty acids. While whole-body studies using indirect calorimetry have shown an increase in fatty acid oxidation caused by cigarette smoking, other studies using metabolic tracers showed a decrease in fatty acid uptake and utilization. However, the findings from these studies, while clearly at odds with each other, did not directly investigate the capacity of the mitochondria to oxidize fatty acids. Therefore, it is still unknown if the alterations to fatty acid metabolism occur at the mitochondrial level or at some other point along the process of fatty acid metabolism.

Lastly, cigarette smoke exposure has been shown to damage isolated mitochondria at several sites along the respiratory chain, most notably complex I and III, and decrease mitochondrial membrane potential, thus resulting in impaired oxidative ATP production. However, the process of isolating mitochondria may damage the mitochondria compared to the permeabilized fiber technique, which could alter the interpretation of these studies. Research has yet to explore the contribution of phosphate transport, ADP sensitivity, and respiratory chain activities to mitochondrial function in permeabilized fibers exposed to cigarette smoke. These findings are critical to identifying the molecular targets of cigarette smoke within the mitochondria.

1.4. Purpose & Aims

Considering the existing gaps in the literature, the overarching goal of this project is to advance the understanding of the underlying causes of cigarette smoke-induced mitochondrial dysfunction – specifically targeting tissue-specific susceptibility to cigarette smoke toxicity, alterations to mitochondrial substrate oxidation, and identifying key mitochondrial targets of cigarette smoke-induced dysfunction using an *in situ* mouse model.

In specific aim 1, we will determine the extent of tissue-specific susceptibility to cigarette smoke for the aorta, cardiac muscle, and oxidative and glycolytic skeletal muscles. Our working hypothesis is that each tissue will display different susceptibility to cigarette smoke, with the cardiac muscle and aorta being more susceptible to cigarette smoke based on epidemiological evidence suggesting the greater relative risks for tobacco-related diseases in these tissues relative to others (Gandini et al., 2008).

In specific aim 2, we will determine the cigarette smoke-induced alterations to the mitochondrial oxidation of palmitoylcarnitine, a long-chain fatty acid, and pyruvate, a product of glycolysis in the skeletal muscle (glycolytic gastrocnemius fibers and oxidative soleus fibers). Our working hypothesis is that cigarette smoke will decrease the sensitivity and maximal capacity to oxidize palmitoylcarnitine oxidation relative to pyruvate.

In specific aim 3, we will determine the extent of cigarette smoke-induced perturbations to the exchange of phosphates, ADP sensitivity, and mitochondrial respiratory chain activity. Based upon prior studies in epithelial cells (Wu et al., 2020), our working hypothesis is that cigarette smoke will primarily affect phosphate exchange by decreasing the activity of ANT, which in turn will decrease ADP sensitivity, and ultimately result in lower mitochondrial respiration in permeabilized fibers from both glycolytic gastrocnemius muscle and oxidative soleus muscle.

CHAPTER 2

LITERATURE REVIEW

Exposure to cigarette smoke is a significant health concern domestically and globally, as cigarette smoke is related to many adverse public health outcomes and ultimately increases mortality risk. While smoking tobacco and other substances have been worldwide religious and medicinal practices for millennia – especially in the Americas where the tobacco plant originated (Gilman & Zhouu, 2004) – the health concerns of smoke exposure were not elucidated until 1925, when German physician Fritz Lickint (Gourd, 2014; Lickint, 1930) established the link between tobacco smoke and cancer. This initial research sparked decades of investigation into adverse smoking-related outcomes, leading to the release of *Smoking and Health: Report of the Advisory Committee of the Surgeon General of the Public Health Service* in January 1964 (United States Department of Health and Human Services, 2014). Since the publication of this monumental document, cigarette smoking has taken the forefront of public health concerns in the United States. This report – now part of a series referred to as the *Surgeon General's Report* – was written by US Surgeon General, Luther L. Terry, under President John F. Kennedy's request to review decades of research surrounding the detrimental public health effects of smoke exposure and establish national health recommendations related to smoking (United States Department of Health and Human Services, 2014) with emphasis on encouraging people to avoid smoke exposure and practice behaviors which encourage smoking cessation. Furthermore, these monumental reports began pushing US public policy changes to mitigate cigarette smoke exposure, such as the Congressional vote to ban inflight smoking in 1987.

Despite these numerous attempts to deter tobacco use by Americans, cigarette smoking remains a significant health concern in the United States. The Surgeon General's most recent report published in 2014 (United States Department of Health and Human Services, 2014) estimated that 18% of Americans continue to smoke. While this is a stark decrease compared to the 42% of smokers in 1965, the economic costs of cigarette smoke for the years 2009-2012 were between \$289-332.5 billion. These costs included direct medical care for adults (\$132.5-175.9 billion), lost productivity due to premature death (\$151 billion), and lost productivity due to secondhand smoke exposure (\$5.6 billion). Furthermore, cigarette smoking contributes to over 480,000 annual deaths and millions of additional smoke-related disabilities, including cardiovascular and cerebrovascular diseases, respiratory disorders, metabolic diseases, cancer, fetal development issues, and many other conditions (United States Department of Health and Human Services, 2014). Altogether, these risks associated with chronic cigarette smoke exposure result in a 10-year reduction in life expectancy compared to those who abstain from smoke exposure. Therefore, cigarette smoke exposure remains a significant public health concern and requires immediate attention to remedy these negative societal impacts.

While cigarette smoke is most commonly associated with detrimental impacts to the airway and lungs, cigarette smoke exposure also negatively influences peripheral organs, such as skeletal muscle and vasculature. The impact to the airways and lungs is multifaceted and involves several pathways related to chronic inflammation and cellular stress (Vaart et al., 2004), which ultimately degrade tissues and result in fibrotic tissues. However, most smoking-related deaths – nearly 40%

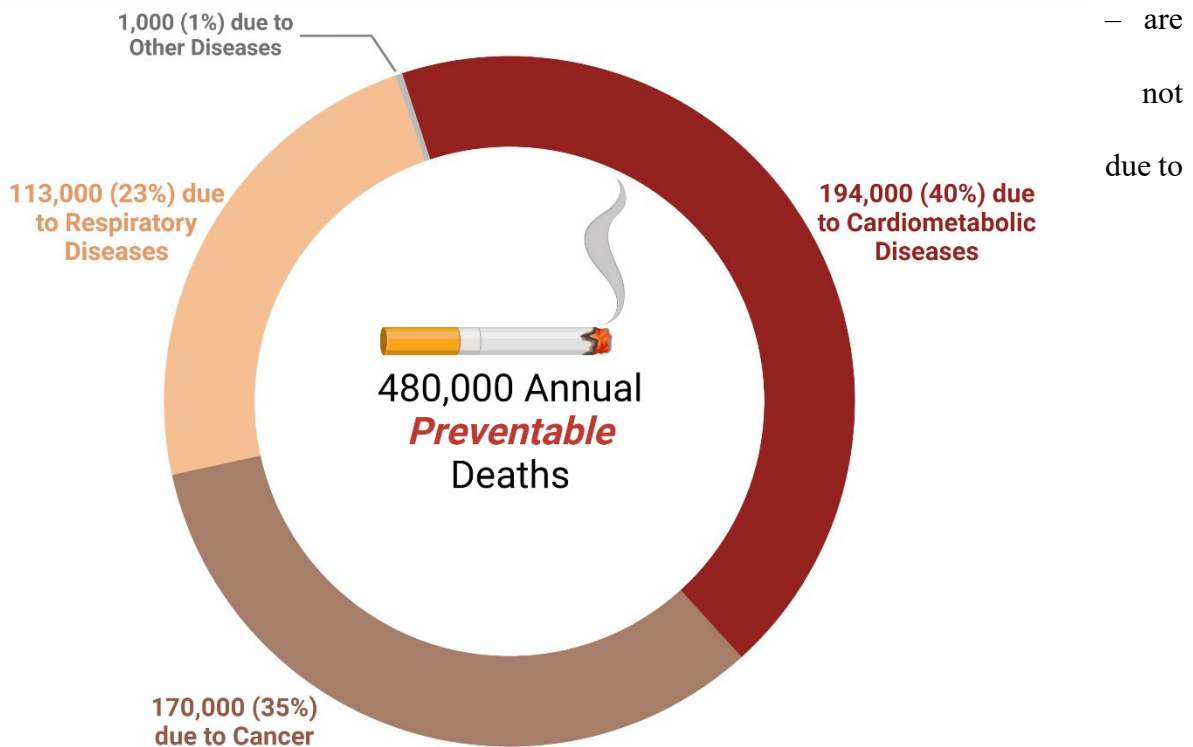


Figure 2-1. Estimated number of annual deaths due to smoking-related diseases.

complications of lung or airway tissues; instead, they are due to extrapulmonary diseases, such as cardiovascular and metabolic disease (Figure 2-1) (United States Department of Health and Human Services, 2014). Considering the biological roles of skeletal muscle, such as locomotion and the immense contribution to whole-body energy expenditure, and the vasculature, such as regulating the transport of blood and nutrients, the health of both systems is critical to the prevention of cardiometabolic diseases. Thus, addressing the mechanisms underlying the cigarette smoke-induced peripheral impairments – specifically those related to skeletal muscle and vascular tissues – is critical to improving the health outcomes of those exposed to regular cigarette smoke.

2.1. Peripheral Manifestations of Cigarette Smoke Exposure

Cigarette smoking is a leading modifiable risk factor for the early development of several chronic conditions related to skeletal muscle and vascular dysfunction – including muscle wasting, diabetes, peripheral artery disease, atherosclerosis, frailty, and cancer (United States Department of Health and Human Services, 2014). Because many of these conditions generally appear in the late stages of life, cigarette smoke exposure is thought to induce “accelerated aging” of various tissues throughout the body (Bernhard et al., 2007). The enhanced deterioration of peripheral tissues – especially skeletal muscle and vascular tissues – caused by cigarette smoke exposure has many significant physiological implications that result in the progressive loss of function and early mortality.

Skeletal muscle, the largest organ in the human body by mass and primary organ for locomotion, is an important contributor to whole-body energy expenditure – representing ~20% of resting oxygen consumption, a relevant indicator of energy expenditure (Gallagher et al., 1998; Illner et al., 2000; Zurlo et al., 1990). Cellular energy in resting skeletal muscle, mainly in the form of adenosine triphosphate (ATP), is primarily used for thermoregulatory and homeostatic purposes, such as maintaining cellular ion concentrations and enzyme activities. However, during the transition to exercise, the cellular demand for ATP may exceed 100-fold that of resting conditions in order to generate contractile force within the cross-bridge cycle, and calcium recycling by the sarcolemma and sarcoplasmic reticulum, all of which consume large quantities of ATP and produce ADP, inorganic phosphate (Pi), and energy via various ATPases (Equation 2-1) (Gaitanos et al., 1993).



Simultaneously, with the increase in energy demand in skeletal muscle during the transition from rest to exercise, the demand for an adequate supply of oxygen (O_2) increases dramatically. Incredibly, whole-body $\dot{V}O_{2\max}$ is typically 10-15 times greater than resting oxygen consumption ($\dot{V}O_2$). Considering the Fick equation (Equation I-1) and the importance of oxygen transport to the active muscle, blood flow to the active muscle must also increase 100-fold, mirroring the increase in muscle ATP demands (Hawley et al., 2014). Though there are many factors involved in transporting oxygen to active muscle, the cardiovascular system's ability to deliver blood to active muscle while maintaining blood pressure is heavily influenced by the ability of blood vessels to appropriately dilate the arteries that supply active tissues (Hawley et al., 2014). The importance of vessel diameter on blood flow to tissue can very easily be determined by Poiseuille's Law (Equation 2-2), which describes the flow of fluids through vessels as follows:

$$Q = \frac{\pi P r^4}{8\eta l} \quad (2-2)$$

Where Q is the rate of blood flow, P is blood pressure, r is the radius of the blood vessel, η is the blood viscosity, and l is the vessel's length. Thus, assuming a constant viscosity, vessel length, and mean arterial pressure, blood vessels' ability to dilate is paramount to maintaining energetic and homeostatic balance during high stress and demand events, such as intense exercise, as even small changes to vessel diameter can cause substantial increases in blood flow (Poole et al., 2020). Therefore, these two systems must work with each other in a coordinated manner to ensure optimal performance and – from an evolutionary perspective – survival (Figure 2-2).

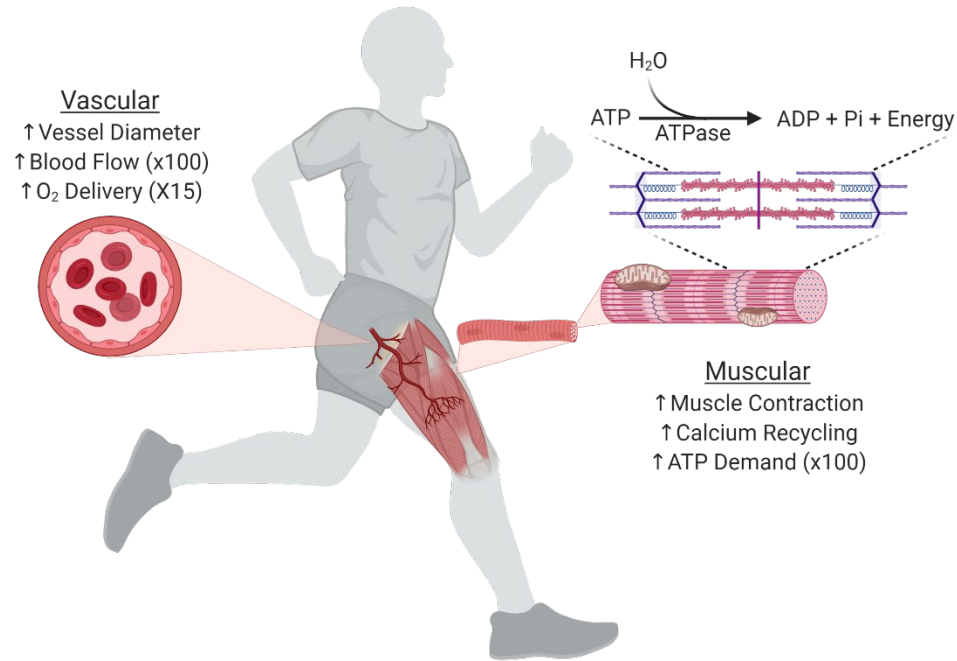


Figure 2-2. The coordination of active muscle and blood vessels during exercise. Blood vessels must increase in diameter in order to increase blood flow to match muscle energy demands during exercise.

2.1.1. Cigarette Smoke Exposure Impairs Skeletal Muscle Function

Chronic cigarette smoke exposure, and more so in patients with COPD, is associated with several muscular ailments (Figure 2-3) – most notably loss of strength, muscle atrophy, shifts in muscle fiber type, and mitochondrial dysfunction (Nyberg et al., 2015). Several reports have shown that active smokers have reduced quadriceps strength compared to age-matched nonsmokers, indicating a loss of contractile ability and force production associated with smoke exposure (Barreiro et al., 2010; Kok et al., 2012; Sadaka et al., 2021; Seymour et al., 2010). The smoke-related loss of strength often coincides with lower muscle cross-sectional area (CSA) (Marques et al., 2020) and type I fiber-specific (Cheung et al., 2020; Montes De Oca et al., 2008b) atrophy; and also may be related to impaired fatigue resistance (Wüst et al., 2008), as cigarette

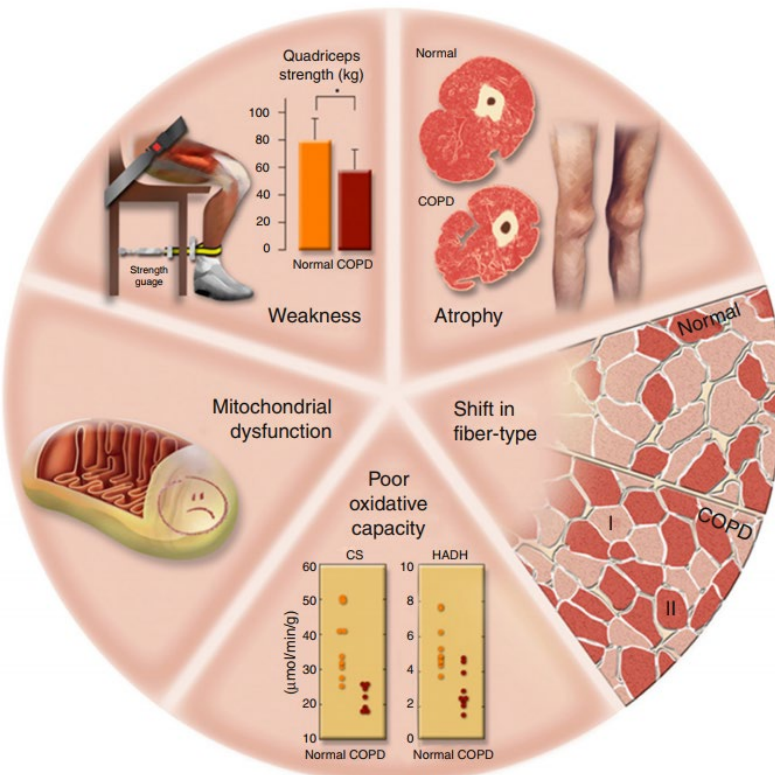


Figure 2-3. Common shifts in muscle size, strength, and metabolism in patients with COPD. Adapted from Nyberg et al. (2015).

smoke exposure directly alters sarcoplasmic calcium handling (Nogueira et al., 2018). Furthermore, skeletal muscle mitochondria appear to be negatively impacted in humans chronically exposed to cigarette smoke, as mitochondrial respiration is impaired in patients with COPD (Gifford et al., 2018b; Naimi et al., 2011; Puente-Maestu et al., 2009). Lastly, many of these impairments also improve upon smoking cessation (Ajime et al., 2020), indicating adverse outcomes directly related to cigarette smoke.

However, these observations are not without caveats. While many studies support a direct link between cigarette smoke exposure and muscular impairments, others have shown no or minimal differences in overall muscle function between smokers and nonsmokers (Richardson et al., 2004; Van Den Borst et al., 2011). There is, however, accumulating evidence that the loss of

skeletal muscle function – especially the mitochondrial bioenergetic deficits – results from reduced physical activity in smokers and individuals with COPD, rather than cigarette smoke exposure, *per se*, as these differences become lessened when participants are closely matched for physical activity (J. G. Gea et al., 2001; Layec, Haseler, et al., 2011; Shields et al., 2015; Wüst et al., 2008). Furthermore, many of the impairments to muscle mitochondria are restored after physical training (Bowen et al., 2017; Brønstad et al., 2012; McKeough et al., 2006). A recent report, which exposed sedentary mice to 8 months of cigarette smoke (equivalent to ~20-30 years of cigarette smoke exposure in humans) revealed that, while cigarette smoke exposure resulted in several alterations to skeletal muscle such as decreased mitochondrial protein expression and enhanced oxidative stress, mitochondrial function was similar to that of the control mice (Decker, Kwon, Zhao, Hoidal, Huecksteadt, et al., 2021). Collectively, these studies raise the possibility that physical inactivity may be the primary cause of cigarette smoke-related impairments in skeletal muscle function and that cigarette smoke itself may play a lesser role than previously thought. Nonetheless, there is considerable evidence to support a direct cigarette smoke-induced mitochondrial impairment of various tissues – including alveolar epithelial cells (Ballweg et al., 2014) and peripheral blood mononuclear cells (Alonso et al., 2004).

Indeed, recent experiments have shown that concentrations of cigarette smoke extract as low as 0.1% may acutely induce mitochondrial dysfunction in isolated mitochondria (Khattri et al., 2022). Furthermore, these studies also showed that individual cigarette smoke components, such as nicotine and o-cresol, can directly inhibit complex I-driven respiration in isolated mitochondria, offering direct evidence of a negative impact of cigarette smoke on the electron transport chain. However, the low sample size and the homogenization of several muscle groups

in this study limit the overall applications of these data, as it cannot be confirmed if the effects of cigarette smoke are more likely to affect fast- or slow-twitch muscles more adversely. Therefore, despite these numerous studies, evidence of a direct effect of cigarette smoke on intact skeletal muscle mitochondria has yet to be fully elucidated.

2.1.2. Cigarette Smoke Exposure Impairs Vascular Function

Alternatively, chronic and acute exposure to cigarette smoke adversely impacts the vascular system (Csizsar et al., 2009), and exposure to cigarette smoke remains a significant risk factor for vascular conditions, such as atherosclerosis and peripheral artery disease (Powell, 1998; United States Department of Health and Human Services, 2014). Mechanistically, many of the negative consequences of cigarette smoke exposure are related to impaired nitric oxide (NO) signaling, which plays a major role in regulating vascular tone via vasodilation (Powell, 1998). Chronic cigarette smoke exposure has long been shown to blunt the NO-mediated flow-mediated dilation (FMD) response (Celermajer et al., 1996; Poredoš et al., 1999), which improves upon cessation of smoke exposure (Celermajer et al., 1993; Johnson et al., 2010). Furthermore, acute exposure to cigarette smoke in young, nonsmoking individuals directly blunted the NO-dependent, but not NO-independent (via nitroglycerin injection), dilation in response to FMD (Giannini et al., 2007), thereby indicating that cigarette smoke directly impairs NO-mediated vasorelaxation. Indeed, much of this cigarette smoke-induced vascular impairment is secondary to decreased NO bioavailability (Raij et al., 2001). This represents a critical mechanism underlying the link between cigarette smoke exposure and adverse health outcomes, as poor endothelial function due to a loss

of NO bioavailability is closely tied to cardiovascular diseases, such as hypertension (Csordas & Bernhard, 2013; Endemann & Schiffrin, 2004).

While much of the research investigating cigarette smoke's impacts on vascular tissues has been related to the impairments to NO synthesis and vasodilation, little research has been conducted on cigarette smoke-induced mitochondrial impairments in vascular tissues. It is widely believed that mitochondria within the vasculature contribute mainly to vascular tone regulation, as adenosine triphosphate (ATP), the primary source of cellular energy, is generated mainly from glycolysis rather than oxidative phosphorylation (Webb, 2003). However, recent investigations have shown that mitochondria within the vasculature respond similarly to skeletal muscle when provided stimuli such as exercise training (S. Y. Park et al., 2016) and caloric restriction (Ungvari et al., 2010), are altered with advancing age (S. H. S. Y. Park et al., 2018), and respire at similar rates to skeletal and cardiac muscle when normalized for mitochondrial volume (S. Y. Park et al., 2014); ultimately implying that vascular mitochondria may play a more significant physiological role than previously thought. Thus, vascular mitochondria's role in maintaining vascular homeostasis and the extent to which cigarette smoke exposure impacts vascular mitochondria are essential subjects in physiology that have yet to be thoroughly explored.

While the causes of cigarette smoke-induced peripheral dysfunction are multifaceted and complex, current evidence points to excessive reactive oxygen species (ROS) production as a significant factor in developing both vascular and muscular impairments. Under conditions of exacerbated ROS production, such as during exposure to cigarette smoke, cellular ROS and the resulting oxidative stress result in damage to DNA, proteins, and lipids (Liguori et al., 2018), causing detrimental effects to critical cellular functions and are linked to skeletal muscle weakness

and atrophy (Moylan & Reid, 2007), mitochondrial dysfunction (Cui et al., 2012), and vascular dysfunction (Weseler & Bast, 2010). This state of cellular dysfunction can further exacerbate ROS formation, thereby creating a vicious cycle of ROS formation and exaggerated cellular dysfunction. Therefore, understanding the underlying mechanisms of how these ROS are formed and identifying interventions to mitigate the cigarette smoke-induced cellular damage may be crucial to addressing the peripheral dysfunction and health detriments observed in cigarette smoke-exposed individuals.

2.2. ROS are a Result of Cigarette Smoke Exposure

Although endogenously-derived ROS are, in many respects, beneficial to the cellular environment by mediating several critical pathways, including apoptosis (Redza-Dutordoir &

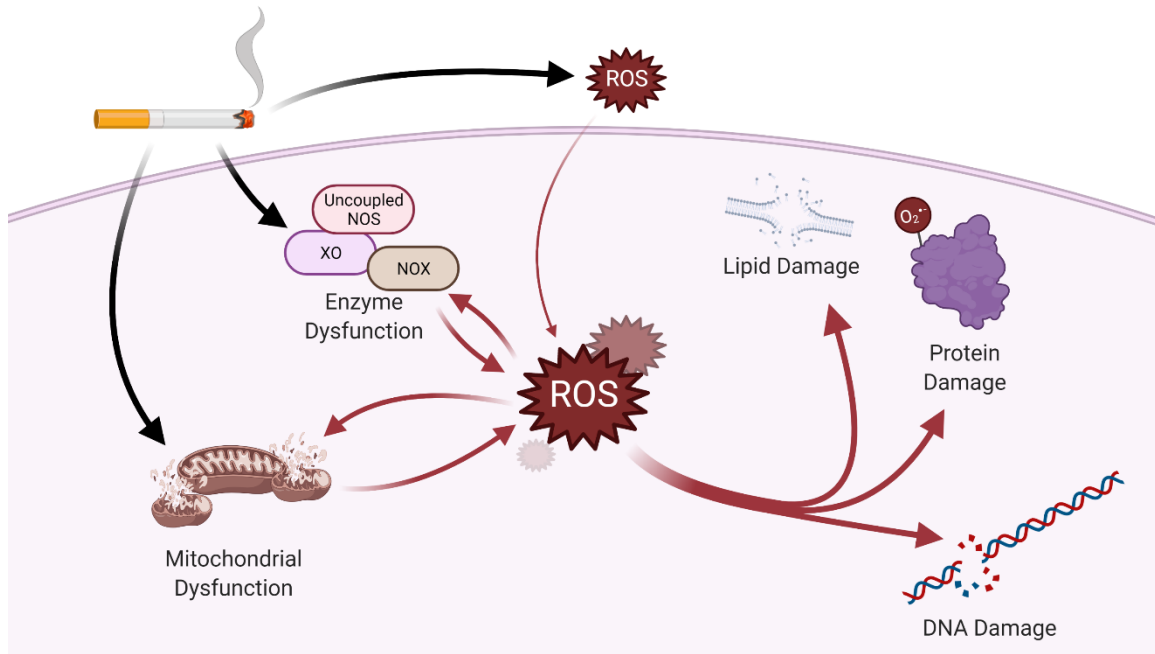


Figure 2-4. The Role of cigarette smoke-induced ROS formation in cells. Smoke-derived ROS may cause mitochondrial or enzyme dysfunction, which can induce further generation of ROS. These ROS can damage critical components of the cell, such as lipids, proteins, and DNA, leaving the cell damaged and dysfunctional ultimately leading to disease and death.

Averill-Bates, 2016) and activation of the antioxidant defense pathways (Ma, 2013), maintenance of a delicate balance of ROS production and clearance is crucial for cell survival. Overproduction and accumulation of ROS are involved in the process of accelerated aging (Davalli et al., 2016) and many chronic conditions (Liu et al., 2018). Indeed, it is the case that ROS production is also highly involved in the development of complications due to chronic cigarette smoking (Kirkham & Barnes, 2013). Moreover, inhaled cigarette smoke is a potent source of ROS (Figure -4), both directly (Huang et al., 2005; Zhao & Hopke, 2012) and indirectly through effects on mitochondrial dysfunction (van der Toorn et al., 2009) and enzymes such as NADPH oxidase (NOX) (Chang et al., 2017), uncoupled NO synthase (NOS) (Abdelghany et al., 2018; Satoh et al., 2005), and xanthine oxidase (XO) (Kim et al., 2013). However, inhaled ROS are unlikely to breach the plasma membrane of alveolar epithelial cells (Brzezinska et al., 2005; Mao & Poznansky, 1992). Therefore, it is more likely that endogenously derived ROS sources produced via pro-oxidant substances found in select water-soluble (Pryor et al., 1998) and lipid-soluble (van der Toorn et al., 2009) components of cigarette smoke or ROS produced as the result of a smoke-induced immune response (Strzelak et al., 2018) are the likely cause of heightened cellular ROS production.

2.2.1. Mitochondria are Major Sources of ROS

Skeletal muscle and vascular mitochondria are dynamic organelles sensitive to environmental factors, such as oxygen availability, toxicants, and ROS (J. N. Meyer et al., 2013). The primary role of mitochondria is the aerobic generation of ATP via mitochondrial oxidative phosphorylation, a highly intricate process involving the oxidation and reduction of several proteins embedded within the inner mitochondrial membrane – collectively known as the electron

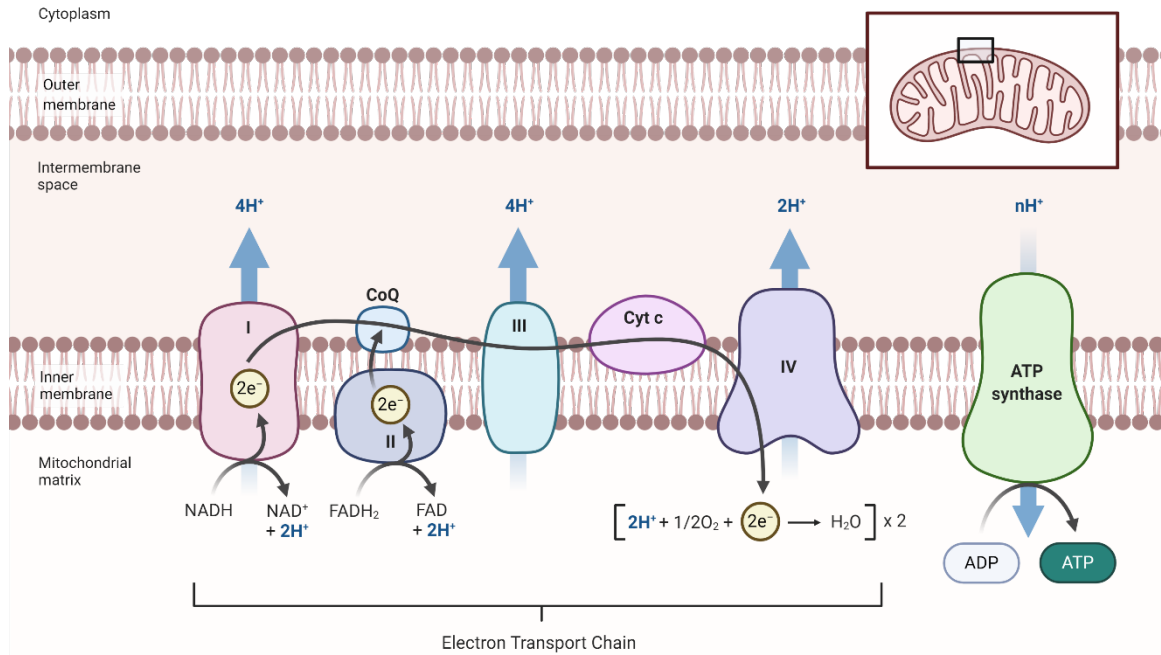


Figure 2-5 A representative schematic of the Electron Transport Chain (ETC). I – Complex I; II – Complex II; III – Complex III; IV – Complex IV; CoQ – Coenzyme Q; Cyt C – Cytochrome C.

transport chain (ETC; Figure 2-5). The first two reactions in this process are the oxidation of NADH to NAD^+ via NADH:ubiquinone Oxidoreductase (Complex I), and the oxidation of FADH_2 into FAD via Succinate Dehydrogenase (Complex II), respectively. The oxidation of NADH and FADH_2 reduces the molecule ubiquinone (Q), which is used as a shuttle to pass through the ETC. In addition to the oxidation of NADH, Complex I also pumps protons into the mitochondrial intermembrane space. The electrons generated from these two initial steps are then transferred via Coenzyme Q (CoQ) to CoQ:cytochrome C – oxidoreductase (Complex III), which transfers these electrons to Cytochrome C (Cyt-C), also pumping protons into the intermembrane space. The terminal reaction of the ETC is the oxidation of Cyt-C via Cytochrome C Oxidase (Complex IV), which consumes the electrons from Cyt-C and oxygen to generate water, pumping protons into the intermembrane space in the process. The accumulation of protons pumped into the intermembrane space via the ETC's reactions generates a chemiosmotic energy gradient, or membrane potential

$(\Delta\Psi_m)$, that drives the energy-yielding reaction that drives the phosphorylation of adenosine diphosphate (ADP) into ATP via ATP synthase (Mitchell, 1961).

Cigarette smoke-derived toxicants are well-known to directly impair the mitochondrial ETC in isolated mitochondria (Figure 2-6). Nicotine and o-cresol have been shown to be inhibitors of complex I and decrease overall mitochondrial respiration in mitochondria isolated from mouse skeletal muscle (Khattri et al., 2022). Both CO (Alonso et al., 2003) and cyanide (Pettersen & Cohen, 1993) inhibit Complex IV through competitive inhibition of the oxygen-binding domain and non-competitive inhibition, respectively. At the same time, lung-secreted ceramides infiltrate peripheral tissues and inhibit mitochondrial respiration via the release of Cyt-C from the inner mitochondrial membrane (Di Paola et al., 2000; Ghafourifar et al., 1999). These alterations to the

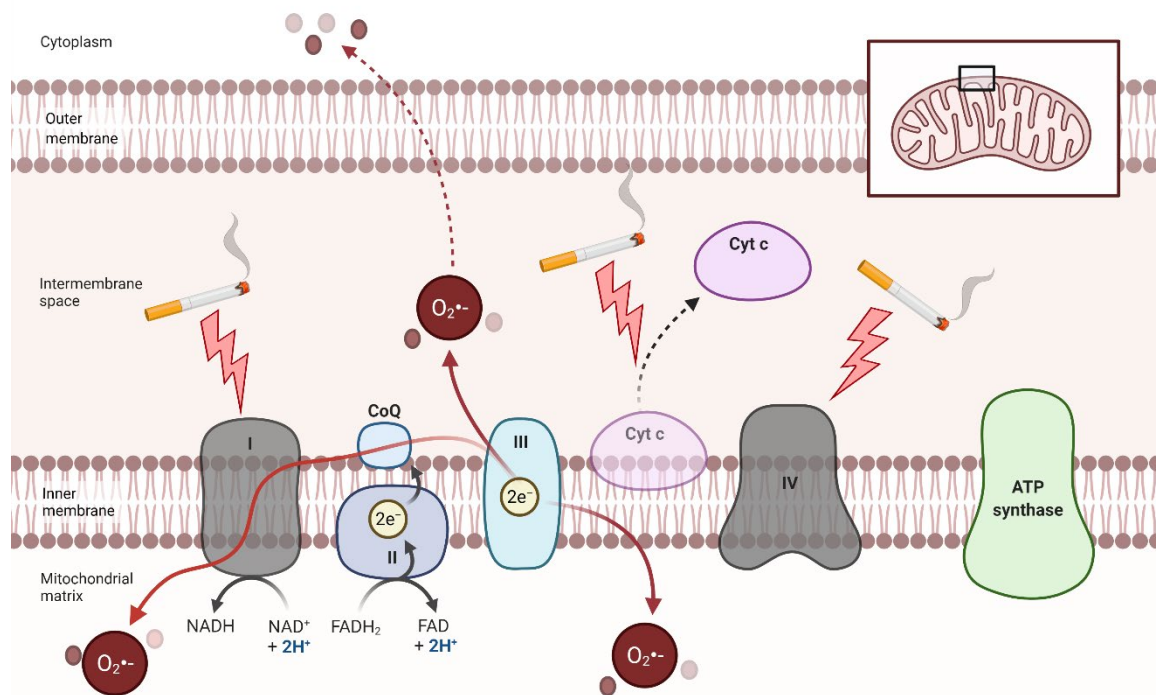


Figure 2-6. A representative schematic of cigarette smoke-induced mitochondrial superoxide (O_2^-) generation.

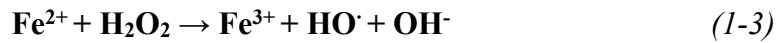
mitochondrial ETC impair the flow of electrons and the subsequent pumping of protons into the intermembrane space, thus lowering the $\Delta\Psi_m$ and decreasing mitochondrial ATP production.

In addition to the decrease in $\Delta\Psi_m$ resulting from the inhibition of Complex IV and release of Cyt-C, electrons passed along the ETC may become “blocked” from passage to the next oxidation-reduction step, resulting in the leak of electrons, primarily at the sites of Complex I and Complex III. The spillage of electrons from Complex I, also known as Reverse Electron Transport (RET), results from the combination of a high $\Delta\Psi_m$ and an over-reduced CoQ pool (Jastroch et al., 2010; Robb et al., 2018). If Complex III or IV are rendered dysfunctional, as can be the case with exposure to CO or cyanide (major components of cigarette smoke), the drive for electrons to travel along the ETC is blunted, rendering electrons unable to be passed from CoQ to Complex III and IV (Scialò et al., 2017). In the presence of adequate FADH₂ donors (such as succinate), this results in transferring electrons back to Complex I, where they can be released into the mitochondrial matrix and produce superoxide (O_2^-), a potent ROS family member. Likewise, inhibition of the reduction of ubiquinone and ubiquinol (QH₂) in Complex III and subsequent transfer of electrons to Cyt-C results in the release of electrons from the Q-cycle into both sides of the inner mitochondrial membrane (Jastroch et al., 2010), resulting in O_2^- formation in the mitochondrial matrix and intermembrane space (Muller et al., 2004), where it can freely diffuse into the cytosol and cause cellular damage.

2.2.2. *ROS Scavenging*

Under normal circumstances, O_2^- is scavenged by a family of superoxide dismutases (SOD), which are composed of 3 isoforms: cytosolic Cu-ZnSOD (SOD1), mitochondrial MnSOD

(SOD2), and extracellular Cu-ZnSOD (SOD3). (Fukai & Ushio-Fukai, 2011) Each of these SOD isoforms catalyzes the reaction that consumes O_2^- to produce hydrogen peroxide (H_2O_2), as shown in Equation 1-1. Because H_2O_2 is still a form of ROS (although more stable and less damaging than O_2^-), it must be further scavenged by catalase (Equation 1-2) or the glutathione pathway; otherwise, it may be converted to the highly reactive hydroxyl radical (HO^\cdot) via the Fenton or Haber-Weiss reaction (Equations 1-3 & 1-4, respectively).



However, individuals chronically exposed to cigarette smoke have a lower antioxidant capacity than nonsmokers, as reflected by decreased catalase and SOD activities, lower glutathione, and increased blood biomarkers oxidative stress, such as malondialdehyde and oxidized low-density lipoproteins (Barreiro et al., 2010; Bloomer, 2007; Neves et al., 2016). Thus, not only does cigarette smoke induce the creation of endogenous ROS, but the ability of the cell to defend itself against these ROS is also impaired. The resulting state of uncontrolled oxidative stress wreaks havoc across cells in many tissues, leading to DNA, protein and lipid damage, cell dysfunction, and premature aging (Liochev, 2013). These findings collectively point to a critical role for oxidative stress in the development of vascular and muscular impairments in individuals exposed to cigarette smoke.

2.2.3. Other Endogenous Sources of ROS

While mitochondria are the most significant ROS producers, several other enzymes produce endogenous ROS, especially in the vasculature. Indeed, reports have demonstrated that the NOX family of enzymes present in vascular tissue, which are dormant under normal conditions (Griendling et al., 2000), are significantly induced by cigarette smoke exposure (Jaimes et al., 2004). The increase in NOX activity increases the rate of O_2^- production through a reaction that consumes NADPH and O₂ and produces O₂⁻, NADP⁺, and H⁺ (equation 1-5).



The O₂⁻ generation in cigarette smoke-exposed vascular endothelium was significantly lessened in the presence of a NOX inhibitor, diphenyleneiodonium, signifying a critical role of NOX-derived O₂⁻ production in the presence of cigarette smoke. Furthermore, treatment of mice with the NOX inhibitor apocynin attenuated skeletal muscle atrophy in mice (Bernardo et al., 2018), therefore, implying NOX is a common source of ROS-induced peripheral dysfunction across various tissues. Another enzyme, XO, which is involved in the catabolism of purines to create uric acid, is also involved in endothelium-derived ROS production. Like NOX, inhibition of XO may reverse endothelial dysfunction in heavy smokers (Guthikonda et al., 2003), though *in vitro* support for this is lacking (Jaimes et al., 2004). One other ROS source that is central to cigarette smoke-induced vascular impairments is uncoupled endothelial NOS (eNOS). Typically, eNOS (like other NOS isoforms) consumes L-arginine, NADPH, and oxygen to produce NO, L-citrulline, NADP⁺, and water. However, under conditions of oxidative stress or lack of tetrahydrobiopterin (BH₄) – an essential cofactor for eNOS – eNOS becomes uncoupled and cannot produce NO, instead generating O₂⁻ and NADP⁺ (Roe & Ren, 2012). The O₂⁻ generated from this process can

then react with nearby NO, oxidizing it to produce peroxynitrite (ONOO^-) (Peluffo et al., 2009), diminishing NO bioavailability and further impairing vascular function (Figure 2-7). Furthermore, these cellular ROS can oxidize BH₄ to BH₂, thereby decreasing the bioavailability of BH₄ and increasing the generation of ROS. Indeed, cigarette smoke induces eNOS uncoupling and ROS generation by decreasing the availability of BH₄ (Abdelghany et al., 2018). As a result, supplementation with BH₄ has been shown to improve vascular function in smokers (Heitzer et al., 2000; Ueda et al., 2000) and patients with COPD (Rodriguez-Miguel et al., 2018), presumably by mitigating endothelial ROS production and increasing NO bioavailability (Heitzer et al., 2000), thus pointing toward cigarette smoke-induced BH₄ depletion as a significant cause of endogenous ROS production.

2.3. Cigarette Smoke Disrupts Mitochondrial Bioenergetics

While mitochondrial ROS formation is indeed an important aspect of cigarette smoke-induced cellular dysfunction, the mitochondria are also impaired by other avenues as a direct result of the constituents of cigarette smoke, such as direct inhibition of Complex I and II as well as increased proton leak through ANT, all of which can alter $\Delta\Psi_{\text{mt}}$ and result in decreased ATP production.

2.3.1. Cigarette Smoke Constituents Inhibit the Mitochondrial Electron Transport Chain

Several studies have provided evidence for a direct inhibition of Complexes I and II of the ETC via cigarette smoke constituents. In isolated liver mitochondria, complex I activity declines by up to 25% with only 0.05% CSE, and may decline by ~80% in concentrations up to 10% CSE

(van der Toorn et al., 2007). Although slightly likely less sensitive than complex I, complex II activity is similarly diminished by 25% with 1% of CSE, and may be inhibited up to 70% with 30% CSE. The loss of function of these two complexes contributed to the significant loss of $\Delta\Psi_{\text{mt}}$ and concurrent decrease in ATP production. Therefore, it is likely that these two complexes are critical sites involved in the bioenergetic deficits induced by CSE.

Indeed, more recent studies have highlighted the inhibitory effects of CSE constituents – especially nicotine and o-cresol – on complex I activity. In a series of experiments, Khattri et al. (2022) elegantly showed that incubation of isolated mitochondria in CSE for 10 minutes impairs pyruvate-and-malate-driven state III respiration, but not succinate-driven respiration, indicating a direct impairment of complex I due to CSE. Follow-up experiments determined that out of 29 chemicals with concentrations $\geq 0.02\text{mM}$ found in CSE (as determined by proton NMR spectroscopy), only three individual chemicals – nicotine, o-cresol, and decanoic acid – inhibited complex I-driven respiration significantly. However, of those three, only nicotine and o-cresol inhibited complex I- and II-driven respiration, indicating that nicotine and o-cresol are critical components of the CSE-induced inhibition of mitochondrial respiration in isolated mitochondria.

2.3.2. Cigarette Smoke Increases Proton Leak Through ANT

In addition to the loss of complex I activity via components of CSE, recent reports have shown that CSE also increases the permeability of the mitochondria via activation of ANT (Wu et al., 2020). ANT is a crucial gatekeeper that facilitates the exchange of nucleotides (i.e., ADP and ATP) (The ADP and ATP Transport in Mitochondria and Its Carrier, 2008). However, ANT also serves as an important site of proton leak and mitochondrial uncoupling (Bertholet et al., 2019b),

regulating mitochondrial apoptosis (Zhivotovsky et al., 2009). Therefore, increases in ANT activity, and thereby lower $\Delta\Psi_{\text{mt}}$ could be another pathway by which CSE induces bioenergetic deficits.

However, there are several limitations to these studies. First, isolation of mitochondria – as performed in both studies – can bias the yield of the mitochondria, thereby exaggerating mitochondrial dysfunction that may not represent the *in vivo* conditions (Picard et al., 2010). Second, recent insights into the mitochondrial network indicate that mitochondrial networks, especially those found in skeletal muscle, are highly adaptive to disruptions in the electron transport chain due to the distributive nature of the mitochondrial reticulum (Glancy & Balaban, 2021). Recent evidence has shown that this highly integrated network of mitochondria may be able to compensate for the localized disruption of the mitochondrial network by maintaining the proton motive force across the entire mitochondrial reticulum via undisturbed components of the ETC that are located elsewhere within the reticulum (Glancy et al., 2015, 2017). Therefore, isolation procedures may disrupt the morphology of the mitochondrial reticulum and may be misrepresentative of mitochondrial function within an intact muscle fiber. Lastly, the investigation into the CSE-induced mitochondrial deficits is limited in skeletal muscle and requires more research to uncover the role of other factors, such as skeletal muscle fiber type (i.e., glycolytic vs. oxidative fibers), as mitochondrial dysfunction specific to the oxidative capacity of muscle may be contributory to the fiber type-specific atrophy associated with cigarette smoke, as is the case in inactivity- (Hyatt et al., 2019) and age-induced (Shally & McDonagh, 2020) muscle atrophy.

2.4. Tissue-Specific Susceptibility to Cigarette Smoke

Although cigarette smoke-induced ROS production appears to impact ROS production and $\Delta\Psi_{mt}$ ubiquitously in smoke-exposed rodents and humans, there is accumulating evidence that there are different tissue-specific inhibitory kinetics of cigarette smoke-induced mitochondrial dysfunction.

2.4.1. Tissue-Specific Variation of Cigarette Smoke-Induced ROS Production

Mice exposed to cigarette smoke for 6 months show much greater ROS production – as indicated by levels of reactive carbonyl groups, 4-HNE, and MDA – in the gastrocnemius muscle than the diaphragm muscles, indicating that the diaphragm muscles may be more susceptible to cigarette smoke-induced ROS production than ambulatory skeletal muscles (Barreiro et al., 2012). Similarly, Raza et al. (2013) showed that mice exposed to 4 consecutive days of nose-only cigarette

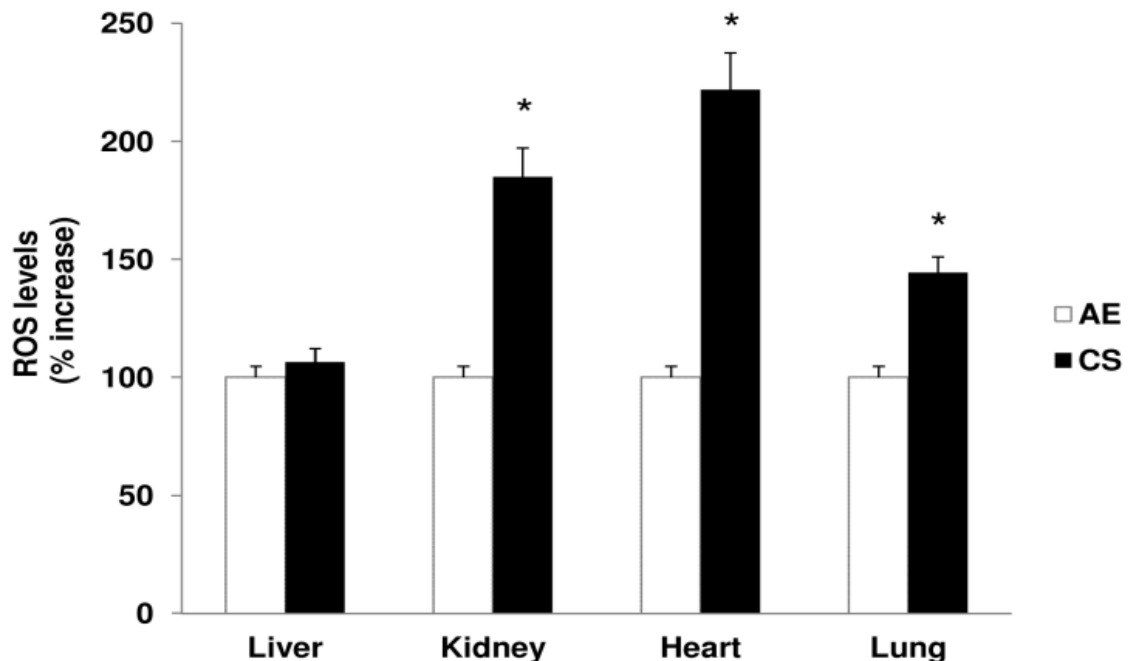


Figure 2-7. Tissue-specific changes in ROS levels induced by 4 days of nose-only cigarette smoke exposure. Reprinted from Raza et al., 2013.

smoke exposure exhibit a two-fold increase in ROS production in the heart and kidney, but only a 50% increase in ROS levels in the lungs and no increase in ROS levels in the liver of these same mice (Figure 2-7), further supporting a tissue-specific susceptibility to cigarette smoke-induced cellular dysfunction. Interestingly, the mice in this study also showed varying alterations to the content of mitochondrial Complex I and the activity of Complex IV. Considering the critical role in Complexes I and IV in the production of mitochondrial-derived ROS (as discussed in previous sections) and the generation of a proton gradient to drive ATP production, it is possible that these tissue-specific alterations in ROS generation and ETC activities may reflect a mitochondrial-specific susceptibility to cigarette smoke-induced mitochondrial dysfunction for each tissue. However, the studies by Raza et al. did not report any measures of mitochondrial membrane potential.

2.4.2. Tissue-Specific Variation of Cigarette Smoke-Induced Membrane Potential

Despite the shortcomings in the studies by Raza et al. (2013), several other studies have shown tissue-specific susceptibility to cigarette smoke-induced bioenergetic deficits. In humans with COPD, isolated lung mitochondria have greater losses of $\Delta\Psi_{\text{mt}}$ compared to mitochondria isolated from the quadriceps muscles, despite similar increases in both mitochondrial and cellular ROS (Haji et al., 2020). Furthermore, tissue samples from the lungs, but not the quadriceps, showed a significant decrease in mitochondrial complexes I, II, III, and ATP synthase protein expression, indicating that the lungs of smokers, at least in the long run, are more susceptible to cigarette smoke-induced bioenergetic deficits than is ambulatory skeletal muscle. These findings are supported by other experiments, such as the ones conducted by van der Toorn et al. (2007). In

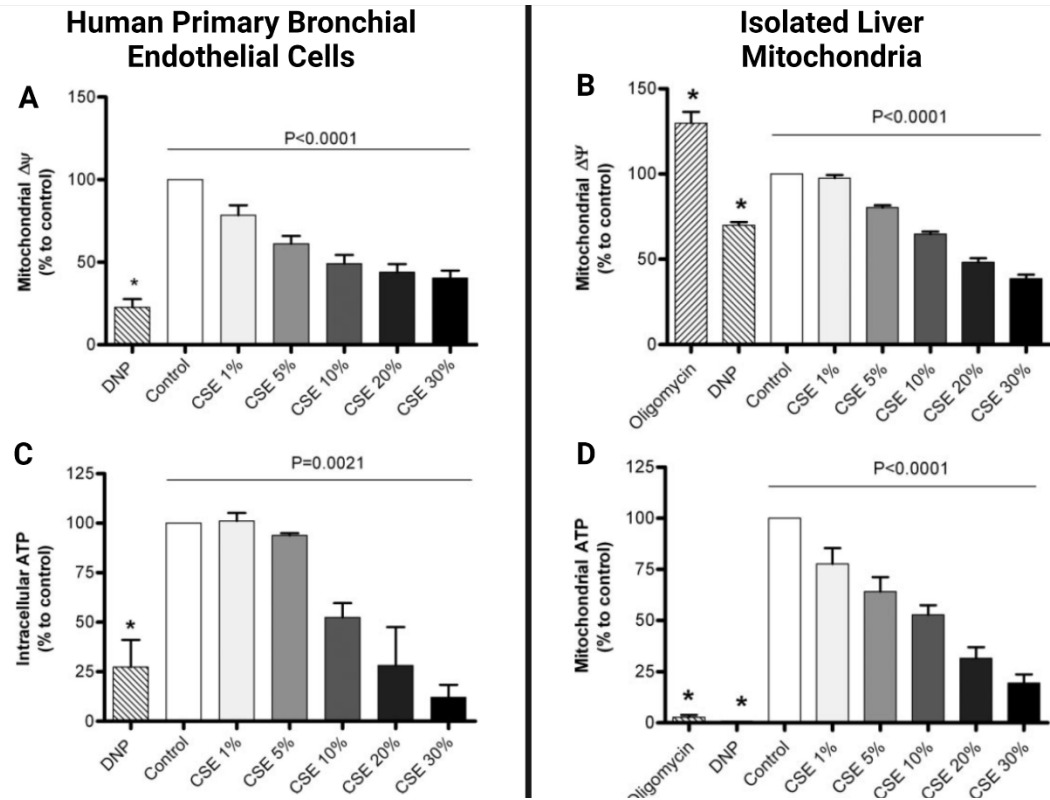


Figure 2-8. Cigarette smoke-induced changes to $\Delta\Psi_{mt}$ in human primary bronchial endothelial cells (A) and isolated liver mitochondria (B), as well as changes to ATP in human primary bronchial endothelial cells (C) and isolated liver mitochondria (D). Adapted from van der Toorn (2007).

these series of experiments, it was shown that mitochondria from human primary bronchial epithelial cells (Figure 2-8A) are more susceptible to loss of $\Delta\Psi_{mt}$ induced by cigarette smoke than are mitochondria isolated from the liver (Figure 2-8B). However, ATP production appeared to be impacted to a lesser extent in the bronchial endothelial cells (Figure 2-8C) than in the liver (Figure 2-8D). Furthermore, the changes to $\Delta\Psi_{mt}$ in isolated liver mitochondria appeared to reflect decreased rates in mitochondrial oxygen consumption. Still, the respiration rates of the bronchial endothelial cells were not reported in this study.

In a series of studies, Naserzadeh et al. (2013 & 2015) examined the time- and dose-dependent $\Delta\Psi_{mt}$ collapse induced by cigarette smoke extract in mitochondria isolated from the mouse eye, fetus, kidney, liver, and skin (Figure 2-9). Collectively, these results reveal a wide

range of dose- and time-dependent bioenergetic deficits induced by cigarette smoke extract, which can cause a $\Delta\Psi_{mt}$ collapse upwards of 300% in some tissues, such as the fetus and kidney, but may only cause 50% collapse in other tissues, such as the skin, after 45 minutes of 100% cigarette smoke exposure.

While the collective contributions of these studies make a compelling case for a role of tissue specificity in the development of cigarette smoke-induced bioenergetic deficits in muscle and the vasculature, no studies have directly examined the susceptibility of cardiac and skeletal muscle, or the aorta to cigarette smoke-induced bioenergetic changes. Furthermore, the inhibitory kinetics of cigarette smoke on mitochondrial respiration have not been determined. Establishing the susceptibility to cigarette smoke in cardiac muscle, oxidative skeletal muscle, glycolytic skeletal muscle, and vascular tissues has several important implications in understanding how cigarette smoke impacts the mitochondria of extrapulmonary tissues. First, because the mitochondria in these tissues play critical roles in cellular energy metabolism and the regulation of various critical biological functions (locomotion, oxygen delivery, etc.), it is essential to determine the direct extent to which cigarette smoke can inhibit mitochondrial bioenergetics in these tissues and cause peripheral dysfunctions. Second, this information can be used to establish

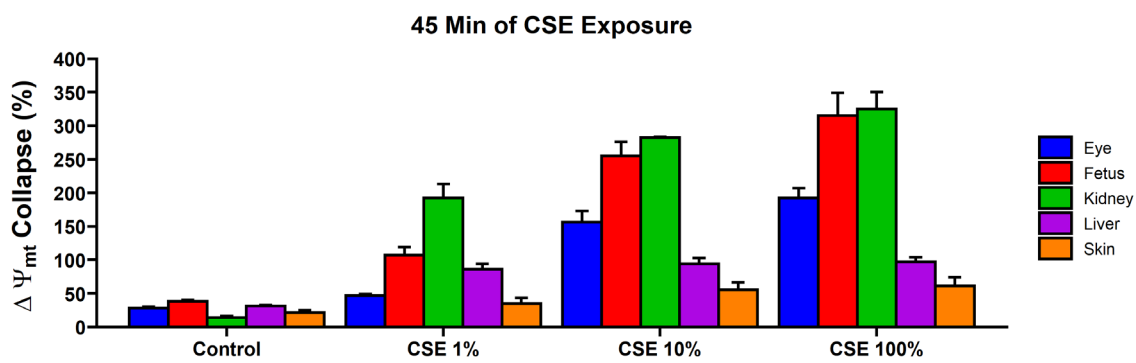


Figure 2-9. Percentage of $\Delta\Psi_{mt}$ collapse induced by cigarette smoke extract in mitochondria isolated from the mouse eye, fetus, kidney, liver, and skin. Adapted from Naserzadeh et al. (2013 & 2015)

the toxicological properties of cigarette smoke on the mitochondria of these tissues, which will help construct future research protocols to explore the impacts of cigarette smoke on these, and other tissues.

2.5. Cigarette Smoke-Induced Shifts in Mitochondrial Substrate Utilization

2.5.1. Whole-body Observations of Shifts in Substrate Utilization

Several observations of whole-body shifts in substrate oxidation have been documented in smokers and patients with COPD. Early studies using indirect calorimetry, such as those by Jensen et al. (Jensen et al., 1995), documented an increase in whole-body fatty acid oxidation proportional to the amount of urinary cotinine, a metabolite of nicotine. These findings imply that nicotine consumption is directly linked to greater oxidation of fatty acids and may partially explain the weight gain often observed during smoking cessation. These findings were later expanded upon in studies by Bergman et al. (2009), which showed that an acute session of smoking causes an increase in the incorporation and oxidation of ^{13}C -labeled palmitate into skeletal muscle (Figure 2-10). The greater incorporation and oxidation of fatty acids was also linked to a decrease in insulin

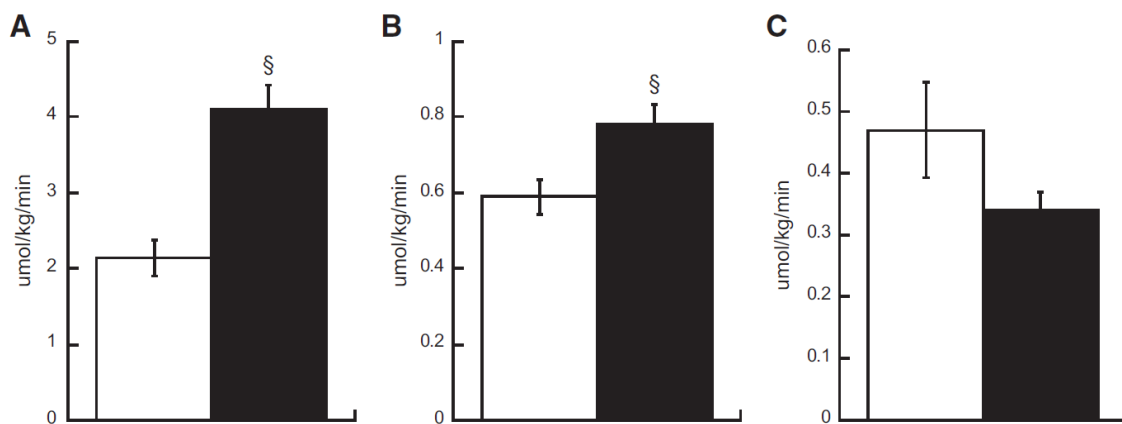


Figure 2-10. Whole-body palmitate rate of appearance (A), oxidation (B), and incorporation (C) into IMTG in nonsmokers (white) and smokers (black). Reprinted from Bergman et al. (2012).

sensitivity due to IRS-1 Ser⁶³⁶ phosphorylation, thus inhibiting the skeletal muscle insulin signaling cascade and inducing insulin resistance. The smoke-induced changes in insulin sensitivity and fatty acid oxidation were found to be only partially transient, as smoking cessation was not able to completely restore insulin sensitivity and fatty acid oxidation, indicating some residual impacts of smoking on these parameters (Bergman et al., 2012).

However, other findings have shown greater serum triglycerides and fatty acids in smokers (Hellerstein et al., 1994; Muscat et al., 1991a; Neese et al., 1994). Experiments by Muscat et al. (1991) found a dose-response relationship between cigarette consumption and serum cholesterol. Later studies by Hellerstein et al. (1994) expanded upon these findings while also documenting increased fatty acid and glycerol fluxes in addition to increased lipolysis. However, despite the increase in fatty acid availability, smoking was not associated with increased whole-body fatty acid oxidation, indicating greater fatty acid storage rather than oxidation, which was not reversed following one week of smoking cessation (Neese et al., 1994). Finally, more recent findings using data from the Coronary Artery Risk Development in Young Adults (CARDIA) Study, a cross-sectional, multi-center study of 3,000 subjects, showed that smoking was associated with an increase in intramuscular adipose tissue (IMAT) and IMAT to lean tissue ratio, as measured by computed tomography. Together, these findings show inhibition of fatty acid oxidation in skeletal muscle. Therefore, there is a conundrum in the whole-body literature related to the smoke-related changes to mitochondrial oxidation of fatty acids in skeletal muscle that must be resolved by directly measuring mitochondrial fatty acid oxidation.

2.5.2. In vitro Evidence of Altered Mitochondrial Substrate Preference

While the literature of smoke-induced changes in substrate oxidation is clearly at odds, no studies have directly investigated changes in mitochondrial substrate utilization with cigarette smoke exposure. In a study using C2C12 myotubes conditioned in media from smoke-exposed lung cells and smoke-exposed mice, Thatcher et al. (2014) documented impaired mitochondrial respiratory capacity using TCA cycle substrates (glutamate, malate, and succinate), impaired glucose tolerance, and ceramide accumulation. Ceramides, part of the sphingolipid family, are a species of lipids that accumulate due to an imbalance between fatty acid supply and oxidation (Watt et al., 2012). Thus, as the supply and storage of fatty acids accumulate in cells, whether due to decreased oxidation of fatty acids or other causes, so do ceramides. Furthermore, these authors demonstrated that injection with myriocin, an inhibitor of ceramide formation, increased mitochondrial respiration in both the control and cigarette smoke-exposed groups and concluded that ceramide formation is a direct cause of cigarette smoke-induced mitochondrial dysfunction. However, the authors did not measure mitochondrial fatty acid oxidation. Consequently, it is unclear whether the accumulation of ceramides in these experiments *caused* mitochondrial dysfunction or if the accumulation of ceramides occurred *secondary* to a shift in mitochondrial substrate utilization caused by cigarette smoke exposure.

2.6. Purpose

Therefore, considering the critical role that the mitochondria play in cellular energy metabolism and redox homeostasis and the negative consequences that cigarette smoke may inflict upon the mitochondria, it is imperative that we better understand the causal mechanisms

underlying cigarette smoke-induced mitochondrial dysfunction in order to identify possible therapeutic targets. Specifically, it is critical to understand the functional alterations that cigarette smoke can cause on mitochondria in skeletal and cardiac muscle and vascular tissues, as these are the primary tissues involved in developing cardiometabolic diseases, which amount to the most significant cause of smoking-related deaths. However, there are currently several gaps in the literature that require reconciliation.

First, while it is apparent that tissue susceptibility to cigarette smoke-mitochondrial dysfunction is variable across organs, the sensitivities of skeletal and cardiac muscles and vascular tissues have not been characterized in the literature. Therefore, it is unknown if the mitochondria in the arteries, cardiac muscle, or type I and type II skeletal muscle fibers have different sensitivities to cigarette smoke, an essential piece of information in identifying which tissues are most susceptible to cigarette smoke-induced damage and more likely to be the targets of therapies.

Second, cigarette smoke alters the metabolism of many energy-generating substrates, especially fatty acids. While many whole-body studies have shown an increase in fatty acid oxidation caused by cigarette smoking, other studies using a reductionist approach showed a decrease in fatty acid uptake and utilization. However, the findings from these studies, while clearly at odds with each other, did not directly address the capacity of the mitochondria to oxidize fatty acids. Therefore, it is still unknown if the alterations to fatty acid metabolism occur at the mitochondrial level or at some other point along the process of fatty acid metabolism.

Lastly, cigarette smoke exposure has been shown to damage isolated mitochondria at several sites along the respiratory chain, most notably complex I and III, and decrease mitochondrial membrane potential, thus resulting in impaired oxidative ATP production.

However, the process of isolating mitochondria may damage the mitochondria compared to the permeabilized fiber technique, which could alter the interpretation of these studies. Research has yet to explore the contribution of phosphate transport, ADP sensitivity, and respiratory chain activities to mitochondrial function in permeabilized fibers exposed to cigarette smoke. These findings are critical to identifying the molecular targets of cigarette smoke within the mitochondria.

2.6.1. Purpose Statement

Considering the existing gaps in the literature, the overarching goal of this project is to advance the understanding of the underlying causes of cigarette smoke-induced mitochondrial dysfunction – specifically targeting tissue-specific susceptibility to cigarette smoke toxicity, alterations to mitochondrial substrate oxidation, and identifying key mitochondrial targets of cigarette smoke-induced dysfunction using an *in situ* mouse model.

2.7. Aims

2.7.2. Aim 1 – Acute Effects of Cigarette Smoke Condensate on Mitochondrial Respiration

In specific aim 1, we will determine the extent of tissue-specific susceptibility to cigarette smoke for the aorta, cardiac muscle, and type I and type II skeletal muscles. Our working hypothesis is that each tissue will display different susceptibility to cigarette smoke, with the cardiac muscle and aorta being more susceptible to cigarette smoke based on epidemiological evidence suggesting the greater relative risks for tobacco-related diseases in these tissues relative to others (Gandini et al., 2008).

2.7.3. Aim 2 – Effects of Cigarette Smoke Exposure on Mitochondrial Substrate Utilization

In specific aim 2, we will determine the cigarette smoke-induced alterations to the mitochondrial oxidation of palmitoylcarnitine, a long-chain fatty acid, and pyruvate, a product of glycolysis in the skeletal muscle (glycolytic gastrocnemius fibers and oxidative soleus fibers). Our working hypothesis is that cigarette smoke will decrease the sensitivity and maximal capacity to oxidize palmitoylcarnitine oxidation relative to pyruvate.

2.7.3. Aim 3 – Mechanisms of Cigarette Smoke-Induced Mitochondrial Dysfunction

In specific aim 3, we will determine the extent of cigarette smoke-induced perturbations to the exchange of phosphates, ADP sensitivity, and mitochondrial respiratory chain activity. Based upon prior studies in epithelial cells (Wu et al., 2020), our working hypothesis is that cigarette smoke will primarily affect phosphate exchange by decreasing ANT activity, which in turn will decrease ADP sensitivity, and ultimately result in lower maximal mitochondrial respiration in permeabilized fibers from both glycolytic gastrocnemius muscle and oxidative soleus muscle.

CHAPTER 3

METHODS

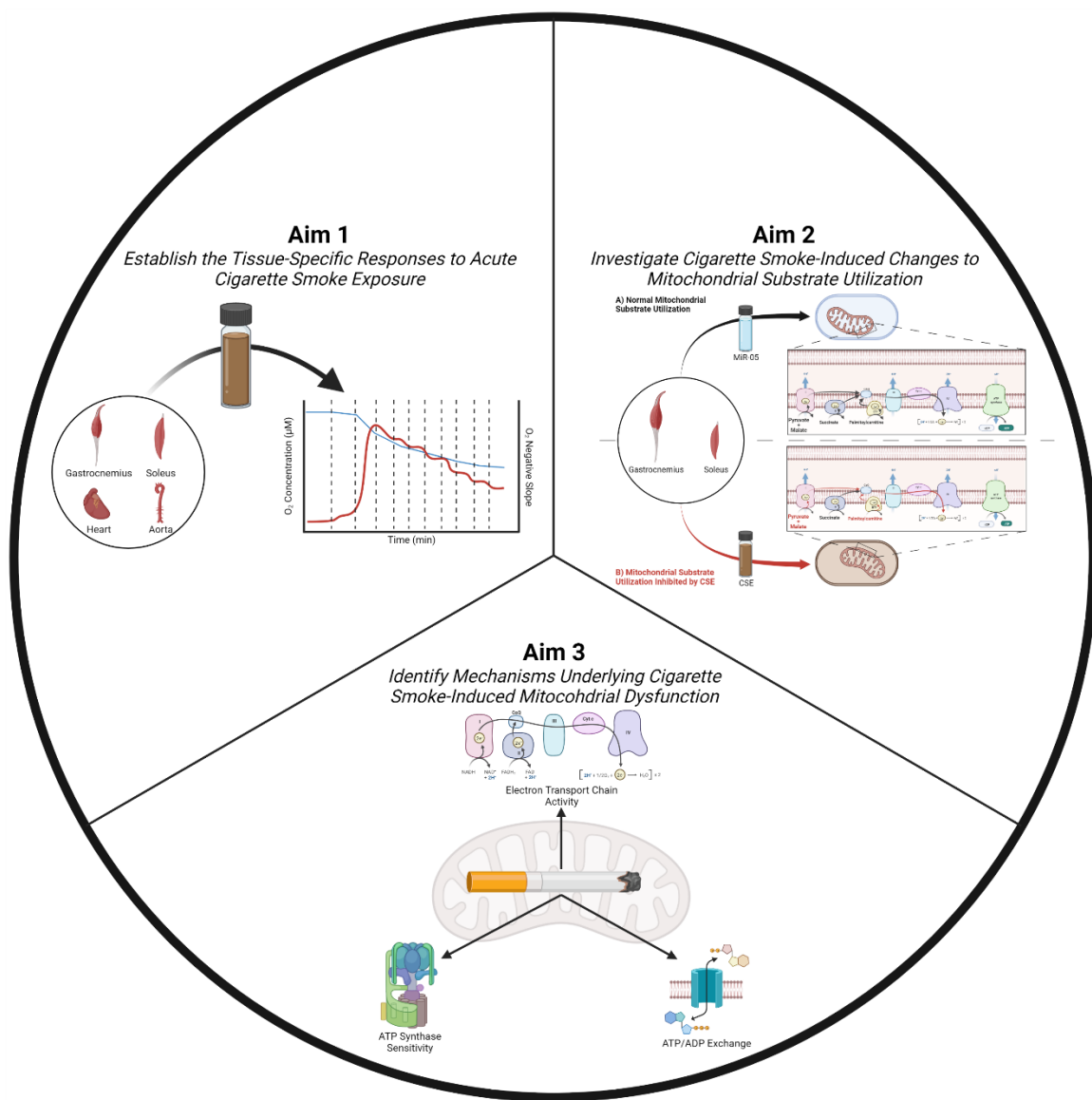


Figure 3-1. Overview of the 3 aims proposed for this project.

3.1. Animal Care and Ethics Approval

3.1.1. Animal Selection and Care

All animal use and husbandry will follow protocols that will be approved by the University of Massachusetts Institutional Animal Care and Use Committee (IACUC). C57BL/6 mice will be obtained from Charles River Laboratories. Mice will be housed in cages containing groups of no more than 5 mice per cage, with *ad libidum* access to water and standard chow. All mice will be exposed to 12-hour light:dark cycles and will not have access to running wheels.

3.1.2. Euthanasia

At 3-6 months of age (i.e., adult maturity), mice will be transported to an isoflurane anesthesia unit approved by the University of Massachusetts IACUC. The mice will be euthanized by an overdose of 5% isoflurane, followed by cervical dislocation as a secondary method of euthanasia.

3.1.3. Tissue Harvesting

Following the euthanasia protocols, the left venticule, the gastrocnemius and soleus hindlimb muscles and the aorta will be harvested, as shown in Figure 3-2. The isolated muscles and aorta will be immediately transferred to a solution of ice-cold BIOPS for preservation.

3.2. Chemical and Tissue Preparations

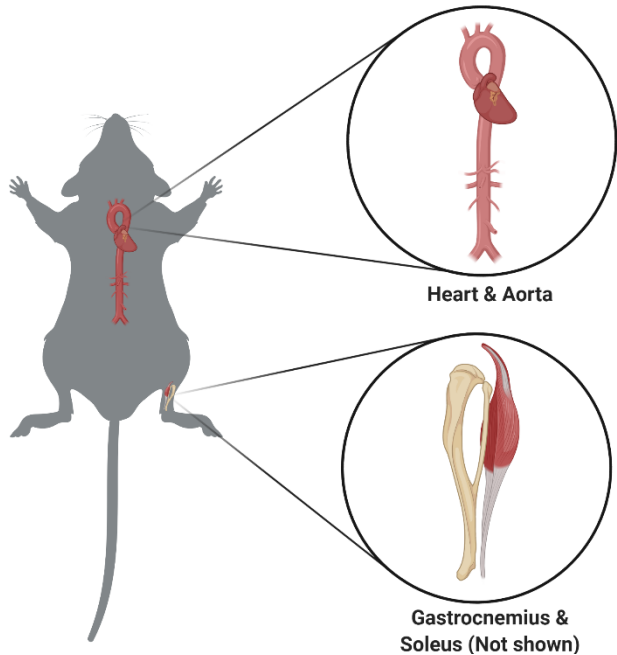


Figure 3-2. Cartoon image of tissues used in this study.

3.2.1. Tissue Preservation Solution (BIOPS)

The preservation of tissue samples in a suitable medium is a critical step in maintaining mitochondrial quality post-extraction. Thus, the choice of a tissue preservation solution is a critical component of ensuring adequate quality control of *in situ* mitochondrial respiration. It is important to note that several preservation solutions have been utilized by several research groups in the literature (Boushel et al., 2007; Fontana-Ayoub et al., 2014; Gnaiger et al., 2000; Kuznetsov et al., 2008b; Perry et al., 2011; Yamashita & Kanki, 2018), all with slight modifications (Table 3-1). BIOPS is a preservation solution commonly used (Boushel et al., 2007; Gifford et al., 2016, 2018b; Gnaiger et al., 2000; Layec, Bringard, et al., 2011) and the recommended solution according to the manufacturer of our high-resolution respirometer, Oroboros Instruments (Innsbruck, AT) (Fontana-Ayoub et al., 2014; Yamashita & Kanki, 2018). A similar buffer, Buffer X, is also a

common preservation solution that contains slightly less phosphocreatine and ATP. On the other hand, Medium A contains K₂HPO₄ (a buffering agent) and leupeptin (a protease inhibitor), and lacks dithiothreitol, a mild antioxidant. Although similar mitochondrial respiration rates have been reported regardless of the preservation solution used indicating mitochondria are preserved in all of the listed solutions, no studies have directly compared each of the preservation solutions on their abilities to maintain mitochondrial respiration after prolonged periods of time. Therefore, based on previous reports published by our group, BIOPS will be the preservation solution used for all experiments (Decker, Kwon, Zhao, Hoidal, Huecksteadt, et al., 2021; Gifford et al., 2016; Layec et al., 2018).

It is also important to acknowledge the role which time plays in the preservation of mitochondrial preparations. Unlike other tissues and homogenized samples (Acin-Perez et al., 2020), mitochondrial quality of permeabilized whole tissue (as will be used in this study) is well-documented to decline within several hours (Gnaiger et al., 2000; Kuznetsov et al., 2003; S. Larsen, Wright-Paradis, et al., 2012), and mitochondrial quality may only be conserved in a preservation solution for up to 20 hours post-harvest (Skladal et al., 1994). Furthermore, while several attempts have been made to establish cryopreservation protocols for the long-term storage of permeabilized skeletal muscle samples (Kuznetsov et al., 2003; A. Meyer et al., 2014), current cryopreservation methods do not prevent the progressive, time-dependent loss of mitochondrial respiratory function. Therefore, to minimize the time-dependent loss of mitochondrial function, all samples will be prepared immediately following harvest, and mitochondrial respiration experiments will be performed on the day of harvest.

Table 3-1. Comparison of three commonly used different tissue preservation solutions.

		BIOPS (Fontana-Ayoub et al., 2014; Gnaiger et al., 2000; Yamashita & Kanki, 2018)	Buffer X (Perry et al., 2011)	Medium A (Kuznetsov et al., 2008b)
Final pH		7.1	7.1	7.1
CaK₂EGTA	Creates free concentration of Ca ²⁺ in physiological range; chelates toxic metals	2.77 mM	2.77 mM	2.77 mM
K₂EGTA	Creates free concentration of Ca ²⁺ in physiological range; chelates toxic metals	7.23 mM	7.23 mM	7.23 mM
ATP	Energy carrier	5.77 mM	5.7 mM	5.7 mM
MgCl₂	Maintains free Mg ²⁺	6.56 mM	6.56 mM	9.5 mM
Taurine	Membrane stabilizer; antioxidant	20 mM	20 mM	20 mM
Phosphocreatine	Energy carrier	15 mM	14.3 mM	15 mM
Imidazole	Antioxidant; chelates toxic metals	20 mM	20 mM	20 mM
Dithiothreitol	Antioxidant	0.5 mM	0.5 mM	—
K⁺-MES	Buffering agent	50 mM	50 mM	49 mM
Leupeptin	Ca-activated protease inhibitor	—	—	1 μM
K₂HPO₄	Maintains levels of inorganic phosphate	—	—	3 mM

3.2.2. Mitochondrial Respiration Medium (MiR-05)

In addition to a tissue preservation solution, high-resolution respirometry experiments require a respiration medium to maintain a stable concentration of dissolved oxygen and not disrupt the mitochondrial environment. Several different mitochondrial respiration media have been used in high-resolution respirometry experiments (Table 3-2). However, these solutions' composition varies considerably more than the preservation solutions, which may influence the sample quality during experimental conditions (Komlódi et al., 2018; Wollenman et al., 2017; Yamashita & Kanki, 2018). K-lactobionate and sucrose-based solutions, namely MiR05, are recommended by Oroboros Instruments (Fontana-Ayoub et al., 2014). However, other solutions such as Buffer Z (Perry et al., 2011) (a K-MES and KCl-based solution), Medium B (Kuznetsov et al., 2008b) (a K-lactobionate-based solution), and other ionic-based solutions (Bose et al., 2003; Glancy et al., 2013; Vinnakota et al., 2011) are commonly used throughout the literature. Two independent studies have thus far compared the different mitochondrial respiration media to determine respiration solution's influence on mitochondrial oxygen consumption (Komlódi et al., 2018; Wollenman et al., 2017); however, it is essential to note that these experiments were conducted using isolated mitochondria, which may respond differently to the respiration media than permeabilized fibers due to environmental factors (Kuznetsov et al., 2008b).

In a series of experiments, (Wollenman et al., 2017) examined the impacts of different respiration solutions and substances on isolated guinea pig cardiac mitochondria. The data from these experiments showed that sucrose-based solutions or solutions low in chloride consistently yield greater mitochondrial respiration rates than traditional ionic-based solutions (Bose et al., 2003; Glancy et al., 2013; Vinnakota et al., 2011), indicating a role for chloride in the inhibition

of the adenine nucleotide translocator, the dicarboxylate carrier, and the alpha-ketoglutarate exchanger. Other experiments by (Komlódi et al., 2018) compared MiR05, Buffer Z, a solution containing a mix of MiR05 and Buffer Z, and MiRK03 (a KCl-based solution similar to other ionic-based solutions). In agreement with Wollenman et al., this study also concluded that ionic-based solutions with greater chloride concentrations (MiRK03) consistently yield lower mitochondrial respiration rates compared to solutions containing lower chloride (MiR05 and Buffer Z). MiR05 and Buffer Z displayed similar respiration rates and H₂O₂ production rates (measured via fluorescence); however, fluorescence sensitivity and stability differed between MiR05 and Buffer Z, therefore indicating that there may be a need for careful consideration of respiration media when performing H₂O₂ production experiments using fluorescence. Therefore, considering the findings of these two studies, MiR05 will be used as the respiration media for all experiments involving high-resolution respirometry.

Table 3-2. Comparisons of commonly-used mitochondrial respiration media for *in situ* mitochondrial respiration experiments.

	Purpose	MiR-05	Buffer Z	Medium B	Ionic-based Buffer
Final pH		7.1	7.4	7.1	7.0
EGTA	Chelates toxic metals	0.5 mM	1 mM	0.5 mM	1 mM
MgCl₂	Maintains free Mg ²⁺	3 mM	5 mM	3 mM	10 mM
Lactobionic Acid	Prevents mitochondrial swelling; chelates Ca ²⁺	60 mM	—	60 mM	—
Taurine	Membrane stabilizer; antioxidant	20 mM	—	20 mM	—
K₂HPO₄	Maintains levels of inorganic phosphate	10 mM	10 mM	10 mM	—
HEPES	Buffering agent	20 mM	—	20 mM	—
Sucrose	Antioxidant	110 mM	—	—	—
Bovine Serum Albumin	Membrane stabilizer; antioxidant; chelates transition metals	1 g/L	5 mg/mL	1 g/L	0.2% (w/v)
K⁺-MES	Buffering agent	—	105 mM	—	—
KCl	Protects ionic environment	—	30 mM	—	100 mM
Glutamate	Mitochondrial substrate	—	0.005 mM	—	—
Malate	Mitochondrial substrate	—	0.002 mM	—	—
Mannitol	Antioxidant	—	—	110 mM	—
Dithiothreitol	Antioxidant	—	—	0.3 mM	—
MOPS	Buffering agent	—	—	—	50 mM
Glucose	Mitochondrial substrate	—	—	—	20 mM
NaCl	Maintains ionic gradient	—	—	—	15 mM

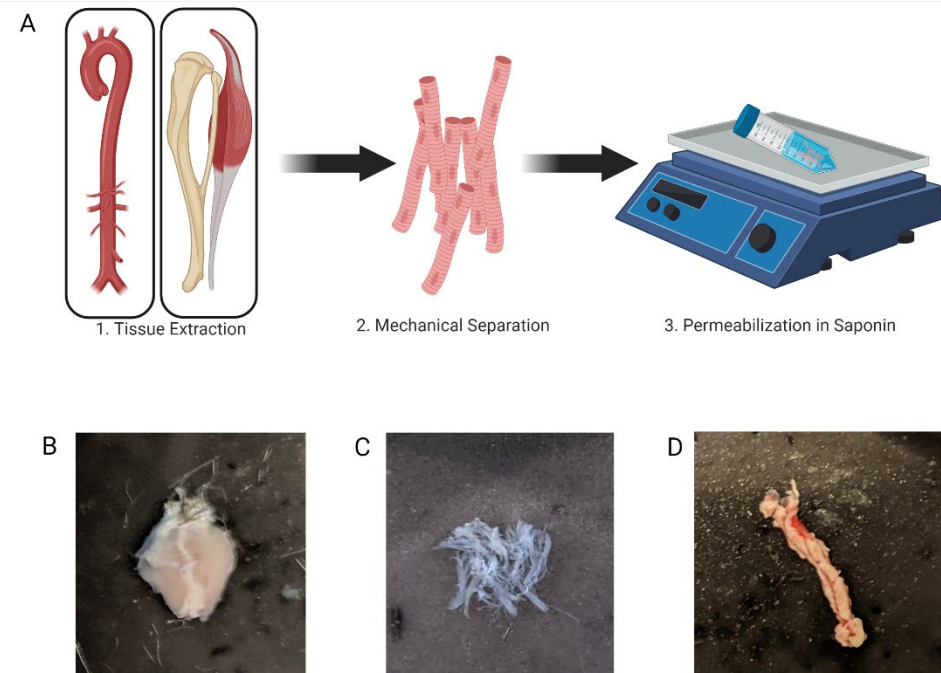


Figure 3-3. General workflow of the protocols used to permeabilize the tissues for this project. (A) Tissues will be harvested, then mechanically teased to expose individual fibers, then placed in a solution containing saponin solution. Representative images of gastrocnemius muscle before mechanical dissection (B), gastrocnemius after mechanical dissection (C), and of the aorta (D)

3.2.3. Tissue Permeabilization

Heart, Gastrocnemius, and Soleus

The preparation and permeabilization of tissues for these studies are based on the methods outlined by (Kuznetsov et al., 2008) and other standard practices in the literature (Figure 3-3A) (Gifford et al., 2015, 2016; Yamashita & Kanki, 2018). Immediately upon tissue extraction, heart, gastrocnemius, and soleus samples will be placed in BIOPS solution and remained on a rotator at 4° until further dissection and permeabilization. Within 120 minutes of the beginning of the respiration measurements, the extracted tissue will have all connective tissue and visible fat removed using sharp forceps (Figure 3-3B) while remaining in cold BIOPS. Following the removal of connective tissue and fat, the muscle tissue will be further dissected to form several thin muscle

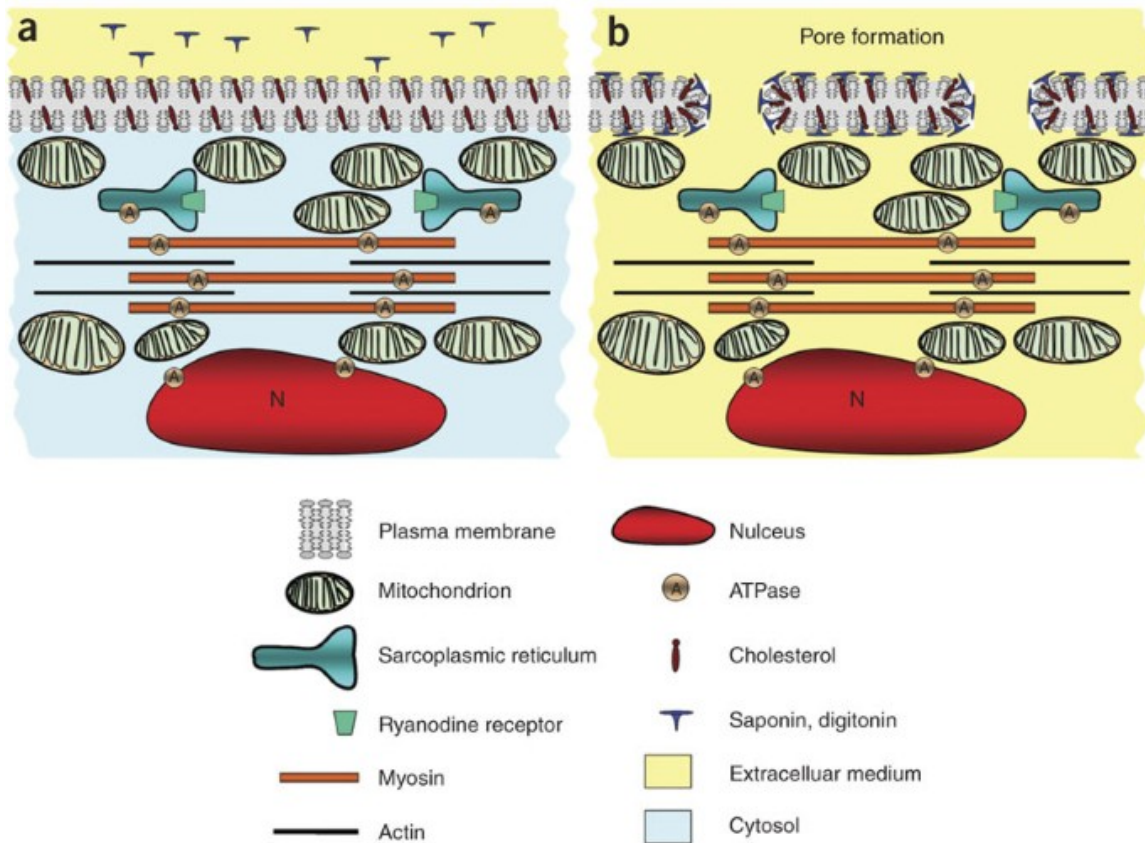


Figure 3-4. Diagram illustrating the chemical process of saponin permeabilization. Reprinted from Kuznetsov et al.

fiber bundles weighing 2-5 mg each (Figure 3-3C). Once the tissue has been appropriately mechanically permeabilized, the fiber bundles will be placed into 2 mL of cold BIOPS containing 50 µg/mL saponin solution for chemical permeabilization (Figure 3-4) of the sarcolemma and gently mixed on a rocker for 30 minutes.

Following chemical permeabilization, the permeabilized muscle fiber bundles will be placed in ~2-3 mL of MiR05 and mixed gently to wash out the saponin and ATP for 10 minutes. The washout step will be repeated a second time to completely remove the saponin and other metabolites. Once the washout steps are completed, the muscle fiber bundles will be removed from the MiR05 and gently dabbed dry on a task wiper to remove excess liquid, then weighed and separated into 1-2 mg portions before being placed into the Oxygraph O2K (Oroboros Instruments;

Innsbruck AT) chambers containing 2 mL of MiR05. All experiments involving the Oxygraph O2K will be conducted at 37°C and stirrers inside the chamber will maintain a rate of 750 rpm. To prevent any limitations from the O₂ concentration and/or diffusive ability of O₂ to enter the mitochondria in the gastrocnemius and soleus, O₂ concentrations within the chambers will be maintained at 170-250 µM by carefully injecting O₂ into the chambers and allowing the O₂ consumption rate to stabilize prior to collecting measurements or further adding substrates or inhibitors. For the heart, O₂ concentrations will be maintained between 350-450 µM.

Aorta

The preparation of the aorta for these studies is based on previously published protocols (S. H. S. Y. Park et al., 2018; S. Y. Park et al., 2014, 2016). Immediately upon tissue extraction, aorta samples will be placed in BIOPS solution and remain on a rotator at 4° until further dissection and permeabilization. Within 120 minutes of the beginning of the respiration measurements, the extracted tissue will have all connective tissue and visible fat removed using sharp forceps (Figure 3-3D) while remaining in cold BIOPS. Following the removal of connective tissue and fat, the aorta will be further dissected to form pieces weighing 2-5 mg each. Once the tissue has been appropriately mechanically permeabilized, the pieces will be placed into 2 mL of cold BIOPS containing 50 µg/mL saponin solution for chemical permeabilization of the sarcolemma and gently mixed on a rocker for 40 minutes. Following chemical permeabilization, the permeabilized aorta pieces will be placed in ~2-3 mL of MiR05 and mixed gently to wash out the saponin and ATP for 10 minutes. The washout step will be repeated a second time to remove the saponin completely and other metabolites. Once the washout steps are completed, the aorta pieces will be removed from the MiR05 and gently dabbed dry on a task wiper to remove excess liquid, then weighed and

separated into 1-2 mg portions before being placed into the O2k-FluroRespirometer (Oroboros Instruments, Innsbruck, AT; see section 3.3.1) chambers containing 2 mL of MiR05. All experiments involving the O2k-FluroRespirometer will be conducted at 37°C. To avoid any limitations from the O₂ concentration and/or diffusive ability of O₂ to enter the mitochondria, O₂ concentrations within the chambers will be maintained at 170-250 µM by carefully injecting O₂ into the chambers and allowing the O₂ consumption rate to stabilize prior to collecting measurements or further adding substrates or inhibitors (Perry et al., 2011).

3.3. Equipment

3.3.1. Mitochondrial Respiration: Oroboros O2k-FluroRespirometer

Hardware

The Oroboros O2k-FluroRespirometer (Innsbruck, AT) is a dual closed-chamber multisensory device equipped with Clark-type polarographic oxygen sensors to measure oxygen concentration within medium and additional fluorometric modules that allow for the measurement of ROS production, mitochondrial membrane potential, or Ca²⁺ or ATP production (Yamashita & Kanki, 2018). Each chamber contains a polarographic oxygen sensor made of a gold cathode and Ag/AgCl anode connected electrically by a KCl electrolyte solution and separated by a 0.25 µm O₂-permeable fluorinated ethylene propylene membrane. The sensors detect oxygen within the chamber by measuring the electrical current generated by the reduction of O₂ to water, which is linearly proportional to the partial pressure of oxygen (Po₂). This system averages one hundred data points at each sampling interval (represented as a single data point) and has a limit of detection of O₂ concentration that extends to 0.005 µM O₂. Each chamber is also equipped with an air-tight stopper to prevent the exchanges of gases between the chamber and ambient air, as well as a non-

Teflon magnetic stirrer bar capable of 750 revolutions per minute to allow adequate diffusion of gases and chemicals.

The conversion of P_{O_2} to O_2 concentration (C_{O_2}) is determined by the raw signal (V) obtained at air saturation of the medium, the raw signal obtained at zero O_2 (V; determined using sodium dithionite), experimental temperature (T; measured in thermoregulated copper blocks), barometric pressure (kPa; measured by an electronic pressure transducer), P_{O_2} (kPa), O_2 solubility in water (S_{O_2} ; $\mu M/kPa$), and the O_2 solubility factor of the respiration medium (0.92 for MiR05 at 30 and 37°C) (Gnaiger E, 2020). Based on these factors, the C_{O_2} at standard barometric pressure (100 kPa) and 37°C is 207.3 μM in ambient air and 191 μM in MiR05 (Yamashita & Kanki, 2018).

Software (DatLab 7.4)

The Orobos O2k-FluroRespirometer is accompanied by the software analysis program, DatLab, of which the current version (DatLab 7.4) will be used to analyze the mitochondrial respiration data for this project. One of the main features of DatLab 7.4 is the calculation of O_2 consumption (J_{O_2} ; measured in pmol/mL/s) expressed as the negative time derivative of the measured O_2 concentration, which is able to detect O_2 flux down to 1 pmol/s/mL (0.001 $\mu M/s$) (Yamashita & Kanki, 2018). The calculation of J_{O_2} can be described by equation 3-1.

$$J_{O_2} = \frac{dC_{O_2}}{dt} \cdot v_{O_2}^{-1} \cdot SF \quad (3-1)$$

Where C_{O_2} is O_2 concentration measured at time t , $d C_{O_2}/dt$ is the positive time derivative of O_2 concentration, $v_{O_2}^{-1}$ is the stoichiometric coefficient for the reaction of O_2 consumption (in this case, -1 because oxygen is being consumed), and SF is the scaling factor (in this case, 1000 to convert the amount of O_2 from nmol to pmol). The default settings in DatLab – which will be used

in this study – set the data recording interval at every 2 seconds. Because the CO_2 is measured by the polarographic sensors every 10 milliseconds, an average of 200 sensor signal points are averaged to generate a single J_{O_2} value, as shown in Figure 3-5.

Following an experimental protocol (such as a substrate-uncoupler-inhibitor titration protocol), marks are manually generated by the user in the DatLab program to assess J_{O_2} at each stage of the protocol. These marks, which contain the individual J_{O_2} data points, are typically placed along timepoints that show the attainment of a stable steady-state that lasts 1-2 minutes (Figure 3-5). After these marks are made for each titration step, the user may collect descriptive parameters (mean, median, standard deviation, etc.) of the data within each mark. These parameters (typically the mean, as is used in these experiments) are then reported as the respiration rates for each experimental step.

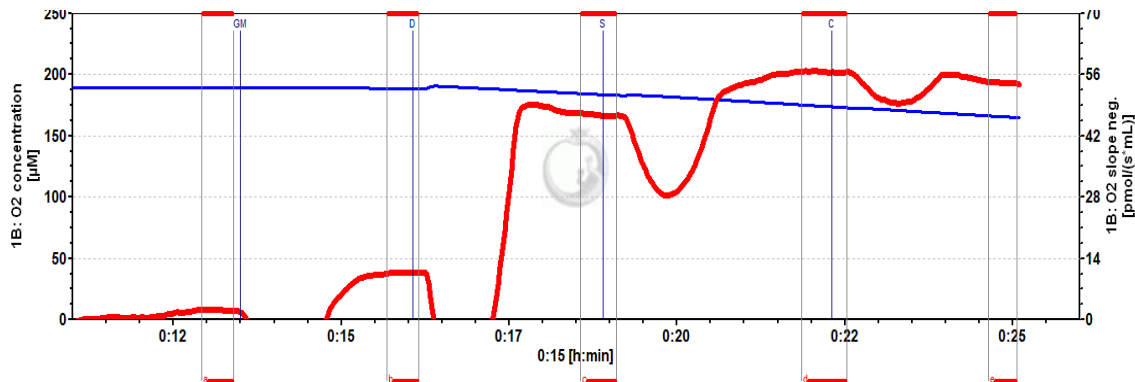


Figure 3-5. Screenshot taken from the DatLab Software output created by Oroboros Instruments. Absolute oxygen concentrations are traced in the blue lines, while the oxygen negative slope is traced in the red lines. Marks (red boxes) are placed to calculate the average oxygen consumption for a given respiration state.

3.4. Acute Effects of Cigarette Smoke Condensate on Mitochondrial Respiration (Aim 1)

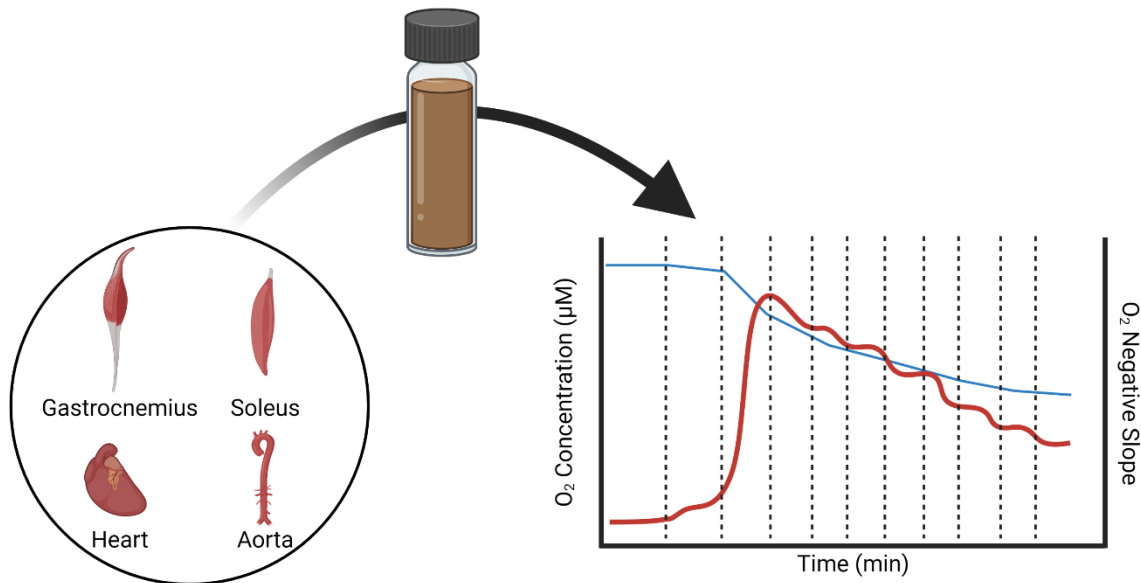


Figure 3-6. Overview of Aim 1.

3.4.1. Mitochondrial Respiration Protocols and Measurements

The experimental overview for Aim 1 is outlined in Figure 3-6, while the experimental protocol and data collection sheet are shown in Table 3-3 and Appendix A, respectively. Each experiment will be run in duplicate and averaged as a single measurement to account for sample variability and technical issues. After allowing 5-10 minutes for the oxygen concentration to stabilize and the oxygen flux to reach a steady-state (as assessed by a plateau in the J_{O_2}), basal respiration – i.e., oxygen consumption in the absence of mitochondrial substrates or ADP – will be measured. After the measurement of basal respiration, saturating amounts of glutamate (G; 10 mM), malate (M; 2 mM), ADP (D; 5 mM), and succinate (S; 10 mM) will be added to the chambers to achieve maximal ADP-stimulated respiration (state III Complex I & II linked respiration; abbreviated as GMDS) (Gifford et al., 2015; Yamashita & Kanki, 2018). Under these conditions, oxygen consumption is tightly coupled to maximal ATP generation, therefore indicating the

maximum ADP-driven rate of ATP production via oxidative phosphorylation. Following the collection of state III respiration rates at a steady state for 1-2 minutes, cytochrome C (C; final concentration 10 µM) will be added to assess the outer mitochondrial membrane integrity. This step is necessary to ensure that the permeabilization or mechanical dissection has not damaged the mitochondrial membranes. All tissues with a cytochrome c response >10% of the previous condition will be removed from the analysis (Perry et al., 2013). Once integrity of the outer mitochondrial membrane has been established, increasing concentrations of cigarette smoke condensate (Murty Pharmaceuticals, Lexington, KY; stock solution 40 mg/mL; dissolved in MiR05 and stored at -80°C) will be added to the respiration chambers to achieve the following final concentrations: 0.004 µg/mL, 0.04 µg/mL, 0.4 µg/mL, 4.0 µg/mL, 40 µg/mL, 400 µg/mL, 800 µg/mL, 1200 µg/mL, 1600 µg/mL, 2000 µg/mL, and 2400 µg/mL. These concentrations were chosen based on previous studies (Csiszar et al., 2008; Orosz et al., 2007), which calculated that the cigarette-containing constituents within these concentrations likely overlap the concentration of constituents that are contained in the blood after smoking a single cigarette. These calculations expanded upon previous studies that showed that plasma nicotine may exceed 25 ng/mL after smoking a single cigarette and that individuals who smoke more than one cigarette per day have plasma nicotine concentrations >50ng/mL (Mendelson et al., 2003). The cigarette smoke condensate that will be used in this study contains 6% nicotine; thus, the range of nicotine that the tissues will be exposed to range from 0.24 ng/mL to 144,000 ng/mL, well within the range of nicotine reported in the blood after a cigarette, as well as the concentration of nicotine in the blood of individuals who smoke more than one cigarette per day. Before increasing the concentration of

cigarette smoke condensate, respiration rates will be allowed to reach a steady-state lasting 1-2 minutes.

3.4.2. Citrate Synthase Activity

The analysis of CS activity will be performed using standard methods as described by Picard et al. (Picard et al., 2010). Tissues (gastrocnemius, soleus, heart, and aorta) will be harvested and then immediately placed in 2 mL of either MiR-05 or 6% CSC dissolved in MiR-05 and incubated for 20 minutes. Following incubation, each tissue will be snap frozen in liquid nitrogen and stored at -80°C for later analysis. At a later date, tissues will be thawed and homogenized on ice in a buffer containing 250 mM sucrose, 40 mM KCl, 2 mM EGTA, and 20 mM Tris-HCl (Qiagen, Hilden, Germany). Samples will be transferred to a 96-well plate where spectrophotometric analysis of CS activity will be assessed using a multi-mode reader (Synergy HTX BioTek Instruments, Winooski, VT) by detecting the increase in absorbance at 412 nm at 30°C.

Table 3-3. Experimental protocol for Aim 1.

Step	Stock Solution	Amount	Final Concentration in Chamber
1	Glutamate	10 µL	10 mM
	Malate	5 µL	2 mM
	ADP 5000	20 µL	5 mM
	Succinate	20 µL	10 mM
2	Cytochrome C	5 µL	10 µM
3	4.0 µg/mL CSC	2.0 µL	0.004 µg/mL
4	4.0 µg/mL CSC	18.0 µL	0.04 µg/mL
5	400 µg/mL CSC	1.8 µL	0.4 µg/mL
6	400 µg/mL CSC	18.0 µL	4 µg/mL
7	40 mg/mL CSC	1.8 µL	40 µg/mL
8	40 mg/mL CSC	18.0 µL	400 µg/mL
9	40 mg/mL CSC	1.8 µL	40 µg/mL
10	40 mg/mL CSC	18.0 µL	400 µg/mL
11	40 mg/mL CSC	20 µL	800 µg/mL
12	40 mg/mL CSC	20 µL	1200 µg/mL
13	40 mg/mL CSC	20 µL	1600 µg/mL
14	40 mg/mL CSC	20 µL	2000 µg/mL
15	40 mg/mL CSC	20 µL	2400 µg/mL

3.4.3. Data Analysis & Sample Size Estimates

The rate of O₂ consumption will be expressed relative to muscle tissue size in picomoles of O₂ per second per milligram of wet weight (pmolO₂/s/mg_{wt}). The assessment of the normality and the homoscedasticity of the data will be statistically determined using a Shapiro-Wilk test and Levene's test, respectively. If the data are found to comply with the assumptions of normality and homoscedasticity, a one-way analysis of variance (ANOVA) will be used to determine the overall impact of cigarette smoke on mitochondrial respiration for each of the tissues. If the ANOVA results are found to be significant, as indicated by p < 0.05, the differences in mitochondrial respiration between state III respiration (GMDS) and each of the cigarette smoke condensate titration steps will be assessed using an *a priori* planned comparisons t-test with a Holm-Šídák adjustment (Holm, 1979). If the data violate the assumptions of normality and homoscedasticity, a nonparametric Kruskal-Wallis test will be used to determine the overall effect of cigarette smoke condensate on mitochondrial respiration. If the Kruskal-Wallis test is significant, nonparametric Mann-Whitney tests will be used to determine significance between state III respiration (GMDS) and each cigarette smoke titration step. All statistical analyses will be performed using R version 4.2.

Citrate Synthase Activity

CS Activity will first be tested for normality and homoscedasticity will be performed using the methods previously described. If the data are found to comply with the assumptions of normality and homoscedasticity, dependent samples t-test will be performed to determine statistical significance between the control and smoke-exposed samples. If the data are found to

violate the assumptions of normality and homoscedasticity, nonparametric Wilcoxon Signed-Rank tests will be performed.

Sample Size Estimates

The sample size estimates (Appendix B) have been determined using the pwr package for R version 4.2 (Helios & Rosario, 2020). Pilot data for these experiments collected from our lab estimate an effect size (Cohen's f) of 1.08, 1.03, 0.98, and 1.81 for the gastrocnemius, soleus, aorta, and heart, respectively. Based on the methods above, and assuming $\alpha = 0.05$ and $\beta = 0.95$, these experiments are estimated to require a minimum sample size of 3 samples per tissue.

3.5. Effects of Cigarette Smoke Exposure on Mitochondrial Substrate Utilization (Aim 2)

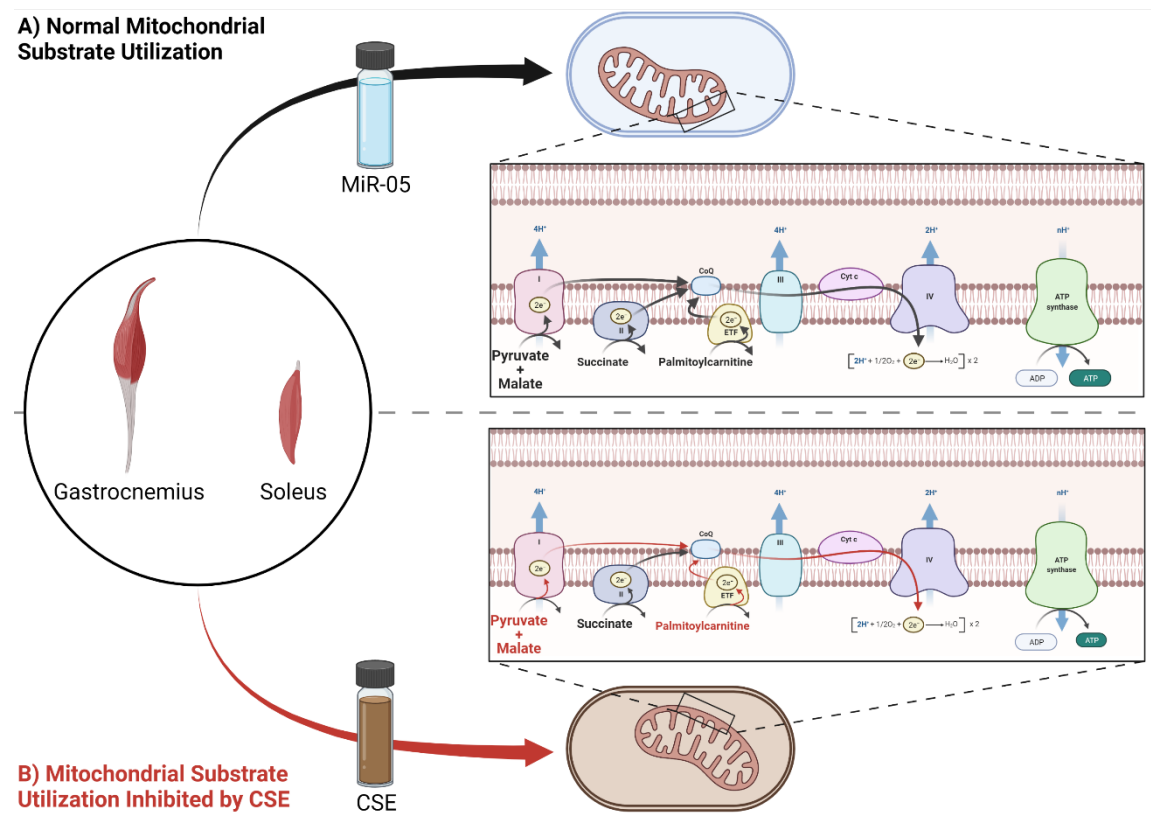


Figure 3-7. Overview of Aim 2

3.5.1. Preparation and Incubation of Tissues

The experimental overview for aim 2 is displayed in Figure 3-7. First, tissues will be harvested according to the procedures outlined in section 3.1.3. Following the collection of tissues, pieces of the gastrocnemius and soleus muscles will be gently dissected and permeabilized (as outlined in section 3.2.3) and placed in separate containers with a 2 mL solution of MiR05 (control) or 4% cigarette smoke concentrate. These concentrations of cigarette smoke were chosen based on pilot studies showing that this concentration induces a ~25% decrease in state III mitochondrial respiration in permeabilized fibers from the gastrocnemius muscle. The tissue-containing solutions will be rocked gently in a 4°C cold room for 1-hour. Following the incubation period, the tissues will be removed from the cigarette smoke solutions and immediately placed in respiration chambers to assess mitochondrial respiration.

3.5.2. Mitochondrial Respiration and Measurements

The experimental protocols for aim 2 are outlined in Tables 3-4 and 3-5. The same data sheets will be used for aim 2 as were used in aim 1 (Appendix A). Following the tissue permeabilization steps, tissue samples will be weighed and placed in the respirometry chambers in MiR05, as previously described. After allowing ample time for the oxygen concentration to stabilize and the oxygen flux to reach a steady-state, saturating concentrations of malate (M; 2 mM) and ADP (D; 5mM) will be added to the chambers. In the presence of saturating amounts of ADP, the mitochondria are in a phosphorylating state, and oxygen consumption is tightly coupled with ATP production (Brand & Nicholls, 2011).

Following this step, one of two protocols will be performed. The first protocol (Table III-4) consists of stepwise titrations of pyruvate into the respiration chambers ranging from final

concentrations of 0.1 mM to 5 mM. Pyruvate, the end product of glycolysis, is transferred into the mitochondria via the voltage-dependent anion channel (VDAC1) and the mitochondrial pyruvate carrier, where it can then be further processed in the Tricarboxylic Acid (TCA) Cycle (McCommis & Finck, 2015). Entry into the TCA cycle produces 3 moles of NADH and 1 mole of FADH₂, which can be oxidized by Complex I and Complex II of the ETC, thus stimulating glucose-derived ATP production. Afterward, cytochrome c (C; 10 µM) will be added to the chamber to assess the outer mitochondrial membrane's integrity, followed by inhibition of ATP synthase via Oligomycin (Omy; 5 nM) and inhibition of Complex III via Antimycin A (AmA; 2.5 µM). All samples with a cytochrome c response >10% will be excluded from the analysis.

Table 3-4. Experimental protocol for aim 2, part 1.

Step	Substrate	Amount	Final Concentration	Mechanism
1	Malate	5 µL	2 mM	CI Agonist
	ADP 5000	20 µL	5 mM	CV Agonist
2	Pyruvate	1 µL	0.1 mM	CI Agonist
3	Pyruvate	1.5 µL	0.25 mM	
4	Pyruvate	2.5 µL	0.5 mM	
5	Pyruvate	5 µL	1 mM	
6	Pyruvate	40 µL	5 mM	
7	Cytochrome C	5 µL	10 µM	Membrane Integrity
8	Antimycin A	1 µL	2.5 µM	CIII Inhibitor
	Oligomycin	1 µL	5 nM	CV Inhibitor

The second protocol (Table 3-5) consists of stepwise titrations of the carnitine-bound long-chain fatty acid, palmitoylcarnitine, ranging from final concentrations of 0.0025 mM to 0.04 mM. Palmitoylcarnitine is a carnitine-bound derivative of the palmitic acid, which is transferred into the mitochondria via membrane-bound carnitine palmitoyltransferase and carnitine-acylcarnitine translocase (Pande, 1975), where it can then undergo β -oxidation to produce Acetyl-CoA (which can enter the TCA cycle) and reduces the electron transfer flavoprotein (ETF) complex, which can then pump electrons through the ETC and stimulate fatty acid-derived mitochondrial ATP production (Ojuka et al., 2016; Ruzicka & Beinert, 1977). Following the palmitoylcarnitine titration, pyruvate will be titrated stepwise into the respiration chambers ranging from final concentrations of 1 mM to 5 mM. The titration of pyruvate following saturating concentrations of palmitoylcarnitine will be used to determine the inhibitory capacity of fatty acids on pyruvate oxidation, and thus substrate competition within the mitochondria, as well as the influence of cigarette smoke on mitochondrial substrate utilization (Abdul-Ghani et al., 2008a). Afterward, cytochrome c (C; 10 μ M) will be added to the chamber to assess the outer mitochondrial membrane's integrity, followed by inhibition of ATP synthase via Oligomycin (Omy; 5 nM) and inhibition of Complex III via Antimycin A (AmA; 2.5 μ M). All samples with a cytochrome c response $>10\%$ will be excluded from the analysis.

Table 3-5. Experimental protocol for aim 2, part 2.

Step	Substrate	Amount	Final Concentration	Mechanism
1	Malate	5 µL	2 mM	CI Agonist
	ADP 5000	20 µL	5 mM	CV Agonist
2	Palmitoylcarnitine	0.5 µL	0.0025 mM	ETF Agonist
3	Palmitoylcarnitine	0.5 µL	0.005 mM	
4	Palmitoylcarnitine	1.5 µL	0.0125 mM	
5	Palmitoylcarnitine	2.5 µL	0.025 mM	
6	Palmitoylcarnitine	3 µL	0.04 mM	
7	Pyruvate	1 µL	0.1 mM	CI Agonist
8	Pyruvate	1.5 µL	0.25 mM	
9	Pyruvate	2.5 µL	0.5 mM	
10	Pyruvate	5 µL	1 mM	
11	Pyruvate	40 µL	5 mM	
12	Cytochrome C	5 µL	10 µM	Membrane Integrity
13	Antimycin A	1 µL	2.5 µM	CIII Inhibitor
	Oligomycin	1 µL	5 nM	CV Inhibitor

3.5.3. Data Analysis & Sample Size Estimates

Sample Size Estimates

The sample size estimates (Appendix B) have been determined using the *pwr* package for R version 4.2 (Helios & Rosario, 2020). Pilot data for these experiments collected from our lab estimate an effect size (Cohen's *f*) of 0.41. Based on the methods above, and assuming $\alpha = 0.05$ and $\beta = 0.95$, these experiments are estimated to require a minimum sample size of 13 samples per group.

Mitochondrial Respiration

The rate of O₂ consumption will be expressed relative to muscle sample size in picomoles of O₂ per second per milligram of wet weight (pmolO₂/s/mg_{wt}). The assessment of normality and homoscedasticity of the data will be statistically determined using a Shapiro-Wilk test and Levene's test, respectively. If the data are found to comply with the assumptions of normality and homoscedasticity, a two-way repeated-measures ANOVA (respiration state \times cigarette smoke) for each tissue will be used to determine the significance of the main effects of cigarette smoke exposure on respiration, as well as the interaction effects. If the ANOVA results are found to be significant, as indicated by $p < 0.05$, pairwise comparisons will be conducted with a Holm-Šídák adjustment. If the data violate the assumptions of normality and homoscedasticity, a nonparametric aligned rank transform (ART) ANOVA (Oliver-Rodríguez & Wang, 2015; Wobbrock et al., 2011) will be used to determine the significance of the main effects of respiration state and cigarette smoke exposure on respiration, as well as the interaction effects. If the ART ANOVA is significant, pairwise comparisons using nonparametric Mann-Whitney tests will be performed. All statistical analyses will be performed using R version 4.2.

Michaelis-Menten Kinetics

The sensitivity of the mitochondria to pyruvate, octanoylcarnitine, and pyruvate in the presence of octanoylcarnitine will be determined by estimating the Michaelis-Menten kinetics using the equation 3-1:

$$V = \frac{V_{max}[S]}{K_m + [S]} \quad (3-1)$$

where V is the rate of the enzymatic reaction (in this case, indicated by the mitochondrial respiration rate) under given conditions, $[S]$ is the concentration of the substrate used for the reaction (pyruvate or octanoylcarnitine), V_{max} is the maximal rate of the enzymatic reaction at saturating concentrations, K_m is the Michaelis-Menten constant, or the concentration of a substrate when the velocity of the reaction (V) is 50% of the V_{max} .

After calculating the K_m and V_{max} for pyruvate, octanoylcarnitine, and pyruvate in the presence of octanoylcarnitine in both the control and cigarette smoke groups, the assessment of normality and homoscedasticity of the data will be statistically determined using methods as previously described. If both of these tests show compliance, a two-way repeated-measures ANOVA and Holm-Šídák adjustment will be used to determine statistical significance. If the assumptions of an ANOVA are violated, an ART ANOVA will be used to establish statistical significance. All calculations and statistical analyses will be performed using R version 4.2.

3.6. Mechanisms of Cigarette Smoke-Induced Mitochondrial Dysfunction (Aim 3)

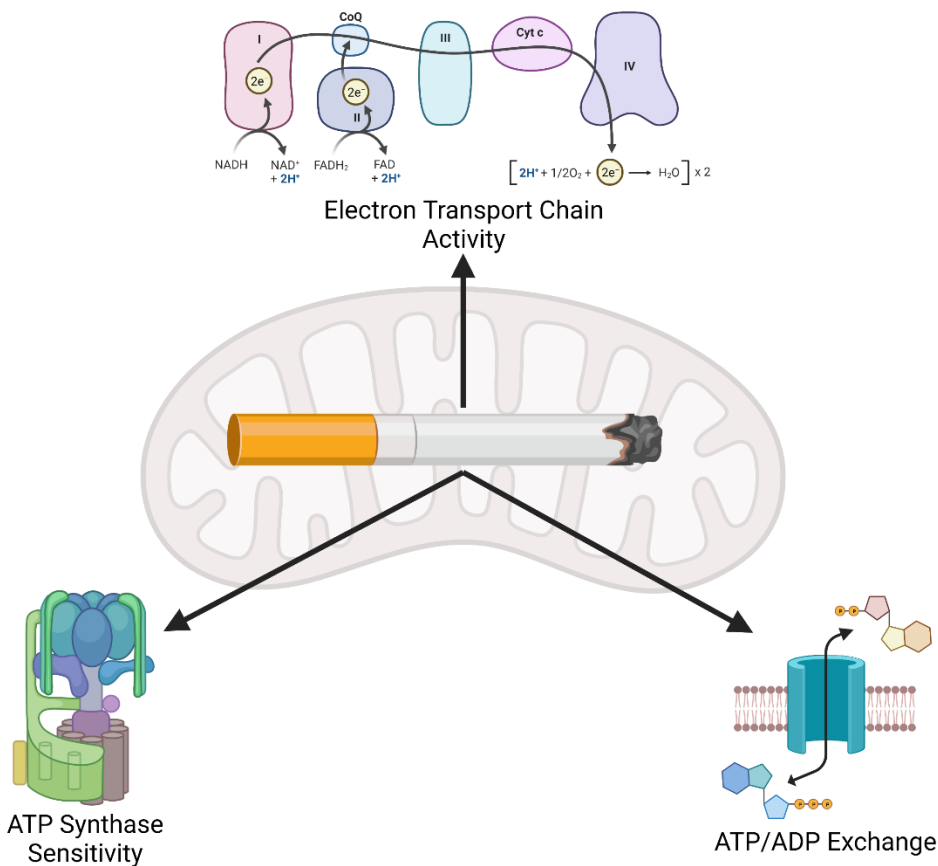


Figure 3-8. Overview of Aim 3.

3.6.1. Preparation and Incubation of Tissues

The experimental overview for aim 3 is displayed in Figure 3-8. The same preparation methods will be used as outlined in section 3.5.1.

3.6.2. Mitochondrial Respiration Measurements

The protocol that will be used to assess mitochondrial respiration for aim 3 is outlined in Table 3-6. The same data sheets will be used for aim 3 as were used in aims 1 and 2 (Appendix

A). Following the tissue permeabilization steps, tissue samples will be weighed and placed in the respirometry chambers in MiR05, as previously described.

The mitochondrial respiration protocol used in aim 3 is designed to several mechanisms by which cigarette smoke condensate impairs mitochondrial function, and will be performed as follows: First, saturating concentrations of glutamate (G; 10 mM) and malate (M; 2 mM) will be added to the chambers. The addition of glutamate and malate without the presence of ADP (also known as state IV respiration) represents a non-phosphorylating state where the oxygen consumed by the mitochondria is linked to the leak of protons from the mitochondrial intermembrane space (Brand & Nicholls, 2011). After attaining a steady-state, ADP (D) will be added in 5 titration steps: 1) 0.025 mM (D₂₅), 2) 0.05 mM (D₅₀), 3) 0.10 mM (D₁₀), 4) 0.25 mM (D₂₅₀), and 3) 5 mM (D₅₀₀₀). These concentrations were chosen as they are reflective of: 1) the concentrations of ADP observed at the end of an acute high-intensity exercise bout (~50 μM) as measured by ³¹P Magnetic Resonance Spectroscopy (Argov et al., 1996; Kemp et al., 2007; Vanderthommen et al., 2003; Vanhatalo et al., 2014); 2) the reported K_m of ADP for mitochondrial respiration (~250 μM) in permeabilized skeletal muscle fibers (Bygrave & Lehninger, 1967; Kuznetsov et al., 1996; Perry et al., 2011; Veksler et al., 1995); and 3) the concentration of ADP at V_{max} for mitochondrial respiration in permeabilized skeletal muscle fibers (5 mM). Following this step, saturating amounts of succinate (S; 10 mM) will be added to the chambers to assess maximal complex I & II-driven mitochondrial respiration. Cytochrome c (C; 10 μM) will be added to the chamber to assess the outer mitochondrial membrane's integrity. All samples with a cytochrome c response >10% will be excluded from the analysis. Following the addition of cytochrome c, carboxyatractyloside (CAT) will be added in 5 steps with final concentrations of 0.05 μM, 0.1 μM, 0.2 μM, 1.0 μM,

and 5.0 μM . A potent ANT inhibitor, CAT will be titrated near concentrations reflective of the inhibition constant (IC_{50}), or the concentration at which CAT inhibits the activity of ANT by 50%, and at the concentration which results in maximal inhibition (I_{\max}). Pilot experiments from our lab ($n = 1$; Figure 3-9) estimated IC_{50} at approximately 0.42 μM , well within the range of other reports (Vignais et al., 1976; Wisniewski et al., 1995). Following this, carbonyl cyanide m-chlorophenyl hydrazone (FCCP) will be added to assess the excess capacity of the mitochondrial ETC. FCCP is a potent ionophore and quickly allows protons to exit the mitochondrial intermembrane space, effectively uncoupling electron transport and oxygen consumption from ATP synthesis and diminishing $\Delta\Psi_m$, and allowing the uninhibited flow of electrons through the ETC (Brand & Nicholls, 2011). Rotenone (ROT; 0.5 μM), a complex I inhibitor, will then be added to the chamber to assess complex II-linked respiration. Lastly, oligomycin (Omy; 2.5 μM), an inhibitor of ATP synthase, and antimycin A (AmA; 2.5 μM), a complex III inhibitor, will be added to the chambers to assess residual, or non-mitochondrial, oxygen consumption. Following the conclusion of these

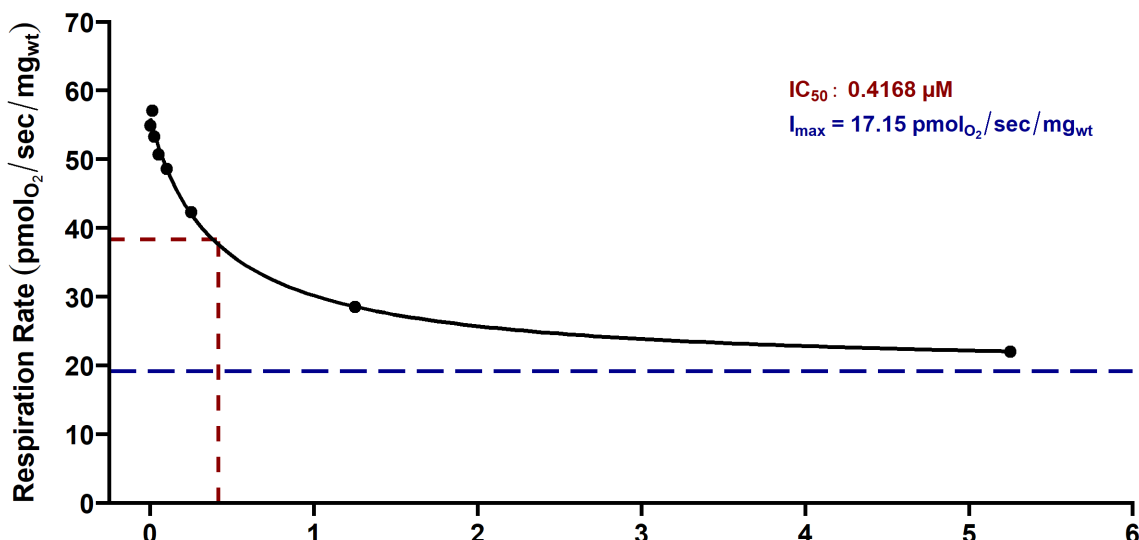


Figure 3-9. Results of a pilot experiment ($n = 1$) demonstrating kinetics of CAT, including IC_{50} (red dashed line) and the I_{\max} (blue dashed line).

experiments, tissue samples will be snap frozen in liquid nitrogen and stored at -80°C for later analysis of CS activity.

3.6.3. Citrate Synthase Activity

The analysis of CS activity will be performed using standard methods as described by Picard et al. (Picard et al., 2010). Frozen muscle samples from the mitochondrial respiration experiments (2-4 mg wet weight) will be thawed and homogenized on ice in a buffer containing 250 mM sucrose, 40 mM KCl, 2 mM EGTA, and 20 mM Tris-HCl (Qiagen, Hilden, Germany). Samples will be transferred to a 96-well plate where spectrophotometric analysis of CS activity will be assessed using a multi-mode reader (Synergy HTX BioTek Instruments, Winooski, VT) by detecting the increase in absorbance at 412 nm at 30°C.

Table 3-6. Experimental protocol for aim 3.

Step	Substrate	Amount	Final Concentration	Mechanism
1	Malate	5 µL	2 mM	CI Agonist
	Glutamate	10 µL	5 mM	CI Agonist
2	ADP (50 mM)	1 µL	25 µM	CV Agonist
3	ADP (50 mM)	1 µL	50 µM	
4	ADP (50 mM)	2 µL	100 µM	
5	ADP (200 mM)	1.5 µL	250 µM	
6	ADP (500 mM)	20 µL	5 mM	
7	Succinate	20 µL	10 mM	CII Agonist
8	Cytochrome C	5 µL	10 µM	Membrane integrity
9	Carboxyatractyloside (0.05 mM)	2 µL	0.05 µM	ANT Inhibitor
10	Carboxyatractyloside (0.05 mM)	2 µL	0.1 µM	ANT Inhibitor
11	Carboxyatractyloside (0.05 mM)	4 µL	0.2 µM	ANT Inhibitor
12	Carboxyatractyloside (2 mM)	0.8 µL	1.0 µM	ANT Inhibitor
13	Carboxyatractyloside (2 mM)	4 µL	5 µM	ANT Inhibitor (at I _{max})
14	FCCP (stepwise)	1 µL (per step)	—	Uncoupler
15	Rotenone	1 µL	0.5 µM	CI Inhibitor
16	Antimycin A	1 µL	2.5 µM	CIII Inhibitor
	Oligomycin	1 µL	5 nM	CV Inhibitor

3.6.6. Data Analysis

Sample Size Estimation

The sample size estimates (Appendix B) have been determined using the pwr package for R version 4.2 (Helios & Rosario, 2020). Pilot data for these experiments collected from our lab estimate an effect size (Cohen's d) of 1.56. Based on the methods above, and assuming $\alpha = 0.05$ and $\beta = 0.95$, these experiments are estimated to require a minimum sample size of 8.

Mitochondrial Respiration

The rate of O₂ consumption will be expressed relative to muscle tissue size in picomoles of O₂ per second per milligram of wet weight (pmolO₂/s/mg_{wt}) and in picomoles of O₂ per second per CS activity (pmolO₂/s/CSAU). The assessment of normality and homoscedasticity of the data will be statistically determined using a Shapiro-Wilk test and Levene's test, respectively. If the data are found to comply with the assumptions of normality and homoscedasticity, a two-way repeated-measures ANOVA (cigarette smoke concentration \times respiration state) for each tissue will be used to determine the significance of the main effects of cigarette smoke concentration on respiration, as well as the interaction effects. If the ANOVA results are found to be significant, as indicated by $p < 0.05$, *a priori* pairwise comparisons between the control and cigarette smoke conditions for each respiration state will be conducted and adjusted using the Holm-Šídák method. If the data violate the assumptions of normality and homoscedasticity, a nonparametric aligned rank transform (ART) ANOVA (Oliver-Rodríguez & Wang, 2015; Wobbrock et al., 2011) will be used to determine the significance of the main effects of respiration state and cigarette smoke, as well as the interaction effects. If the ART ANOVA is significant, pairwise comparisons using

nonparametric Wilcoxon Signed-Rank tests will be performed. All statistical analyses will be performed using R version 4.2.

Respiratory Control Ratio

The respiratory control ratio (RCR), or the ratio of state III (GMDS) to state IV (GM), is widely used as an indicator of mitochondrial substrate capacity (Brand & Nicholls, 2011) and overall mitochondrial dysfunction. After calculating the RCR for each tissue, tests for normality and homoscedasticity will be performed using the methods previously described. If the data are found to comply with the assumptions of normality and homoscedasticity, dependent samples t-test will be performed to determine statistical significance between the control and smoke-exposed samples. If the data are found to violate the assumptions of normality and homoscedasticity, nonparametric Wilcoxon Signed-Rank tests will be performed.

ADP Sensitivity

The sensitivity of the ETC to ADP, or K_m , will be determined by the Michaelis-Menten Kinetics as outlined in section 3.5.3. If Michaelis-Menten Kinetics cannot be estimated, the

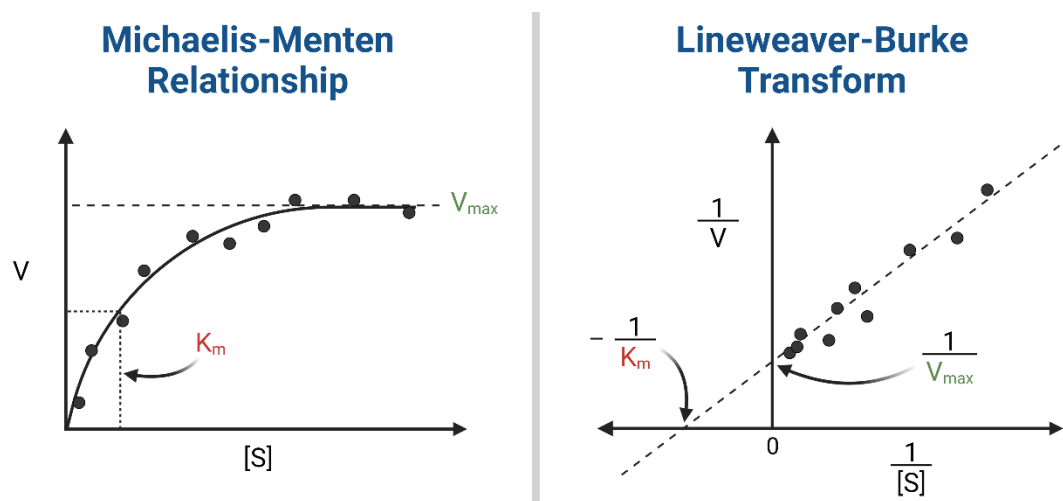


Figure 3-10. Diagram illustrating the conversion of the Michaelis-Menten curve to a Lineweaver-Burke Plot.

Lineweaver-Burke method (Lineweaver & Burk, 1934), which is an extension of the Michaelis-Menten equation (Equation III-1), will be used. This method, illustrated in Figure 3-8, calculates the K_m and V_{max} of a reaction by taking the reciprocal of the reaction velocity (V) and plotting it against the substrate concentration ($[S]$), and can therefore be represented as shown in Equation 3-2. For the purpose of this study, V will be the rate of oxygen consumption and $[S]$ will be the final ADP concentrations used in our protocol (0.05 mM, 0.25 mM, and 5 mM).

$$\frac{1}{V} = \frac{K_m}{V_{max} [S]} + \frac{1}{V_{max}} \quad (3-2)$$

After determining the reciprocals of V and $[S]$, a linear regression model may be performed on these values to calculate the slope and x- and y-intercepts. The slope represents the relationship $\frac{K_m}{V_{max}}$, while the x-intercept is equal to $-\frac{1}{K_m}$ and the y-intercept is equal to $\frac{1}{V_{max}}$. From these parameters, the K_m and V_{max} for each of the tissue samples may be calculated.

Following calculation of the K_m and V_{max} for each tissue, tests for normality and homoscedasticity will be performed using the methods previously described. If the data are found to comply with the assumptions of normality and homoscedasticity, dependent samples t-test will be performed to determine statistical significance between the control and smoke-exposed samples. If the data are found to violate the assumptions of normality and homoscedasticity, nonparametric Wilcoxon Signed-Rank tests will be performed.

Citrate Synthase Activity

CS Activity will first be tested for normality and homoscedasticity will be performed using the methods previously described. If the data are found to comply with the assumptions of

normality and homoscedasticity, dependent samples t-test will be performed to determine statistical significance between the control and smoke-exposed samples. If the data are found to violate the assumptions of normality and homoscedasticity, nonparametric Wilcoxon Signed-Rank tests will be performed.

CHAPTER 4

ADDENDA TO THE PROPOSAL & PILOT STUDIES

Due to unforeseen factors and methodological changes, the following changes have been made to the proposal:

Aim 1 Citrate Synthase Activity – In a separate cohort of mice, tissues (gastrocnemius, soleus, heart, and aorta) were harvested as stated earlier and then immediately placed in 2 mL of MiR-05 and incubated for 20 minutes. Each sample was snap frozen in liquid nitrogen after incubation and stored at -80°C for later analysis. Tissues were thawed and homogenized on ice in a buffer containing 1 mM EDTA and 50 mM triethanolamine, as described previously (Picard et al., 2010). Samples were transferred to a 96-well plate containing 200 µM Acetyl CoA, 200 µM DTNB, and 70 µM oxaloacetate, where spectrophotometric analysis of CS activity was assessed using a multi-mode reader (Synergy HTX BioTek Instruments, Winooski, VT) by detecting the increase in absorbance at 412 nm at 30°C (Picard et al., 2010).

Aims 2 & 3 Lineweaver-Burke Plots – The Lineweaver-Burke methods will no longer be used to estimate the K_m and V_{max} of ADP or carboxyatractyloside. Instead, extra titration steps will be added to each protocol and fitted to the Michaelis-Menten equation. Details of the procedures are outlined in each respective manuscript in chapters V-V.

Aim 3 Citrate Synthase Activity – Due to the within-tissues design of the study, I have opted to exclude the analysis of citrate synthase activity from the study. I do not believe that these results, or lack thereof, will impact the overall results of the scope of the study.

Discussion – In lieu of the formal results and discussion section, the sections of the manuscript (Chapter 5-8) are comprised of the three primary manuscripts that will be submitted for publication based on the experiments performed as a part of this dissertation work.

Pilot Studies to Determine CSC Concentrations and Duration for Aims 2 & 3 – Extensive work was performed to identify an appropriate concentration and exposure duration of CSC to the gastrocnemius and soleus. Studies examining human mitochondrial respiration after cigarette smoke exposure (Brønstad et al., 2011; Gifford et al., 2018a; Layec, Haseler, et al., 2011) and mouse models (Ajime et al., 2020; Thatcher et al., 2014) have consistently shown a ~25% decrease in mitochondrial respiration induced by cigarette smoke exposure. Therefore, to increase the translational aspects of these studies, we sought to create an *in situ* model of CSC-induced mitochondrial dysfunction without causing irreversible cellular damage (Martinou et al., 2000), as indicated by a >10% increase in mitochondrial respiration in the presence of cytochrome C. The results of these pilot investigations in the gastrocnemius and soleus muscles are shown in figures 4-1 and 4-2, respectively. Our data show that incubating these skeletal muscles in a solution containing 4% CSC for 1 hour was sufficient to induce a ~25% decrease in maximal mitochondrial

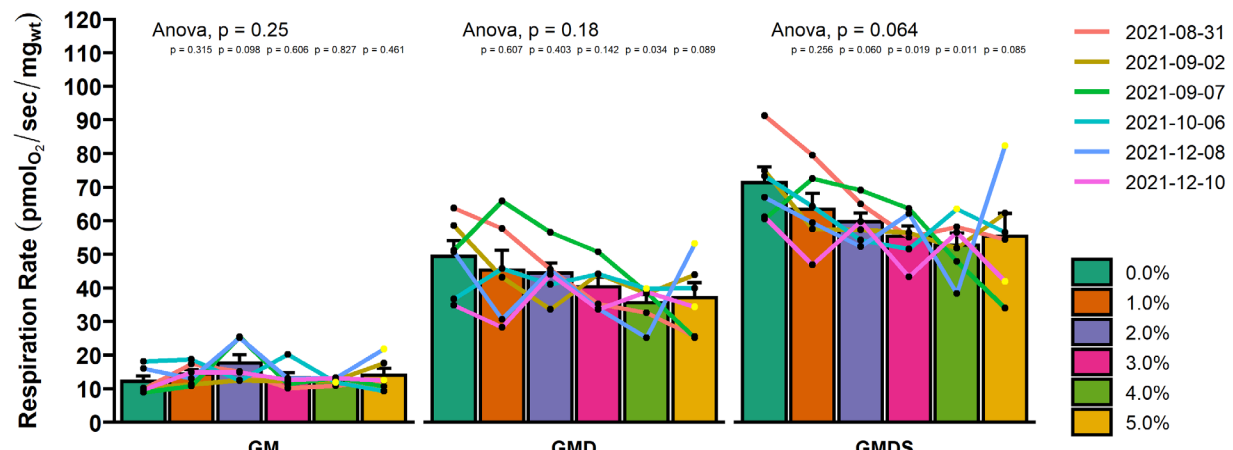


Figure 4-1. Pilot data to determine the appropriate CSC concentration in gastrocnemius muscle.

respiration in the gastrocnemius and a >10% decrease in the soleus. However, further increases in CSC concentrations were more likely to result in irreversible cellular damage, as indicated by the increase in the frequency of cytochrome C responses. Furthermore, the duration of exposure did not appear to influence the loss of mitochondrial respiration (data not shown). Therefore, for aims 2 and 3, we will expose the gastrocnemius and soleus muscles to CSC concentrations of 4% for 1 hour, thus increasing the translational abilities of these studies to reflect the observations of cigarette smoke-induced mitochondrial dysfunction reported *in vivo*.

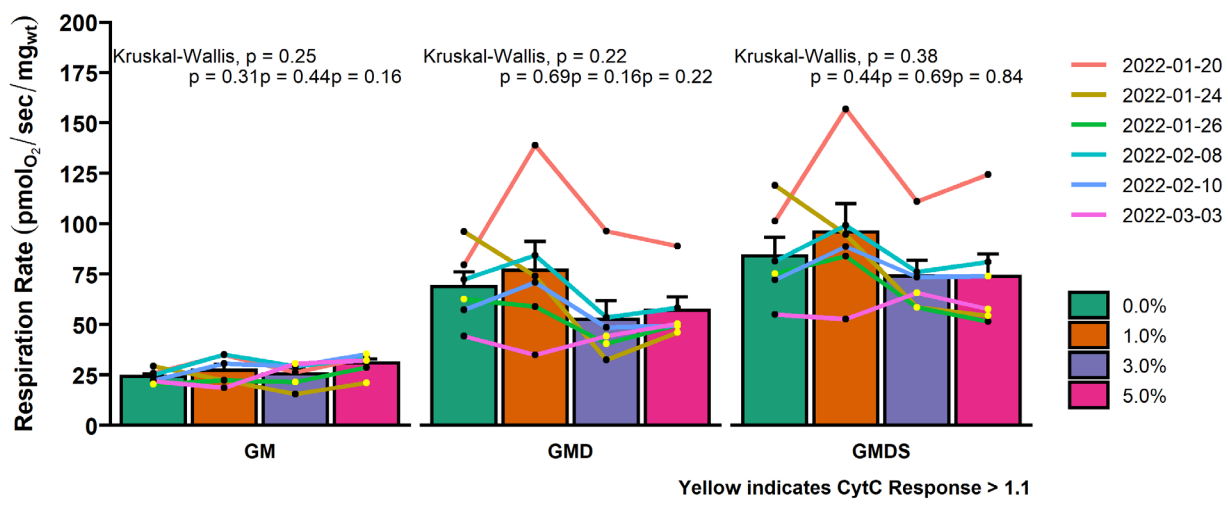


Figure 4-2. . Pilot data to determine the appropriate CSC concentration in soleus muscle.

CHAPTER 5

AIM I RESULTS AND DISCUSSION

5.1 Tissue specificity of mitochondrial toxicity induced by cigarette smoke in striated muscles and aorta

Stephen T Decker¹, Alexs A Matias¹, Adolfo E Cuadra², M Enes Erol¹, Corinna Serviente^{1,3}, Karine Fenelon^{2,3}, Gwenael Layec^{1,3}

Departments of Kinesiology, University of Massachusetts Amherst, USA¹

Department of Biology, University of Massachusetts Amherst, USA²

Institute for Applied Life Science, University of Massachusetts Amherst, USA³

Running Title: Tissue Specificity of Mitochondrial Cigarette Smoke Toxicity in Muscle and Aorta

Keywords: Skeletal Muscle, Aorta, Cardiac Muscle, High-Resolution Respirometry, Cigarette Smoke

Corresponding Author: Gwenael Layec

Life Sciences Laboratories, 240 Thatcher Rd, Amherst, Ma 01003

Email: glayec@umass.edu

5.2. Abstract

Epidemiological and clinical evidence suggests that cigarette smoke exposure elicits a tissue-specific and dose-dependent insult to mitochondrial function, possibly leading to cardiometabolic disease. However, the susceptibility and sensitivity of skeletal, cardiac, and vascular smooth muscle to cigarette smoke-induced mitochondrial dysfunction is unknown. Accordingly, using a piecewise linear regression to estimate the breakpoint and slope following the breakpoint, this study aimed to establish the tissue-specific susceptibility and sensitivity to cigarette smoke-induced inhibition of mitochondrial respiration in the gastrocnemius, soleus, heart, and aorta. In terms of absolute respiration, the aorta (BREAKPOINT: $480.2 \pm 243.1 \mu\text{g/mL}$) was the least susceptible compared to the heart (BREAKPOINT: $107.5 \pm 37.3 \mu\text{g/mL}$; $p = 0.001$) and the gastrocnemius (BREAKPOINT: $147.5 \pm 113.0 \mu\text{g/mL}$; $p = 0.005$), but not soleus (BREAKPOINT: $213.8 \pm 124.2 \mu\text{g/mL}$). Likewise, the heart (SLOPE: $-145.1 \pm 45.5 \text{ JO}_2/\text{[CSC]}$) was the most sensitive, followed by the soleus (SLOPE: $-54.6 \pm 13.3 \text{ JO}_2/\text{[CSC]}$), and, lastly, the gastrocnemius (SLOPE: $-21.8 \pm 7.9 \text{ JO}_2/\text{[CSC]}$) and the aorta (SLOPE: $-15.3 \pm 9.5 \text{ JO}_2/\text{[CSC]}$; all $p < 0.05$). However, when normalized for differences in mitochondrial content between tissues, only the aorta (SLOPE: $-0.8 \pm 0.4 \text{ JO}_2/\text{CS/[CSC]}$) was significantly less sensitive than the heart (SLOPE: $-2.6 \pm 1.4 \text{ JO}_2/\text{CS/[CSC]}$; $p = 0.021$), soleus (SLOPE: $-3.4 \pm 1.0 \text{ JO}_2/\text{CS/[CSC]}$; $p < 0.001$), and gastrocnemius (SLOPE: $-3.8 \pm 1.5 \text{ JO}_2/\text{CS/[CSC]}$; $p < 0.001$), suggesting intrinsic properties of the aorta that protect against cigarette smoke-induced mitochondrial toxicity. Our findings underscore the tissue specificity involved in cigarette smoke-induced mitochondrial toxicity, with the heart being most vulnerable to bioenergetic deficits induced by cigarette smoke,

and mitochondria in the aorta being inherently most resistant to dysfunction. These differences may explain the variation in risks of developing cardiometabolic diseases in these tissues.

5.3. New & Noteworthy

While cigarette smoke exposure is a well-known risk factor for the development of cardiometabolic disorders, the susceptibilities and sensitivities to cigarette smoke of the mitochondria in tissues central to the pathophysiology of cardiometabolic diseases are unknown. Herein, we demonstrate that the heart is the most vulnerable to bioenergetic insults induced by cigarette smoke. On the other hand, the mitochondria in the aorta exhibited an intrinsically distinct resistance to cigarette smoke-induced dysfunction. With this evidence, we demonstrate that the mitochondrial damage induced by cigarette smoke is, in fact, tissue-specific, thus providing mechanisms to explain the variations in the tissue-specific pathophysiology of cigarette smoke-associated cardiometabolic diseases.

5.4 Introduction

Cigarette smoke exposure is a well-known and significant health concern in the United States, contributing to 480,000 premature deaths and costing an estimated \$300 billion annually in direct and indirect costs (United States Department of Health and Human Services, 2014). Chronic cigarette smoking has a causative role in the development of respiratory diseases. In addition, mounting evidence indicates a dose-dependent increase in the risks for cardiovascular and metabolic diseases, skeletal muscle atrophy and weakness, or frailty in smokers (Jo et al., 2019; Lee & Choi, 2019; Maddatu et al., 2017b; Münzel et al., 2020). Despite the tight epidemiological link between cigarette smoking and numerous adverse health outcomes, the exact cellular mechanisms mediating the toxicity of cigarette smoke on multiple organs are still not fully elucidated.

Mitochondria are the primary source of cellular energy across numerous organ systems and are now recognized to play a key role in maintaining redox balance, calcium homeostasis, and apoptosis throughout the body. Interestingly, a growing number of studies seem to implicate the mitochondria as a mediator of the multi-systemic defects induced by cigarette smoke. Mainstream cigarette smoke is indeed composed of over 4,800 different chemicals, including reactive oxygen species (ROS) and toxins (Rodgman & Green, 2016), which can impair mitochondrial function. Specifically, acute exposure to reactive oxygen species can lower the activity of several enzymes of the Krebs cycle and maximal respiration in isolated mitochondria (Nulton-Persson & Szweda, 2001). Also, direct exposure to cigarette smoke compounds, specifically nicotine and o-cresol, has been demonstrated to inhibit maximal respiration using a similar *in vitro* preparation (Khattri et al., 2022). However, the use of isolated mitochondria in these studies is an important caveat, as

this approach exaggerates mitochondrial susceptibility to dysfunction in skeletal muscle (Picard et al., 2010).

In lung epithelial cells, it is well described that acute exposure to cigarette smoke condensate elicits substantial bioenergetic perturbations and redox stress. Specifically, mitochondrial membrane potential and ATP production are lowered by cigarette smoke condensate as a result of increased proton leak, which in turn stems from the activation of the mitochondrial ADP/ATP transporter (van der Toorn et al., 2007, 2009; Wu et al., 2020). These energetic changes are accompanied by greater mitochondrial-derived ROS generation (van der Toorn et al., 2007, 2009; Wu et al., 2020) and increased susceptibility to apoptosis (Aoshiba et al., 2001a). In contrast, the mitochondrial toxicity of cigarette smoke on other organs or tissues has been scarcely described. For instance, acute exposure to cigarette smoke or nicotine, a major constituent of tobacco, resulted in lower proton driving force and increased mitochondrial-derived ROS production in cultured cardiomyocytes (Jia et al., 2020) and carotid arteries (Csiszar et al., 2008; Orosz et al., 2007).

While these studies have been instrumental in elucidating the mechanisms behind cigarette smoke-induced mitochondrial dysfunction, the cigarette smoke concentrations used (upwards of 20% of the total solution) in those preparations were well above the physiological range of cigarette smoke particulate in the blood of smokers (Benowitz et al., 1982; Mendelson et al., 2003), making the findings from these studies challenging to translate to the human condition. Also, although intrinsic mitochondrial function may vary between tissues (Patel et al., 2009) and the susceptibility to the harmful effects of cigarette smoke differs across organs, as illustrated by the

greater relative risks for disease of some tissues (Gandini et al., 2008; Münzel et al., 2020), the tissue-dependent toxicity of cigarette smoke on mitochondrial function remains unknown.

An essential step in toxicology is to characterize the dose-response (Aronson, 2007) to determine the susceptibility and sensitivity of the organs to toxicant damage. Surprisingly, no studies to date have examined the dose-response to cigarette smoke toxicity on the mitochondrial function of skeletal, cardiac, or smooth muscles. Therefore, this study aimed to comprehensively characterize the toxicity of acute exposure to cigarette smoke condensate (CSC) on mitochondrial function in intact permeabilized muscle tissues. Herein, we used high-resolution respirometry coupled with increasing concentrations of cigarette smoke condensate – both physiological and supraphysiological – in permeabilized skeletal muscle (gastrocnemius and soleus) fibers, ventricular cardiac muscle fibers, and smooth muscles from the aorta. Based on prior epidemiological studies demonstrating an elevated cardiovascular disease burden in smokers (Münzel et al., 2020), we hypothesized that there would be a significant tissue-dependent difference, with greater susceptibility and sensitivity to CSC-induced mitochondrial toxicity in cardiac and smooth muscle tissues than in skeletal muscles.

5.5 Methods

5.5.1 Animals and Experimental Design

Three-to-twelve-month-old male and female C57BL/6 mice were used for this study. All animals were maintained on a 12-hour dark/light cycle without access to running wheels and were fed standard chow *ad libidum*. Following euthanasia by 5% isoflurane, the gastrocnemius, soleus, left ventricle, and aorta were extracted and placed in ice-cold BIOPS preservation solution. The gastrocnemius and soleus were specifically chosen due to the similarities in mitochondrial respiratory rates per unit of mass compared to those of human vastus lateralis muscle (Jacobs et al., 2013), and to encompass tissues that contain varying amounts of type I and type II skeletal muscle (Augusto et al., 2004).

5.5.2. Cigarette Smoke Condensate Preparation

Cigarette Smoke Condensate (Murty Pharmaceuticals Inc, Lexington, Kentucky, USA) containing 40 milligrams of cigarette smoke particulate matter per milliliter (henceforth considered 100%) was diluted in MiR05 (in mM: 110 Sucrose, 0.5 EGTA, 3 MgCl₂, 60 K-lactobionate, 20 taurine, 10KH₂PO₄, 20 HEPES, BSA 1g.L⁻¹, pH 7.1) and stored at -80°C until use.

5.5.3 Preparation of Permeabilized Muscle Fibers & Mitochondrial Respiration Measurements

The tissue preparation and respiration measurement techniques were adapted from established methods (Kuznetsov et al., 2008a; Pesta & Gnaiger, 2012) and have been previously described (Layec et al., 2018). Briefly, BIOPS-immersed fibers (2.77mM CaK₂EGTA, 7.23mM

K₂EGTA, 50mM K⁺ MES, 6.56 mM MgCl₂, 20mM Taurine, 5.77mM ATP, 15mM PCr, 0.5mM DTT, 20mM Imidazole) were carefully separated with fine-tip forceps and subsequently bathed in a BIOPS-based saponin solution (50 µg saponin.ml⁻¹ BIOPS) for 30 minutes for the gastrocnemius, soleus, and heart; and 40 minutes for the aorta. Following saponin treatment, muscle fibers were rinsed twice in ice-cold mitochondrial respiration fluid (MIR05, in mM: 110 Sucrose, 0.5 EGTA, 3 MgCl₂, 60 K-lactobionate, 20 taurine, 10KH₂PO₄, 20 HEPES, BSA 1g.L⁻¹, pH 7.1) for 10 minutes each. After the muscle sample was gently dabbed with a paper towel to remove excess fluid, the wet weight of the sample (1-2 mg) was measured using a standard, calibrated scale. The muscle fibers were then placed in the respiration chamber (Oxygraph O2K, Oroboros Instruments, Innsbruck, Austria) with 2 ml of MIR05 solution warmed to 37°C. Oxygen was added to the chambers, and oxygen concentration was maintained between 175-250 µM for the gastrocnemius, soleus, and aorta; and between 350-450 µM for the right ventricle. After allowing the permeabilized muscle sample to equilibrate for 5 minutes, mitochondrial respiratory function was assessed in duplicate. To determine maximal state III mitochondrial respiration, glutamate (10 mM), malate (2 mM), ADP (5 mM), succinate (10 mM) were added to the chamber (GMDS). Cytochrome c (10 µM) was then added to the chamber to assess mitochondrial membrane integrity (Perry et al., 2013). Samples that demonstrated impaired mitochondrial membrane integrity (more than a 10% increase in respiration in response to cytochrome C) were excluded from the analysis. Following determining membrane integrity, cigarette smoke condensate was injected into each chamber at concentrations starting from 0.004 µg/mL (0.00001%) to 2,400 µg/mL (6%). In each condition, the respiration rate was recorded until a steady state of at least 30-seconds (at a sampling rate of 2 seconds) was reached, the average of which was used for data analysis. The rate of O₂

consumption was expressed relative to muscle sample mass (in picomoles O₂ per second per milligram of wet weight), or normalized to CS activity (in picomoles O₂ per second per CS).

5.5.4. Citrate Synthase (CS) Activity

In a separate cohort of mice (n = 7), tissues (gastrocnemius, soleus, heart, and aorta) were harvested as stated earlier and then immediately placed in 2 mL of MiR-05 and incubated for 20 minutes. Each sample was snap frozen in liquid nitrogen after incubation and stored at -80°C for later analysis. Tissues were thawed and homogenized on ice in a buffer containing 1 mM EDTA and 50 mM triethanolamine, as described previously (Picard et al., 2010). Samples were transferred to a 96-well plate containing 200 µM Acetyl CoA, 200 µM DTNB, and 70 µM oxaloacetate, where spectrophotometric analysis of CS activity was assessed using a multi-mode reader (Synergy HTX BioTek Instruments, Winooski, VT) by detecting the increase in absorbance at 412 nm at 30°C (Picard et al., 2010).

5.5.5. Data Analysis

The assessment of the normality and homoscedasticity was performed using a Shapiro-Wilk and Levene test for all variables. The effects of cigarette smoke condensate on mitochondrial respiration were determined using a nonparametric two-way (tissue × concentration) Aligned Ranks Transform (ART) ANOVA (Wobbrock et al., 2011). Planned comparisons of the effect of cigarette smoke concentrations on state III respiration (GMDS), as established *a priori*, were determined using Dunn's tests with a Holm-Šidák adjustment. A piecewise linear regression model

was used to estimate breakpoints in the dose-dependent changes to mitochondrial respiration. The differences between the breakpoints of each tissue were determined using a nonparametric Kruskal-Wallis test, followed by *post hoc* pairwise Dunn's Test with a Holm-Šidák adjustment. Statistical significance was accepted at $p \leq 0.05$. All statistical analyses were performed using R, version 4.1. Breakpoint analyses were performed using the 'segmented' (Muggeo, 2008) package. Effect sizes (partial η^2 and Cohen's d for ANOVA and *post hoc* tests, respectively) were calculated using the 'emmeans' package. Results are presented as mean \pm SD in the text and mean \pm SEM in the figures.

5.6. Results

5.6.1. Effects of CSC on Absolute Rates of Mitochondrial Respiration

Absolute mitochondrial respiration rates are shown in Figure 5-1. There were significant main effects of CSC ($p < 0.001$; partial $\eta^2 = 0.72$) and tissue type ($p < 0.001$; partial $\eta^2 = 0.72$), as well as a significant interaction effect ($p < 0.001$; partial $\eta^2 = 0.33$). *Post hoc* analyses for each tissue (Figure 5-2) revealed that the respiration rates of the gastrocnemius, soleus, heart, and aorta were significantly (adjusted $p < 0.05$) inhibited by cigarette smoke starting at 1200 (3%), 400 (1%), 1600 (4%), and 2000 (5%) $\mu\text{g}/\text{mL}$, respectively.

Results of the piecewise linear regression are shown in Figure 5-3. Results from the one-way ANOVA revealed a significant main effect of tissue type on the breakpoint at which CSC mitochondrial respiration ($p = 0.001$; partial $\eta^2 = 0.37$; Figure 5-3A). *Post hoc* analysis revealed that the [CSC] at which the breakpoint occurs in the aorta ($480.2 \pm 243.1 \mu\text{g}/\text{mL}$) was significantly different from the heart ($107.5 \pm 37.3 \mu\text{g}/\text{mL}$; $p = 0.001$; $d = 2.6$) and the gastrocnemius ($147.5 \pm$

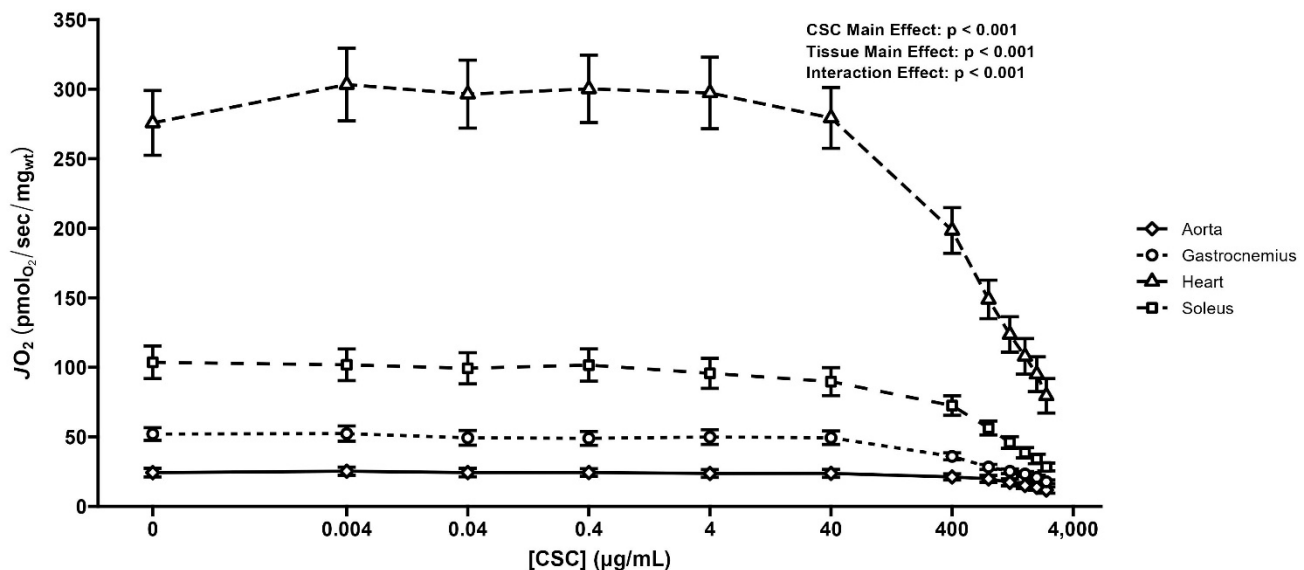


Figure 5-1. Absolute Respiration Rates for the heart ($n = 9$; triangles), soleus ($n = 11$; squares), gastrocnemius ($n = 11$; circles), and aorta ($n = 8$; diamonds). Values are represented as mean \pm SEM..

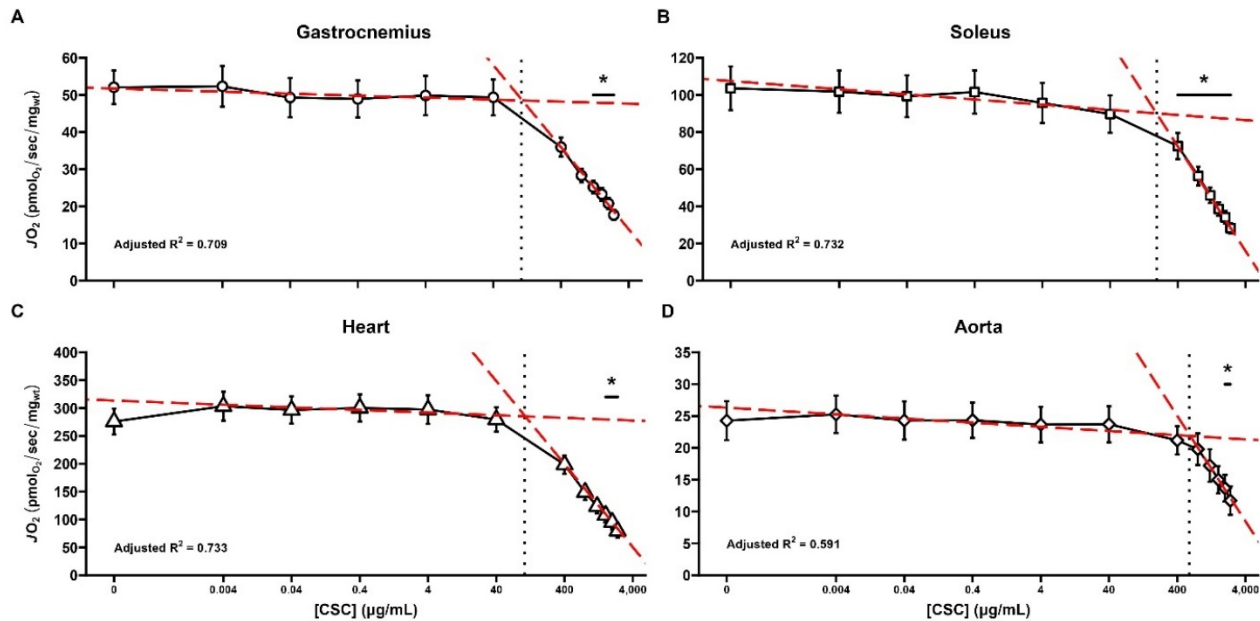


Figure 5-2. Absolute Respiration Rates for gastrocnemius ($n = 11$; A), soleus ($n = 11$; B), the heart ($n = 9$; C), and aorta ($n = 8$; D). Breakpoints are indicated by the dotted black line. Slopes of the piecewise linear regression are indicated by the red dashed lines. Values are represented as mean \pm SEM.

$113.0 \mu\text{g/mL}$; $p = 0.005$, $d = 2.3$), but not soleus ($213.8 \pm 124.2 \mu\text{g/mL}$; $p = 0.081$; $d = 0.7$).

However, there were no significant differences between the soleus and the gastrocnemius ($p = 0.187$; $d = 0.5$) or heart ($p = 0.081$; $d = 0.7$); nor were there differences between the gastrocnemius and the heart ($p = 0.209$; $d = 0.3$).

Likewise, tissue type had a significant main effect on the slope following the break ($p < 0.001$; partial $\eta^2 = 0.82$; Figure 5-3B). Post hoc analyses revealed that the rate of CSC-induced inhibition in the heart ($-145.1 \pm 45.5 JO_2/[CSC]$) was significantly different from the soleus ($-54.6 \pm 13.3 JO_2/[CSC]$; $p = 0.047$, $d = 3.5$), gastrocnemius ($-21.8 \pm 7.9 JO_2/[CSC]$; $p < 0.001$, $d = 4.8$), and aorta ($-15.3 \pm 9.5 JO_2/[CSC]$; $p < 0.001$, $d = 5.0$). Likewise, the rate of CSC-induced inhibition in the soleus was significantly different than the gastrocnemius ($p = 0.018$, $d = 1.3$) and the aorta ($p = 0.002$, $d = 1.5$). However, there was not a significant difference between the rate of CSC-induced inhibition in the gastrocnemius and the aorta ($p = 0.169$, $d = 0.7$).

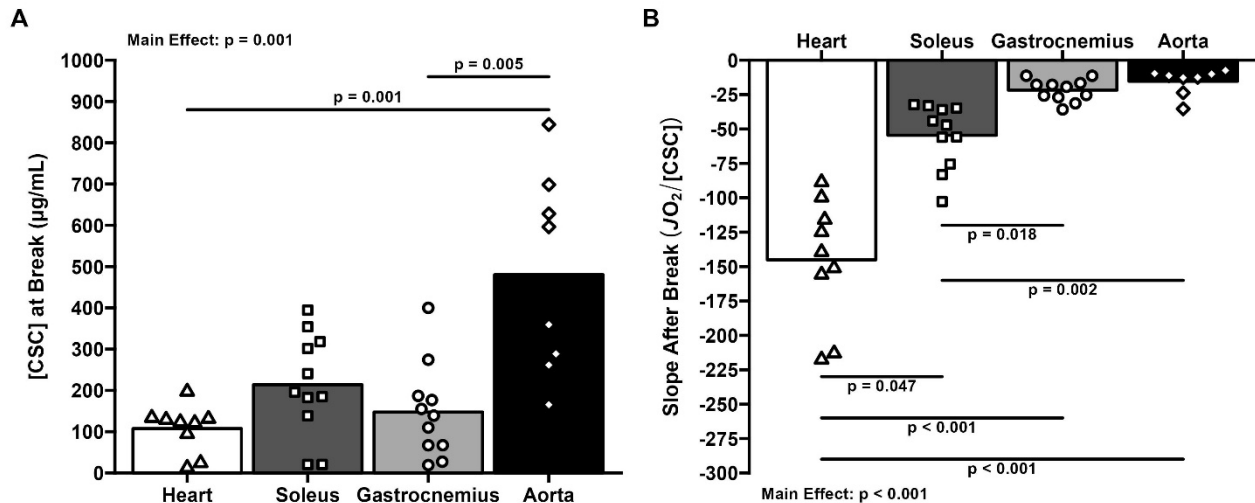


Figure 5-3. Results of the piecewise linear regression in absolute rates of mitochondrial respiration. Estimates of the breakpoint (A) and the slope following the breaking point (B) for the heart ($n = 9$; white), soleus ($n = 11$; dark grey), gastrocnemius ($n = 11$; light grey), and aorta ($n = 7$; black). Values are represented as mean \pm SEM.

5.6.2. Citrate Synthase Activities

CS activities for each tissue are shown in Figure 5-4. There was a significant main effect of tissue type on the CS activity ($p < 0.001$; partial $\eta^2 = 0.94$). Post hoc analyses revealed that CS activity in the heart (63.8 ± 6.4 AU) was significantly different from the soleus (22.3 ± 5.4 AU; $p < 0.001$, $d = 6.4$), gastrocnemius (9.4 ± 3.4 AU; $p < 0.001$, $d = 8.4$), and aorta (36.4 ± 9.3 AU; $p = 0.025$, $d = 4.3$). Likewise, the rate of CSC-induced inhibition in the soleus was significantly different than the gastrocnemius ($p = 0.025$, $d = 2.0$) and the aorta ($p < 0.001$, $d = 2.2$). Lastly, there was also a significant difference between the rate of CSC-induced inhibition in the gastrocnemius and the aorta ($p = 0.027$, $d = 4.2$).

5.6.3. Effects of CSC on Mitochondrial Respiration Normalized to CS Activity

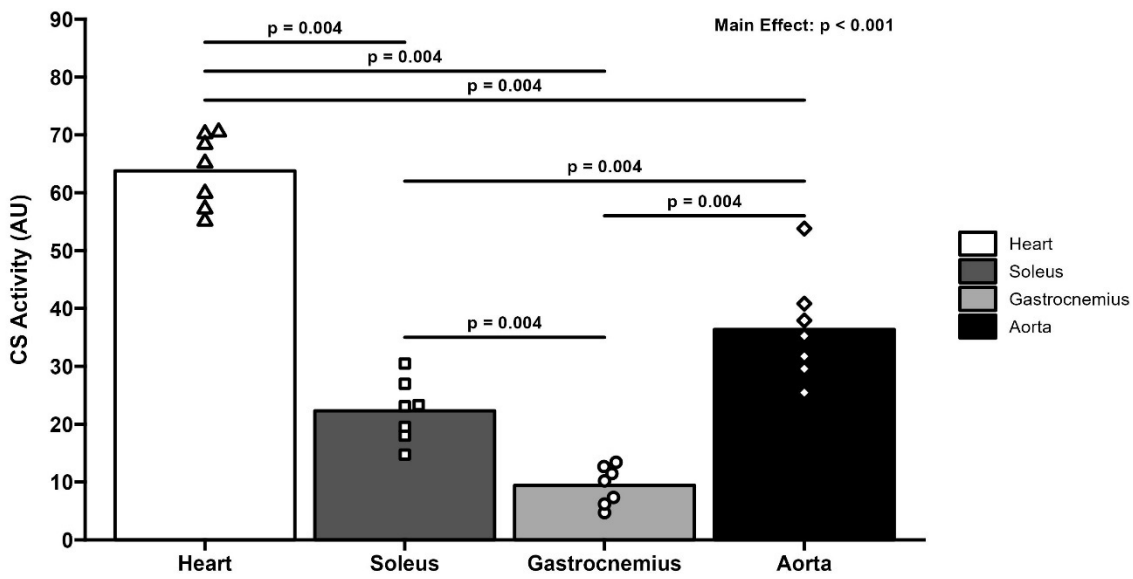


Figure 5-4. Citrate synthase activity for the heart (white), soleus (dark grey), gastrocnemius (light grey) and aorta (black). n = 7 for all tissues. Values are represented as mean \pm SEM.

Mitochondrial respiration rates normalized to CS activity of control tissues are shown in Figure 5-5. There were significant main effects of CSC ($p < 0.001$; partial $\eta^2 = 0.72$) and tissue type ($p < 0.001$; partial $\eta^2 = 0.72$), as well as a significant interaction effect ($p < 0.001$; partial $\eta^2 = 0.33$). Post hoc analyses for each tissue (Figure 5-6 A-D) revealed that the normalized respiration rates of the gastrocnemius, soleus, heart, and aorta were significantly (adjusted $p < 0.05$) inhibited by cigarette smoke starting at 1200 (3%), 400 (1%), 1600 (4%), and 2000 (5%) $\mu\text{g}/\text{mL}$, respectively.

Results of the piecewise linear regression are shown in Figure 5-6. Results from the one-way ANOVA revealed a significant main effect of tissue type on the breakpoint at which CSC mitochondrial respiration ($p = 0.001$; partial $\eta^2 = 0.37$; Figure 5-6A). Post hoc analysis revealed that the [CSC] at which the breakpoint occurs in the aorta ($480.2 \pm 243.1 \mu\text{g}/\text{mL}$) was significantly different from the heart ($107.5 \pm 37.3 \mu\text{g}/\text{mL}$; $p = 0.001$; $d = 2.6$) gastrocnemius ($147.5 \pm 113.0 \mu\text{g}/\text{mL}$; $p = 0.005$, $d = 2.3$), and soleus ($213.8 \pm 124.2 \mu\text{g}/\text{mL}$; $p = 0.001$; $d = 0.7$). However, there

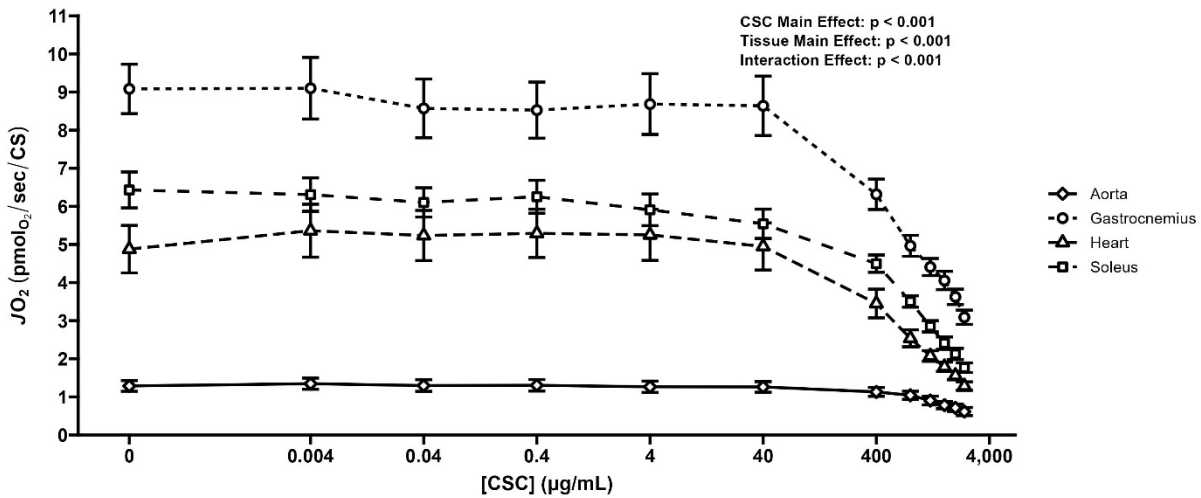


Figure 5-5. Respiration rates normalized to CS activity for the heart ($n = 9$; triangles), soleus ($n = 11$; squares), gastrocnemius ($n = 11$; circles), and aorta ($n = 8$; diamonds). Values are represented as mean \pm SEM.

were no significant differences between the soleus and the aorta ($p = 0.081$; $d = 1.9$), gastrocnemius ($p = 0.187$; $d = 0.5$), or heart ($p = 0.081$; $d = 0.7$); nor were there differences between the gastrocnemius and the heart ($p = 0.209$; $d = 0.3$).

Likewise, tissue type had a significant main effect on the slope following the break ($p < 0.001$; partial $\eta^2 = 0.53$; Figure 5-6B). Post hoc analyses revealed that the rate of CSC-induced inhibition in the aorta ($-0.8 \pm 0.4 J_O_2/CS/[CSC]$) was significantly different from the heart ($-2.6 \pm 1.4 J_O_2/CS/[CSC]$; $p = 0.021$, $d = 1.6$), soleus ($-3.4 \pm 1.0 J_O_2/CS/[CSC]$; $p < 0.001$, $d = 2.2$), and gastrocnemius ($-3.8 \pm 1.5 J_O_2/CS/[CSC]$; $p < 0.001$, $d = 2.6$). However, there were no significant differences between the heart and the gastrocnemius ($p = 0.138$, $d = 1.0$) or the soleus ($p = 0.193$, $d = 0.6$); nor were there significant differences between the gastrocnemius and the soleus ($p = 0.340$, $d = 0.4$).

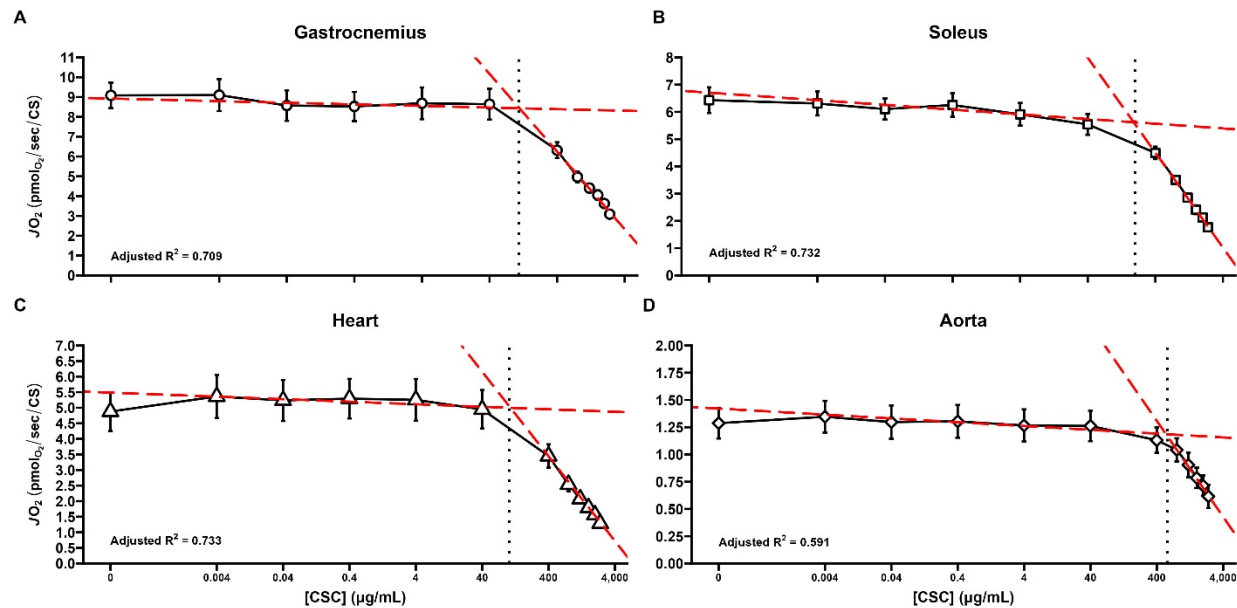


Figure 5-6. Respiration rates normalized for CS activity for gastrocnemius ($n = 11$; A), soleus ($n = 11$; B), the heart ($n = 9$; C), and aorta ($n = 8$; D). Breakpoints are indicated by the dotted black line. Slopes of the piecewise linear regression are indicated by the red dashed lines. Values are represented as mean \pm SEM.

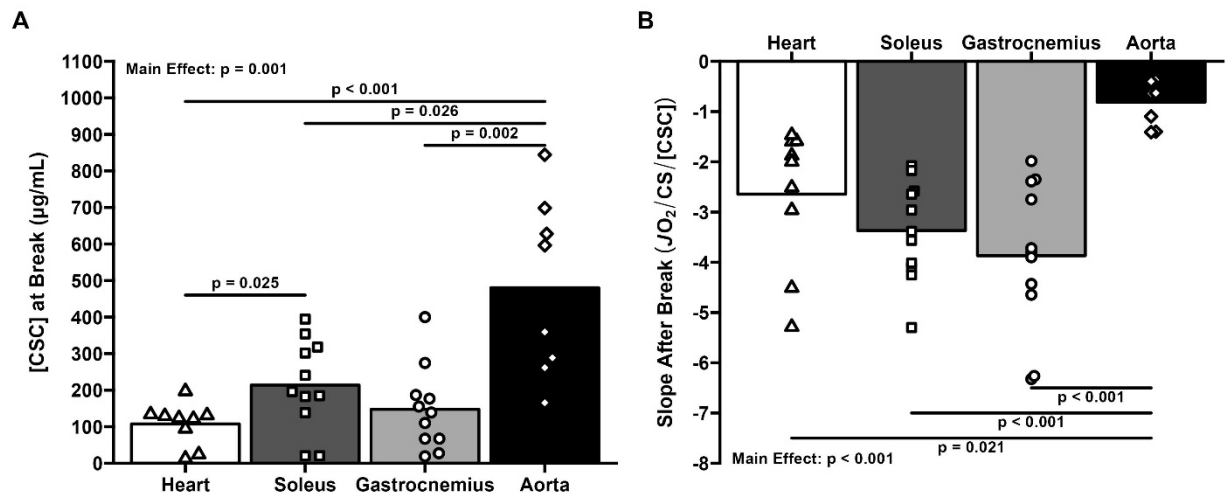


Figure 5-7. Results of the piecewise linear regression in mitochondrial respiration rates normalized to CS activity. Estimates of the breakpoint (A) and the slope following the breaking point (B) for the heart ($n = 9$; white), soleus ($n = 11$; dark grey), gastrocnemius ($n = 11$; light grey), and aorta ($n = 7$; black). Values are represented as mean \pm SEM.

5.7. Discussion

Cigarette smoke exposure is implicated in the pathophysiology of several cardiometabolic diseases, of which mitochondrial dysfunction may play a significant role. However, the direct effects of cigarette smoke on mitochondrial function have not been fully characterized. Therefore, this study aimed to determine the acute dose-response relationship between cigarette smoke condensate (CSC) and mitochondrial function on intact permeabilized skeletal muscle, heart, and aorta. Indeed, cigarette smoke condensate directly impaired mitochondrial respiration in each of these tissues. Furthermore, as indicated by tissue-dependent breakpoints in the CSC-induced inhibition of mitochondrial respiration, our results reveal a distinct threshold at which CSC directly impairs mitochondrial respiration in these tissues, suggesting a tissue-specific susceptibility to the negative impacts of cigarette smoke. In line with our hypothesis, cardiac muscle mitochondria exhibited the greatest loss of mitochondrial respiration per [CSC], indicating a greater susceptibility of the heart to CSC-induced bioenergetic deficits than other tissues used in this study. Alternatively, the aorta was the least sensitive and susceptible to CSC-induced mitochondrial impairments. When normalized to CS activity in order to account for differences in mitochondrial content between tissues (S. Larsen, Nielsen, et al., 2012), however, cardiac mitochondria were equally susceptible to CSC as the gastrocnemius and similarly sensitive to CSC as the gastrocnemius and soleus. However, the aorta remained the least susceptible and least sensitive to CSC-induced mitochondrial dysfunction, indicating an intrinsic quality of mitochondria in vascular smooth muscle which protects from CS-induced toxicity. Together, these findings are the first to establish the susceptibility and sensitivity of the skeletal muscle, cardiac muscle, and vascular tissue to cigarette smoke-induced mitochondrial impairments and indicate that, compared

to striated muscles, vascular smooth muscle mitochondria have intrinsic characteristics which provide greater protection from smoke-induced toxicity.

5.7.1. Cigarette Smoke Condensate Directly Impairs Mitochondrial Respiration

Cigarette smoke condensate had an inhibitory effect on mitochondrial respiration in all tissues examined in the present study, as shown in Figures V-1 and V-2. As indicated by attenuated mitochondrial respiration, bioenergetic deficits were observed at concentrations as low as 40 µg/mL (0.1%) CSC and, at greater concentrations, resulted in up to a ~10% decrease in mitochondrial respiration in several tissues used in the present study. Moreover, at the final concentration of 2400 µg/mL (6%) CSC, mitochondrial respiration was inhibited by up to ~60% compared to maximal state III respiration in the gastrocnemius, soleus, and heart, and by ~40% in the aorta. These findings collectively demonstrate that cigarette smoke directly induces mitochondrial bioenergetic deficits in a dose-dependent manner, thus resulting in decreased oxidative ATP production that may drive cellular dysfunction in these tissues, ultimately leading to the development of cardiometabolic disease and increased risk of premature death.

The tissue-specific inhibitory effects of CSC on mitochondrial function observed in the present study were similar to those previously used to induce mitochondrial dysfunction in mitochondria isolated from a range of tissues, including lung epithelial tissue, carotid arteries, cardiac muscle, and skeletal muscle. (Csiszar et al., 2009; Khattri et al., 2022; Naserzadeh et al., 2015; Naserzadeh & Pourahmad, 2013; Orosz et al., 2007; Thatcher et al., 2014; van der Toorn et al., 2007, 2009). However, the present study extends the findings of these other studies by adding the novelty of using intact permeabilized tissues rather than isolated mitochondria. The use of

permeabilized tissues, compared with isolated mitochondria, has the added benefit of maintaining the structural integrity of the surrounding cellular environment, which, considering that mitochondria form a vast reticulum across cells (Glancy et al., 2015), preserves the mitochondrial structure and prevents potential bias (Picard et al., 2010) and better reflects the *in vivo* condition (Jacobs et al., 2013; Kuznetsov et al., 2008a; Layec et al., 2016).

Considering these methodological differences between the use of isolated mitochondria and permeabilized fibers, it is essential to note that these differences result in significant changes to the susceptibility of the mitochondria to CSC. For example, Khattri et al. (2022) found that incubating mitochondria isolated from a mixture of mouse skeletal muscles in 0.02%, 0.1%, and 1.0% CSC solution for 10 minutes impaired state III mitochondrial respiration by 5%, 22%, and 61%, respectively. Alternatively, the present study provides evidence that permeabilized skeletal muscle fibers are more resistant to CSC than mitochondria isolated from skeletal muscle, as much higher (~2-10 times) CSC concentrations were needed study to elicit similar decrements in mitochondrial respiration as Khattri et al. The increased resistance to CSC in permeabilized fibers, as opposed to isolated mitochondria, are likely due to diffusion limitations caused by structural components of the mitochondria and the surrounding cellular components of skeletal muscle, as is the case with ADP diffusion (V. Saks et al., 1991; V. A. Saks et al., 2010). Therefore, while CSC is indeed able to induce mitochondrial dysfunction, there appear to be distinct differences in the concentration of CSC required to cause acute dysfunction between isolated mitochondria and intact tissue samples, likely due to the loss of the reticular structure as a result of the isolation procedures (Picard et al., 2011).

5.7.2. Aorta is Intrinsically Less Susceptible and Sensitive to CSC Than Gastrocnemius, Soleus, or Heart

An important aspect of the present study is that we were able to characterize the susceptibility and sensitivity to CSC of the aorta, heart, and two physically unique skeletal muscles, which has not yet been done. Using a piecewise linear regression, we identified a breakpoint at which cigarette smoke significantly begins to alter mitochondrial respiration (Figures 3A & 6A). Based on this analysis, we estimate that the mitochondria in the aorta exhibit deficits in mitochondrial respiration beginning at ~500 µg/mL CSC – between two and five times the amount required to change the slope of the CSC-induced loss of respiration of the gastrocnemius and soleus, and heart, respectively. These changes were also observed following normalizing for the differences in mitochondrial content. Moreover, the sensitivity (Figures V-4B & V-6B) of the aorta to CSC-induced mitochondrial dysfunction was the lowest of the tissues used in the present study by 2-5 fold, especially when normalized for CS activity. Therefore, we provide evidence that the mitochondria in the aorta are intrinsically less susceptible to the negative impacts of cigarette smoke exposure than mitochondria in skeletal and cardiac muscle.

These findings are rather surprising, as mitochondria from cardiac muscle, skeletal muscle, and skeletal muscle feed arteries have been shown to have similar respiration rates when these tissues are normalized for differences in mitochondrial content, as measured by citrate synthase activity (S. Y. Park et al., 2014). Additionally, much like skeletal muscle, mitochondria in the skeletal muscle feed arteries respond positively to exercise training (S. Y. Park et al., 2016) and become impaired with advancing age (S. H. Park et al., 2018), indicating functional similarities between mitochondria in the vasculature and skeletal muscle. However, the CS activities of the

skeletal muscle feed arteries in these studies were much lower than the CS activity in the present study. While we cannot fully explain the wide discrepancies between our results and the other studies, there may be inherent differences in the mitochondrial content across the vascular tree. Furthermore, considering the wide diversity of the structural and functional components of vascular tissues (Lacolley et al., 2017), mitochondria may have very distinct morphological properties across the vascular tree. Specifically, it is widely considered that the main role of peripheral arteries, such as skeletal muscle feed arteries, is to regulate local blood flow and maintain mean arterial pressure, while the role of more centrally-located arteries, such as the aorta, is to withstand the extremely high pressure invoked by systolic contractions of the heart (Lacolley et al., 2017). As such, to maintain arterial compliance in response to large variations in pressure, central arteries are composed of tissues that maintain arterial stiffness (i.e., elastin, collagen), which become less abundant in peripheral arteries (Lacolley et al., 2017). These changes in artery composition may play important roles in also shaping the morphology of the mitochondrial reticulum (Glancy et al., 2017) in the specific regions of the vascular tree, thus altering the regional function of the mitochondria. However, further research is needed to determine the structural properties of mitochondria across the vascular network.

5.7.3. Sensitivity to CSC in Striated Muscle is Dependent on Mitochondrial Content

In contrast to the resistance to CSC observed in the aorta, the other tissues used in the present study, specifically the heart and the soleus, were extremely sensitive to CSC-induced deficits in mitochondrial bioenergetics. As such, the heart exhibited a loss of mitochondrial respiration per [CSC] at a rate 3 times greater than the soleus and 6 times greater than the

gastrocnemius. Similarly, the soleus decreased at a rate 2 times greater than the gastrocnemius. However, these significant findings were abolished when the CSC-induced decreases in respiration were normalized to CS activity. Therefore, these findings suggest that the differences in sensitivity between striated muscles can be attributed solely to the vast differences in mitochondrial content of these tissues rather than some other inherent property of the tissue.

Cigarette smoke exposure is associated with dramatic increases in numerous chronic cardiovascular and muscular ailments, including peripheral artery disease, heart failure, type II diabetes, and sarcopenia (Jo et al., 2019; Lee & Choi, 2019; Maddatu et al., 2017c; Münzel et al., 2020; Steffl et al., 2015). The mitochondrial density-dependent responses to CSC observed in striated muscles in the present study explain, in part, the high incidence of cardiomyopathies in chronic smokers (i.e., heart failure) and why type I muscle fibers are more apt to atrophy and cellular dysfunction than type II fibers in chronic smokers (Degens et al., 2015; Gosker et al., 2007, 2009). Indeed, several reports from our lab (Decker, Kwon, Zhao, Hoidal, Heuckstadt, et al., 2021) and others (Gosker et al., 2007, 2009; Kapchinsky et al., 2018; Montes De Oca et al., 2008a) have reported more pronounced cigarette smoke-induced atrophy of type I skeletal muscle fibers compared to type II fibers, thereby inducing a shift towards anaerobic metabolism and increased susceptibility to fatigue (Amann et al., 2010; Nogueira et al., 2018). Likewise, these explain why ventricular remodeling is a common manifestation in several models of smoke exposure in animals (Kaplan et al., 2017) and humans (Barutcu et al., 2008; Minicucci et al., 2012; Nadruz et al., 2016). Given the greater mitochondrial density of the left ventricle and the soleus (~6- and ~2-fold greater than the gastrocnemius, respectively), these tissues, as our data suggest, would likely be more prone to CSC-induced deficits in mitochondrial bioenergetics due to their greater reliance on

oxidative ATP production. The bioenergetic deficits in the soleus muscles and, even more so, cardiac muscles, which have a greater portion of slow-twitch muscle fibers (Augusto et al., 2004; Gorza et al., 1986), could then activate cellular mechanisms which result in severe muscle atrophy (Hyatt et al., 2019) specific to these tissues and often reported in chronic smokers (Montes De Oca et al., 2008a). Thus, our findings support the hypothesis that striated muscle fibers with a greater mitochondrial density are more sensitive to CSC-induced deficits in mitochondrial bioenergetics due to a mismatch between absolute, but not relative, oxidative energy supply and demand. These decrements result in a mismatch between ATP supply and demand that, ultimately, leads to contractile dysfunction and loss of cellular function, leading to poor health outcomes.

5.8. Conclusions

In conclusion, this study revealed the sensitivity and susceptibility characteristics of cigarette smoke-induced mitochondrial dysfunction in gastrocnemius, soleus, heart, and aorta (Figure 5-7). Collectively, the results from these studies suggest that inherent characteristics of mitochondria in the aorta increase the resistance to CSC-induced bioenergetic deficits. On the other hand, the CSC-induced insults to mitochondrial respiration in striated muscles are largely dependent on the mitochondrial density of these tissues. However, considering the range of bioenergetic demand in these tissues, especially cardiac muscle, even minor deficits in oxidative ATP production could lead to severe bioenergetic deficits and cellular dysfunction. Thus, the findings in the present study characterized the direct changes to mitochondrial respiration in a range of muscle types that are severely altered by cigarette smoke exposure, thus contributing cigarette smoke exposure to the development of several chronic cardiometabolic diseases.

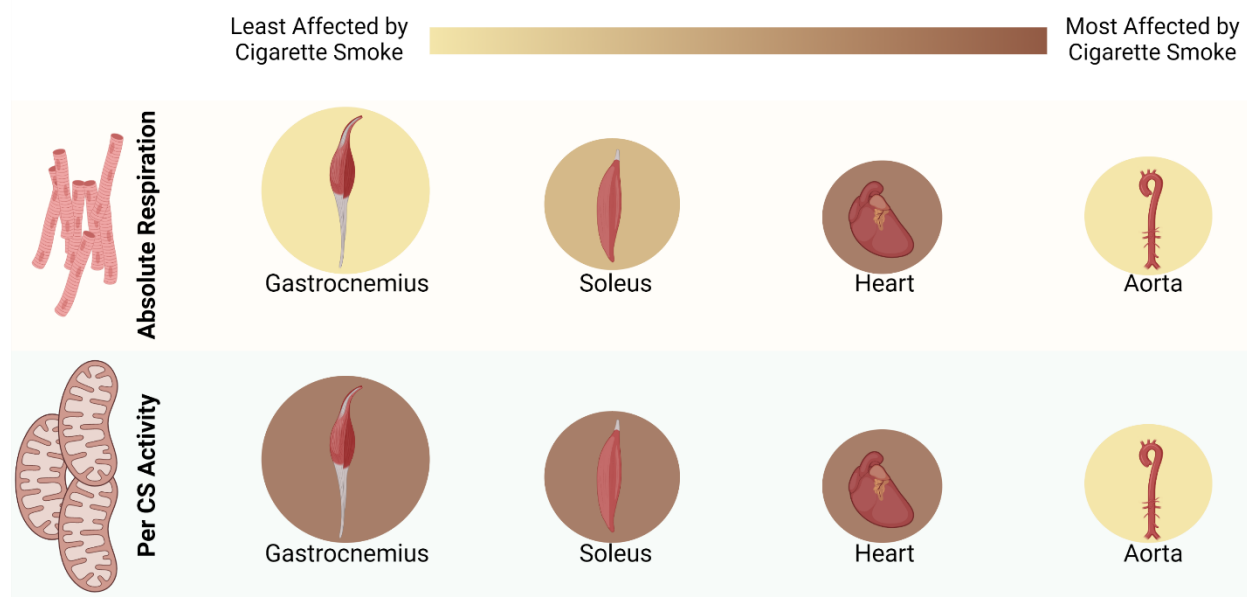


Figure 5-8. Summary of findings from Aim 1.

CHAPTER 6

AIM II RESULTS AND DISCUSSION

6.1. Effects of Cigarette Smoke on *In Situ* Mitochondrial Substrate Oxidation of Slow- and Fast-Twitch Skeletal Muscles

Stephen T Decker¹, Alexs A Matias¹, Sean T Bannon¹, Jack P Madden¹, Nadia Alexandrou-Majaj³, Gwenael Layec^{1,2}

Department of Kinesiology¹, Department of Psychological & Brain Sciences³, and the Institute for Applied Life Science²

University of Massachusetts Amherst, USA

Running Title: Cigarette Smoke Alterations to Mitochondrial Substrate Oxidation

Keywords: Skeletal Muscle, High-Resolution Respirometry, Palmitoylcarnitine, Pyruvate, Cigarette Smoke

Corresponding Author: Gwenael Layec

Life Sciences Laboratories, 240 Thatcher Rd, Amherst, MA 01003

Email: glayec@umass.edu

6.2. Abstract

Epidemiological and clinical evidence suggests that cigarette smoke exposure alters glucose and fatty acid metabolism, leading to greater susceptibility to metabolic disorders. However, the effects of cigarette smoke exposure on mitochondrial substrate oxidation in the skeletal muscle are still poorly understood. Accordingly, this study aimed to examine the acute effects of cigarette smoke on mitochondrial respiratory capacity, sensitivity, and concurrent utilization of palmitoylcarnitine (PC), a long-chain fatty acid, and pyruvate, a product of glycolysis, in permeabilized gastrocnemius and soleus muscle fibers. Cigarette smoke decreased both mitochondrial respiratory capacity (CONTROL: $50.4 \pm 11.8 \text{ pmol O}_2/\text{sec/mg}_{\text{wt}}$ and SMOKE: $22.3 \pm 4.4 \text{ pmol O}_2/\text{sec/mg}_{\text{wt}}$, $p < 0.01$) and sensitivity for pyruvate (CONTROL: $0.10 \pm 0.04 \text{ mM}$ and SMOKE: $0.11 \pm 0.04 \text{ mM}$, $p < 0.01$) in the gastrocnemius muscle. In the soleus, only the sensitivity for pyruvate-stimulated mitochondrial respiration trended towards a decrease (CONTROL: $0.11 \pm 0.04 \text{ mM}$ and SMOKE: $0.23 \pm 0.15 \text{ mM}$, $p = 0.08$). In contrast, cigarette smoke did not significantly alter palmitoylcarnitine-stimulated mitochondrial respiration in either muscle. In the control condition, pyruvate-supported respiration was inhibited by the concurrent addition of palmitoylcarnitine in the fast-twitch gastrocnemius muscle ($-27.1 \pm 19.7\%$, $p < 0.05$), but not in the slow-twitch soleus ($-9.2 \pm 17.0\%$). With cigarette smoke, the addition of palmitoylcarnitine augmented the maximal respiration rate stimulated by the concurrent addition of pyruvate in the gastrocnemius ($+18.5 \pm 39.3\%$, $p < 0.05$). However, cigarette smoke still significantly impaired mitochondrial respiratory capacity with combined substrates than control ($p < 0.05$). Our findings underscore that cigarette smoke directly impairs mitochondrial respiration of carbohydrate-derived substrates and is a primary mechanism underlying cigarette smoke-

induced muscle dysfunction, which leads to a vicious cycle involving excess glucose conversion into fatty acids and lipotoxicity.

6.3. New & Noteworthy

While cigarette smoke exposure is a well-known risk factor for the development of metabolic disorders, it is unclear how mitochondrial substrate metabolism is directly affected by cigarette smoke. Herein, while acute cigarette smoke exposure did not significantly alter fatty acid metabolism, cigarette smoke significantly impaired mitochondrial pyruvate oxidation. Furthermore, acute cigarette smoke exposure augmented mitochondrial respiration in the presence of competing substrates. With this evidence, we demonstrate that pyruvate oxidation is directly impaired by cigarette smoke, thus providing mechanistic insights into the link between cigarette smoking and the development of metabolic diseases.

6.4. Introduction

Cigarette smoke exposure is accountable for up to 480,000 premature deaths per year in the United States (United States Department of Health and Human Services, 2014), and is considered an independent risk factor for metabolic diseases such as type 2 diabetes (Pan et al., 2015), metabolic syndrome (Sun et al., 2012), and non-alcoholic fatty liver disease (Rezayat et al., 2018). Phenotypically, tobacco smoke exposure results in higher central adiposity (Canoy et al., 2005; Chiolero et al., 2008), ectopic fat accumulation (Sinha-Hikim et al., 2014; Terry et al., 2020), and lower muscle mass (Ajime et al., 2020; Terry et al., 2020). Despite abundant evidence of its negative impact on health, the mechanisms underlying the metabolic toxicity of cigarette smoke are, however, still poorly understood.

Dyslipidemia is common in cigarette smokers who exhibit higher levels of circulating cholesterol (Muscat et al., 1991b), intramuscular saturated or non-saturated triglycerides (Bergman et al., 2009; Terry et al., 2020), and saturated diacylglycerol (Bergman et al., 2009) compared to non-smokers. In this regard, acute exposure to cigarette smoke has been documented to increase circulating free fatty acids (FFA) (Hellerstein et al., 1994) and whole-body palmitate rate of appearance and oxidation measured by ¹³C isotope tracers during fasting conditions in young adults (Bergman et al., 2009). Similar alterations to lipid metabolism were observed in chronic smokers, which were attenuated upon smoking cessation (Bergman et al., 2012). Together, these findings suggest that cigarette smoke stimulates adipose tissue lipolysis coupled to incomplete fatty acid oxidation in peripheral tissues, thus resulting in ectopic fat accumulation in the skeletal muscle. However, whether incomplete oxidation of fatty acids is attributable to direct smoke-induced inhibition of mitochondrial capacity to utilize fatty acids is still unknown.

Cigarette smoke is also strongly linked to glucose metabolism abnormalities and the development of skeletal muscle insulin resistance (Artese et al., 2017; Bergman et al., 2009), which is partly mediated by insulin receptor inhibition on the muscle cell membrane (Bergman et al., 2012). Interestingly, exposure to cigarette smoke also impairs muscle mitochondrial respiratory capacity using substrates replicating the Krebs cycle (glutamate, malate, and succinate) (Thatcher et al., 2014) as we have shown in aim 1, thus also implicating mitochondrial dysfunction in the pathogenesis of insulin resistance with cigarette smoke. Of note, inhibition of ceramide formation, a fatty acid of the sphingolipid family, by myriocin resulted in higher *in situ* respiratory capacity in skeletal muscle permeabilized fibers (Thatcher et al., 2014), which alluded to a potential role for ceramide accumulation and lipotoxicity in the inhibition of mitochondrial respiration by cigarette smoke. However, mitochondrial fatty acid oxidation was not assessed, and ceramide inhibition improved mitochondrial respiration regardless of smoking status in this study, which suggests that the effects of ceramides were not specific to cigarette smoke exposure. Thus, it is still unclear whether cigarette smoke directly caused ceramide accumulation resulting in mitochondrial dysfunction, or if ceramide accumulation was secondary to a shift in mitochondrial substrate sensitivity and/or impaired respiration with glycolytic products, thus causing glucose conversion into fatty acids and triglycerides.

Accordingly, this study aimed to determine cigarette smoke's acute effects on substrate sensitivity, respiratory capacity, and fuel interaction in skeletal muscles with different metabolic profiles. Specifically, we assessed mitochondrial respiration *in situ* using palmitoylcarnitine (PC), a long-chain fatty acid, and pyruvate, a product of glycolysis, in predominantly fast (white gastrocnemius) and slow-twitch (soleus) skeletal muscle fibers exposed to cigarette smoke

concentrate (CSC). We hypothesized that CSC would impair mitochondrial respiration (sensitivity and maximal capacity) supported by pyruvate, whereas fatty acid-linked respiration will remain unaltered. As a result, mitochondrial substrate preference with CSC would shift toward greater lipid oxidation.

6.5. Methods

6.5.1. Animals and Experimental Design

Eleven mature C57BL/6 mice (male/female: 7/4) were used for this study. All animals were maintained on a 12-hour dark/light cycle and fed standard chow *ad libidum*. Protocols were approved by the Institutional Animal Care and Use Committee of UMASS Amherst. Following euthanasia by 5% isoflurane, the gastrocnemius and soleus were immediately harvested and placed in ice-cold BIOPS preservation solution (Kuznetsov et al., 2008a; Pesta & Gnaiger, 2012). The gastrocnemius and soleus were specifically chosen to encompass tissues with different metabolic properties (Augusto et al., 2004).

6.5.2. Preparation of Permeabilized Muscle Fibers

The tissue preparation and respiration measurement techniques were adapted from established methods (Kuznetsov et al., 2008a; Pesta & Gnaiger, 2012) and have been previously described by our group (Decker, Kwon, Zhao, Hoidal, Heuckstadt, et al., 2021). Briefly, BIOPS-immersed fibers (2.77mM CaK2EGTA, 7.23mM K2EGTA, 50mM K⁺ MES, 6.56 mM MgCl₂, 20mM Taurine, 5.77mM ATP, 15mM PCr, 0.5mM DTT, 20mM Imidazole) were carefully separated with fine-tip forceps and subsequently bathed in a BIOPS-based saponin solution (50 µg saponin.ml⁻¹ BIOPS) for 30 minutes at 4°C. Following saponin treatment, muscle fibers were rinsed twice in ice-cold mitochondrial respiration fluid (MIR05, in mM: 110 Sucrose, 0.5 EGTA, 3 MgCl₂, 60 K-lactobionate, 20 taurine, 10KH₂PO₄, 20 HEPES, BSA 1g.L⁻¹, pH 7.1) for 10 minutes each.

Following chemical permeabilization, tissues were incubated for 1-hour in a 2 mL solution

of MiR05 (control) or MiR05 with 4% (1600 µg/mL) cigarette smoke concentrate (CSC; Murty Pharmaceuticals, Lexington, KY) at 4°C. This concentration of cigarette smoke was chosen based on pilot studies indicating that this concentration replicates the mitochondrial perturbations previously documented in mice and humans chronically exposed to cigarette smoke (Ajime et al., 2020; Gifford et al., 2018a; Thatcher et al., 2014).

After the muscle sample was gently dabbed with a paper towel to remove excess fluid, the wet weight of the sample (1-2 mg) was measured using a standard, calibrated scale. The muscle fibers were then placed in the respiration chamber (Oxygraph O2K, Oroboros Instruments, Innsbruck, Austria) with 2 ml of MIR05 solution warmed to 37°C. Oxygen was added to the chambers, and oxygen concentration was maintained between 190-250 µM. After allowing the permeabilized muscle sample to equilibrate for 5 minutes, mitochondrial respiratory function was assessed in duplicate. Following the addition of each substrate, the respiration rate was recorded until a steady state of at least 30-seconds was reached, the average of which was used for data analysis. To assess mitochondrial respiration supported by glycolysis or fatty acids, the rate of O₂ consumption (picomoles per second per milligram of wet weight) was assessed with 2 protocols:

6.5.3. Protocol 1: Pyruvate-Stimulated Respiration

Saturating concentrations of malate (M; 2mM) and ADP (D; 5 mM) were added to the chamber, followed by a stepwise titration of pyruvate (P) at a final concentration of 0.10, 0.25, 0.50, 1, and 5 mM. Cytochrome c (10 µM) was then added to the chamber to assess mitochondrial membrane integrity (Kuznetsov et al., 2008a; Pesta & Gnaiger, 2012). Finally, antimycin A (2.5 µM) and oligomycin (5 nM) were added to assess residual, non-mitochondrial oxygen

consumption (AmA & Omy).

6.5.4. Protocol 2: Palmitoylcarnitine-Stimulated Respiration and Pyruvate-Palmitoylcarnitine Respiration Interaction

To assess palmitoylcarnitine-stimulated respiration, saturating concentrations of malate (M; 2mM) and ADP (D; 5 mM) were added to the chamber, followed by a stepwise titration of palmitoylcarnitine (Palm), resulting in final concentrations of 0.0025, 0.005, 0.0125, 0.025, and 0.04 mM. Pyruvate was then titrated in the chambers to assess the kinetics of pyruvate in the presence of palmitoylcarnitine using Protocol 1. Membrane integrity was tested with cytochrome C, followed by the addition of antimycin A and oligomycin to assess residual, non-mitochondrial oxygen consumption.

6.5.5. Data Analysis

Apparent K_m and V_{max} were determined using a 3-parameter model of the Michaelis-Menten equation:

$$JO_2 = C + \frac{V_{max} + C}{1 + \frac{K_m}{[S]}}$$

where JO_2 is the respiration rate at the concentration of a given substrate [S], and c is JO_2 when $[S] = 0$.

Samples that demonstrated impaired mitochondrial membrane integrity (more than a 10% increase in respiration in response to cytochrome C) were excluded from the analysis (n=3). All extreme outliers (more extreme than $Q1 - 3 * IQR$ or $Q3 + 3 * IQR$) were also excluded from the

analysis. Normality and homoscedasticity were determined using the Shapiro-Wilk and Levene's tests, respectively. The effects of cigarette smoke and tissue on the K_m and V_{max} for each substrate were determined using a two-way (Smoke x Tissue) non-parametric Aligned Ranks Transform (ART) ANOVA (Oliver-Rodríguez & Wang, 2015). If main effects or interaction effects were determined to be statistically significant ($p < 0.05$), post hoc comparisons were performed using Dunn's test with a Holm-Sidak correction. Effect sizes were determined by calculating the partial eta-squared (η^2) and Cohen's d (d) for both the ART ANOVA and the post hoc comparisons, respectively. For clarity, the results are presented as mean \pm SD in text and tables and mean \pm SEM in the figures.

6.6. Results

6.6.1. Effects of CSC on Mitochondrial Respiration supported by Pyruvate Oxidation

Dose-response curves for pyruvate-supported respiration in each tissue are shown in Figures VI-1A and VI-1B. Smoke and tissue type had significant main (Smoke: $p < 0.001$, partial $\eta^2 = 0.56$; Tissue: $p = 0.008$, partial $\eta^2 = 0.22$) and interaction effects ($p = 0.008$, partial $\eta^2 = 0.22$) on the apparent sensitivity (K_m) of the mitochondria to pyruvate (Fig 1C). Post hoc tests indicated that K_m of the control gastrocnemius (0.10 ± 0.04 mM) was significantly lower than the CSC-exposed gastrocnemius (0.45 ± 0.19 mM, adj. $p < 0.001$, $d = 2.51$) and CSC-exposed soleus (0.23 ± 0.15 mM, adj. $p = 0.045$, $d = 1.23$). Likewise, the control soleus (0.11 ± 0.04 mM) had a

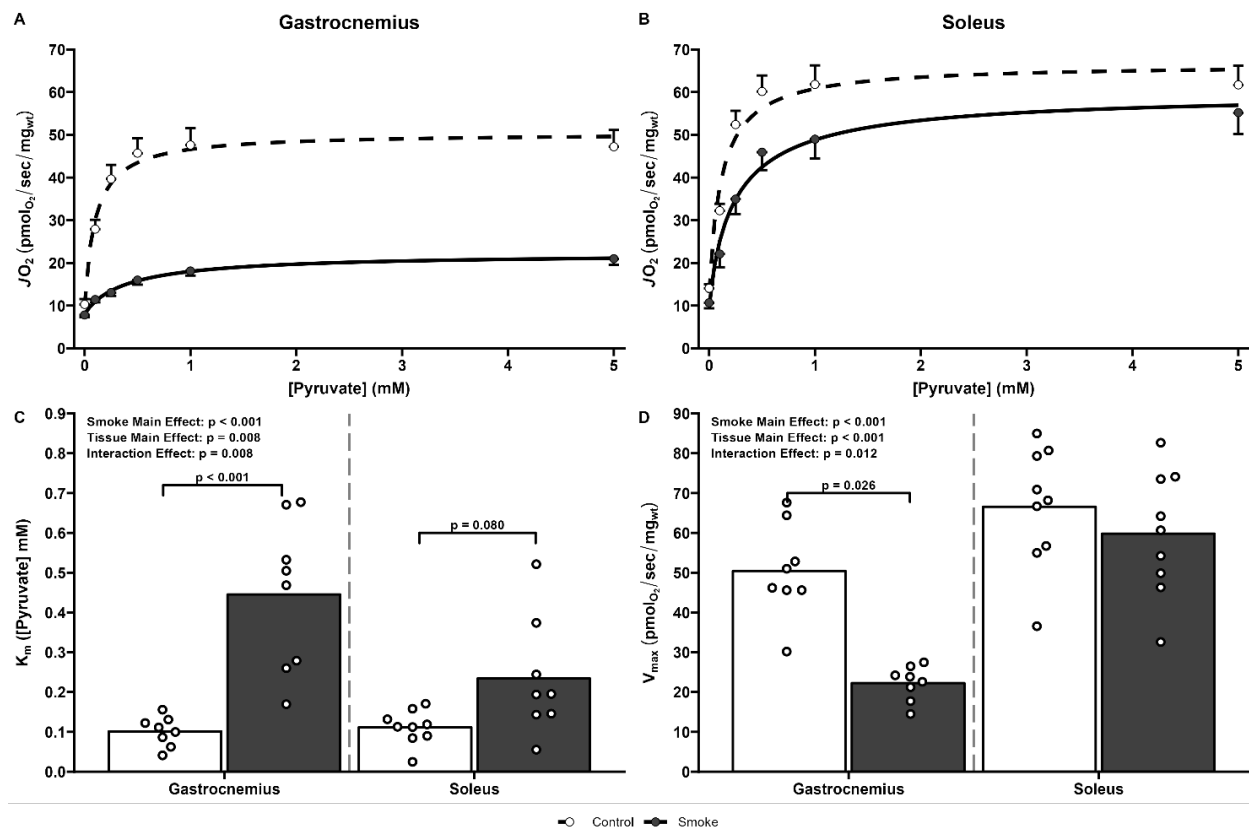


Figure 6-1. Dose-response curve for Pyruvate-stimulated mitochondrial respiration in the Gastrocnemius (A; $n = 8$ per group) and Soleus (B; $n = 8-9$ per group), and the mean estimates for the apparent K_m (C) and V_{max} (D) of mitochondrial respiration to pyruvate for both control (white) and CSC-exposed (grey) fibers. Values are expressed as mean \pm SEM, where appropriate.

significantly lower K_m than the CSC-exposed gastrocnemius (adj. $p = 0.001$, $d = 2.42$) while the difference between the control soleus and the CSC-exposed soleus did not reach significance (adj. $p = 0.080$, $d = 1.13$). There was not a significant difference in the sensitivity to pyruvate between the control gastrocnemius and the control soleus (adj. $p = 0.337$, $d = 0.25$), or the CSC-exposed gastrocnemius and the CSC-exposed soleus (adj. $p = 0.106$, $d = 1.24$).

Similar to the K_m , smoke and tissue type had significant main (Smoke: $p < 0.001$, partial $\eta^2 = 0.35$; Tissue: $p < 0.001$, partial $\eta^2 = 0.52$) and interaction effects ($p = 0.012$, partial $\eta^2 = 0.19$) on the maximal respiration capacity (V_{max}) of the mitochondria to pyruvate (Fig 1D). Post hoc tests indicated that the V_{max} of the CSC-exposed gastrocnemius (22.3 ± 4.4 pmol O_2 /sec/mg_{wt}) was significantly lower than the control gastrocnemius (50.4 ± 11.8 pmol O_2 /sec/mg_{wt}; adj. $p = 0.029$, $d = 3.17$), control soleus (66.6 ± 15.2 pmol O_2 /sec/mg_{wt}; adj. $p < 0.001$, $d = 3.96$), and CSC-exposed soleus (59.8 ± 15.8 pmol O_2 /sec/mg_{wt}; adj. $p = 0.001$, $d = 3.25$). However, there was not a significant difference between the control gastrocnemius and the control soleus (adj. $p = 0.099$, $d = 1.18$), the control soleus and the smoke-exposed soleus (adj. $p = 0.224$, $d = 0.44$), or the control gastrocnemius and the smoke-exposed soleus (adj. $p = 0.258$, $d = 0.67$).

6.6.2. Effect of CSC on Mitochondrial Respiration supported by Palmitoylcarnitine Oxidation

Dose-response curves for PC-supported respiration in each tissue are shown in Figures VI-2A and VI-2B. While tissue type had a significant main effect on mitochondrial PC sensitivity ($p = 0.002$, partial $\eta^2 = 0.32$), we observed no effect of CSC ($p = 0.220$, partial $\eta^2 = 0.06$) or an interaction effect ($p = 0.220$, partial $\eta^2 = 0.06$; Fig VI-2C). Post hoc analysis of the tissue main

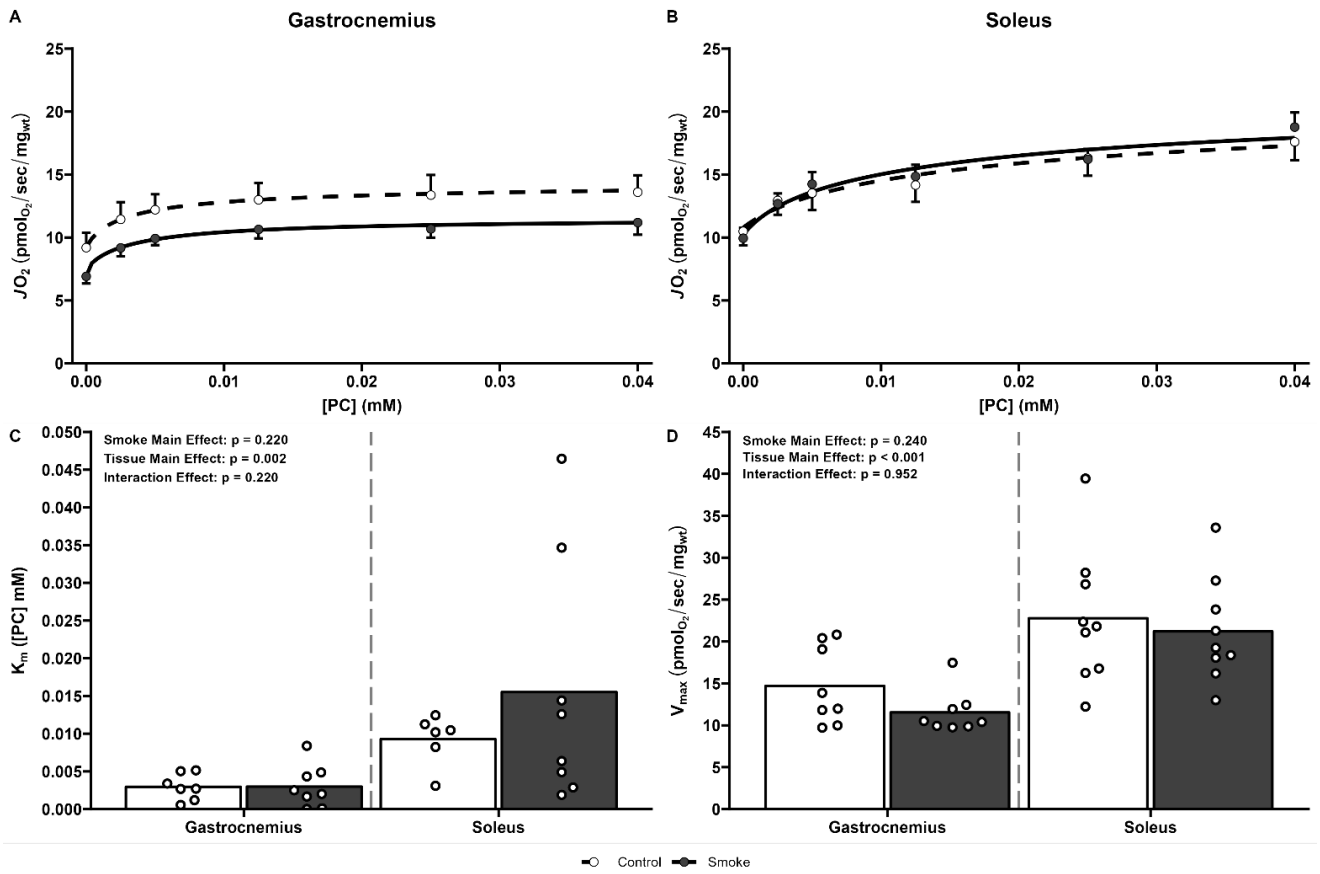


Figure 6-2. Dose-response curve for palmitoylcarnitine-stimulated mitochondrial respiration in the Gastrocnemius (A; $n = 7-8$ per group) and Soleus (B; $n = 8-9$ per group), and the mean estimates for the apparent K_m (C) and V_{max} (D) of mitochondrial respiration to palmitoylcarnitine (PC) for both control (white) and cigarette smoke condensate-exposed (grey) fibers. Values are expressed as mean \pm SEM, where appropriate.

effects indicated that the K_m of the gastrocnemius (Control: 0.0030 ± 0.0017 ; Smoke: 0.0030 ± 0.0027) was significantly lower than the K_m of the soleus (Control: 0.0093 ± 0.0033 ; Smoke: 0.0155 ± 0.0164) for both the control (adj. $p = 0.014$, $d = 2.38$) and the CSC (adj. $p = 0.009$, $d = 1.07$) conditions.

Furthermore, there was not a main effect of CSC ($p = 0.240$, partial $\eta^2 = 0.05$) or an interaction effect ($p = 0.952$, partial $\eta^2 < 0.01$); however, there was a significant effect of tissue type ($p < 0.001$, partial $\eta^2 = 0.46$) on the maximal rate (V_{max}) of PC-stimulated mitochondrial respiration (Figure 6-2D). Post hoc analysis indicated that the V_{max} of the control gastrocnemius

(14.7 ± 4.7 pmol O_2 /sec/mg_{wt}) was significantly lower than the V_{max} of the control soleus (22.8 ± 8.0 pmol O_2 /sec/mg_{wt}; adj. p = 0.010, d = 1.23). Likewise, the CSC-exposed gastrocnemius (11.5 ± 2.6 pmol O_2 /sec/mg_{wt}) was significantly lower than the CSC-exposed soleus (21.2 ± 6.2 pmol O_2 /sec/mg_{wt}; adj. p = 0.001, d = 2.02).

6.6.3. Effect of CSC on Mitochondrial Respiration with concurrent addition of Pyruvate and Palmitoylcarnitine

Dose-response curves for pyruvate-supported respiration in the presence of 0.04 mM PC in each tissue are shown in Figures VI-3A and VI-3B. Contrary to pyruvate alone, there was no interaction effect (p = 0.344, partial η^2 = 0.03) on the K_m of pyruvate in 0.04 mM PC, however, there was a significant effect of CSC (p = 0.038, partial η^2 = 0.14; Fig VI-3C) and tissue (p = 0.048, partial η^2 = 0.13). Post hoc analysis indicated that there was not a significant difference between the gastrocnemius groups (Gastrocnemius Control: 0.11 ± 0.03 , Gastrocnemius Smoke: 0.12 ± 0.03 ; adj. p = 0.263, d = 0.40), but there was a trend towards significance between the soleus control fibers (0.12 ± 0.04 mM) and the soleus CSC-exposed fibers (0.20 ± 0.12 mM; adj. p = 0.066, d = 0.85). No significant post hoc differences were detected between the control fibers (p = 0.241, d = 0.48) and the CSC-exposed fibers (p = 0.081, d = 0.93).

Tissue type (p < 0.001, partial η^2 = 0.68) and cigarette smoke (p = 0.035, partial η^2 = 0.14) had significant main effects on the V_{max} of pyruvate in 0.04 mM of PC (Figure 6-4D); however, there was not a significant interaction effect (p = 0.276, partial η^2 = 0.04). Post hoc analysis indicated that the control gastrocnemius (35.2 ± 8.1 pmol O_2 /sec/mg_{wt}) was significantly different than the control soleus (60.1 ± 17.1 pmol O_2 /sec/mg_{wt}; adj. p = 0.005, d = 1.86). Likewise, the CSC-

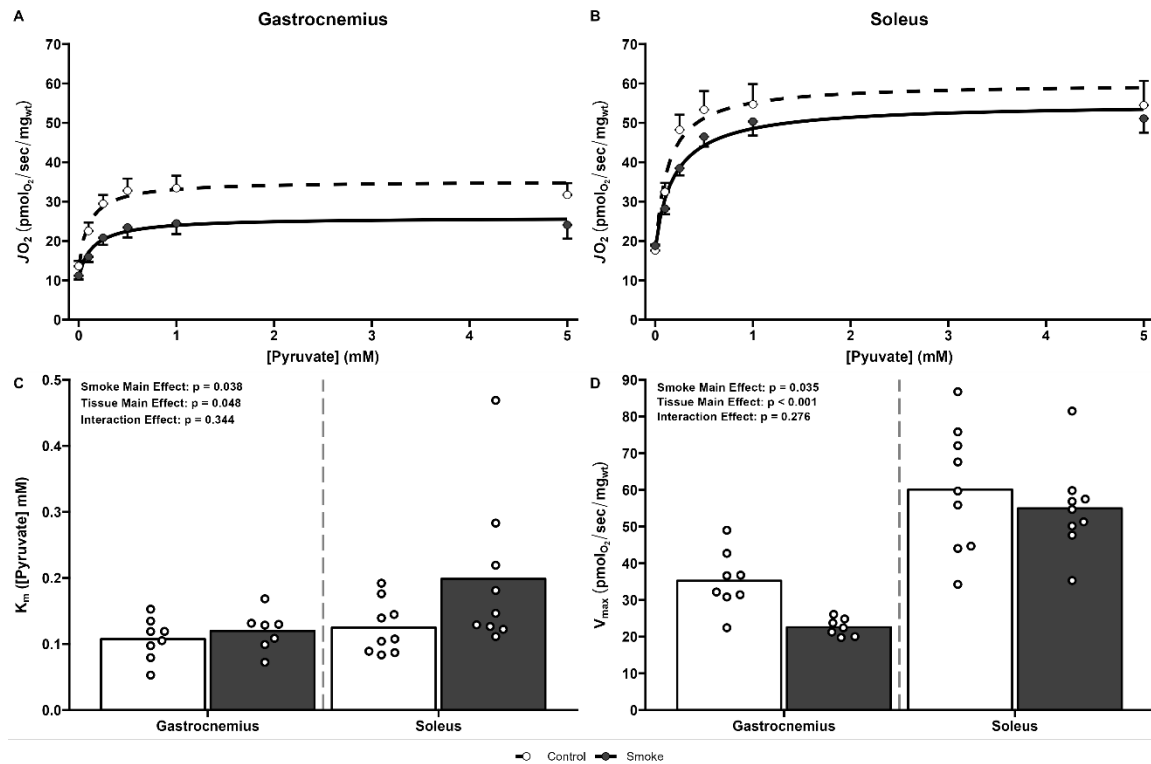


Figure 6-3. Dose-response curve for Pyruvate-stimulated mitochondrial respiration in the presence of 0.04 mM PC for the Gastrocnemius (A; $n = 7-8$ per group) and Soleus (B; $n = 7-9$ per group), and the mean estimates for the apparent K_m (C) and V_{max} (D) of mitochondrial respiration to pyruvate for both control (white) and cigarette smoke condensate-exposed (grey) fibers. Values are expressed as mean \pm SEM, where appropriate.

exposed gastrocnemius ($22.6 \pm 2.4 \text{ pmol O}_2/\text{sec/mg}_{\text{wt}}$) was significantly different than the CSC-exposed soleus ($55.0 \pm 12.3 \text{ pmol O}_2/\text{sec/mg}_{\text{wt}}$; adj. $p < 0.001$, $d = 3.65$). However, we did not identify any significant post hoc effects between the control gastrocnemius and CSC-exposed gastrocnemius ($p = 0.104$, $d = 2.12$) or between the soleus control and the CSC-exposed soleus ($p = 0.385$, $d = 0.34$)

6.6.4. Specific Effect of CSC on Palmitoylcarnitine induced inhibition of Pyruvate supported respiration

To determine the effect of smoke on the PC-induced inhibition of pyruvate oxidation, we normalized the K_m and V_{max} of Pyruvate with concurrent addition of PC to the K_m and V_{max} of

pyruvate in the absence of PC (Figure 6-4). CSC had a significant main effect ($p < 0.001$, partial $\eta^2 = 0.43$) on the change in K_m (Fig. VI-4A), but there was no main effect of tissue type ($p = 0.250$, partial $\eta^2 = 0.05$) or an interaction effect ($p = 0.156$, partial $\eta^2 = 0.07$). Post hoc analysis indicated that the change in K_m to the CSC-exposed gastrocnemius ($-63 \pm 22\%$) was significantly lower than the control gastrocnemius ($24 \pm 67\%$; $p < 0.001$, $d = 1.75$). However, the change in K_m to the CSC-exposed soleus ($-24 \pm 36\%$) only trended toward being significantly different from the control soleus ($8 \pm 34\%$; $p = 0.053$, $d = 0.35$).

Similarly, CSC had a significant main effect ($p = 0.027$, partial $\eta^2 = 0.15$) on the change in V_{max} (Fig VI-4B), but there was no main effect of tissue type ($p = 0.843$, partial $\eta^2 < 0.01$) or an interaction effect ($p = 0.095$, partial $\eta^2 = 0.09$). Post hoc analysis indicated that the differences between the control ($-27 \pm 20\%$) and CSC-exposed gastrocnemius ($19 \pm 39\%$; $p = 0.001$, $d = 1.47$) were significant, but not the differences between the control ($-9 \pm 17\%$) and CSC-exposed soleus ($-5 \pm 30\%$; $p = 0.131$, $d = 0.35$).

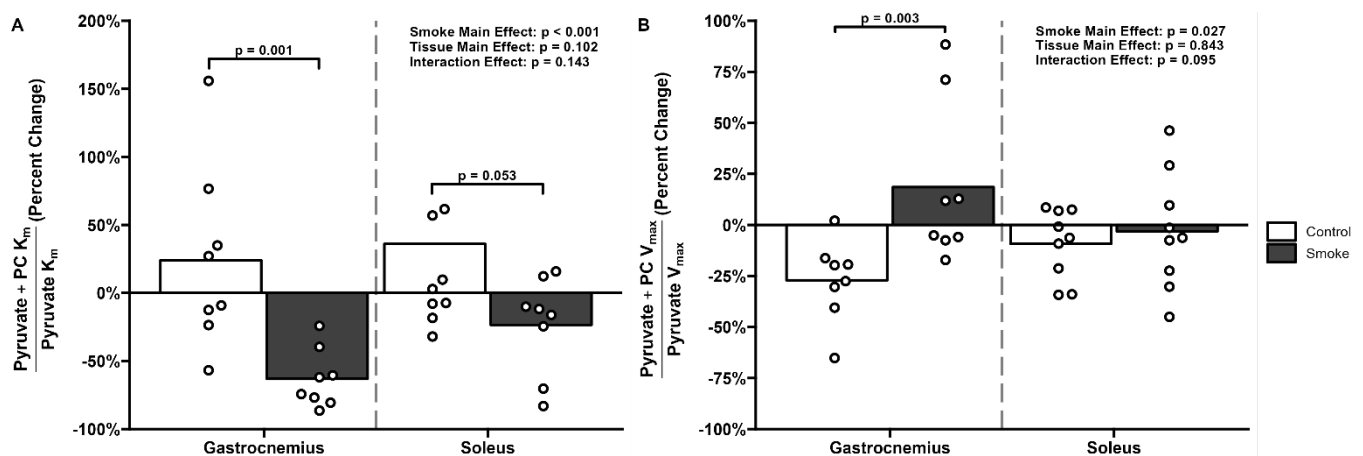


Figure 6-4. Change in the K_m (A; $n = 8$ per group) and V_{max} (B; $n = 8-9$ per group) of mitochondrial pyruvate oxidation in the presence of saturating (0.04 mM) concentration of palmitoylcarnitine relative to mitochondrial pyruvate oxidation without palmitoylcarnitine in control (white) and cigarette smoke condensate-exposed (grey) white gastrocnemius and soleus fiber bundles.

6.7. Discussion

Cigarette smoking is closely linked to the development of metabolic disorders. However, the mechanisms underlying the metabolic toxicity of cigarette smoke remain unclear. Therefore, this study aimed to determine cigarette smoke's acute effects on substrate sensitivity, respiratory capacity, and fuel interaction in skeletal muscles with different metabolic characteristics. Consistent with our hypothesis, cigarette smoke condensate directly impaired mitochondrial respiration supported by pyruvate, a product of glycolysis, in the fast-twitch gastrocnemius and, albeit to a lesser extent, the slow-twitch soleus muscles. Specifically, CSC exposure decreased both muscle respiration sensitivity and maximal capacity linked to pyruvate oxidation. In contrast, the sensitivity and maximal respiration supported by the fatty acid palmitoylcarnitine were unaffected by cigarette smoke in the gastrocnemius or soleus tissues. In the control condition, respiration supported by pyruvate was inhibited by the concurrent addition of palmitoylcarnitine in the fast-twitch gastrocnemius muscle but not in the soleus muscle. With cigarette smoke, the addition of palmitoylcarnitine augmented the maximal respiration rate stimulated by the concurrent addition of pyruvate in the gastrocnemius. However, mitochondrial respiratory capacity with combined substrates remained significantly lower in cigarette smoke than in controls for both muscles, indicating impaired mitochondrial metabolic flexibility. Together, the results from the present study lend support to the concept that cigarette smoke directly impairs the mitochondrial capacity to use the products of glucose breakdown rather than fatty acids in skeletal muscles with different metabolic properties.

6.7.1. CSC Impairs Skeletal Muscle Mitochondrial Respiration Supported by Pyruvate

Consistent with our hypothesis, CSC drastically impaired pyruvate-supported skeletal muscle respiration. Specifically, there was more than a 4-fold decrease in the sensitivity (~440% increase in K_m , Figure 6-1C), and the maximal rate of mitochondrial respiration linked to pyruvate oxidation was decreased by ~58% (lower V_{max} , Figure 6-1D) in the fast-twitch gastrocnemius muscle. This inhibitory effect of CSC was attenuated in the slow-twitch soleus muscle, for which the sensitivity of mitochondrial respiration to pyruvate was decreased only by 2.5-fold (Figure 6-1C), and muscle respiratory capacity was not significantly affected by CSC incubation (Figure 6-1D).

The present study's findings align with the results of studies performed by Thatcher et al. (2014), which reported a ~60% decrease in maximal glutamate-and-malate-stimulated respiration in cultured myotubes exposed to smoke-conditioned media for 4 hours. This study also reported a ~50% decrease in maximal ADP-stimulated respiration with complex I substrates, glutamate-and-malate, in the gastrocnemius muscle of mice exposed to mainstream cigarette smoke for 6 weeks. Our results, therefore, confirm and extend these findings to submaximal rates, thus revealing a smoke-induced decrease in sensitivity for pyruvate oxidation in the fast-twitch gastrocnemius muscle, with this effect being attenuated in slow-twitch soleus muscle due to a relatively lower proportion of type II glycolytic muscle fibers compared to the gastrocnemius (Augusto et al., 2004).

In conjunction with the present results *in situ*, the findings from Thatcher et al. (2014) support the concept of a direct inhibitory effect of cigarette smoke on mitochondrial oxidation of glucose-derived substrates. Further supporting this interpretation, constituents of cigarette smoke,

specifically nicotine and o-cresol, have been identified as inhibitors of mitochondrial Complex I, the primary site of NADH oxidation, in isolated mitochondria (Khattri et al., 2022). As the ultimate energy-producing fate of glucose oxidation is to support the reduction of NAD⁺ to NADH to support complex I-driven respiration, the direct inhibition of complex I function by cigarette smoke is likely to be an important mechanism contributing to impaired glucose oxidation, and the greater risk of hyperglycemia and insulin resistance often observed in smokers (Pan et al., 2015).

6.7.2. Skeletal Muscle Mitochondrial Respiration Supported by Fatty Acids is Unaffected by CSC

Unlike pyruvate oxidation, fatty acid-stimulated mitochondrial respiration was not significantly affected by CSC in either muscle group (Figure 6-2A-D). For example, in the gastrocnemius muscle, CSC had almost no (~1%) effect on the K_m of mitochondrial respiration for fatty acid substrates. Likewise, CSC did not significantly alter the V_{max} in the soleus (-7%). Overall, these results with different conditions of substrate availability in permeabilized fibers rule out a direct effect of cigarette smoke on the mitochondrial oxidation of fatty acids in the skeletal muscle.

Our findings in an *in situ* muscle preparation somewhat contrast with whole-body studies in humans, reporting a ~30% increase in the oxidation of ¹³C-palmitate in the quadriceps muscles of humans during an active smoking session (Bergman et al., 2009). Also, Jensen et al. (1995) documented a significant correlation ($r = 0.57$) between urine cotinine excretion and fat oxidation measured by indirect calorimetry. A possible explanation for this discrepancy between *in situ* and *in vivo* studies might be the calorogenic effects of cigarette smoke and one of its main constituents, nicotine, which can confound the interpretation of the whole-body results. For instance, smoking

and nicotine have been demonstrated to increase 24-h (Hofstetter et al., 1986) and resting energy expenditure (Perkins et al., 1989, 1990). A strength of our study design was that our skeletal muscle preparation *in situ* allowed us to parse out the direct effects of cigarette smoke on mitochondrial respiratory function with fatty acid substrates from the confounding changes in metabolic demand. Therefore, our findings seem to discount a smoke-induced defect in mitochondrial capacity to oxidize lipids as a factor responsible for dyslipidemia and ectopic fat accumulation in chronic smokers, as observed by several epidemiological studies (Canoy et al., 2005; Chiolero et al., 2008; Sinha-Hikim et al., 2014; Terry et al., 2020).

6.7.3. CSC Alters Skeletal Muscle Mitochondrial Respiration with Competing Substrates

A unique feature of the experimental design in the present study was the assessment of mitochondrial respiration rates with competing substrates (fatty acids and pyruvate) using experimental conditions that replicate the transition from fasting to the fed state, and thus the transition from fatty acid utilization to carbohydrate utilization, to examine mitochondrial metabolic flexibility (Figure 6-3A-D). In line with work conducted in mitochondria isolated from fast-twitch muscles (Abdul-Ghani et al., 2008b), we observed an inhibitory effect of palmitoylcarnitine on pyruvate-stimulated mitochondrial respiration (increased K_m and lower V_{max}) in both the control gastrocnemius and soleus muscles *in situ* (Figure 6-4). Specifically, the results of these experiments in permeabilized fibers indicated that palmitoylcarnitine decreased the sensitivity of the mitochondria to pyruvate by ~20-40% and decreased the maximal respiration capacity (V_{max}) of pyruvate by ~10-25% in the fast-twitch gastrocnemius and slow-twitch soleus muscles (Figure 4A-B). Consistent with these results in the skeletal muscle *in situ*,

palmitoylcarnitine inhibited maximal respiration capacity linked to pyruvate oxidation by 34% in mitochondria isolated from fast-twitch mouse muscles (Abdul-Ghani et al., 2008b).

We then sought to examine whether CSC exposure would alter the inhibition induced by palmitoylcarnitine on pyruvate-stimulated respiration. Interestingly, with CSC, palmitoylcarnitine had an additive effect and improved mitochondrial respiration sensitivity for pyruvate by 20-60% in the gastrocnemius and soleus muscles. Similarly, the pyruvate-stimulated V_{max} in the gastrocnemius was increased by ~20% (Figure 6-3C-D). However, it is important to note that mitochondrial respiratory capacity with combined substrates remained significantly lower in cigarette smoke than in controls, indicating impaired mitochondrial metabolic flexibility. These findings may reconcile the conflicting results between experiments in humans using whole-body indirect calorimetry and isotope tracers (Bergman et al., 2009; Jensen et al., 1995), which indicated a CSC-induced increase in substrate oxidation, and studies *in vitro* (Khattri et al., 2022; Thatcher et al., 2014), which demonstrated CSC-induced impairment in substrate oxidation by the mitochondria. In light of the present results obtained in permeabilized muscle fibers *in situ*, it is apparent that the oxidation by the mitochondria of the glycolytic product (e.g., pyruvate) or downstream tricarboxylic acid cycle (TCA) intermediates (e.g., glutamate and malate) is impaired by cigarette smoke exposure. This inhibition was substantial when depending solely on those substrates (Figure 6-1), whereas the effect was attenuated but still statistically significant, using a combination of glucose- and fatty acid-derived substrates at submaximal amounts (Figure 6-3), as is the case in a physiological system. Future studies using simultaneous measurements of the fluxes through the TCA cycle and β -oxidation, combined with direct measurements of the electrochemical potential in conditions of competing substrates, are therefore needed to elucidate

the thermodynamic mechanisms underlying these findings.

6.7.4. Clinical Perspectives

Herein, we investigated the impacts of cigarette smoke on substrate oxidation at the mitochondrial level — the final site of substrate oxidation for the generation of ATP. Our study in a skeletal muscle preparation *in situ* revealed that, while maximal mitochondrial respiration with fatty acid substrates was unaffected by cigarette smoke exposure, mitochondrial respiration supported by carbohydrate-derived substrates, alone or in combination with fatty acids, was significantly impaired in the skeletal muscle. Clinically, these findings of impaired mitochondrial metabolic flexibility could explain both the decline in insulin sensitivity and the increase in triglyceride storage associated with chronic smoking (Canoy et al., 2005; Chiolero et al., 2008; Pan et al., 2015; Sinha-Hikim et al., 2014; Terry et al., 2020). Conceptually, the inhibition of pyruvate oxidation in the mitochondria can decrease cellular glucose oxidation. As excess carbohydrates are converted into fatty acids in the liver, those can then be incorporated into triglycerides and cholesterol to be transported in the blood or converted into sphingolipids and/or ceramide (Li et al., 2021; Telenga et al., 2014). These excess lipid species would then be taken up and stored in ectopic fat depots, such as skeletal muscle and liver (Figure 6-5), with adverse effects (lipotoxicity) on these organs (Watt et al., 2012). Therefore, impaired pyruvate oxidation induced by cigarette smoke leads to a vicious cycle whereby the incorporated lipid species further impair mitochondrial respiration and cause further cellular damage, as observed in individuals chronically

exposed to cigarette smoke.

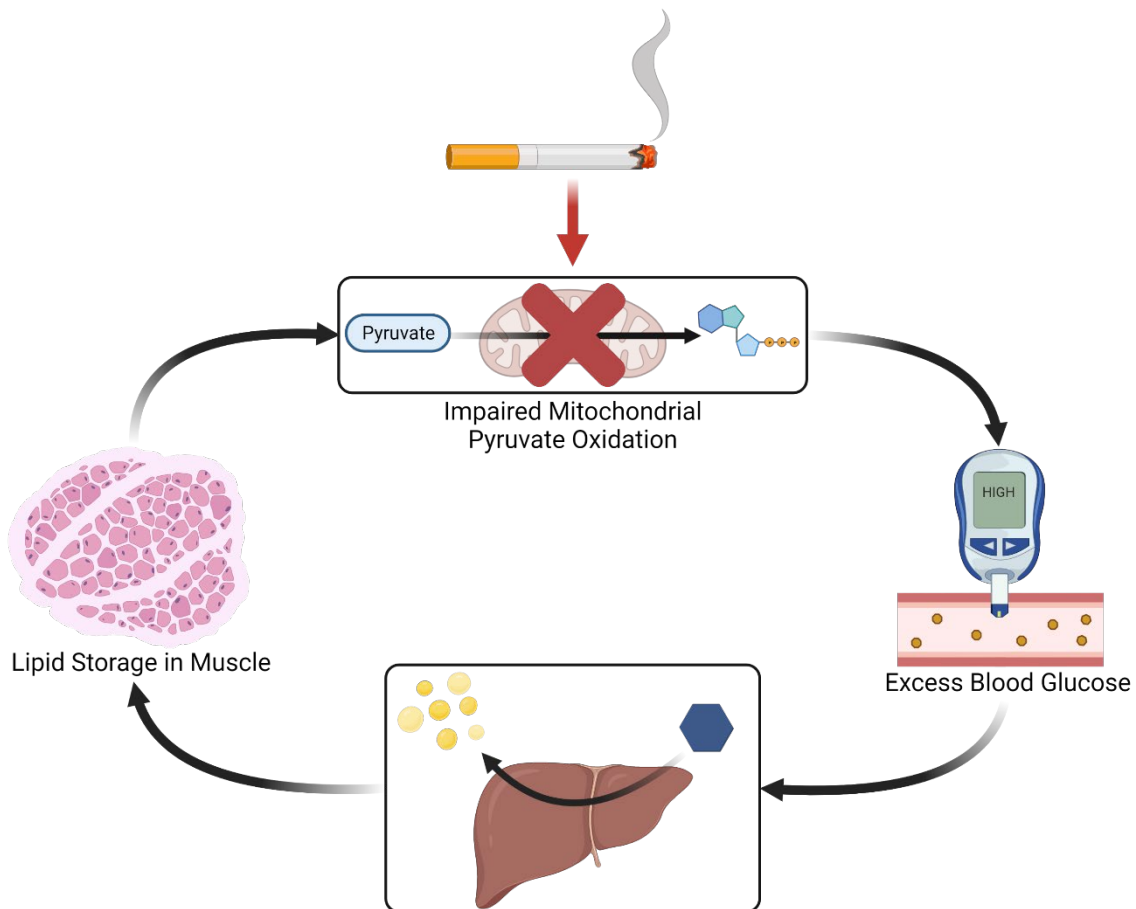


Figure 6-5. Schematic outlining the hypothesized mechanisms by which cigarette smoke induces skeletal muscle mitochondrial dysfunction and the downstream effects. Cigarette smoke inhibits the oxidation of pyruvate, a carbohydrate-derived substrate. This contributes to excess blood glucose, which is converted to fatty acids and other lipid species via the liver. These excess lipids are transported back into the bloodstream, where they are taken up and stored in muscle.

6.8. Conclusion

In conclusion, this study revealed that cigarette smoke condensate acutely impaired mitochondrial respiration supported by pyruvate, a product of glycolysis, in the fast-twitch gastrocnemius and, to a lesser extent, the slow-twitch soleus muscle. In contrast, the sensitivity and maximal respiration supported by the fatty acid palmitoylcarnitine were unaffected by cigarette smoke in either the gastrocnemius or soleus tissues. In a condition replicating the transition from fasting to the fed state, respiration supported by pyruvate was inhibited by the concurrent addition of palmitoylcarnitine in the fast-twitch gastrocnemius muscle. Interestingly, palmitoylcarnitine increased pyruvate utilization at submaximal respiration rates in conditions with cigarette smoke in the gastrocnemius. However, this additive effect of fatty acids was insufficient to restore mitochondrial respiration to the level of the control condition, thus still indicating an impaired mitochondrial metabolic flexibility. Our findings underscore that impaired metabolism of carbohydrate-derived substrates are the primary mechanism underlying cigarette smoke-associated muscle mitochondrial dysfunction, which leads to a vicious cycle involving excess glucose conversion into fatty acids and lipotoxicity, which further skeletal muscle and mitochondrial abnormalities commonly observed in humans chronically exposed to cigarette smoke.

CHAPTER 7

AIM III RESULTS AND DISCUSSION

7.1. Effects of Acute Cigarette Smoke Exposure on Mitochondrial Energy Transfer in Fast and Slow Twitch Skeletal Muscle

Stephen T Decker¹, Nadia Alexandrou-Majaj³, Gwenael Layec^{1,2}

Department of Kinesiology¹, Department of Psychology and Brain Sciences³, and the Institute for Applied Life Science²

University of Massachusetts Amherst, USA

Running Title: Cigarette Smoke Alterations to Mitochondrial Function

Keywords: Skeletal Muscle, Electron Transport Chain, Mitochondrial Leak, ADP/ATP transport
Cigarette Smoke

Corresponding Author: Gwenael Layec

Life Sciences Laboratories, 240 Thatcher Rd, Amherst, Ma 01003

Email: glayec@umass.edu

7.2. Abstract

Cigarette smoke has been shown to induce mitochondrial dysfunction, thus leading to the development of chronic disease. However, the mechanisms underlying cigarette smoke-induced mitochondrial dysfunction in the skeletal muscle are still poorly understood. Accordingly, this study aimed to elucidate the molecular targets of cigarette smoke in the mitochondria of permeabilized gastrocnemius and soleus muscle fibers. Cigarette smoke decreased complex-I-driven mitochondrial respiration in the gastrocnemius (CONTROL: 45.4 ± 11.2 pmol_{O₂}/sec/mg_{wt} and SMOKE: 27.5 ± 12.0 pmol_{O₂}/sec/mg_{wt}; p = 0.04) and soleus (CONTROL: 63.0 ± 23.8 pmol_{O₂}/sec/mg_{wt} and SMOKE: 44.6 ± 11.1 pmol_{O₂}/sec/mg_{wt}; p = 0.038), resulting in a greater overall contribution of complex II on maximally stimulated respiration. The maximal activity of the electron transport chain was also significantly inhibited by cigarette smoke. Furthermore, ADP/ATP transport also appeared to be impaired in cigarette smoke-exposed gastrocnemius, as the contribution of ANT to total mitochondrial respiration was decreased (CONTROL: 2.23 ± 0.69 ; SMOKE: 1.21 ± 0.08 ; p = 0.001). However, these effects were attenuated in the soleus (CONTROL: 1.66 ± 0.42 ; SMOKE: 1.30 ± 0.16 ; p = 0.076). Interestingly, cigarette smoke did not significantly alter any markers of mitochondrial quality or thermodynamic coupling. Our findings underscore that cigarette smoke directly impairs the mitochondrial electron transport chain, especially at the site of complex I, as well as ANT, which facilitates the exchange of ADP/ATP across the inner mitochondrial membrane. These concurrent effects result in the maintenance of mitochondrial efficiency; however, total mitochondrial ATP production is indeed impaired in smoke-exposed fibers. The findings in these studies elucidate the primary targets of smoke-induced mitochondrial dysfunction and provide targets of interest for therapeutic approaches.

7.3. New & Noteworthy

While cigarette smoke exposure is well-known to induce mitochondrial dysfunction, the molecular targets of cigarette smoke within the mitochondrial are unknown. Herein, we show that complex I of the electron transport chain is a primary target of cigarette smoke-induced mitochondrial dysfunction. Furthermore, cigarette smoke also targets ANT, thus inhibiting the exchange of ADP/ATP across the inner mitochondrial membrane. With this evidence, we demonstrate that concurrent inhibition of the electron transport chain and ADP/ATP exchange by cigarette smoke is the primary mechanism by which cigarette smoke induces mitochondrial dysfunction and bioenergetic deficits in skeletal muscle.

7.4. Introduction

Cigarette smoke exposure is a significant risk factor for frailty, sarcopenia, and the development of numerous chronic diseases, thus causing over 480,000 premature deaths in the United States (United States Department of Health and Human Services, 2014). Additionally, increased muscle fatigability (Wüst et al., 2008) and lower exercise tolerance (Papathanasiou et al., 2007b) are typical in chronic smokers, which contribute to impaired quality of life. The underlying causes of cigarette smoke-induced exacerbations in fatigability are multifaceted and include impaired oxygen transport and diffusion (Morse et al., 2008; Tang et al., 2010), deficits in myofiber contractile function (Nogueira et al., 2018; Robison et al., 2017), and mitochondrial dysfunction (Ajime et al., 2020; Pérez-Rial et al., 2020; Thatcher et al., 2014; Tippetts et al., 2014).

Regarding mitochondrial alterations, chronic cigarette smoking elicits substantial changes in mitochondrial characteristics such as impaired skeletal muscle oxidative phosphorylation capacity (Thatcher et al., 2014; van der Toorn et al., 2007, 2009; aim 1), altered substrate utilization (aim 2), decreased oxidative enzymes (Barreiro et al., 2012; Decker, Kwon, Zhao, Hoidal, Heuckstadt, et al., 2021; Gosker et al., 2009), and enhanced mitochondrial-derived ROS production (Barreiro et al., 2012; Decker, Kwon, Zhao, Hoidal, Heuckstadt, et al., 2021; Haji et al., 2020). Interestingly, the mechanisms by which energy transduction in the mitochondria is directly impaired by cigarette smoke have recently received some attention in the skeletal muscle. Specifically, acute exposure to cigarette smoke condensate (0.02-1%) inhibited ADP-stimulated respiration supported by complex I and II in isolated mitochondria from the hindlimb muscles of mice (Khattri et al., 2022). In addition, complex-II supported respiration was slightly less sensitive than complex I to the inhibitory effects of cigarette smoke condensate (Khattri et al., 2022).

Another interesting finding was the documentation of a decreased mitochondrial proton leak-driven respiration with cigarette smoke condensate exposure, which alluded to direct impairments of the electron transport system.

Other reports in epithelial cells exposed to cigarette smoke condensate pointed toward an increase in mitochondrial membrane permeability via activation of the adenine nucleotide translocase (ANT) (Wu et al., 2020), a crucial transporter responsible for the exchange of nucleotides (i.e., ADP and ATP) across the mitochondrial inner mitochondrial membrane (Klingenberg, 2008). ANT also serves as an important site of proton leak and mitochondrial uncoupling (Bertholet et al., 2019a), effectively regulating $\Delta\Psi_{\text{mt}}$ and, when activated, decreasing the protonmotive force driving ATP production. Based on the above evidence obtained *in vitro* in isolated mitochondria or cultured cells, cigarette smoke may impair mitochondrial ATP production through three potential mechanisms: decreased supply of reducing equivalent in the electron transport, increased proton leak, and/or decreased ATP turnover (ATP synthesis and transportation). However, whether these mechanisms are involved and their relative contribution to the bioenergetic deficits induced by cigarette smoke in the skeletal muscle remains to be elucidated. It is also unknown whether these mechanisms are fiber-type specific. In this regard, it is noteworthy that chronic smokers and patients with chronic obstructive pulmonary disease, a disorder mainly caused by cigarette smoking, are characterized by metabolic abnormalities and specific atrophy of type I fibers (Maltais et al., 2000; Nyberg et al., 2015; Whittom et al., 1998).

Therefore, the purpose of the present study was to determine the effect of cigarette smoke on the function of the electron transport system, ADP transport into the mitochondria, and changes in ATP synthase kinetics in permeabilized muscle fiber of skeletal muscles with differing

metabolic characteristics. To achieve these aims, we assessed *in situ* mitochondrial respiration via titrations of ADP and carboxyatractyloside, a potent ANT inhibitor, in predominantly fast (white gastrocnemius) and slow-twitch (soleus) skeletal muscle fibers acutely exposed to cigarette smoke concentrate (CSC). We hypothesized that CSC would inhibit mitochondrial respiration (sensitivity and maximal capacity) supported by ADP, which would be attributed to impairments in ANT activity, decreased electron flow through the respiratory complexes, and greater proton leak.

7.5. Methods

7.5.1. Animals and Experimental Design

Eleven three- to eleven-month-old male ($n = 7$) and female C57BL/6 mice were used for this study. All animals were maintained on a 12-hour dark/light cycle without access to running wheels and were fed standard chow *ad libidum*. Following euthanasia by 5% isoflurane, the gastrocnemius and soleus were immediately extracted and placed in an ice-cold BIOPS preservation solution (Pesta & Gnaiger, 2012). The gastrocnemius and soleus were specifically chosen due to the similarities in mitochondrial respiratory rates per unit of mass compared to those of human vastus lateralis muscle (Jacobs et al., 2013), and to encompass tissues that contain varying amounts of type I and type II skeletal muscle fibers (Augusto et al., 2004).

7.5.2. Preparation of Permeabilized Muscle Fibers

The tissue preparation and respiration measurement techniques were adapted from established methods (Kuznetsov et al., 2008a; Pesta & Gnaiger, 2012) and have been previously described (Layec et al., 2018). Briefly, BIOPS-immersed fibers (2.77mM CaK2EGTA, 7.23mM K2EGTA, 50mM K⁺ MES, 6.56 mM MgCl₂, 20mM Taurine, 5.77mM ATP, 15mM PCr, 0.5mM DTT, 20mM Imidazole) were carefully separated with fine-tip forceps and subsequently bathed in a BIOPS-based saponin solution (50 µg saponin.ml⁻¹ BIOPS) for 30 minutes. Following saponin treatment, muscle fibers were rinsed twice in ice-cold mitochondrial respiration fluid (MIR05, in mM: 110 Sucrose, 0.5 EGTA, 3 MgCl₂, 60 K-lactobionate, 20 taurine, 10 KH₂PO₄, 20 HEPES, BSA 1g.L⁻¹, pH 7.1) for 10 minutes each.

Following chemical permeabilization, tissues were placed in separate containers with a 2

mL solution of MiR05 (control) or 4% cigarette smoke concentrate (CSC; Murty Pharmaceuticals, Lexington, KY). These concentrations of cigarette smoke were chosen based on pilot studies showing that this concentration induces a ~25% decrease in state III mitochondrial respiration in permeabilized fibers from the gastrocnemius muscle, which reflects the perturbations in mitochondrial respiration reported in mice and humans chronically exposed to cigarette smoke (Ajime et al., 2020; Gifford et al., 2018a; Thatcher et al., 2014). The tissue-containing solutions were rocked gently in a 4°C cold room for 1 hour.

After the muscle sample was gently dabbed with a paper towel to remove excess fluid, the wet weight of the sample (1-2 mg) was measured using a standard, calibrated scale. The muscle fibers were then placed in the respiration chamber (Oxygraph O2K, Oroboros Instruments, Innsbruck, Austria) with 2 ml of MIR05 solution warmed to 37°C. Oxygen was added to the chambers, and oxygen concentration was maintained between 190-250 µM. After allowing the permeabilized muscle sample to equilibrate for 5 minutes, mitochondrial respiratory function was assessed in duplicate. Following the addition of each substrate, the respiration rate was recorded until a steady state of at least 30-seconds (at a sampling rate of 2 seconds) was reached, the average of which was used for data analysis. The rate of O₂ consumption was expressed relative to muscle sample mass (in picomoles per second per milligram of wet weight).

7.5.4. Measurement of Mitochondrial Respiration

The mitochondrial respiration protocol used in the present study was designed to test several mechanisms by which cigarette smoke condensate impairs mitochondrial function and was performed as follows: First, saturating concentrations of glutamate (G; 10 mM) and malate (M; 2

mM) were added to the chambers. The addition of glutamate and malate without the presence of ADP (also known as state IV respiration) represents a non-phosphorylating state where the oxygen consumed by the mitochondria is linked to the leak of protons from the mitochondrial intermembrane space (Brand & Nicholls, 2011). After attaining a steady-state, ADP was added in 5 titration steps: 1) 0.025 mM, 2) 0.05 mM, 3) 0.10 mM, 4) 0.25 mM, and 3) 5 mM (ADP₅₀₀₀). These concentrations were chosen as they are reflective of: 1) the concentrations of ADP observed at the end of an acute high-intensity exercise bout (~50 µM) as measured by ³¹P Magnetic Resonance Spectroscopy (Argov et al., 1996; Kemp et al., 2007; Vanderthommen et al., 2003; Vanhatalo et al., 2014); 2) the reported Km of ADP for mitochondrial respiration (~250 µM) in permeabilized skeletal muscle fibers (Bygrave & Lehninger, 1967; Kuznetsov et al., 1996; Perry et al., 2011; Veksler et al., 1995); and 3) the concentration of ADP at Vmax for mitochondrial respiration in permeabilized skeletal muscle fibers (5 mM). Following this step, saturating amounts of succinate (S; 10 mM) were added to the chambers to assess maximal complex I & II-driven mitochondrial respiration. Cytochrome c (C; 10 µM) was added to the chamber to assess the outer mitochondrial membrane's integrity (Perry et al., 2013).

Following the addition of cytochrome C, carboxyatractylamide (CAT; Cayman Chemical no. 21120) was added in 5 steps with final concentrations of 0.05 µM, 0.1 µM, 0.2 µM, 1.0 µM, and 5.0 µM. A potent ANT inhibitor, CAT was titrated near concentrations reflective of the inhibition constant (IC₅₀), or the concentration at which CAT inhibits the activity of ANT by 50%, and at the concentration which results in maximal inhibition (I_{max}). Pilot experiments from our lab estimated IC₅₀ at approximately 0.42 µM, well within the range of other reports (Vignais et al., 1976; Wisniewski et al., 1995). Following this, carbonyl cyanide m-chlorophenyl hydrazone

(FCCP) was added to assess the excess capacity of the mitochondrial ETC. FCCP is a potent ionophore that quickly allows protons to exit the mitochondrial intermembrane space, effectively uncoupling electron transport and oxygen consumption from ATP synthesis, diminishing $\Delta\Psi_{\text{mt}}$ and allowing the uninhibited flow of electrons through the ETC (Brand & Nicholls, 2011). Rotenone (Rot; 0.5 μM), a complex I inhibitor, will then be added to the chamber to assess complex II-linked respiration. Lastly, oligomycin (Omy; 2.5 μM), an inhibitor of ATP synthase, and antimycin A (AmA; 2.5 μM), a complex III inhibitor, was added to the chambers to assess residual, or non-mitochondrial, oxygen consumption. Following the conclusion of these experiments, tissue samples were snap frozen in liquid nitrogen and stored at -80°C for later analysis of CS activity.

7.5.5. Data Analysis

The rate of O₂ consumption (J_{O_2}) was expressed relative to muscle sample mass (in picomoles per second per milligram of wet weight). Samples that demonstrated impaired mitochondrial membrane integrity (more than a 10% increase in respiration in response to cytochrome C) were excluded from the analysis (n = 2-3). All extreme outliers (more extreme than Q1 - 3 * IQR or Q3 + 3 * IQR) were also excluded from the analysis. The respiratory control ratio (RCR) was calculated as the ratio of maximal state III-driven respiration (GMDS) to leak respiration (GM). The relative contribution of Complex II to maximal uncoupled respiration was determined by calculating the ratio of Rot:FCCP_{Peak}.

Thermodynamic coupling (q) is another method of quantifying mitochondrial respiratory capacity (Larsen 2011) and estimates all enzymatic processes and free energy changes that occur during oxidative phosphorylation. Furthermore, thermodynamic coupling changes are theorized to

reflect changes in the P/O ratio. Thermodynamic coupling was calculated by:

$$q = \sqrt{1 - \frac{CAT_{5.0}}{FCCP_{Peak}}}$$

CSC-induced changes to the ETS ($\Delta FCCP_{Peak}$) in the gastrocnemius and soleus was determined by calculating the difference in uncoupled respiration ($FCCP_{Peak}$) between the smoke and control tissues expressed as a percentage of the control fibers. CSC-induced inhibition to ANT for each tissue was calculated as follows:

$$CSC\text{-}Induced\ ANT\ Inhibition\ (\%) = \frac{(GMDS_{Smoke} - CAT_{5.0\ Smoke}) - (GMDS_{Control} - CAT_{5.0\ Control})}{GMDS_{Control}}$$

Apparent K_m and V_{max} were determined using a 3-parameter model of the Michaelis-Menten equation:

$$JO_2 = C + \frac{V_{max} - C}{1 + \frac{K_m}{[S]}}$$

where JO_2 is the respiration rate at the concentration of a given substrate $[S]$, V_{max} is the maximal rate of respiration, K_m is the concentration of $[S]$ at 50% of V_{max} , and C is JO_2 when $[S] = 0$. Likewise, the inhibitory kinetics of CAT was fitted to the same equation but modified as follows:

$$JO_2 = I_{max} + \frac{C - I_{max}}{1 + \frac{IC_{50}}{[S]}}$$

where I_{max} is the minimum rate of respiration induced CAT and IC_{50} is the respiration rate at 50% I_{max} .

Normality and homoscedasticity were determined using the Shapiro-Wilk test and Levene's test, respectively. The effects of cigarette smoke and tissue on all parameters were determined

using a two-way (Smoke x Tissue) Aligned Ranks Transform (ART) ANOVA (Oliver-Rodríguez & Wang, 2015). If main effects or interaction effects were determined to be statistically significant ($p < 0.05$), post hoc comparisons were performed using Dunn's test with a Holm-Sidak correction. A nonparametric Wilcoxon's test was used for the comparison between the difference in FCCP_{Peak} between the gastrocnemius and soleus. Effect sizes were determined by calculating the partial eta-squared (η^2) and Cohen's d for both the ANOVA and the post hoc comparisons, respectively. For clarity, the results are presented as mean \pm SD in text and tables and mean \pm SEM in the figures.

7.6. Results

7.6.1. Effects of CSC on Components of the Mitochondrial Respiratory System

Mitochondrial respiration rates are shown in Figure VII-1A and Table 7-S1. Leak (GM) respiration did not exhibit an effect of CSC ($p = 0.314$, partial $\eta^2 = 0.03$) nor an interaction effect ($p = 0.308$, partial $\eta^2 = 0.03$), however there was a significant effect of tissue type ($p < 0.001$, partial $\eta^2 = 0.61$). *Post hoc* analysis revealed that respiration in the soleus tissues exhibited greater leak respiration than the gastrocnemius in control (Gastrocnemius control: 16.8 ± 4.6 pmol_{O₂}/sec/mg_{wt}; Soleus control: 27.6 ± 4.4 pmol_{O₂}/sec/mg_{wt}; adjusted $p = 0.001$, $d = 2.38$) and CSC-exposed (Gastrocnemius CSC: 12.6 ± 3.9 pmol_{O₂}/sec/mg_{wt}; Soleus CSC: 26.4 ± 7.2 pmol_{O₂}/sec/mg_{wt}; adjusted $p < 0.001$, $d = 2.38$) conditions. Both CSC exposure ($p < 0.001$, partial $\eta^2 = 0.32$) and tissue type ($p = 0.001$, partial $\eta^2 = 0.28$) had main effects on complex-I-driven state III respiration (GMD₅₀₀₀), but there was no interaction effect ($p = 0.604$, partial $\eta^2 = 0.01$). As determined by *post hoc* tests, smoke had a significant effect on the gastrocnemius (Gastrocnemius control: 45.4 ± 11.2 pmol_{O₂}/sec/mg_{wt}; Gastrocnemius CSC: 27.5 ± 12.0 pmol_{O₂}/sec/mg_{wt}; adjusted $p = 0.014$, $d = 1.54$) and soleus (Soleus control: 63.0 ± 23.8 pmol_{O₂}/sec/mg_{wt}; Soleus CSC: 44.6 ± 11.1 pmol_{O₂}/sec/mg_{wt}; adjusted $p = 0.038$, $d = 0.99$). Likewise there was a significant difference between the control gastrocnemius and control soleus (adjusted $p = 0.048$, $d = 0.95$) and the CSC-exposed gastrocnemius and the CSC-exposed soleus (adjusted $p = 0.019$, $d = 1.48$).

Maximal State III respiration (GMDS) also exhibited significant main effects of smoke ($p < 0.001$, partial $\eta^2 = 0.27$), tissue ($p < 0.001$, partial $\eta^2 = 0.47$), but not an interaction effect ($p = 0.542$, partial $\eta^2 = 0.01$). *Post hoc* analysis revealed trends toward significance between the control and CSC-exposed gastrocnemius muscles (Gastrocnemius control: 57.1 ± 10.6 pmol_{O₂}/sec/mg_{wt};

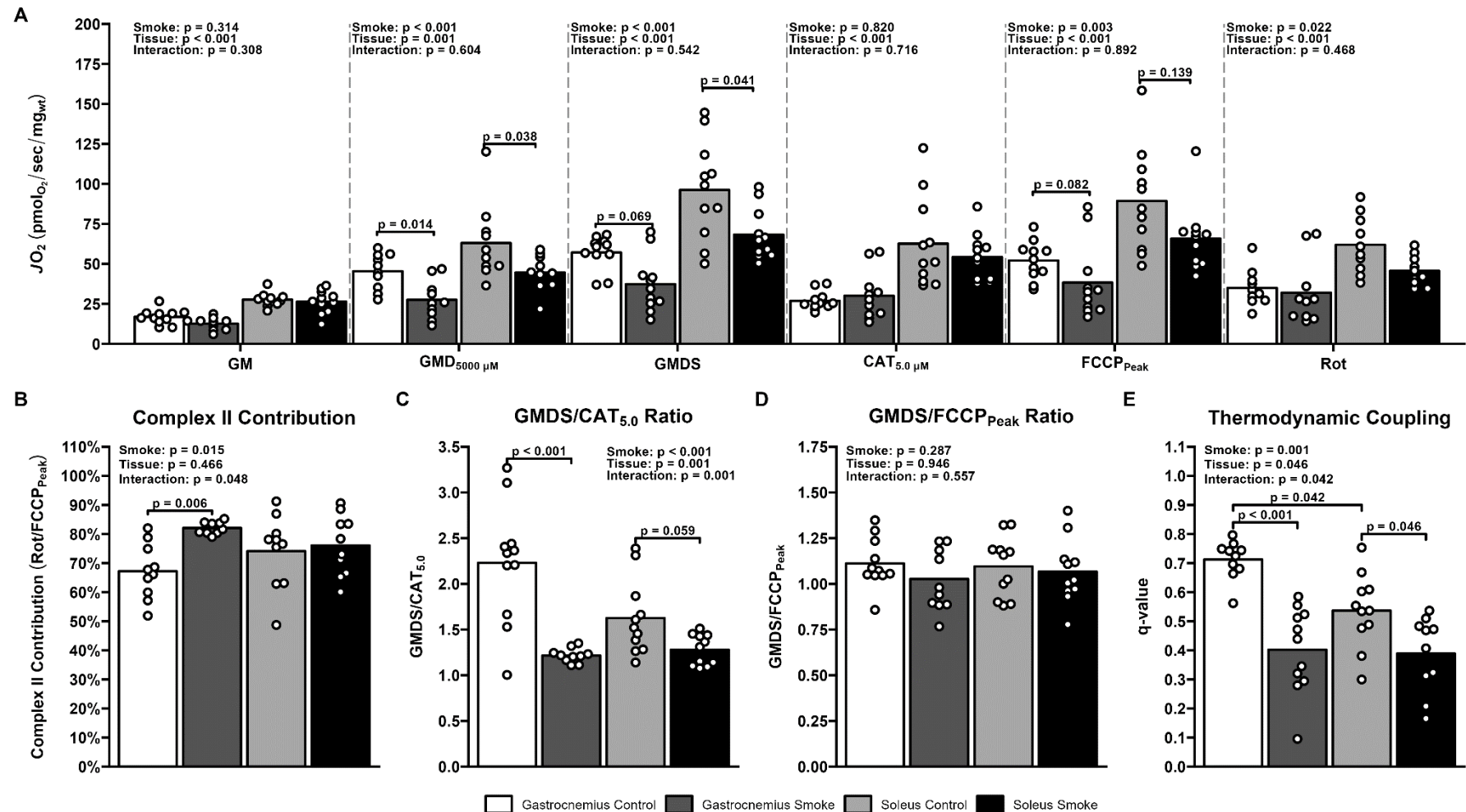


Figure 7-1. Respiration rates (JO_2) of permeabilized gastrocnemius (white bars) and soleus (light grey bars) skeletal muscle fibers, and their respective CSC-exposed counterparts (dark grey bars and black bars) normalized to the wet weight of the sample (A). Also shown are the contribution of complex II (B), ratio of GMDS to $CAT_{5.0}$ (C), Respiratory Control Ratio (D), and thermodynamic coupling (E). n = 9-10 per group. Values are expressed as mean \pm SEM, where appropriate. G: glutamate; M: malate; D: ADP; S: succinate; CAT: carboxyatractyloside; Rot: rotenone.

Gastrocnemius CSC: 37.3 ± 17.5 pmol_{o2}/sec/mg_{wt}; adjusted p = 0.069, d = 1.37), but there were significant differences between the control and CSC-exposed soleus muscles (Soleus control: 96.2 ± 30.9 pmol_{o2}/sec/mg_{wt}; Soleus CSC: 68.2 ± 16.0 pmol_{o2}/sec/mg_{wt}; adjusted p = 0.041, d = 1.14). On the other hand, soleus muscles exhibited significantly greater respiration rates than the gastrocnemius muscles for both the control (adjusted p = 0.004, d = 1.69) and CSC-exposed groups (adjusted p = 0.006, d = 1.85).

However, there was no effect of cigarette smoke on the respiration rates on state II respiration when inhibited with CAT (CAT_{5.0}) (p = 820, partial $\eta^2 < 0.001$ nor an interaction effect (p = 0.716, partial $\eta^2 < 0.01$), but there was a significant main effect of tissue (p < 0.001, partial $\eta^2 = 0.58$). *Post hoc* tests determined significant differences between tissues in the control (Gastrocnemius control: 26.8 ± 5.8 pmol_{o2}/sec/mg_{wt}; Soleus control: 62.6 ± 28.1 pmol_{o2}/sec/mg_{wt}; adjusted p < 0.001, d = 1.76) and CSC-exposed (Gastrocnemius CSC: 30.1 ± 15.0 pmol_{o2}/sec/mg_{wt}; Soleus CSC: 54.3 ± 14.8 pmol_{o2}/sec/mg_{wt}; adjusted p < 0.001, d = 1.62) groups.

Similar to maximal state III respiration, uncoupled respiration (FCCP_{Peak}) was significantly affected by cigarette smoke (p = 0.003, partial $\eta^2 = 0.20$) and tissue type (p < 0.001, partial $\eta^2 = 0.36$), however, there was not a significant interaction effect (p = 0.892, partial $\eta^2 < 0.01$). *Post hoc* analyses failed to determine significant CSC-induced effects in the gastrocnemius (Gastrocnemius control: 52.1 ± 12.0 pmol_{o2}/sec/mg_{wt}; Gastrocnemius CSC: 38.3 ± 23.3 pmol_{o2}/sec/mg_{wt}; adjusted p = 0.082, d = 0.74) or soleus (Soleus control: 89.3 ± 32.1 pmol_{o2}/sec/mg_{wt}; Soleus CSC: 65.7 ± 10.9 pmol_{o2}/sec/mg_{wt}; adjusted p = 0.139, d = 0.87) tissues. However, there were significant effects between the control tissues (p = 0.006, d = 1.54) and the

CSC-exposed tissues ($p = 0.004$, $d = 1.24$).

Complex II-specific respiration (Rot) was affected by CSC ($p = 0.022$, partial $\eta^2 = 0.14$) and tissue type ($p < 0.001$, partial $\eta^2 = 0.37$), but there was not an interaction effect ($p = 0.468$, partial $\eta^2 = 0.01$). *Post hoc* analysis demonstrated non-significant differences between the control group and the CSC-exposed group for the gastrocnemius (Gastrocnemius control: 34.9 ± 11.4 pmol_{O₂}/sec/mg_{wt}; Gastrocnemius CSC: 31.9 ± 20.3 pmol_{O₂}/sec/mg_{wt}; adjusted $p = 0.303$, $d = 0.18$) and soleus (Soleus control: 61.9 ± 18.0 pmol_{O₂}/sec/mg_{wt}; Soleus CSC: 45.5 ± 9.3 pmol_{O₂}/sec/mg_{wt}; adjusted $p = 0.136$, $d = 1.14$). However, there were tissue-specific differences in the control ($p = 0.002$, $d = 1.79$) and CSC-exposed groups ($p = 0.015$, $d = 0.86$). Lastly, residual oxygen consumption (AmA & Omy) was affected by tissue type ($p < 0.001$, partial $\eta^2 = 0.65$), but not CSC ($p = 0.072$, partial $\eta^2 = 0.10$), and there was no interaction effect ($p = 0.535$, partial $\eta^2 = 0.01$). *Post hoc* analysis revealed significant differences between the gastrocnemius and soleus tissues for the control (Gastrocnemius control: 11.9 ± 3.6 pmol_{O₂}/sec/mg_{wt}; Soleus control: 19.9 ± 4.0 pmol_{O₂}/sec/mg_{wt}; adjusted $p < 0.001$, $d = 2.09$) and CSC-exposed (Gastrocnemius CSC: 8.1 ± 2.0 pmol_{O₂}/sec/mg_{wt}; Soleus CSC: 17.8 ± 3.3 pmol_{O₂}/sec/mg_{wt}; adjusted $p = 0.003$, $d = 3.53$) groups.

7.6.2. Effects of CSC on Complex I/II and ANT Contributions and Mitochondrial Quality

There was a significant main effect of smoke ($p = 0.015$, partial $\eta^2 = 0.16$) and an interaction effect ($p = 0.048$, partial $\eta^2 = 0.11$), but no main effect of tissue ($p = 0.466$, partial $\eta^2 = 0.02$) on the relative contribution of complex II respiration (Figure VII-1B). *Post hoc* analysis revealed a significant difference between the control gastrocnemius and the CSC-exposed

gastrocnemius (Gastrocnemius control: $67.2 \pm 9.5\%$; Gastrocnemius CSC: $82.1 \pm 2.1\%$; adjusted $p = 0.006$, $d = 2.16$). No significant differences were observed between the control soleus and smoke soleus (Soleus control: $74.1 \pm 12.6\%$; Soleus CSC: $76.1 \pm 10.4\%$; adjusted $p = 0.323$, $d = 0.17$), control gastrocnemius (adjusted $p = 0.240$, $d = 0.62$), or the CSC-exposed gastrocnemius (adjusted $p = 0.154$, $d = 0.88$); nor were there differences between the CSC-exposed soleus and the control (adjusted $p = 0.161$, $d = 0.89$) or the CSC-exposed gastrocnemius (adjusted $p = 0.190$, $d = 0.80$).

There were significant main effects of smoke ($p < 0.001$ partial $\eta^2 = 0.52$), tissue ($p = 0.001$, partial $\eta^2 = 0.25$), and an interaction effect ($p = 0.001$, partial $\eta^2 = 0.25$) on the ratio of GMDS to CAT_{5.0} (Figure VII-1C). *Post hoc* analysis revealed significant differences between the control and CSC-exposed gastrocnemius (control: 2.23 ± 0.65 ; CSC: 1.22 ± 0.08 ; adjusted $p < 0.001$, $d = 2.05$), but only trended in the soleus (control: 1.63 ± 0.41 ; CSC: 1.28 ± 0.17 ; adjusted $p = 0.059$, $d = 1.10$). There were no differences between the tissues in the control groups (adjusted

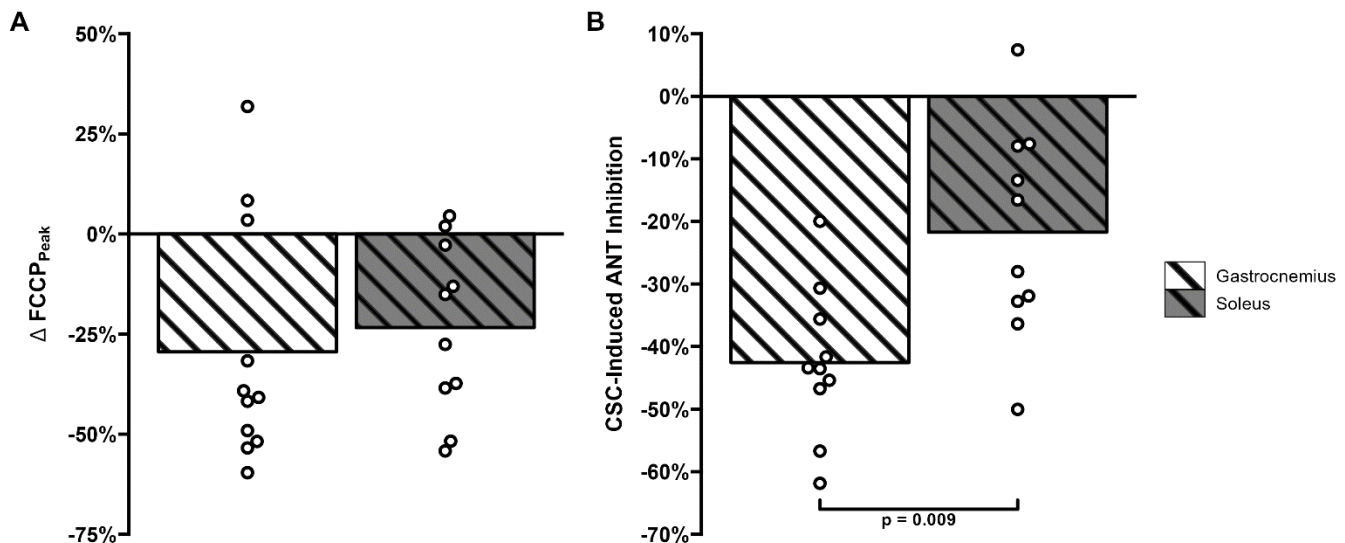


Figure 7-2. The relative differences in uncoupled (FCCP_{Peak}) respiration (A) and the CSC-induced inhibition of ANT (B) between the control and CSC-exposed fibers for the gastrocnemius (white) and soleus (grey) muscle fibers.

$p = 0.135$, $d = 1.11$) or the CSC-exposed groups (adjusted $p = 0.330$, $d = 0.13$).

There were no significant effects of CSC ($p = 0.287$, partial $\eta^2 = 0.03$) or tissue ($p = 0.946$, partial $\eta^2 < 0.01$), nor an interaction effect ($p = 0.557$, partial $\eta^2 < 0.01$) on the ratio of GMDS to FCCP_{Peak} (Figure VII-1D). Significant main effects of CSC ($p < 0.001$, partial $\eta^2 = 0.58$), tissue ($p = 0.015$, partial $\eta^2 = 0.15$), and an interaction effect ($p = 0.025$, partial $\eta^2 = 0.12$) were observed on the thermodynamic coupling (Figure VII-1E). Post hoc analysis revealed significant differences between the control and CSC-exposed gastrocnemius (control: 0.71 ± 0.07 , CSC: 0.40 ± 0.15 ; adjusted $p < 0.001$, $d = 2.70$) and soleus (control: 0.54 ± 0.13 , CSC: 0.39 ± 0.12 ; adjusted $p = 0.046$, $d = 1.18$). Furthermore, there were significant differences between the control gastrocnemius and control soleus (adjusted $p = 0.042$, $d = 1.74$) and the control gastrocnemius and the CSC-exposed soleus (adjusted $p < 0.001$, $d = 3.27$). No significant differences were observed between the CSC-exposed gastroc and the control soleus (adjusted $p = 0.063$, $d = 0.98$) or the CSC-exposed gastrocnemius and the CSC-exposed soleus (adjusted $p = 0.380$, $d = 0.09$).

Respiratory Control Ratio (not shown) was also significantly affected by CSC ($p = 0.025$, partial $\eta^2 = 0.12$), but not tissue ($p = 0.570$, partial $\eta^2 < 0.01$), nor was there an interaction effect ($p = 0.571$, partial $\eta^2 < 0.01$). Post hoc analysis revealed a trend toward significance between the control and CSC-exposed soleus (control: 3.25 ± 0.85 , CSC: 2.70 ± 0.70 ; adjusted $p = 0.057$, $d = 0.71$), but no difference between the control and CSC-exposed gastrocnemius (control: 3.71 ± 1.54 , CSC: 2.71 ± 0.86 ; adjusted $p = 0.105$, $d = 0.81$).

7.6.3. Effects of CSC on ETS Activity

The difference in uncoupled respiration (FCCP_{Peak}) between the control and smoke groups

for both the gastrocnemius and soleus are shown in Figure 7-2A. There were no significant differences ($p = 0.426$; $d = 0.23$) between the gastrocnemius ($-29.4\% \pm 30.0\%$) and the soleus ($-23.3\% \pm 21.6\%$). CSC-induced ANT inhibition is shown in Figure VII-2B. There was a significant difference ($p = 0.009$; $d = 0.93$) in the ability for CSC to inhibit ANT between the gastrocnemius ($-42.6\% \pm 12.0\%$) and the soleus ($-21.8\% \pm 17.0\%$).

7.6.4. Effects of CSC on ADP Kinetics

Dose kinetics for ADP are shown in Figure VII-2A. There were significant main effects of CSC ($p < 0.001$, partial $\eta^2 = 0.35$) and tissue ($p < 0.001$, partial $\eta^2 = 0.38$), as well as significant interaction effects ($p < 0.001$, partial $\eta^2 = 0.37$) in the apparent K_m of ADP (Figure VII-2B). *Post hoc* analysis revealed that the soleus control ($316.8 \pm 213.5 \mu\text{M}$ ADP) was significantly greater than the control gastrocnemius ($26.4 \pm 18.5 \mu\text{M}$ ADP; adjusted $p = 0.001$, $d = 1.92$), CSC-exposed gastrocnemius ($37.7 \pm 42.4 \mu\text{M}$ ADP; adjusted $p = 0.001$, $d = 1.81$), and the CSC-exposed soleus ($43.6 \pm 9.7 \mu\text{M}$ ADP; adjusted $p = 0.042$, $d = 1.81$). No significant differences were observed between the gastrocnemius control and gastrocnemius smoke (adjusted $p = 0.431$, $d = 0.35$), the gastrocnemius control and the soleus smoke ($p = 0.277$, $d = 1.03$), or the CSC-exposed gastrocnemius and CSC-exposed soleus (adjusted $p = 0.242$, $d = 0.19$).

Similarly, CSC ($p < 0.001$, partial $\eta^2 = 0.35$) and tissue type ($p < 0.001$, partial $\eta^2 = 0.46$) had significant main effects on the apparent V_{max} of ADP (Figure VII-3C); however, there was not a significant interaction effect ($p = 0.813$, partial $\eta^2 < 0.01$). *Post hoc* analysis revealed significant differences between the control gastrocnemius and CSC-exposed gastrocnemius (Gastrocnemius control: $44.5 \pm 10.8 \text{ pmol O}_2/\text{sec/mg}_{\text{wt}}$; Gastrocnemius CSC: $27.3 \pm 12.4 \text{ pmol O}_2/\text{sec/mg}_{\text{wt}}$; adjusted

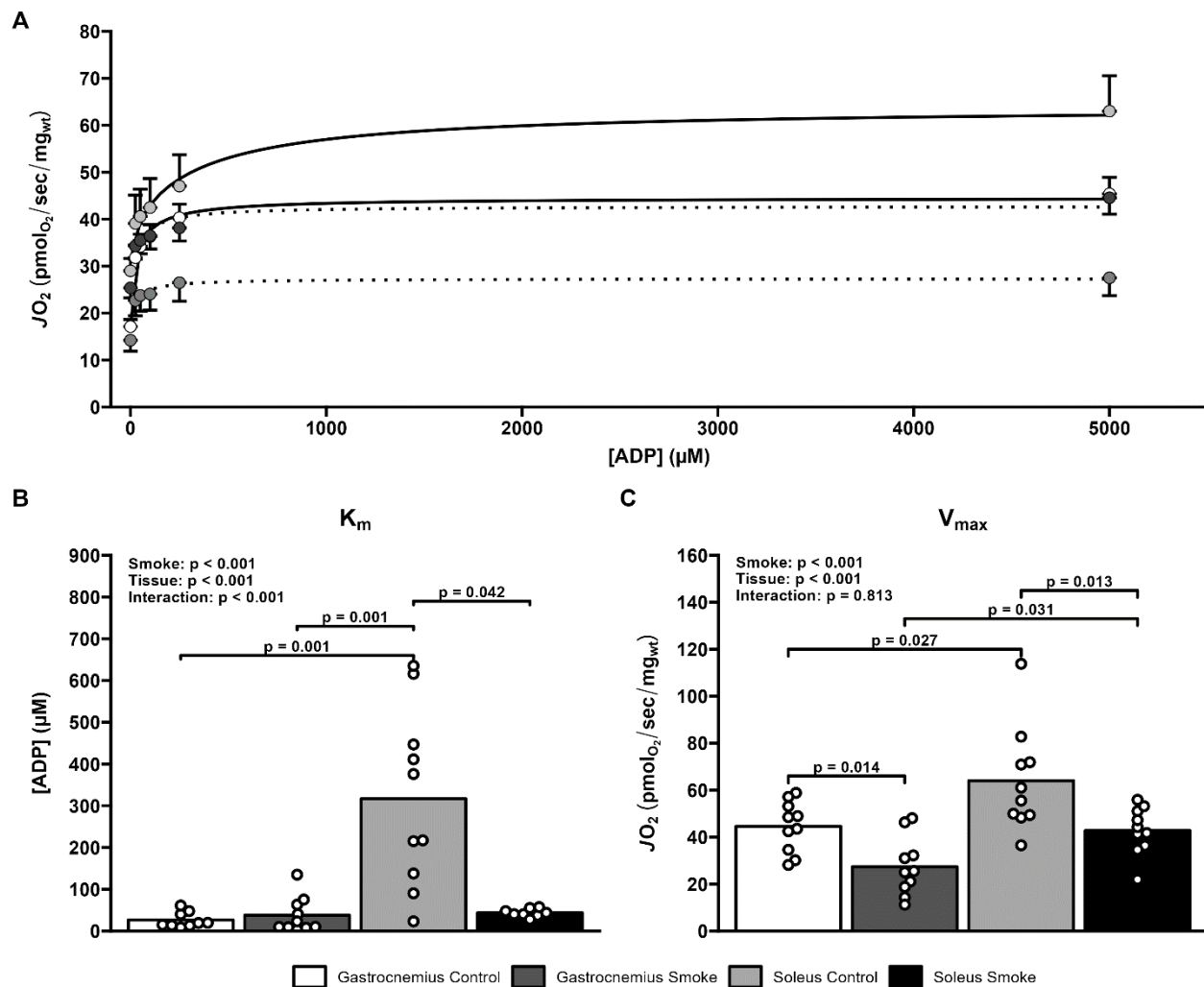


Figure 7-3. Dose-response kinetic curves for ADP-stimulated respiration (A) in the gastrocnemius (white; $n = 9-10$) and soleus (light grey; $n = 10$) and their respective CSC-exposed counterparts (dark grey and black; $n = 8-10$); and mean estimates for the apparent K_m (B) and V_{max} (C). Values are expressed as mean \pm SEM, where appropriate.

$p = 0.014$, $d = 1.48$) as well as the control soleus and CSC-exposed soleus (Soleus control: 64.0 ± 22.2 pmol₂/sec/mg_{wt}; Soleus CSC: 42.7 ± 10.1 pmol₂/sec/mg_{wt}; adjusted $p = 0.013$, $d = 1.23$). Likewise, there were significant differences between the tissues in the CSC-exposed groups ($p = 0.032$, $d = 1.37$), but only a trend towards significant differences between the control groups ($p = 0.028$, $d = 1.11$).

7.6.3. Effects of CSC on ANT-dependent Mitochondrial Respiration

Dose kinetics for CAT are shown in Figure VII-3A. CSC ($p = 0.004$, partial $\eta^2 = 0.21$) and tissue ($p < 0.001$, partial $\eta^2 = 0.43$) type had significant effects on the initial rate (C) of respiration before the addition of CAT (Figure VII-3B); however, there was no a significant interaction effect ($p = 0.717$, partial $\eta^2 < 0.01$). *Post hoc* analysis failed to find any significant effects of CSC on the gastrocnemius (Gastrocnemius control: 57.1 ± 10.6 pmol₂/sec/mg_{wt}; Gastrocnemius CSC: 39.0 ± 19.9 pmol₂/sec/mg_{wt}; adjusted $p = 0.113$, $d = 1.14$) or the soleus tissues (Soleus control: 93.9 ± 34.6 pmol₂/sec/mg_{wt}; Soleus CSC: 68.8 ± 18.0 pmol₂/sec/mg_{wt}; adjusted $p = 0.073$, $d = 1.03$). There were, however, significant effects of tissue type for both the control (adjusted $p = 0.005$, $d = 1.56$) and CSC-exposed tissues (adjusted $p = 0.008$, $d = 1.66$).

There were no significant main effects of CSC ($p = 0.644$, partial $\eta^2 < 0.01$) and tissue ($p = 0.516$, partial $\eta^2 = 0.01$), nor a significant interaction effect ($p = 0.581$, partial $\eta^2 < 0.01$) in the apparent IC₅₀ of CAT (Figure VII-3C). Similarly, we failed to detect a significant main effect of CSC ($p = 0.059$, partial $\eta^2 = 0.10$) or an interaction effect ($p = 0.506$ partial $\eta^2 = 0.01$); however, there was a significant effect of tissue type ($p < 0.001$, partial $\eta^2 = 0.41$) on the apparent I_{max} of CAT (Figure VII-3D). *Post hoc* analysis revealed significant differences between the

gastrocnemius and soleus tissues in the control groups (Gastrocnemius control: 18.3 ± 10.0 pmol₂/sec/mg_{wt}; Soleus control: 40.3 ± 9.1 pmol₂/sec/mg_{wt}; adjusted p = 0.002, d = 2.30) and the CSC-exposed (Gastrocnemius CSC: 27.4 ± 12.3 pmol₂/sec/mg_{wt}; Soleus CSC: 42.8 ± 17.8 pmol₂/sec/mg_{wt}; adjusted p = 0.013, d = 1.01) groups.

On the other hand, there were significant main effects of CSC (p < 0.001, partial $\eta^2 = 0.61$), tissue type (p = 0.048, partial $\eta^2 = 0.11$), and an interaction effect (p = 0.004, partial $\eta^2 = 0.22$) on the relative inhibitory effects of CAT (Figure VII-3E). *Post hoc* analysis revealed a significant difference between the control and CSC-exposed gastrocnemius (Gastrocnemius control: $-70.5 \pm 17.6\%$; Gastrocnemius CSC: $-27.7 \pm 10.4\%$; adjusted p < 0.001, d = 2.96), but only trended in the soleus (Soleus control: $47.2 \pm 15.7\%$; Soleus CSC: $30.5 \pm 6.9\%$; adjusted p = 0.077, d = 1.37). Furthermore, the control gastrocnemius exhibited significantly greater inhibition than the CSC-exposed soleus (adjusted p = 0.001, d = 3.00), but not the control soleus (p = 0.076, d = 3.00), while the CSC-exposed gastrocnemius exhibited significantly greater inhibition than the control soleus (p = 0.024, d = 1.46). *Post hoc* tests failed to identify a significant difference between the CSC-exposed gastrocnemius and the CSC-exposed soleus (p = 0.305, d = 0.31).

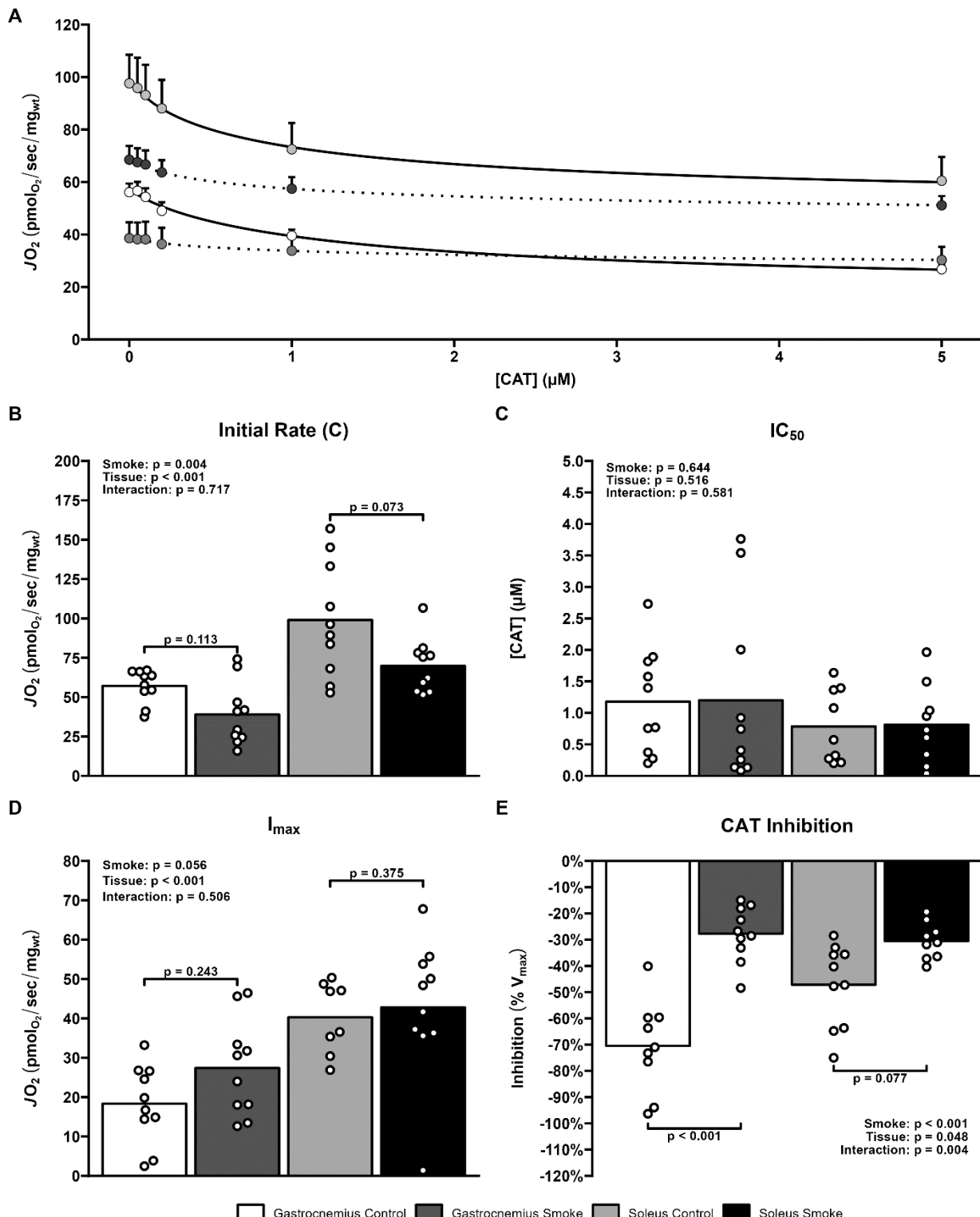


Figure 7-4. Dose-response kinetic curves for carboxyatractyloside-inhibited respiration (A) in the gastrocnemius (white; $n = 9-10$) and soleus (light grey; $n = 10$) and their respective CSC-exposed counterparts (dark grey and black; $n = 8-10$). Mean estimates for the initial rate (B), apparent IC_{50} (C), I_{max} (D), and the inhibitory effect of CAT relative to the initial rate (E). Values are expressed as mean \pm SEM, where appropriate.

7.7. Discussion

The present study aimed to comprehensively examine the effect of cigarette smoke on mitochondrial energy transfer involving the electron transport chain, ADP transport into the mitochondria, and respiratory control by ADP in permeabilized fibers from skeletal muscles with different metabolic characteristics. Consistent with our hypothesis, acute cigarette smoke exposure significantly inhibited maximal ADP-stimulated respiration in slow- and fast-twitch skeletal muscle fibers. Despite quantitatively similar impairments in maximal ETC capacity, the site of CSC-induced inhibition of mitochondrial respiration appeared to be tissue-dependent. Specifically, the fast-twitch gastrocnemius muscle exhibited a greater decrease of Complex-I-specific respiration than the slow-twitch soleus. In comparison, Complex II-linked respiration was marginally affected by CSC, such that its relative contribution to muscle respiratory capacity was increased in the CSC-exposed gastrocnemius muscle relative to controls. CSC also elicited a tissue-dependent effect on respiratory control as mitochondrial respiration sensitivity for ADP was significantly increased in the soleus but not the gastrocnemius.

Moreover, the effect of carboxyatractyloside-induced inhibition of nucleotide transfer was markedly attenuated in smoke-exposed fibers compared to control tissues, suggesting that cigarette smoke impairs the ANT-mediated exchange of ATP/ADP across the inner mitochondrial membrane. This mechanism contributed to the cigarette smoke-induced loss of mitochondrial oxidative capacity and was accentuated in the fast-twitch gastrocnemius muscle. However, cigarette smoke did not significantly affect mitochondrial proton leak in slow- and fast-twitch skeletal muscle fibers. Finally, mitochondrial thermodynamic efficiency was decreased by cigarette smoke in both muscles with, however, a greater relative decline in the gastrocnemius than

the soleus muscle. Collectively, these findings support the theory that cigarette smoke directly impairs mitochondrial respiration, especially in fast-twitch muscles. This acute effect was mediated by inhibiting the mitochondrial ETC capacity, predominantly at the site of complex I, and the impairment of nucleotide exchange by ANT in both muscles.

7.7.1. Complex I is a Primary Site of CSC-Induced Mitochondrial Impairments in Gastrocnemius but not soleus

Consistent with our hypothesis, CSC drastically inhibited complex-I-supported (GMD_{5000}), complex-I-and-II-supported (GMDS), and uncoupled (FCCP_{Peak}) mitochondrial respiration in fast- and slow-twitch skeletal muscle fibers (Figure VII-1A). Specifically, CSC decreased complex-I-supported respiration by ~40% in the gastrocnemius and by ~30% in the soleus. In comparison, complex-I-and-II-driven respiration was decreased by ~35% and ~30% in the gastrocnemius and soleus muscles, respectively. Furthermore, CSC elicited similar inhibitory effects in both the gastrocnemius and soleus to maximal ETC activity assessed by optimal titrations of FCCP (Figure VII-2A). Interestingly, it appears that the gastrocnemius is quite susceptible to CSC-induced impairments in complex-I-specific respiration (Figure VII-1B), as rotenone, an inhibitor of complex I, greatly inhibited mitochondrial respiration in the control gastrocnemius but had a much lesser effect in the CSC-exposed gastrocnemius. These effects were not as pronounced in the soleus fibers, thus suggesting that the gastrocnemius relies more on complex-I-driven respiration than the soleus muscles and that CSC-induced impairments in complex I activity are more detrimental in fast-twitch glycolytic muscle fibers than slow-twitch oxidative fibers. However, despite the greater reliance of the gastrocnemius on complex I-driven respiration, the soleus

exhibited similar global impairments to the mitochondrial ETC, suggesting that other ETC components – such as cytochrome C, complex III, or complex IV – are likely inhibited by cigarette smoke in the soleus.

Overall, the present findings agree with the results of Khattri et al. (2022), which reported a 50-90% inhibition of complex-I-driven respiration (stimulated by glutamate and malate) in CSC-exposed isolated mitochondria from skeletal muscles of different regions of the body. Likewise, using permeabilized gastrocnemius muscle fibers, Thatcher et al. (2014) reported a ~40% decrease in complex-I-driven mitochondrial respiration in mice exposed to airstream cigarette smoke for six weeks. Although the inhibition induced by cigarette smoke on the respiration rate was evident with both preparations, it is interesting to note the smaller effect size using an *in situ* preparation. Specifically, in the present study, the ~40% decrease in complex I supported respiration in the white gastrocnemius muscles following 1 hour of 4% CSC incubation was strikingly similar to the ~40% decrease in the respiration rate of the red gastrocnemius muscles of mice chronically exposed to airstream cigarette smoke for six weeks (Thatcher et al., 2014). In comparison, mitochondria respiration in isolated mitochondria from a mixture of skeletal muscles was inhibited by as much as 93% after exposure to a lower concentration of CSC (1%) for only 10 minutes (Khattri et al., 2022). These findings confirm that mitochondrial isolation procedures exacerbate the susceptibility of the mitochondria to stressors, such as cigarette smoke, whereas the *in situ* preparation more closely recapitulates the extent of mitochondrial dysfunction under conditions that preserve its native morphology (Picard et al., 2011).

Another important result from the present study was the finding that inhibition of complex I respiration with rotenone significantly attenuated the CSC-induced deficit in mitochondrial

respiration, although this effect was fiber-type specific (Figure 1C). Indeed, the relative contribution of complex II-supported respiration was higher in the fast-twitch gastrocnemius muscle after CSC incubation than in control but remained unchanged in the slow-twitch soleus muscle (Figure 1C). The present findings provide additional insights into the metabolic alterations previously documented in the skeletal muscle of patients with Chronic Obstructive Pulmonary Disease (COPD), a disorder typically caused by chronic cigarette smoking. Specifically, the skeletal muscles of these patients are characterized by a greater proportion of type II muscle fibers in the lower limb (Gea et al., 2015; Gosker et al., 2007; Nyberg et al., 2015) and a greater reliance on complex II-driven respiration than healthy controls (Gifford et al., 2015, 2018). The results of the present study would therefore suggest that this shift in the mitochondrial pathways for energy production in the skeletal muscle of patients with COPD is mediated by the direct effect of cigarette smoke on mitochondrial respiration in type II fibers, which becomes the predominant fiber type as the disease progresses.

Moreover, the results in the present study, in conjunction with the findings in Thatcher et al., underscore the translational properties of the use of permeabilized skeletal muscle bundles in models investigating mitochondrial function *in situ* as compared to models using isolated mitochondria. Specifically, the ~40% decrease in mitochondrial respiration in the white gastrocnemius muscles of mice following 1-hour of 4% CSC exposure in the present study are strikingly similar to the ~40% decrease in mitochondrial respiration in the red gastrocnemius muscles of mice exposed to airstream cigarette smoke for 6 weeks reported by Thatcher et al. In comparison, mitochondria isolated from a mixture of skeletal muscles experienced up to a 93% decrease in mitochondrial respiration after exposure to 1% CSC for ~10 minutes. This suggests

that structural alterations to mitochondria caused by the isolation procedures (Picard et al., 2011) drastically exacerbate cigarette smoke-induced impairments in mitochondrial function. Collectively, while there are several comparative advantages of using isolated mitochondria for the investigation of mitochondrial physiology (i.e., high-throughput, cost-effectiveness, etc.), these findings highlight the importance of validating studies utilizing mitochondrial preparations (e.g., tissue homogenate, isolated mitochondria, etc.) with techniques that may be more reflective of the *in vivo* condition (e.g., intact permeabilized tissues, ^{31}P -MRS)(Layec et al., 2016).

7.7.2. Effects of Cigarette Smoke on the Control of Oxidative Phosphorylation in Skeletal Muscle

Unlike the gastrocnemius muscle, the apparent K_m for ADP in the soleus markedly decreased from $\sim 320 \mu\text{M}$ in the control condition to $\sim 40 \mu\text{M}$ with CSC (Figure VII-3A). In the control condition, the apparent K_m values for ADP for the gastrocnemius and soleus muscles are within the range of values previously reported using permeabilized muscle fibers. For instance, slow-twitch oxidative muscles are characterized by an apparent K_m for ADP in the range of 200-500 μM whereas fast-twitch glycolytic muscles exhibit values in the range of 10-40 μM (Burelle & Hochachka, 2002; Ponsot et al., 2005). This lower sensitivity for ADP in slow-twitch oxidative muscles stems from the selective permeability of the mitochondrial outer membrane to ADP, which restricts its diffusion into the matrix. Interestingly, the mitochondrial sensitivity for ADP of slow-twitch oxidative muscles can be substantially increased ($K_m < 100 \mu\text{M}$) with the addition of creatine in the respiration buffer (Burelle & Hochachka, 2002; Ponsot et al., 2005). In slow-twitch oxidative muscles, mitochondrial creatine kinase (Mt-CK) is functionally coupled to ANT and the voltage-dependent anion channel (VDAC), located on the inner and outer mitochondrial

membrane, respectively. Within this functional network, Mt-CK catalyzes the transfer of phosphate groups between the sites of ATP production in the mitochondrial matrix (ATP synthase) and ATP consumption in the cytosol (myosin ATPase and ionic pumps) (Qin et al., 1999; V. Saks et al., 1991; V. Saks et al., 1994; Wallimann et al., 1992).

In light of the Cr/PCr shuttle theory detailed above, the CSC-induced increase in mitochondrial respiration sensitivity for ADP in the permeabilized fibers from the soleus suggests that cigarette smoke disrupted the functional interactions between VDAC, mtCK, and ANT. This disruption resulted in greater permeability of the mitochondrial outer membrane to ADP in the slow-twitch oxidative muscle, which perhaps mediated VDAC/mtCK/ANT interdependence. In support of this interpretation, it has been reported that tubulin structure, which is a cytoskeletal protein present at the mitochondrial surface that binds to VDAC and regulates its conductance (Guzun et al., 2012), can be disrupted by cigarette smoke exposure in lung epithelial cells (Das et al., 2009). The present findings provide evidence for a tissue-dependent effect of cigarette smoke on the control of oxidative phosphorylation mediated by perturbations of the Cr/PCr shuttle in slow-twitch oxidative soleus muscle. Further studies are warranted to examine whether this alteration in the control of oxidative phosphorylation is caused by changes in VDAC conductance, mtCK, or ANT directly.

7.7.3. Cigarette Smoke-Induced Blockade of Nucleotide Exchange Across the Mitochondrial Membrane

A novel aspect of the present study was the use of carboxyatractyloside to investigate the contribution of ANT-facilitated exchange of ADP/ATP to mitochondrial respiration.

Carboxyatractyloside is a non-competitive inhibitor of the enzyme adenine nucleotide translocase (Luciani et al., 1971), which is located on the inner mitochondrial membrane and is responsible for the exchange of ADP/ATP between the mitochondrial intermembrane space and the mitochondrial matrix (Klingenberg, 2008; Kunji et al., 2016), as well as an important site for proton leak (Bertholet et al., 2019a). Similarly to its analog, atracyloside, CAT binds to the ANT from the cytosolic side of the mitochondrial inner membrane, locking ANT in a cytoplasmic-facing open conformation and preventing the exchange of ADP/ATP (Pebay-Peyroula et al., 2003). However, unlike atracyloside, CAT is not influenced by the concentrations of ADP or ATP, thus increasing its effectiveness in blocking the transfer of adenine nucleotides between the inner mitochondrial membrane (Luciani et al., 1971). Therefore, by using CAT to inhibit ANT in the present study, we were able to measure the functional contribution of ANT to the control of mitochondrial respiration under our experimental conditions.

Using this specific inhibitor (Barbour et al., 1984; Burelle & Hochachka, 2002; Qin et al., 1999; V. Saks et al., 1991; V. A. Saks et al., 1994; Wallimann et al., 1992), the differences in maximal ADP-stimulated respiration between CSC and control conditions were abolished under saturating concentrations of CAT in the gastrocnemius and the soleus (CAT_{5.0}, Figure VII-1). Likewise, there were significant CSC-induced differences in the apparent sensitivity (IC₅₀) or maximal inhibitory capacity (I_{max}) of CAT (Figure VII-4C & VII-4D). As a result, the relative inhibition induced by CAT was significantly lower in CSC-exposed fibers (~30%) than in control fibers (~70-50%, Figure VII-4E) for both muscles, although the magnitude of this effect was tissue-dependent. Specifically, the inhibitory effect of cigarette smoke on ANT-dependent respiration was markedly higher in the gastrocnemius (~43%) than the soleus (~22%, Figure VII-

2B). Additionally, the ratio of maximal respiration (GMDS) to ANT-inhibited respiration (CAT_{5.0}) was significantly impaired by cigarette smoke in both the gastrocnemius and soleus (Figure VII-1C). In contrast, cigarette smoke exposure had no significant effect on the ratio of maximal ADP-dependent respiration (GMDS) to maximal ADP-independent respiration (FCCP_{Peak}), as shown in Figure VII-1D, which rules out impairments of the phosphorylation capacity of the F₁-F₀ ATP Synthase as a contributor to the decline in maximal ADP-stimulated respiration induced by cigarette smoke. Therefore, these collective findings suggest that, in addition to impairments to the electron transport chain, cigarette smoke also greatly impairs the exchange of ADP/ATP via inhibiting the functionality of ANT. Furthermore, maximal uncoupled respiration (FCCP_{Peak}), in which mitochondrial respiration is not coupled with ATP production and is independent of ADP availability, was less affected by CSC exposure than was maximal coupled respiration (GMDS). Accordingly, maximal coupled respiration was significantly impaired in the CSC-exposed fibers by 40% and 35% in the gastrocnemius and soleus, respectively (Figure VII-1A), while uncoupled respiration was nonsignificantly impaired in the CSC-exposed fibers by ~25% in both the gastrocnemius and soleus, respectively (Figure VII-2A). Altogether, our results suggest that ANT blockade is another mechanism by which cigarette smoke produces a bioenergetic insult to skeletal muscle mitochondria. . A study in human lung epithelial A459 cells has also previously implicated ANT in the deleterious effects of cigarette smoke on mitochondrial function (Wu *et al.*, 2020). However, the difference in protocols (10% versus 4% CSC, intact cells versus permeabilized fibers, 6 versus 1 hour incubation, carboxyatractyloside prolonged incubation versus acute titration) precluded any direct comparison between the study by Wu *et al.* and the present work. Interestingly, the gastrocnemius was nearly twice as susceptible to CSC-induced ANT

inhibition than the soleus muscles (Figure VII-2B). Considering the differences in expression of Mt-CK between the white gastrocnemius and soleus muscles, it is likely that these observations are due to differing mechanisms which regulate the exchange of adenine nucleotides between the mitochondrial intermembrane space and matrix. Indeed, several models estimate that Mt-CK-facilitated exchange of nucleotides accounts for up to ~80% of energy transfer from the matrix to the cytosol (Aliev et al., 2011; Guzun et al., 2012; Perry et al., 2012; Wallimann et al., 2011). Thus, the sMt-CK present in soleus muscles, which is interdependent on the activity of ANT, could act as a buffer system to better maintain energy transfer between the sarcoplasm and the mitochondrial matrix. Alternatively, the lack of Mt-CK in white gastrocnemius would increase the reliance of these tissues on ANT for energy transfer and, therefore, would increase the susceptibility of the white gastrocnemius to CSC-induced ANT-dependent bioenergetic dysfunction, as observed in the present study.

7.7.4. Mitochondrial Quality is Impaired with CSC Exposure

Mitochondrial thermodynamic coupling (q-value) was significantly impaired by cigarette smoke exposure in both muscles (Figure VII-1E). Interestingly, the smoke-induced loss of energy coupling was accentuated in the fast-twitch gastrocnemius compared to the slow-twitch soleus muscle. This thermodynamic coupling reflects all enzymatic processes and free energy changes during oxidative phosphorylation (Stucki, 1980) and is linked to the mitochondrial P/O ratio (Cairns et al., 1998), thus providing a direct measure of mitochondrial efficiency (Larsen et al., 2011). The present results in skeletal muscle fibers acutely exposed to cigarette smoke are consistent with those of Kyle et al. (Kyle et al., 2013), which reported smoke-induced decreases

in the P/O ratio of mitochondria isolated from the lungs of guinea pigs. Also, patients with COPD, a condition caused by chronic cigarette smoking, are characterized by impaired metabolic efficiency during dynamic contraction (Layec et al., 2011; Richardson et al., 2004).

Conceptually, lower thermodynamic coupling values indicate that mitochondrial respiration was not as tightly coupled to oxidative ATP production following cigarette smoke exposure, which might be mediated by a greater dissipation of the proton gradient via proton leak. However, the lack of significant differences between smoke and control conditions in leak respiration (GM, Figure VII-1A) does not support this mechanism. Alternatively, a decrease in the protons/electrons stoichiometry of the proton pumps caused by slipping of the proton pumps in the respiratory chain (Nicholls & Ferguson, 2013) may account for the effects of cigarette smoke on thermodynamic coupling. In support of this interpretation, cigarette smoke markedly inhibited electron flow in the electron transport chain in both muscles as assessed by the titration of FCCP (Figure 2A). Also, a lower mitochondrial membrane potential has been consistently documented in various tissue preparation (Haji et al., 2020; van der Toorn et al., 2007, 2009; Wu et al., 2020), consistent with lower respiratory coupling. From a translational perspective (Jacobs et al., 2013; Kyle et al., 2013; Picard et al., 2011), the impaired efficiency of ATP production in hindlimb skeletal muscles of mice could explain many of the altered bioenergetic differences commonly reported in the locomotor muscles of persons chronically exposed to cigarette smoke, including increased muscle fatigability (Wüst et al., 2008) and impaired exercise tolerance (Papathanasiou et al., 2007).

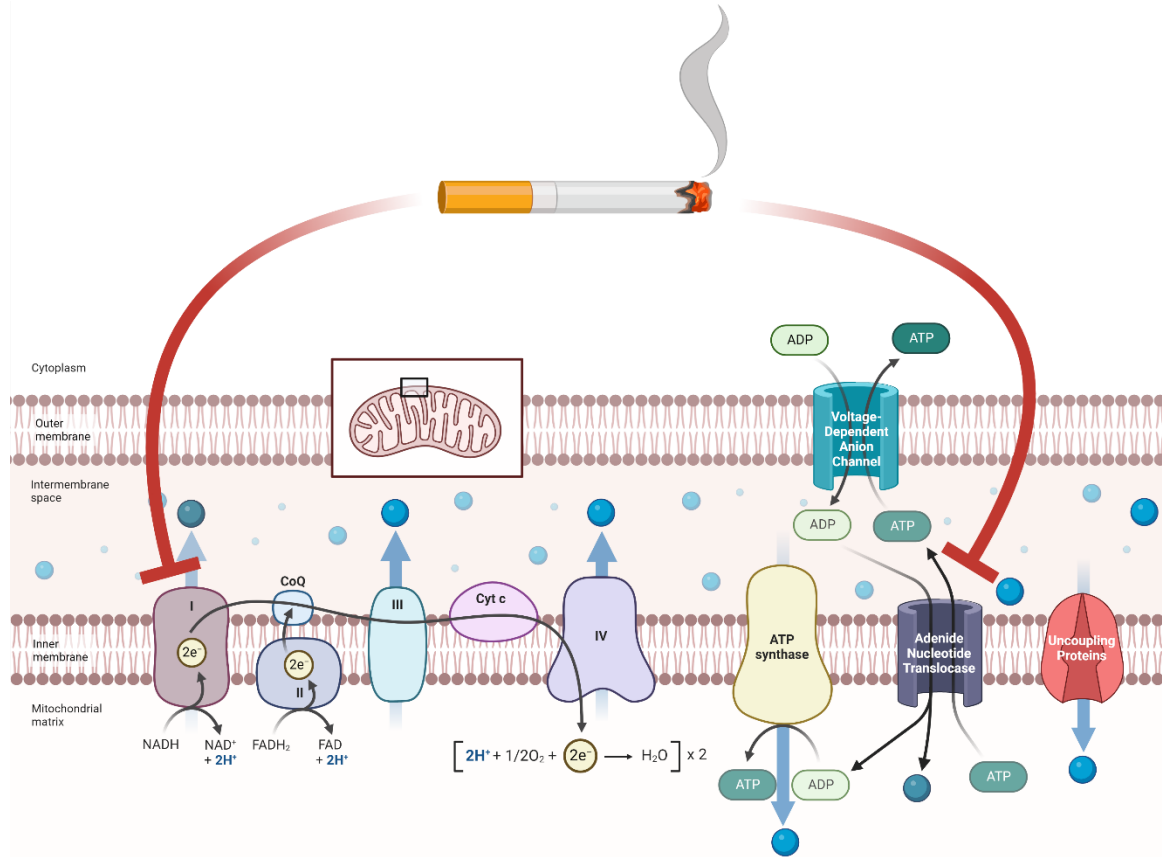


Figure 7-5. Summary of the findings in aim 3. Cigarette smoke induces concurrent blockade of Complex I and ANT, impairing mitochondrial oxidative phosphorylation and ATP generation.

7.7.5. Clinical Perspectives

Herein, we investigated the mechanisms of cigarette smoke-induced impairments to skeletal muscle mitochondrial respiration. The experiments in the present study revealed that, in addition to inhibition of complex I of the ETC, cigarette smoke also impairs the exchange of ADP/ATP between the mitochondrial matrix and cytosol, ultimately resulting in reduced bioenergetic efficiency in the mitochondria of skeletal muscles. Clinically, the impaired efficiency of ATP production in hindlimb skeletal muscles of mice could explain many of the altered bioenergetic differences commonly reported in the locomotor muscles of persons chronically exposed to cigarette smoke, including increased muscle fatigability (Wüst et al., 2008) and

impaired exercise tolerance (Papathanasiou et al., 2007b). Conceptually, deficiencies in sarcoplasmic ATP concentrations — whether due to impaired production of ATP or transport of ATP into the sarcoplasm — could induce fatigue in skeletal muscle directly by impairing ATP availability for myosin ATPase or indirectly by attenuating SERCA-ATPase-dependent calcium recycling into the sarcoplasmic reticulum. These effects of CSC, in conjunction with the direct inhibition of muscular force production and impairment of calcium handling in skeletal muscle (Nogueira et al., 2018), may mechanistically explain the loss of muscle function related to cigarette smoking. However, interventions to address these detriments and restore muscle function have yet to be identified.

7.8. Conclusion

In conclusion, the present study comprehensively examined the effects of cigarette smoke on mitochondrial energy transfer involving the electron transport chain, ADP transport into the mitochondria, and respiratory control by ADP in skeletal muscles with different metabolic characteristics. Acute cigarette smoke exposure significantly inhibited maximal ADP-stimulated respiration in the skeletal muscle. Interestingly, the site of CSC-induced inhibition of mitochondrial respiration appeared to be tissue-dependent. Specifically, the fast-twitch gastrocnemius muscle exhibited a greater decrease of Complex-I-specific respiration than the slow-twitch soleus. CSC also elicited a tissue-dependent effect on respiratory control as mitochondrial respiration sensitivity for ADP was significantly increased in the soleus but not the gastrocnemius.

Furthermore, we provide evidence to suggest that cigarette smoke also directly impairs mitochondrial thermodynamic efficiency and the exchange of ADP/ATP by inhibiting ANT in the inner mitochondrial membrane. Unlike previous studies using *in vitro* preparation which can affect mitochondrial morphology and function, mitochondrial proton leak in slow- and fast-twitch skeletal muscle fibers was not significantly affected by cigarette smoke when assessed *in situ* in permeabilized fibers. Our findings shed light on the mechanisms of energy transfer that mediate the cigarette smoke-induced impairment of mitochondrial production of ATP in the skeletal muscle, leading to bioenergetic deficiencies and ultimately contributing to poor exercise tolerance commonly observed in humans chronically exposed to cigarette smoke.

Table 7-1. Mean Mitochondrial Respiration Rates (pmol_{O₂}/sec/mg). Data represented as mean ± SD. Different letters indicate significant ($p < 0.05$) post hoc differences between groups; like letters indicate lack of significance ($p > 0.05$) between groups.

	Gastrocnemius		Soleus		ANOVA p-values (Partial η^2)		
	Control	Smoke	Control	Smoke	Smoke Effect	Tissue Effect	Interaction Effect
GM	16.8 ± 4.6 ^a	12.6 ± 3.9 ^a	27.6 ± 4.44 ^b	26.4 ± 7.2 ^b	p = 0.313 (0.03)	p < 0.001 (0.61)	p = 0.308 (0.3)
GMD₅₀₀₀	45.4 ± 11.2 ^a	27.5 ± 12.0 ^b	63.0 ± 23.8 ^c	44.6 ± 11.1 ^d	p < 0.001 (0.32)	p < 0.001 (0.28)	p = 0.604 (0.01)
GMDS	57.1 ± 10.6 ^a	37.3 ± 17.5 ^b	96.2 ± 30.9 ^c	68.2 ± 16.0 ^c	p < 0.001 (0.27)	p < 0.001 (0.47)	p = 0.542 (0.01)
CAT_{5.0}	26.8 ± 5.8 ^a	30.1 ± 15.0 ^a	62.6 ± 28.1 ^b	54.3 ± 14.8 ^b	p = 0.820 (<0.01)	p < 0.001 (0.58)	p = 0.716 (<0.01)
FCCP_{Peak}	52.1 ± 12.0 ^a	38.3 ± 23.3 ^a	89.3 ± 32.1 ^b	65.7 ± 20.9 ^b	p = 0.003 (0.20)	p < 0.001 (0.36)	p = 0.892 (<0.01)
Rot	34.9 ± 11.4 ^a	31.9 ± 20.3 ^a	61.9 ± 18.0 ^b	45.5 ± 9.3 ^b	p = 0.022 (0.14)	p < 0.001 (0.37)	p = 0.468 (0.01)
AmA & Omy	11.9 ± 3.6 ^a	8.1 ± 2.0 ^a	19.9 ± 4.0 ^b	17.8 ± 3.3 ^b	p = 0.072 (0.10)	p < 0.001 (0.65)	p = 0.535 (0.01)

CHAPTER 8

CONCLUSION

The overarching goal of this project was to advance the understanding of the underlying causes of cigarette smoke-induced mitochondrial dysfunction – specifically targeting tissue-specific susceptibility to cigarette smoke toxicity, alterations to mitochondrial substrate oxidation, and identifying key mitochondrial targets of cigarette smoke-induced dysfunction using an *in situ* mouse model. To meet this overarching goal, we developed 3 separate experimental aims which would elucidate the mechanisms of cigarette smoke-induced mitochondrial dysfunction:

Aim 1 – Acute Effects of Cigarette Smoke Condensate on Mitochondrial Respiration

In specific aim 1, we determined the extent of tissue-specific susceptibility to cigarette smoke for the aorta, cardiac muscle, and type I and type II skeletal muscles. Our working hypothesis was that each tissue would display different susceptibility to cigarette smoke, with the cardiac muscle and aorta being more susceptible to cigarette smoke based on epidemiological evidence suggesting the greater relative risks for tobacco-related diseases in these tissues relative to others (Gandini et al., 2008).

Aim 2 – Effects of Cigarette Smoke Exposure on Mitochondrial Substrate Utilization

In specific aim 2, we determined the cigarette smoke-induced alterations to mitochondrial oxidation of palmitoylcarnitine, a long-chain fatty acid, and pyruvate, a product of glycolysis in the skeletal muscle (glycolytic gastrocnemius fibers and oxidative soleus fibers). Our working hypothesis was that cigarette smoke would decrease the sensitivity and maximal capacity to oxidize palmitoylcarnitine oxidation.

Aim 3 – Mechanisms of Cigarette Smoke-Induced Mitochondrial Dysfunction

In specific aim 3, we determined the extent of cigarette smoke-induced perturbations to the exchange of phosphates, ADP sensitivity, and mitochondrial respiratory chain activity. Based upon prior studies in epithelial cells (Wu et al., 2020), our working hypothesis was that cigarette smoke would primarily affect phosphate exchange by decreasing ANT activity, which in turn will decrease ADP sensitivity, and ultimately result in lower maximal mitochondrial respiration in permeabilized fibers from both glycolytic gastrocnemius muscle and oxidative soleus muscle.

8.1. Overview of Main Findings

We confirmed several of our initial hypotheses and elucidated many of the mechanisms underlying the detrimental effects of cigarette smoke on mitochondrial function (Figure 8-1). Of note, we provide valuable insight into several mechanisms of cigarette smoke-induced dysfunction.

8.1.1. Summary of Aim 1

Mitochondrial sensitivity and susceptibility to cigarette smoke-induced mitochondrial dysfunction are indeed tissue-dependent. We show that the extent of mitochondrial bioenergetic impairments in striated muscles is dependent on mitochondrial content. On the other hand,

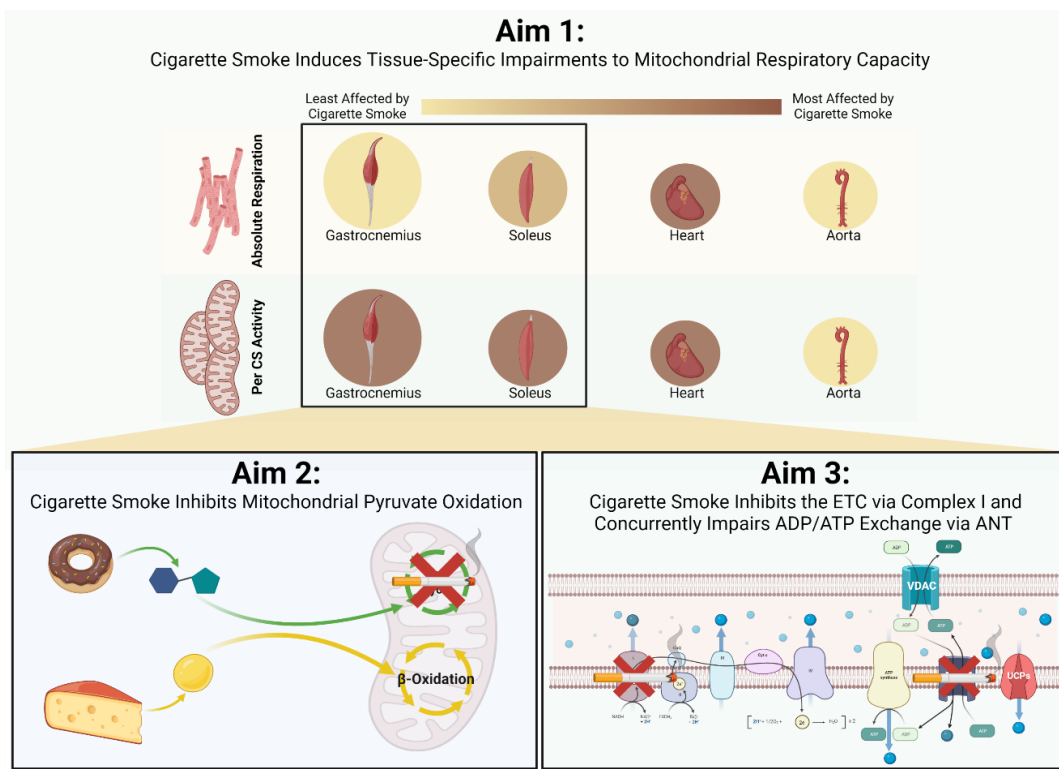


Figure 8-1. Conceptual framework and summary of the main findings in the present work.

mitochondria in the aorta exhibit intrinsic resistance to cigarette smoke-induced mitochondrial dysfunction, suggesting that the mitochondria in vascular smooth muscle contain physically distinct characteristics that may protect against cigarette smoke toxicity. These results suggest that the tissue-specific sensitivity and susceptibility to cigarette smoke alter the bioenergetic profiles (i.e., ATP flux and availability) of these tissues differently, providing further mechanistic insight into the link between cigarette smoke exposure and the development of tissue-specific atrophy and increased risk of cellular dysfunction.

8.1.2. Summary of Aim 2

Cigarette smoke directly impairs mitochondrial pyruvate oxidation, but not palmitoylcarnitine oxidation. Furthermore, while mitochondrial respiration is still decreased in

cigarette smoke-exposed tissues compared to control tissues, we show that the combination of competing substrates (i.e., the combination of pyruvate and palmitoylcarnitine) improved pyruvate-stimulated respiration kinetics in smoke-exposed fibers. These findings have several implications for understanding cigarette smoke-related metabolic dysfunction and provide a potential mechanism that links cigarette smoke exposure to the development of hyperglycemia, insulin resistance, and type II diabetes.

8.1.3. Summary of Aim 3

In permeabilized fibers, cigarette smoke directly impairs complex I of the mitochondrial ETC and inhibits the ADP/ATP transporter, ANT. The overall result of the combination of these effects lowers mitochondrial oxidative capacity without altering several indicators of mitochondrial efficiency, thus suggesting that the mitochondrial P/O ratio is preserved in the presence of cigarette smoke. These findings provide further insight into the specific cellular components that are affected by cigarette smoke and identify future targets of interest for therapies to address cigarette smoke-induced mitochondrial dysfunction.

8.2. Experimental Considerations

There are several experimental considerations in the present work. First, these studies utilized *in situ* reductionist approaches, which included isolating tissues from their whole-body environment and exposing them to supraphysiological concentrations of cigarette smoke to elicit mitochondrial dysfunction. This approach eliminates any systemic effects of cigarette smoke exposure and the inter-organ crosstalk and dependence, which are likely to occur *in vivo* (Aoshiba

et al., 2001b; Nemmar et al., 2013; Sanders et al., 2019). Therefore, the effects of any signaling molecules excreted by the primary organs exposed to cigarette smoke – such as pulmonary macrophages (Aoshiba et al., 2001b; Sanders et al., 2019; Thatcher et al., 2014; van der Toorn et al., 2007) – are removed from the present studies. Furthermore, the concentrations of cigarette smoke condensate used in the present study (0.004 µg/mL to 2400 µg/mL in aim 1, and 1600 µg/mL in aims 2 and 3) are well above the reported range (~0.67 µg/mL) of cigarette smoke particulate in the blood of active smokers (Benowitz et al., 1982, 2009; Mendelson et al., 2003). Assuming a 6% nicotine content in the CSC used in our studies (Csiszar et al., 2008; Jaccard et al., 2019), our concentrations of cigarette smoke were up to ~3,600 times greater than those reported in human blood in aim 1, and ~2,400 times greater than those reported in human blood in aims 2 and 3. However, despite these large concentration differences, the effects on mitochondrial respiration observed in the present studies reflect the effects of airstream cigarette smoke exposure to skeletal muscle mitochondrial function in other mouse models (Ajime et al., 2020; Gosker et al., 2009; Thatcher et al., 2014; Tippetts et al., 2014). Therefore, we feel that the exposure to CSC in these studies reflects the changes that would occur in models utilizing airstream cigarette smoke.

Furthermore, specific to aim 1, it is important to note that there were different sample dissection preparations for the aorta compared to the gastrocnemius, soleus, and heart. Considering that there is a delicate balance between the optimal permeabilization to elicit the highest possible respiration rate of a given tissue without inducing irreversible damage as indicated by a cytochrome C response (>10% increase in cytochrome C-stimulated respiration), we extensively tested our permeabilization protocols for each tissue to optimize mitochondrial respiration while minimizing damage (data not shown). Unlike striated muscle tissues (Figure 8-1A), we could not

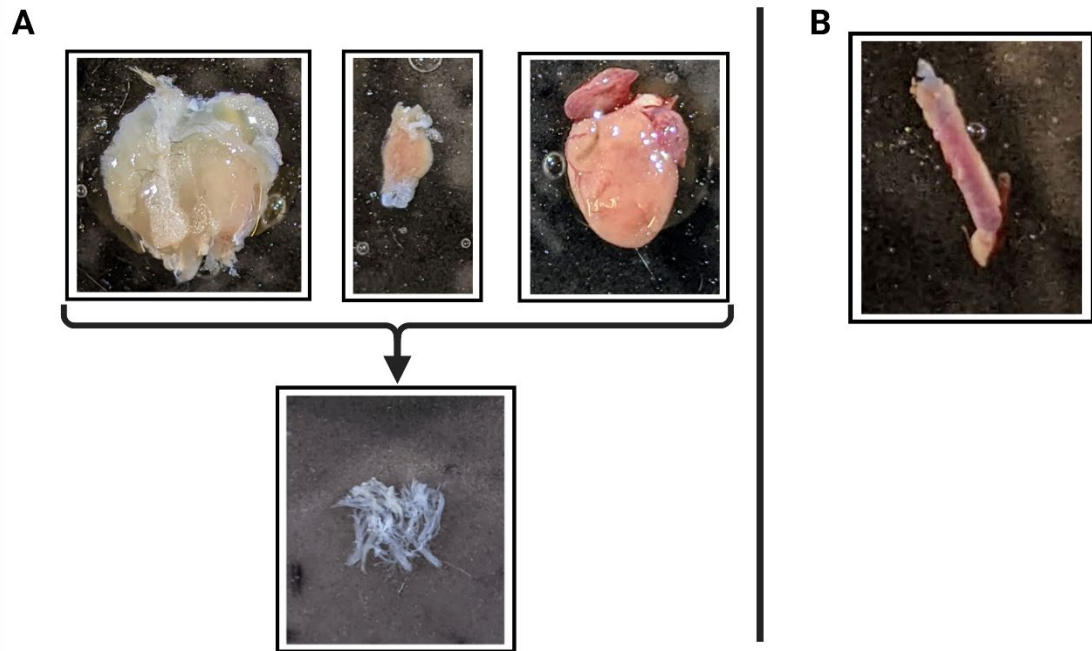


Figure 8-2. Schematic showing the differences in sample preparation between striated muscles (A; left to right: gastrocnemius, soleus, and heart) and the aorta (B), as used in aim 1. Striated muscle samples were mechanically dissected more than the aorta due to high rates of dissection-induced mitochondrial damage to the aorta.

extensively dissect the aorta without inducing high frequencies of irreversible damage. However, despite the aorta remaining relatively intact compared to the striated muscles used in these studies (Figure 8-1B), we reported respiration rates comparable to the rates used in other studies (S. H. S. Y. Park et al., 2018; S. Y. Park et al., 2014, 2016), which utilized similar preparations and respiration protocols. Furthermore, we are confident that the aorta samples used in these studies were adequately permeabilized, as we still observed some cytochrome c responses when running our experiments, albeit much less frequently than when we extensively dissected the aorta.

We did not measure citrate synthase activity (or another marker of mitochondrial content) for aims 2 and 3. Thus, we could not account for variations in respiration due to mitochondrial content, which prevented us from concluding any intrinsic alterations to mitochondrial respiration induced by CSC. Additional experiments from aim 1 show that CSC exposure (6% CSC for 20 minutes) results in a significant increase in citrate synthase activity (main effect of CSC $p = 0.007$;

partial $\eta^2 = 0.16$), as shown in Figure 8-1. These effects were especially pronounced in the gastrocnemius muscles, where the citrate synthase activity in the control fibers (9.42 ± 3.37 AU) was significantly lower than in the CSC-exposed fibers (12.88 ± 3.17 AU; $p = 0.024$, $d = 1.07$). Therefore, any differences in the citrate synthase activities between the control and smoke fibers may not indicate actual changes to mitochondrial content, but rather show an intrinsic increase in the enzymatic activities of citrate synthase. On the other hand, the use of within-sample measurements in aims 2 and 3 by using the same tissue samples (from the same mouse and same hindlimb) for control and CSC-exposed experiments provides confidence that the CSC-induced alterations to mitochondrial respiration are due solely to CSC rather than variations in tissue mitochondrial content. Because we used the same tissues in all the respiration experiments, we would not expect the large changes we reported in mitochondrial respiration to be due to differences in mitochondrial content. Therefore, the within-tissues comparison likely reflects inherent CSC-induced changes to mitochondrial respiration. However, due to the inability to measure citrate synthase activities in the gastrocnemius and soleus of aims 2 and 3, we cannot compare any inherent differences in the mitochondrial adaptations to CSC exposure between tissues.

Additionally, the present studies did not examine potential sex differences nor the influences of lifestyle factors, such as physical activity and/or diet. While studies have shown sex differences in the development of emphysema (DeMeo et al., 2018; Sørheim et al., 2010) and skeletal muscle weakness (Sharanya et al., 2019), we are unaware of any studies that have directly investigated any sex differences in cigarette smoke-induced mitochondrial dysfunction. On the other hand, several studies have performed secondary analyses on potential sex differences in cigarette smoke-induced mitochondrial dysfunction and found no effect (Decker et al., 2021; Khattri et al., 2022); however, it is noteworthy that these studies were not powered to detect sex differences and likely lack the sample size required to detect any significant effects. Likewise, in the present studies, we failed to detect any significant sex differences in CSC-induced mitochondrial dysfunction, likely due to inadequate sample size and exclusion of sex as a variable in our power analysis. Furthermore, diet and exercise are indubitably critical factors that regulate mitochondrial morphology and function (Civitarese et al., 2007; Drew et al., 2003; Lanza & Nair,

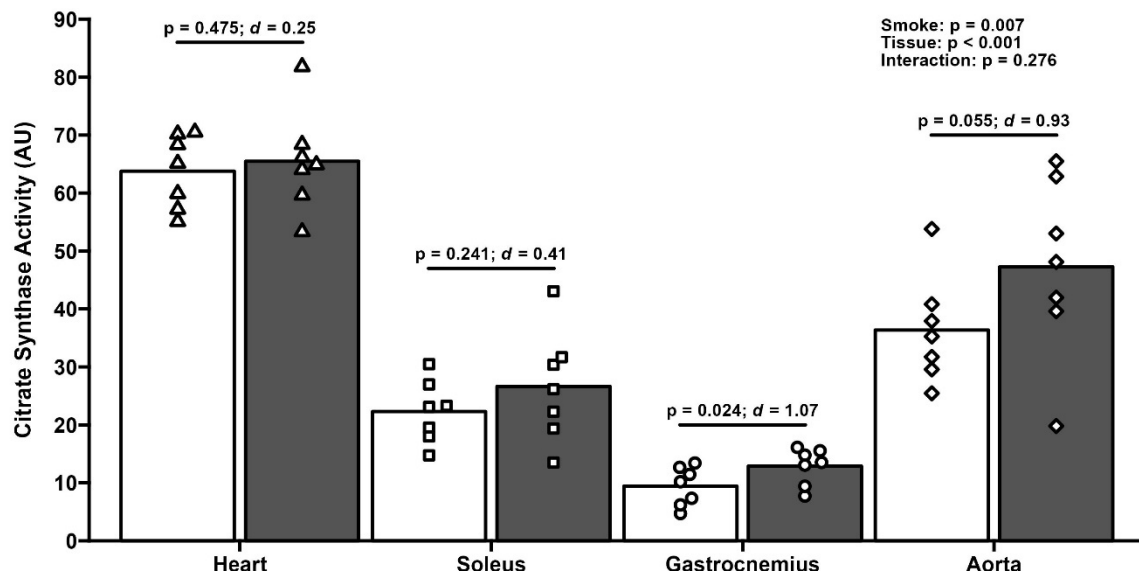


Figure 8-3. Citrate synthase activities of control (white) and CSC-exposed tissues (grey). Tissues were exposed to 6% CSC for 20 minutes.

2009; Putti et al., 2015; Russell et al., 2014). Indeed, several studies have highlighted the role of physical inactivity in the development of cigarette smoke-induced peripheral dysfunction (Barreiro et al., 2009; Decker, Kwon, Zhao, Hoidal, Heuckstadt, et al., 2021; J. Gea et al., 2015; J. G. Gea et al., 2001; Gifford et al., 2015, 2018a; McKeough et al., 2006; Shields et al., 2015). Therefore, we attempted to control for these factors by restricting physical activity (by housing animals in cages without running wheels) and controlling diet (by feeding all animals with standard chow) to critically examine the effects of cigarette smoke on mitochondrial function independently of lifestyle factors. However, it is noteworthy that the interaction between lifestyle factors and cigarette smoke exposure is an important point of consideration when exploring the effects of cigarette smoke exposure on mitochondrial function. More studies are needed to explore these interactions, as well as sex differences, on cigarette smoke-induced mitochondrial dysfunction.

One last experimental consideration for this project is the sample sizes chosen for each of the individual aims. Indeed, the sample size for each of these studies was limited to ~10 mice per group. Although a larger sample size would increase the statistical power of these studies, it is noteworthy that the sample sizes used in these studies are within the range of other studies utilizing similar approaches (Decker, Kwon, Zhao, Hoidal, Heuckstadt, et al., 2021; Khattri et al., 2022; Orosz et al., 2007; Thatcher et al., 2014; van der Toorn et al., 2007, 2009). Furthermore, while many of the *post hoc* analyses reported p values that trended toward significance, many of the main effects of CSC on these outcomes were significantly different, as indicated by the ANOVAs. Therefore, while sample size would have proven to increase the power of the *post hoc* analyses, we are confident that the findings in these studies are not due to a type II error and that the increase in sample size would not change the interpretation of these results.

8.3. Future Directions

While the studies performed in this dissertation are insightful, many questions remain in addressing the public health crisis related to cigarette smoke exposure. Namely, no therapies have been identified which restore mitochondrial function in persons exposed to cigarette smoke, nor have treatments been identified that may reverse the cigarette smoke-induced mitochondrial dysfunction shown in this work. Furthermore, while the present work outlines several mechanisms of cigarette smoke-induced mitochondrial dysfunction, the role of ROS, specifically the contribution of mitochondria-derived ROS to smoke-induced cellular dysfunction, remains unclear. Therefore, more studies are needed to identify the contribution of mitochondria-derived ROS in cellular dysfunction and any potential therapies to address cigarette smoke-induced dysfunction, thus improving the quality of life of persons exposed to cigarette smoke.

APPENDIX A

DATA COLLECTION SHEETS

Mouse Prep Guide/Checklist + Lab Sheet

For Mouse Experiments

Initial Prep

- Thaw 1 tube with >15 mL BIOPS
- Thaw 1 tube with >40 mL MiR05

Saponin Prep

- Prepare stock Saponin (5mg saponin/1mL water)
- Prepare 2 mL BIOPS in the necessary number of 5-mL tubes (one tube for each condition)
- Pipette 20 μ L stock saponin in 2 mL BIOPS for each condition
- Place all tubes on ice

MiR05 Prep

- Prepare 2 mL (each) MiR05 in 2 5-mL tubes (2 for each condition)
- Place all tubes on ice

Once all of this is completed, the blue container with ice for the sacrifice. Be sure to take note of the sex and date of birth from Ernie (needs to be written down or a photo needs to be taken). Take the specimen back up to the 5th floor for dissection immediately.

182

Dissection Steps

Gastroc & Soleus

- Make sure the mouse is firmly anchored to the styrofoam container lid by placing the needles through all 4 feet
- Make an incision with large scissors at the ankle
- Pull back the skin (and fur) to reveal the gastroc
- Cut the Achilles tendon at the distal portion of the lower leg
- Pull the gastroc back from the leg, revealing the soleus
- Sever the proximal end of the gastroc and soleus
- Place in BIOPS
- Separate the gastroc and the soleus by separating the soleus from the gastroc and cutting any remaining attachments

Aorta

- Cut longitudinally down the rib cage and open the chest cavity
- Carefully remove lungs and other organs, but do not disturb the heart
- Locate the aorta (should be near the spine)
- Gently separate the aorta from the spine
- Cut 3-5 cm of the aorta and remove. Place in BIOPS.

Date of Sacrifice (Today's date): _____

Date of Birth (from Ernie): _____

Check one: Male or Female

Tissue: Gastroc Soleus Aorta

Stirrer test normal (F9 on keyboard)? Yes or No

Air Calibration Performed and saved in Excel? Yes or No

<i>Condition (i.e. “% Cigarette Smoke”)</i>	<i>Saponin Start Time (30 min)</i>	<i>Wash 1 Start Time (10 min)</i>	<i>Wash 2 Start Time (10 min)</i>	<i>Cigarette Smoke Start Time (60 min)</i>	<i>Time placed in O2K</i>	<i>Weight</i>	<i>Comments</i>
	<i>Initials:</i>	<i>Initials:</i>	<i>Initials:</i>	<i>Initials:</i>	<i>Initials:</i>	<i>A:</i> _____	
	<i>Initials:</i>	<i>Initials:</i>	<i>Initials:</i>	<i>Initials:</i>	<i>Initials:</i>	<i>A:</i> _____	
	<i>Initials:</i>	<i>Initials:</i>	<i>Initials:</i>	<i>Initials:</i>	<i>Initials:</i>	<i>A:</i> _____	
	<i>Initials:</i>	<i>Initials:</i>	<i>Initials:</i>	<i>Initials:</i>	<i>Initials:</i>	<i>A:</i> _____	
	<i>Initials:</i>	<i>Initials:</i>	<i>Initials:</i>	<i>Initials:</i>	<i>Initials:</i>	<i>A:</i> _____	
	<i>Initials:</i>	<i>Initials:</i>	<i>Initials:</i>	<i>Initials:</i>	<i>Initials:</i>	<i>A:</i> _____	

Comment

APPENDIX B

SAMPLE SIZE ESTIMATES

Proposed Project	Tissue	Estimated Effect	Proposed Sample Size
Aim 1	Gastrocnemius	Cohen's $f = 1.08$	n = 3
	Soleus	Cohen's $f = 1.03$	n = 3
	Heart	Cohen's $f = 1.81$	n = 3
	Aorta	Cohen's $f = 0.98$	n = 3
Aim 2	Gastrocnemius	Cohen's $f = 0.41$	n = 13
	Soleus	Cohen's $f = 0.41$	n = 13
Aim 3	Gastrocnemius	Cohen's $d = 1.56$	n = 8
	Soleus	Cohen's $d = 1.56$	n = 8

BIBLIOGRAPHY

- Abdelghany, T. M., Ismail, R. S., Mansoor, F. A., Zweier, J. R., Lowe, F., & Zweier, J. L.** (2018). Cigarette smoke constituents cause endothelial nitric oxide synthase dysfunction and uncoupling due to depletion of tetrahydrobiopterin with degradation of GTP cyclohydrolase. *Nitric Oxide - Biology and Chemistry*. <https://doi.org/10.1016/j.niox.2018.02.009>
- Abdul-Ghani, M. A., Muller, F. L., Liu, Y., Chavez, A. O., Balas, B., Zuo, P., Chang, Z., Tripathy, D., Jani, R., Molina-Carrion, M., Monroy, A., Folli, F., Van Remmen, H., & DeFronzo, R. A.** (2008a). deleterious action of FA metabolites on ATP synthesis: Possible link between lipotoxicity, mitochondrial dysfunction, and insulin resistance. *American Journal of Physiology - Endocrinology and Metabolism*, 295(3), 678–685. <https://doi.org/10.1152/AJPENDO.90287.2008/ASSET/IMAGES/LARGE/ZH10090854190004.jpeg>
- Abdul-Ghani, M. A., Muller, F. L., Liu, Y., Chavez, A. O., Balas, B., Zuo, P., Chang, Z., Tripathy, D., Jani, R., Molina-Carrion, M., Monroy, A., Folli, F., Van Remmen, H., & DeFronzo, R. A.** (2008b). deleterious action of FA metabolites on ATP synthesis: Possible link between lipotoxicity, mitochondrial dysfunction, and insulin resistance. *American Journal of Physiology - Endocrinology and Metabolism*, 295(3), 678–685. <https://doi.org/10.1152/AJPENDO.90287.2008/ASSET/IMAGES/LARGE/ZH10090854190004.jpeg>
- Acin-Perez, R., Benador, I. Y., Petcherski, A., Veliova, M., Benavides, G. A., Lagarrigue, S., Caudal, A., Vergnes, L., Murphy, A. N., Karamanlidis, G., Tian, R., Reue, K., Wanagat, J., Sacks, H., Amati, F., Darley-Usmar, V. M., Liesa, M., Divakaruni, A. S., Stiles, L., &**

Shirihi, O. S. (2020). A novel approach to measure mitochondrial respiration in frozen biological samples. *The EMBO Journal*, 39(13), e104073. <https://doi.org/10.15252/embj.2019104073>

Agarwal, A. R., Zhao, L., Sancheti, H., Sundar, I. K., Rahman, I., & Cadenas, E. (2012). Short-term cigarette smoke exposure induces reversible changes in energy metabolism and cellular redox status independent of inflammatory responses in mouse lungs. *Am J Physiol Lung Cell Mol Physiol*, 303, 889–898. <https://doi.org/10.1152/ajplung.00219.2012>.-Cigarette
Ahmad, T., Sundar, I. K., Lerner, C. A., Gerloff, J., Tormos, A. M., Yao, H., & Rahman, I. (2015). Impaired mitophagy leads to cigarette smoke stress-induced cellular senescence: implications for chronic obstructive pulmonary disease. *FASEB Journal: Official Publication of the Federation of American Societies for Experimental Biology*, 29(7), 2912–2929. <https://doi.org/10.1096/FJ.14-268276>

Ajime, T. T., Serré, J., Wüst, R. C. I., Messa, G. A. M., Poffé, C., Swaminathan, A., Maes, K., Janssens, W., Troosters, T., Degens, H., & Gayan-Ramirez, G. (2020). Two Weeks of Smoking Cessation Reverse Cigarette Smoke-Induced Skeletal Muscle Atrophy and Mitochondrial Dysfunction in Mice. *Nicotine & Tobacco Research*. <https://doi.org/10.1093/ntr/ntaa016>

Aliev, M., Guzun, R., Karu-Varikmaa, M., Kaambre, T., Wallimann, T., & Saks, V. (2011). Molecular System Bioenergetics of the Heart: Experimental Studies of Metabolic Compartmentation and Energy Fluxes versus Computer Modeling. *International Journal of Molecular Sciences*, 12(12), 9296. <https://doi.org/10.3390/IJMS12129296>

- Alonso, J. R., Cardellach, F., Casademont, J., & Miró, Ò.** (2004). Reversible inhibition of mitochondrial complex IV activity in PBMC following acute smoking. *European Respiratory Journal*. <https://doi.org/10.1183/09031936.03.00038203>
- Alonso, J. R., Cardellach, F., López, S., Casademont, J., & Miró, Ò.** (2003). Carbon monoxide specifically inhibits cytochrome C oxidase of human mitochondrial respiratory chain. *Pharmacology and Toxicology*. <https://doi.org/10.1034/j.1600-0773.2003.930306.x>
- Amann, M., Regan, M. S., Kobitay, M., Eldridge, M. W., Boutellier, U., Pegelow, D. F., & Dempsey, J. A.** (2010). Impact of pulmonary system limitations on locomotor muscle fatigue in patients with COPD. *American Journal of Physiology - Regulatory Integrative and Comparative Physiology*, 299(1). <https://doi.org/10.1152/ajpregu.00183.2010>
- Amato, M., Frigerio, B., Castelnuovo, S., Ravani, A., Sansaro, D., Tremoli, E., Squellerio, I., Cavalca, V., Veglia, F., Sirtori, C. R., Werba, J. P., & Baldassarre, D.** (2013). Effects of smoking regular or light cigarettes on brachial artery flow-mediated dilation. *Atherosclerosis*, 228(1), 153–160. <https://doi.org/10.1016/J.ATHEROSCLEROSIS.2013.02.037>
- Ambrosino, N., & Strambi, S.** (2004). New strategies to improve exercise tolerance in chronic obstructive pulmonary disease. In *European Respiratory Journal*. <https://doi.org/10.1183/09031936.04.00002904>
- Aoshiba, K., Tamaoki, J., & Nagai, A.** (2001a). Acute cigarette smoke exposure induces apoptosis of alveolar macrophages. *American Journal of Physiology. Lung Cellular and Molecular Physiology*, 281(6). <https://doi.org/10.1152/AJPLUNG.2001.281.6.L1392>
- Aoshiba, K., Tamaoki, J., & Nagai, A.** (2001b). Acute cigarette smoke exposure induces apoptosis of alveolar macrophages. *American Journal of Physiology - Lung Cellular and*

Molecular Physiology, 281(6) 25-6).

<https://doi.org/10.1152/AJPLUNG.2001.281.6.L1392/ASSET/IMAGES/LARGE/H51210674009.JPG>

Aravamudan, B., Kiel, A., Freeman, M., Delmotte, P., Thompson, M., R, V., Sieck, G. C., Pabelick, C. M., & Prakash, Y. (2014). Cigarette smoke-induced mitochondrial fragmentation and dysfunction in human airway smooth muscle. *American Journal of Physiology. Lung Cellular and Molecular Physiology*, 306(9).

<https://doi.org/10.1152/AJPLUNG.00155.2013>

Aravamudan, B., Thompson, M., Sieck, G. C., Vassallo, R., Pabelick, C. M., & Prakash, Y. (2017). Functional Effects of Cigarette Smoke-Induced Changes in Airway Smooth Muscle Mitochondrial Morphology. *Journal of Cellular Physiology*, 232(5), 1053–1068.

<https://doi.org/10.1002/JCP.25508>

Argov, Z., De Stefano, N., & Arnold, D. L. (1996). ADP recovery after a brief ischemic exercise in normal and diseased human muscle - A 31P MRS study. *NMR in Biomedicine*, 9(4), 165–172. [https://doi.org/10.1002/\(SICI\)1099-1492\(199606\)9:4<165::AID-NBM408>3.0.CO;2-X](https://doi.org/10.1002/(SICI)1099-1492(199606)9:4<165::AID-NBM408>3.0.CO;2-X)

Aronson, J. K. (2007). Concentration-effect and dose-response relations in clinical pharmacology. *British Journal of Clinical Pharmacology*, 63(3), 255–257.

<https://doi.org/10.1111/J.1365-2125.2007.02871.X>

Arte, A., Stamford, B. A., & Moffatt, R. J. (2017). Cigarette Smoking: An Accessory to the Development of Insulin Resistance. *American Journal of Lifestyle Medicine*, 13(6), 602–605.

<https://doi.org/10.1177/1559827617726516>

Ashok, B. T., & Ali, R. (1999). The aging paradox: free radical theory of aging. *Exp Gerontol*, 34(3), 293–303.

Augusto, V., Padovani, C. R., & Campos, G. E. R. (2004). Skeletal Muscle Fiber Types in C57BL6J Mice. *Brazilian Journal of Morphological Science*, 21(2), 89–94.
<http://www.jms.periodikos.com.br/journal/jms/article/587cb4537f8c9d0d058b45ea>

Ballweg, K., Mutze, K., Königshoff, M., Eickelberg, O., & Meiners, S. (2014). Cigarette smoke extract affects mitochondrial function in alveolar epithelial cells. *American Journal of Physiology - Lung Cellular and Molecular Physiology*.
<https://doi.org/10.1152/ajplung.00180.2014>

Barbour, R. L., Ribaudol, J., & Chanoy, S. H. P. (1984). Effect of creatine kinase activity on mitochondrial ADP/ATP transport. Evidence for a functional interaction. 259(13), 8246–8251. [https://doi.org/10.1016/S0021-9258\(17\)39720-X](https://doi.org/10.1016/S0021-9258(17)39720-X)

Barreiro, E., del Puerto-Nevado, L., Puig-Vilanova, E., Pérez-Rial, S., Sánchez, F., Martínez-Galán, L., Rivera, S., Gea, J., González-Mangado, N., & Peces-Barba, G. (2012). Cigarette smoke-induced oxidative stress in skeletal muscles of mice. *Respiratory Physiology and Neurobiology*. <https://doi.org/10.1016/j.resp.2012.02.001>

Barreiro, E., Peinado, V. I., Galdiz, J. B., Ferrer, E., Marin-Corral, J., Sánchez, F., Gea, J., & Barberà, J. A. (2010). Cigarette smoke-induced oxidative stress: A role in chronic obstructive pulmonary disease skeletal muscle dysfunction. *American Journal of Respiratory and Critical Care Medicine*. <https://doi.org/10.1164/rccm.200908-1220OC>

Barreiro, E., Rabinovich, R., Marin-Corral, J., Barberà, J. A., Gea, J., & Roca, J. (2009).

Chronic endurance exercise induces quadriceps nitrosative stress in patients with severe COPD. *Thorax*. <https://doi.org/10.1136/thx.2008.105163>

Barutcu, I., Esen, A. M., Kaya, D., Onrat, E., Melek, M., Celik, A., Kilit, C., Turkmen, M., Karakaya, O., Esen, O. B., Saglam, M., & Kirma, C. (2008). Effect of acute cigarette

smoking on left and right ventricle filling parameters: a conventional and tissue Doppler echocardiographic study in healthy participants. *Angiology*, 59(3), 312–316.
<https://doi.org/10.1177/0003319707304882>

Benowitz, N. L., Hukkanen, J., & Jacob, P. (2009). Nicotine Chemistry, Metabolism, Kinetics

and Biomarkers. *Handbook of Experimental Pharmacology*, 192(192), 29.
https://doi.org/10.1007/978-3-540-69248-5_2

Benowitz, N. L., Kuyt, F., & Jacob, P. (1982). Circadian blood nicotine concentrations during

cigarette smoking. *Clinical Pharmacology & Therapeutics*, 32(6), 758–764.
<https://doi.org/10.1038/CLPT.1982.233>

Bergman, B. C., Perreault, L., Hunerdosse, D., Kerege, A., Playdon, M., Samek, A. M., &

Eckel, R. H. (2012). Novel and Reversible Mechanisms of Smoking-Induced Insulin Resistance in Humans. *Diabetes*, 61(12), 3156–3166. <https://doi.org/10.2337/DB12-0418>

Bergman, B. C., Perreault, L., Hunerdosse, D. M., Koehler, M. C., Samek, A. M., & Eckel, R. H. (2009). Intramuscular Lipid Metabolism in the Insulin Resistance of Smoking.

Diabetes, 58(10), 2220. <https://doi.org/10.2337/DB09-0481>

- Bernardo, I., Passey, S., Seow, H. J., Bozinovski, S., & Vlahos, R.** (2018). *Targeting NADPH oxidase-2 reduces cigarette smoke-induced lung inflammation and skeletal muscle wasting in mice*. <https://doi.org/10.1183/13993003.congress-2018.oa1945>
- Bernhard, D., Moser, C., Backovic, A., & Wick, G.** (2007). Cigarette smoke - an aging accelerator? In *Experimental Gerontology* (Vol. 42, Issue 3, pp. 160–165). Pergamon. <https://doi.org/10.1016/j.exger.2006.09.016>
- Bertholet, A. M., Chouchani, E. T., Kazak, L., Angelin, A., Fedorenko, A., Long, J. Z., Vidoni, S., Garrity, R., Cho, J., Terada, N., Wallace, D. C., Spiegelman, B. M., & Kirichok, Y.** (2019a). H⁺ transport is an integral function of the mitochondrial ADP/ATP carrier. *Nature*. <https://doi.org/10.1038/s41586-019-1400-3>
- Bertholet, A. M., Chouchani, E. T., Kazak, L., Angelin, A., Fedorenko, A., Long, J. Z., Vidoni, S., Garrity, R., Cho, J., Terada, N., Wallace, D. C., Spiegelman, B. M., & Kirichok, Y.** (2019b). H⁺ transport is an integral function of the mitochondrial ADP/ATP carrier. *Nature*, 571(7766), 515–520. <https://doi.org/10.1038/s41586-019-1400-3>
- Bloomer, R. J.** (2007). Decreased blood antioxidant capacity and increased lipid peroxidation in young cigarette smokers compared to nonsmokers: Impact of dietary intake. *Nutrition Journal*. <https://doi.org/10.1186/1475-2891-6-39>
- Bose, S., French, S., Evans, F. J., Joubert, F., & Balaban, R. S.** (2003). Metabolic network control of oxidative phosphorylation. Multiple roles of inorganic phosphate. *Journal of Biological Chemistry*, 278(40). <https://doi.org/10.1074/jbc.M306409200>

Boushel, R., Gnaiger, E., Schjerling, P., Skovbro, M., Kraunsoe, R., & Dela, F. (2007).

Patients with type 2 diabetes have normal mitochondrial function in skeletal muscle.

Diabetologia, 50(4), 790–796. <https://doi.org/10.1007/s00125-007-0594-3>

Bowen, T., Aakerøy, L., Eisenkolb, S., Kunth, P., Bakkerud, F., Wohlwend, M., Ormbostad, A., Fischer, T., Wisloff, U., Schuler, G., Steinshamn, S., Adams, V., & Bronstad, E.

(2017). Exercise Training Reverses Extrapulmonary Impairments in Smoke-exposed Mice.

Medicine and Science in Sports and Exercise, 49(5), 879–887.

<https://doi.org/10.1249/MSS.0000000000001195>

Brand, M. D., & Nicholls, D. G. (2011). Assessing mitochondrial dysfunction in cells. In

Biochemical Journal (Vol. 435, Issue 2, pp. 297–312). Portland Press Ltd.

<https://doi.org/10.1042/BJ20110162>

Brønstad, E., Rognmo, Ø., Dedichen, H., Kirkeby-Garstad, I., Wisloff, U., & Steinshamn, S.

(2011). Effects of one-leg exercise training on mitochondrial function in COPD patients. *The Clinical Respiratory Journal*. https://doi.org/10.1111/j.1752-699x.2011.00266_11.x

Brønstad, E., Rognmo, O., Tjonna, A. E., Dedichen, H. H., Kirkeby-Garstad, I., Håberg, A. K., Ingul, C. B., Wisloff, U., & Steinshamn, S. (2012). High-intensity knee extensor training

restores skeletal muscle function in COPD patients. *European Respiratory Journal*.

<https://doi.org/10.1183/09031936.00193411>

Brzezinska, A. K., Lohr, N., & Chilian, W. M. (2005). Electrophysiological effects of O₂⁻ on

the plasma membrane in vascular endothelial cells. *American Journal of Physiology - Heart and Circulatory Physiology*. <https://doi.org/10.1152/ajpheart.00132.2005>

Burelle, Y., & Hochachka, P. W. (2002). Endurance training induces muscle-specific changes in mitochondrial function in skinned muscle fibers. *Journal of Applied Physiology*, 92(6), 2429–2438.

<https://doi.org/10.1152/JAPPLPHYSIOL.01024.2001/ASSET/IMAGES/LARGE/DG0621587005.jpeg>

Bygrave, F. L., & Lehninger, A. L. (1967). The affinity of mitochondrial oxidative phosphorylation mechanisms for phosphate and adenosine diphosphate. *Proceedings of the National Academy of Sciences of the United States of America*, 57(5), 1409–1415.
<https://doi.org/10.1073/pnas.57.5.1409>

Cairns, C. B., Walther, J., Harken, A. H., & Banerjee, A. (1998). Mitochondrial oxidative phosphorylation thermodynamic efficiencies reflect physiological organ roles. *American Journal of Physiology - Regulatory Integrative and Comparative Physiology*, 274(5 43-5).
<https://doi.org/10.1152/AJPREGU.1998.274.5.R1376/ASSET/IMAGES/LARGE/AREG70530005X.jpeg>

Canoy, D., Wareham, N., Luben, R., Welch, A., Bingham, S., Day, N., & Khaw, K. T. (2005). Cigarette smoking and fat distribution in 21,828 British men and women: a population-based study. *Obesity Research*, 13(8), 1466–1475. <https://doi.org/10.1038/OBY.2005.177>

Caram, L. M. D. O., Ferrari, R., Bertani, A. L., Garcia, T., Mesquita, C. B., Knaut, C., Tanni, S. E., & Godoy, I. (2016). Smoking and early COPD as independent predictors of body composition, exercise capacity, and health status. *PLoS ONE*.
<https://doi.org/10.1371/journal.pone.0164290>

- Celermajer, D. S., Adams, M. R., Clarkson, P., Robinson, J., McCredie, R., Donald, A., & Deanfield, J. E.** (1996). Passive Smoking and Impaired Endothelium-Dependent Arterial Dilatation in Healthy Young Adults. *New England Journal of Medicine*, 334(3), 150–155. <https://doi.org/10.1056/nejm199601183340303>
- Celermajer, D. S., Sorensen, K. E., Georgakopoulos, D., Bull, C., Thomas, O., Robinson, J., & Deanfield, J. E.** (1993). Cigarette smoking is associated with dose-related and potentially reversible impairment of endothelium-dependent dilation in healthy young adults. *Circulation*. <https://doi.org/10.1161/01.CIR.88.5.2149>
- Chang, K. H., Park, J. M., Lee, C. H., Kim, B., Choi, K. C., Choi, S. J., Lee, K., & Lee, M. Y.** (2017). NADPH oxidase (NOX) 1 mediates cigarette smoke-induced superoxide generation in rat vascular smooth muscle cells. *Toxicology in Vitro*. <https://doi.org/10.1016/j.tiv.2016.10.013>
- Cheung, K. K., Fung, T. K. H., Mak, J. C. W., Cheung, S. Y., He, W., Leung, J. W., Lau, B. W. M., & Ngai, S. P. C.** (2020). The acute effects of cigarette smoke exposure on muscle fiber type dynamics in rats. *PLoS ONE*. <https://doi.org/10.1371/journal.pone.0233523>
- Chevalier, R. B., Bowers, J. A., Bondurant, S., & Ross, J. C.** (1963). Circulatory and ventilatory effects of exercise in smokers and nonsmokers. *Journal of Applied Physiology*, 18, 357–360. <https://doi.org/10.1152/jappl.1963.18.2.357>
- Chiolero, A., Faeh, D., Paccaud, F., & Cornuz, J.** (2008). Consequences of smoking for body weight, body fat distribution, and insulin resistance. *The American Journal of Clinical Nutrition*, 87(4), 801–809. <https://doi.org/10.1093/AJCN/87.4.801>

- Civitarese, A. E., Carling, S., Heilbronn, L. K., Hulver, M. H., Ukropcova, B., Deutsch, W. A., Smith, S. R., & Ravussin, E.** (2007). Calorie restriction increases muscle mitochondrial biogenesis in healthy humans. *PLoS Medicine*, 4(3), 485–494. <https://doi.org/10.1371/JOURNAL.PMED.0040076>
- Cooper, K. H., Gey, G. O., & Bottenberg, R. A.** (1968). Effects of Cigarette Smoking on Endurance Performance. *JAMA: The Journal of the American Medical Association*, 203(3), 189–192. <https://doi.org/10.1001/jama.1968.03140030021006>
- Csiszar, A., Labinskyy, N., Podlutsky, A., Kaminski, P. M., Wolin, M. S., Zhang, C., Mukhopadhyay, P., Pacher, P., Hu, F., de Cabo, R., Ballabh, P., & Ungvari, Z.** (2008). Vasoprotective effects of resveratrol and SIRT1: Attenuation of cigarette smoke-induced oxidative stress and proinflammatory phenotypic alterations. *American Journal of Physiology - Heart and Circulatory Physiology*, 294(6), 2721–2735. <https://doi.org/10.1152/ajpheart.00235.2008>
- Csiszar, A., Podlutsky, A., Wolin, M. S., Losonczy, G., Pacher, P., & Ungvari, Z.** (2009). Oxidative stress and accelerated vascular aging: Implications for cigarette smoking. *Frontiers in Bioscience*. <https://doi.org/10.2735/3440>
- Csordas, A., & Bernhard, D.** (2013). The biology behind the atherothrombotic effects of cigarette smoke. In *Nature Reviews Cardiology*. <https://doi.org/10.1038/nrcardio.2013.8>
- Cui, H., Kong, Y., & Zhang, H.** (2012). Oxidative Stress, Mitochondrial Dysfunction, and Aging. *Journal of Signal Transduction*. <https://doi.org/10.1155/2012/646354>

- Davalli, P., Mitic, T., Caporali, A., Lauriola, A., & D'Arca, D.** (2016). ROS, Cell Senescence, and Novel Molecular Mechanisms in Aging and Age-Related Diseases. In *Oxidative Medicine and Cellular Longevity*. <https://doi.org/10.1155/2016/3565127>
- De Tarso Muller, P., Barbosa, G. W., O'Donnell, D. E., & Alberto Neder, J.** (2019). Cardiopulmonary and muscular interactions: Potential implications for exercise (In)tolerance in symptomatic smokers without chronic obstructive pulmonary disease. In *Frontiers in Physiology*. <https://doi.org/10.3389/fphys.2019.00859>
- Decker, S. T., Kwon, O. S., Zhao, J., Hoidal, J. R., Heuckstadt, T., Sanders, K. A., Richardson, R. S., & Layec, G.** (2021). Skeletal muscle mitochondrial adaptations induced by long-term cigarette smoke exposure. *American Journal of Physiology - Endocrinology and Metabolism*.
- Decker, S. T., Kwon, O. S., Zhao, J., Hoidal, J. R., Huecksteadt, T. P., Richardson, R. S., Sanders, K. A., Layec, G., Heuckstadt, T., Sanders, K. A., Richardson, R. S., & Layec, G.** (2021). Skeletal muscle mitochondrial adaptations induced by long-term cigarette smoke exposure. *American Journal of Physiology - Endocrinology and Metabolism*. <https://doi.org/10.1152/ajpendo.00544.2020>
- Degens, H., Gayan-Ramirez, G., & Van Hees, H. W. H.** (2015). Smoking-induced skeletal muscle dysfunction: From evidence to mechanisms. In *American Journal of Respiratory and Critical Care Medicine*. <https://doi.org/10.1164/rccm.201410-1830PP>
- DeMeo, D. L., Ramagopalan, S., Kavati, A., Vegesna, A., Han, M. K., Yadao, A., Wilcox, T. K., & Make, B. J.** (2018). Women manifest more severe COPD symptoms across the life course. *International Journal of COPD*. <https://doi.org/10.2147/COPD.S160270>

- Di Paola, M., Cocco, T., & Lorusso, M.** (2000). Ceramide interaction with the respiratory chain of heart mitochondria. *Biochemistry*. <https://doi.org/10.1021/bi9924415>
- Dikalov, S., Itani, H., Richmond, B., Vergeade, A., Jamshedur Rahman, S. M., Boutaud, O., Blackwell, T., Massion, P. P., Harrison, D. G., & Dikalova, A.** (2019). Tobacco smoking induces cardiovascular mitochondrial oxidative stress, promotes endothelial dysfunction, and enhances hypertension. *American Journal of Physiology - Heart and Circulatory Physiology*. <https://doi.org/10.1152/ajpheart.00595.2018>
- Doonan, R. J., Hausvater, A., Scallan, C., Mikhailidis, D. P., Pilote, L., & Daskalopoulou, S. S.** (2010). The effect of smoking on arterial stiffness. *Hypertension Research* 2010 33:5, 33(5), 398–410. <https://doi.org/10.1038/hr.2010.25>
- Drew, B., Dirks, P. A., Selman, C., Gredilla, R., Lezza, A., Barja, G., & Leeuwenburgh, C.** (2003). Effects of aging and caloric restriction on mitochondrial energy production in gastrocnemius muscle and heart. *American Journal of Physiology. Regulatory, Integrative and Comparative Physiology*, 284(2). <https://doi.org/10.1152/AJPREGU.00455.2002>
- Endemann, D. H., & Schiffrin, E. L.** (2004). Endothelial dysfunction. In *Journal of the American Society of Nephrology*. <https://doi.org/10.1097/01.ASN.0000132474.50966.DA>
- Fontana-Ayoub, Fasching, M., & Gnaiger, E.** (2014). Selected media and chemicals for respirometry with mitochondrial preparations. *Mitochondrial Physiology Network*, 02(17).
- Fukai, T., & Ushio-Fukai, M.** (2011). Superoxide dismutases: Role in redox signaling, vascular function, and diseases. In *Antioxidants and Redox Signaling*. <https://doi.org/10.1089/ars.2011.3999>

Gaitanos, G. C., Williams, C., Boobis, L. H., & Brooks, S. (1993). Human muscle metabolism

during intermittent maximal exercise. *Journal of Applied Physiology.*

<https://doi.org/10.1152/jappl.1993.75.2.712>

Gallagher, D., Belmonte, D., Deurenberg, P., Wang, Z., Krasnow, N., Pi-Sunyer, F. X., &

Heymsfield, S. B. (1998). Organ-tissue mass measurement allows modeling of ree and

metabolically active tissue mass. *American Journal of Physiology - Endocrinology and*

Metabolism. <https://doi.org/10.1152/ajpendo.1998.275.2.e249>

Gandini, S., Botteri, E., Iodice, S., Boniol, M., Lowenfels, A. B., Maisonneuve, P., & Boyle,

P. (2008). Tobacco smoking and cancer: A meta-analysis. *International Journal of Cancer,*

122(1), 155–164. <https://doi.org/10.1002/IJC.23033>

Gea, J. G., Pasto, M., Carmona, M. A., Orozco-Levi, M., Palomeque, J., & Broquetas, J.

(2001). Metabolic characteristics of the deltoid muscle in patients with chronic obstructive

pulmonary disease. *European Respiratory Journal.*

<https://doi.org/10.1183/09031936.01.17509390>

Gea, J., Pascual, S., Casadevall, C., Orozco-Levi, M., & Barreiro, E. (2015). Muscle

dysfunction in chronic obstructive pulmonary disease: Update on causes and biological

findings. In *Journal of Thoracic Disease.* <https://doi.org/10.3978/j.issn.2072-1439.2015.08.04>

Ghafourifar, P., Klein, S. D., Schucht, O., Schenk, U., Pruschy, M., Rocha, S., & Richter, C.

(1999). Ceramide induces cytochrome c release from isolated mitochondria. Importance of

mitochondrial redox state. *Journal of Biological Chemistry.*

<https://doi.org/10.1074/jbc.274.10.6080>

Giannini, D., Leone, A., Di Bisceglie, D., Nuti, M., Strata, G., Buttitta, F., Masserini, L., & Balbarini, A. (2007). The effects of acute passive smoke exposure on endothelium-dependent brachial artery dilation in healthy individuals. *Angiology*.

<https://doi.org/10.1177/0003319707300361>

Gifford, J. R., Garten, R. S., Nelson, A. D., Trinity, J. D., Layec, G., Witman, M. A., Weavil, J. C., Mangum, T., Hart, C., Etheredge, C., Jessop, J., Bledsoe, A., Morgan, D. E., Wray, D. W., Rossman, M. J., & Richardson, R. S. (2016). Symmorphosis and skeletal muscle

VO₂ max : in vivo and in vitro measures reveal differing constraints in the exercise-trained and untrained human. *J Physiol*, 594(6), 1741–1751. <https://doi.org/10.1113/JP271229>

Gifford, J. R., Trinity, J. D., Kwon, O. S., Layec, G., Garten, R. S., Park, S. Y., Nelson, A. D., & Richardson, R. S. (2018a). Altered skeletal muscle mitochondrial phenotype in COPD:

Disease vs. disuse. *Journal of Applied Physiology*.

<https://doi.org/10.1152/japplphysiol.00788.2017>

Gifford, J. R., Trinity, J. D., Kwon, O. S., Layec, G., Garten, R. S., Park, S. Y., Nelson, A. D., & Richardson, RS. S. (2018b). Altered skeletal muscle mitochondrial phenotype in COPD:

Disease vs. disuse. *Journal of Applied Physiology*.

<https://doi.org/10.1152/japplphysiol.00788.2017>

Gifford, J. R., Trinity, J. D., Layec, G., Garten, R. S., Park, S. Y., Rossman, M. J., Larsen, S., Dela, F., & Richardson, R. S. (2015). Quadriceps exercise intolerance in patients with

chronic obstructive pulmonary disease: the potential role of altered skeletal muscle mitochondrial respiration. *J Appl Physiol* (1985), 119(8), 882–888.

<https://doi.org/10.1152/japplphysiol.00460.2015>

- Gilman, S., & Zhouu, X.** (2004). *Smoke: A Global History of Smoking*. Reaktion Books.
- Glancy, B., & Balaban, R. S.** (2021). Energy Metabolism Design of the Striated Muscle Cell. *Physiol Rev*, 101, 1561–1607. <https://doi.org/10.1152/physrev.00040.2020>
- Glancy, B., Hartnell, L. M., Combs, C. A., Fenmou, A., Sun, J., Murphy, E., Subramaniam, S., & Balaban, R. S.** (2017). Power Grid Protection of the Muscle Mitochondrial Reticulum. *Cell Reports*, 19(3), 487–496. <https://doi.org/10.1016/J.CELREP.2017.03.063>
- Glancy, B., Hartnell, L. M., Malide, D., Yu, Z. X., Combs, C. A., Connelly, P. S., Subramaniam, S., & Balaban, R. S.** (2015). Mitochondrial reticulum for cellular energy distribution in muscle. *Nature* 2015 523:7562, 523(7562), 617–620. <https://doi.org/10.1038/nature14614>
- Glancy, B., Willis, W. T., Chess, D. J., & Balaban, R. S.** (2013). Effect of calcium on the oxidative phosphorylation cascade in skeletal muscle mitochondria. *Biochemistry*, 52(16). <https://doi.org/10.1021/bi3015983>
- Gnaiger E.** (2020). *O2k Quality Control 1: Polarographic oxygen sensors and accuracy of calibration Section Page*.
- Gnaiger, E., Kuznetsov, A. V., Schneeberger, S., Seiler, Rü., Brandacher, G., Steurer, W., & Margreiter, R.** (2000). Mitochondria in the Cold. In *Life in the Cold*. https://doi.org/10.1007/978-3-662-04162-8_45
- Gorza, L., Sartore, S., Thornell, L. E., & Schiaffino, S.** (1986). Myosin types and fiber types in cardiac muscle. III. Nodal conduction tissue. *The Journal of Cell Biology*, 102(5), 1758. <https://doi.org/10.1083/JCB.102.5.1758>

- Gosker, H. R., Langen, R. C. J., Bracke, K. R., Joos, G. F., Brusselle, G. G., Steele, C., Ward, K. A., Wouters, E. F. M., & Schols, A. M. W. J.** (2009). Extrapulmonary manifestations of chronic obstructive pulmonary disease in a mouse model of chronic cigarette smoke exposure. *American Journal of Respiratory Cell and Molecular Biology*. <https://doi.org/10.1165/rcmb.2008-0312OC>
- Gosker, H. R., Zeegers, M. P., Wouters, E. F. M., & Schols, A. M. W. J.** (2007). Muscle fibre type shifting in the vastus lateralis of patients with COPD is associated with disease severity: A systematic review and meta-analysis. In *Thorax*. <https://doi.org/10.1136/thx.2007.078980>
- Gourd, K.** (2014). Fritz Lickint. In *The Lancet Respiratory Medicine*. [https://doi.org/10.1016/S2213-2600\(14\)70064-5](https://doi.org/10.1016/S2213-2600(14)70064-5)
- Graham Barr, R., Mesia-Vela, S., Austin, J. H. M., Basner, R. C., Keller, B. M., Reeves, A. P., Shimbo, D., & Stevenson, L.** (2007). Impaired Flow-mediated Dilation Is Associated with Low Pulmonary Function and Emphysema in Ex-smokers The Emphysema and Cancer Action Project (EMCAP) Study. *American Journal of Respiratory and Critical Care Medicine*, 176, 1200–1207. <https://doi.org/10.1164/rccm.200707-980OC>
- Griendling, K. K., Sorescu, D., & Ushio-Fukai, M.** (2000). NAD(P)H oxidase: Role in cardiovascular biology and disease. In *Circulation Research*. <https://doi.org/10.1161/01.RES.86.5.494>
- Guthikonda, S., Sinkey, C., Barenz, T., & Haynes, W. G.** (2003). Xanthine oxidase inhibition reverses endothelial dysfunction in heavy smokers. *Circulation*. <https://doi.org/10.1161/01.CIR.0000046448.26751.58>

- Guzun, R., Gonzalez-Granillo, M., Karu-Varikmaa, M., Grichine, A., Usson, Y., Kaambre, T., Guerrero-Roesch, K., Kuznetsov, A., Schlattner, U., & Saks, V.** (2012). Regulation of respiration in muscle cells in vivo by VDAC through interaction with the cytoskeleton and MtCK within Mitochondrial Interactosome. *Biochimica et Biophysica Acta*, 1818(6), 1545–1554. <https://doi.org/10.1016/J.BBAMEM.2011.12.034>
- Hahad, O., Arnold, N., Prochaska, J. H., Panova-Noeva, M., Schulz, A., Lackner, K. J., Pfeiffer, N., Schmidtmann, I., Michal, M., Beutel, M., Wild, P. S., Keaney, J. F. Jr., Daiber, A., & Münz, T.** (2021). Cigarette Smoking Is Related to Endothelial Dysfunction of Resistance, but Not Conduit Arteries in the General Population—Results From the Gutenberg Health Study. *Frontiers in Cardiovascular Medicine*, 0, 403. <https://doi.org/10.3389/FCVM.2021.674622>
- Haji, G., Wiegman, C. H., Michaeloudes, C., Patel, M. S., Curtis, K., Bhavsar, P., Polkey, M. I., Adcock, I. M., & Chung, K. F.** (2020). Mitochondrial dysfunction in airways and quadriceps muscle of patients with chronic obstructive pulmonary disease. *Respiratory Research*, 21(1). <https://doi.org/10.1186/S12931-020-01527-5>
- Hara, H., Araya, J., Ito, S., Kobayashi, K., Takasaka, N., Yoshii, Y., Wakui, H., Kojima, J., Shimizu, K., Numata, T., Kawaishi, M., Kamiya, N., Odaka, M., Morikawa, T., Kaneko, Y., Nakayama, K., & Kuwano, K.** (2013). Mitochondrial fragmentation in cigarette smoke-induced bronchial epithelial cell senescence. *American Journal of Physiology. Lung Cellular and Molecular Physiology*, 305(10). <https://doi.org/10.1152/AJPLUNG.00146.2013>
- Hawley, J. A., Hargreaves, M., Joyner, M. J., & Zierath, J. R.** (2014). Integrative biology of exercise. In *Cell*. <https://doi.org/10.1016/j.cell.2014.10.029>

- Heitzer, T., Brockhoff, C., Mayer, B., Warnholtz, A., Mollnau, H., Henne, S., Meinertz, T., & Münz, T.** (2000). Tetrahydrobiopterin improves endothelium-dependent vasodilation in chronic smokers : evidence for a dysfunctional nitric oxide synthase. *Circulation Research*.
<https://doi.org/10.1161/01.RES.86.2.e36>
- Helios, M., & Rosario, D.** (2020). Package “pwr” Title Basic Functions for Power Analysis.
- Hellerstein, M. K., Benowitz, N. L., Neese, R. A., Schwartz, J.-M., Hoh, R., Iii, P. J., Hsieh, J., & Faixi, D.** (1994). Effects of Cigarette Smoking and Its Cessation on Lipid Metabolism and Energy Expenditure in Heavy Smokers. *Journal of Clinical Investigation*, 93, 265–272.
- Hirsch, G. L., Sue, D. Y., Wasserman, K., Robinson, T. E., Hansen, J. E., & Wasser-Man, K.** (1985). *Immediate effects of cigarette smoking on cardiorespiratory responses to exercise*.
- Hofstetter, A., Schutz, Y., Jéquier, E., & Wahren, J.** (1986). Increased 24-hour energy expenditure in cigarette smokers. *The New England Journal of Medicine*, 314(2), 79–82.
<https://doi.org/10.1056/NEJM198601093140204>
- Holm, S.** (1979). A Simple Sequentially Rejective Multiple Test Procedure. *Scandinavian Journal of Statistics*, 6(2), 65–70.
- Huang, M. F., Lin, W. L., & Ma, Y. C.** (2005). A study of reactive oxygen species in mainstream of cigarette. *Indoor Air*. <https://doi.org/10.1111/j.1600-0668.2005.00330.x>
- Hyatt, H., Deminice, R., Yoshihara, T., & Powers, S. K.** (2019). Mitochondrial dysfunction induces muscle atrophy during prolonged inactivity: a review of the causes and effects. *Archives of Biochemistry and Biophysics*, 662, 49.
<https://doi.org/10.1016/J.ABB.2018.11.005>

Illner, K., Brinkmann, G., Heller, M., Bosy-Westphal, A., & Müller, M. J. (2000).

Metabolically active components of fat free mass and resting energy expenditure in nonobese adults. *American Journal of Physiology - Endocrinology and Metabolism*.
<https://doi.org/10.1152/ajpendo.2000.278.2.e308>

Jaccard, G., Djoko, D. T., Korneliou, A., Stabbert, R., Belushkin, M., & Esposito, M. (2019).

Mainstream smoke constituents and in vitro toxicity comparative analysis of 3R4F and 1R6F reference cigarettes. *Toxicology Reports*, 6, 222–231.
<https://doi.org/10.1016/j.toxrep.2019.02.009>

Jacobs, R. A., Díaz, V., Meinild, A. K., Gassmann, M., & Lundby, C. (2013). The C57Bl/6

mouse serves as a suitable model of human skeletal muscle mitochondrial function. *Experimental Physiology*. <https://doi.org/10.1113/expphysiol.2012.070037>

Jaimes, E. A., DeMaster, E. G., Tian, R. X., & Raij, L. (2004). Stable compounds of cigarette

smoke induce endothelial superoxide anion production via NADPH oxidase activation. *Arteriosclerosis, Thrombosis, and Vascular Biology*.
<https://doi.org/10.1161/01.ATV.0000127083.88549.58>

Jastroch, M., Divakaruni, A. S., Mookerjee, S., Treberg, J. R., & Brand, M. D. (2010).

Mitochondrial proton and electron leaks. *Essays in Biochemistry*.
<https://doi.org/10.1042/BSE0470053>

Jensen, E. X., Fusch, C., Jaeger, P., Peheim, E., & Horber, F. (1995). Impact of chronic

cigarette smoking on body composition and fuel metabolism. *The Journal of Clinical Endocrinology and Metabolism*, 80(7), 2181–2185.
<https://doi.org/10.1210/JCE.80.7.7608276>

- Jia, G., Meng, Z., Liu, C., Ma, X., Gao, J., Liu, J., Guo, R., Yan, Z., Christopher, T., Lopez, B., Liu, W., Dai, H., Lau, W. B., Jiao, X., Zhao, J., Wang, Z. X., Cao, J., & Wang, Y.** (2020). Nicotine induces cardiac toxicity through blocking mitophagic clearance in young adult rat. *Life Sciences*, 257. <https://doi.org/10.1016/J.LFS.2020.118084>
- Jo, Y., Linton, J. A., Choi, J., Moon, J., Kim, J., Lee, J., & Oh, S.** (2019). Association between Cigarette Smoking and Sarcopenia according to Obesity in the Middle-Aged and Elderly Korean Population: The Korea National Health and Nutrition Examination Survey (2008–2011). *Korean Journal of Family Medicine*, 40(2), 87. <https://doi.org/10.4082/KJFM.17.0078>
- Johnson, H. M., Gossett, L. K., Piper, M. E., Aeschlimann, S. E., Korcarz, C. E., Baker, T. B., Fiore, M. C., & Stein, J. H.** (2010). Effects of smoking and smoking cessation on endothelial function: 1-year outcomes from a randomized clinical trial. *Journal of the American College of Cardiology*. <https://doi.org/10.1016/j.jacc.2010.03.002>
- Kapchinsky, S., Vuda, M., Miguez, K., Elkrief, D., de Souza, A. R., Baglioni, C. J., Aare, S., MacMillan, N. J., Baril, J., Rozakis, P., Sonjak, V., Pion, C., Aubertin-Leheudre, M., Morais, J. A., Jagoe, R. T., Bourbeau, J., Taivassalo, T., & Hepple, R. T.** (2018). Smoke-induced neuromuscular junction degeneration precedes the fibre type shift and atrophy in chronic obstructive pulmonary disease. *Journal of Physiology*. <https://doi.org/10.1113/JP275558>
- Kaplan, A., Abidi, E., Ghali, R., Booz, G. W., Kobeissy, F., & Zouein, F. A.** (2017). Functional, Cellular, and Molecular Remodeling of the Heart under Influence of Oxidative Cigarette Tobacco Smoke. *Oxidative Medicine and Cellular Longevity*, 2017. <https://doi.org/10.1155/2017/3759186>

- Kemp, G. J., Meyerspeer, M., & Moser, E.** (2007). Absolute quantification of phosphorus metabolite concentrations in human muscle in vivo by ^{31}P MRS: A quantitative review. In *NMR in Biomedicine* (Vol. 20, Issue 6, pp. 555–565). <https://doi.org/10.1002/nbm.1192>
- Khattri, R. B., Thome, T., Fitzgerald, L. F., Wohlgemuth, S. E., Hepple, R. T., & Ryan, T. E.** (2022). NMR Spectroscopy Identifies Chemicals in Cigarette Smoke Condensate That Impair Skeletal Muscle Mitochondrial Function. *Toxics 2022, Vol. 10, Page 140, 10(3)*, 140. <https://doi.org/10.3390/TOXICS10030140>
- Kim, B. S., Serebreni, L., Hamdan, O., Wang, L., Parniani, A., Sussan, T., Scott Stephens, R., Boyer, L., Damarla, M., Hassoun, P. M., & Damico, R.** (2013). Xanthine oxidoreductase is a critical mediator of cigarette smoke-induced endothelial cell DNA damage and apoptosis. *Free Radical Biology and Medicine*. <https://doi.org/10.1016/j.freeradbiomed.2013.01.023>
- Kirkham, P. A., & Barnes, P. J.** (2013). Oxidative stress in COPD. *Chest*. <https://doi.org/10.1378/chest.12-2664>
- Klingenberg, M.** (2008). The ADP and ATP transport in mitochondria and its carrier. In *Biochimica et Biophysica Acta - Biomembranes*. <https://doi.org/10.1016/j.bbamem.2008.04.011>
- The ADP and ATP transport in mitochondria and its carrier, 1778 *Biochimica et Biophysica Acta - Biomembranes* 1978 (2008). <https://doi.org/10.1016/j.bbamem.2008.04.011>
- Kojima, G., Iliffe, S., & Walters, K.** (2015). Smoking as a predictor of frailty: a systematic review. *BMC Geriatrics 2015 15:1, 15(1), 1–7*. <https://doi.org/10.1186/S12877-015-0134-9>

Kok, M. O., Hoekstra, T., & Twisk, J. W. R. (2012). The longitudinal relation between smoking and muscle strength in healthy adults. *European Addiction Research*.
<https://doi.org/10.1159/000333600>

Komlódi, T., Sobotka, O., Krumschnabel, G., Bezuidenhout, N., Hiller, E., Doerrier, C., & Gnaiger, E. (2018). Comparison of mitochondrial incubation media for measurement of respiration and hydrogen peroxide production. In *Methods in Molecular Biology* (Vol. 1782).
https://doi.org/10.1007/978-1-4939-7831-1_8

Krumholz, R. A., Chevalier, R. B., & Ross, J. C. (1964). *Cardiopulmonary Function in Young Smokers A Comparison of Pulmonary Function Measurements and Some Cardiopulmonary Responses to Exercise Between a Group of Young Smokers and a Comparable Group of Nonsmokers*.

Kunji, E. R. S., Aleksandrova, A., King, M. S., Majd, H., Ashton, V. L., Cerson, E., Springett, R., Kibalchenko, M., Tavoulari, S., Crichton, P. G., & Ruprecht, J. J. (2016). The transport mechanism of the mitochondrial ADP/ATP carrier. *Biochimica et Biophysica Acta (BBA) - Molecular Cell Research*, 1863(10), 2379–2393.
<https://doi.org/10.1016/J.BBAMCR.2016.03.015>

Kuznetsov, A. V., Kunz, W. S., Saks, V., Usson, Y., Mazat, J. P., Letellier, T., Gellerich, F. N., & Margreiter, R. (2003). Cryopreservation of mitochondria and mitochondrial function in cardiac and skeletal muscle fibers. *Analytical Biochemistry*, 319(2), 296–303.
[https://doi.org/10.1016/S0003-2697\(03\)00326-9](https://doi.org/10.1016/S0003-2697(03)00326-9)

Kuznetsov, A. V., Tiivel, T., Sikk, P., Kaambre, T., Kay, L., Daneshrad, Z., Rossi, A., Kadaja, L., Peet, N., Seppet, E., & Saks, V. A. (1996). Striking Differences Between the Kinetics of

Regulation of Respiration by ADP in Slow-Twitch and Fast-Twitch Muscles In Vivo.

European Journal of Biochemistry, 241(3), 909–915. <https://doi.org/10.1111/j.1432-1033.1996.00909.x>

Kuznetsov, A. v., Veksler, V., Gellerich, F. N., Saks, V., Margreiter, R., & Kunz, W. S. (2008a). Analysis of mitochondrial function in situ in permeabilized muscle fibers, tissues and cells. *Nature Protocols*. <https://doi.org/10.1038/nprot.2008.61>

Kuznetsov, A. V., Veksler, V., Gellerich, F. N., Saks, V., Margreiter, R., & Kunz, W. S. (2008b). Analysis of mitochondrial function in situ in permeabilized muscle fibers, tissues and cells. *Nature Protocols*, 3(6), 965–976. <https://doi.org/10.1038/nprot.2008.61>

Kyle, J. L., Riesen, W. H., & Riesen, W. H. (2013). Stress and Cigarette Smoke Effects on Lung Mitochondrial Phosphorylation. <Https://Doi.Org/10.1080/00039896.1970.10667277>, 21(4), 492–497. <https://doi.org/10.1080/00039896.1970.10667277>

Lacolley, P., Regnault, V., Segers, P., & Laurent, S. (2017). Vascular smooth muscle cells and arterial stiffening: Relevance in development, aging, and disease. *Physiological Reviews*, 97(4), 1555–1617. <https://doi.org/10.1152/PHYSREV.00003.2017>

Lanza, I. R., & Nair, K. S. (2009). Muscle mitochondrial changes with aging and exercise. *American Journal of Clinical Nutrition*. <https://doi.org/10.3945/ajcn.2008.26717D>

Larsen, F. J., Schiffer, T. A., Borniquel, S., Sahlin, K., Ekblom, B., Lundberg, J. O., & Weitzberg, E. (2011). Dietary inorganic nitrate improves mitochondrial efficiency in humans. *Cell Metabolism*, 13(2), 149–159. <https://doi.org/10.1016/J.CMET.2011.01.004>

Larsen, S., Nielsen, J., Hansen, C. N., Nielsen, L. B., Wibrand, F., Stride, N., Schroder, H. D., Boushel, R., Helge, J. W., Dela, F., & Hey-Mogensen, M. (2012). Biomarkers of

mitochondrial content in skeletal muscle of healthy young human subjects. *Journal of Physiology*. <https://doi.org/10.1113/jphysiol.2012.230185>

Larsen, S., Wright-Paradis, C., Gnaiger, E., Helge, J. W., & Boushel, R. (2012). Cryopreservation of human skeletal muscle impairs mitochondrial function. *Cryo-Letters*, 33(3), 170–176.

Larson-Meyer, D. E., Newcomer, B. R., Hunter, G. R., Hetherington, H. P., & Weinsier, R. L. (2000). *31P MRS measurement of mitochondrial function in skeletal muscle: reliability, force-level sensitivity and relation to whole body maximal oxygen uptake*. NMR in Biomedicine.

[https://analyticalsciencejournals.onlinelibrary.wiley.com/doi/pdf/10.1002/\(SICI\)1099-1492\(200002\)13:1%3C14::AID-NBM605%3E3.0.CO;2-0](https://analyticalsciencejournals.onlinelibrary.wiley.com/doi/pdf/10.1002/(SICI)1099-1492(200002)13:1%3C14::AID-NBM605%3E3.0.CO;2-0)

Larson-Meyer, D. E., Newcomer, B. R., Hunter, G. R., Joanisse, D. R., Weinsier, R. L., & Bamman, M. M. (2001). Relation between in vivo and in vitro measurements of skeletal muscle oxidative metabolism. *Muscle and Nerve*, 24(12), 1665–1676.
<https://doi.org/10.1002/mus.1202>

Larsson, L., & Örlander, J. (1984). Skeletal muscle morphology, metabolism and function in smokers and non-smokers. A study on smoking-discordant monozygous twins. *Acta Physiologica Scandinavica*. <https://doi.org/10.1111/j.1748-1716.1984.tb07394.x>

Layec, G., Blain, G. M., Rossman, M. J., Park, S. Y., Hart, C. R., Trinity, J. D., Gifford, J. R., Sidhu, S. K., Weavil, J. C., Hureau, T. J., Amann, M., & Richardson, R. S. (2018). Acute high-intensity exercise impairs skeletal muscle respiratory capacity. *Medicine and Science in Sports and Exercise*. <https://doi.org/10.1249/MSS.0000000000001735>

- Layec, G., Bringard, A., Le Fur, Y., Vilmen, C., Micallef, J. P., Perrey, S., Cozzone, P. J., & Bendahan, D.** (2011). Comparative determination of energy production rates and mitochondrial function using different 31P MRS quantitative methods in sedentary and trained subjects. *NMR Biomed*, 24(4), 425–438. <https://doi.org/10.1002/nbm.1607>
- Layec, G., Gifford, J. R., Trinity, J. D., Hart, C. R., Garten, R. S., Park, S. Y., Le Fur, Y., Jeong, E. K., & Richardson, R. S.** (2016). Accuracy and precision of quantitative 31P-MRS measurements of human skeletal muscle mitochondrial function. *Am J Physiol Endocrinol Metab*, 311(2), E358-66. <https://doi.org/10.1152/ajpendo.00028.2016>
- Layec, G., Haseler, L. J., Hoff, J., & Richardson, R. S.** (2011). Evidence that a higher ATP cost of muscular contraction contributes to the lower mechanical efficiency associated with COPD: preliminary findings. *Am J Physiol Regul Integr Comp Physiol*, 300(5), R1142-7. <https://doi.org/10.1152/ajpregu.00835.2010>
- Lee, N., & Choi, C. J.** (2019). Smoking and Diabetes as Predictive Factors of Accelerated Loss of Muscle Mass in Middle-Aged and Older Women: A Six-Year Retrospective Cohort Study. *Journal of Women's Health* (2002), 28(10), 1391–1398. <https://doi.org/10.1089/JWH.2018.7527>
- Li, R., Adamo, A., Chang, C. C., Tseng, C. H., Hsiai, T. K., & Rossiter, H. B.** (2021). Serum Acylglycerols Inversely Associate with Muscle Oxidative Capacity in Severe COPD. *Medicine and Science in Sports and Exercise*, 53(1), 10–18. <https://doi.org/10.1249/MSS.0000000000002441>
- Lickint, F.** (1930). Tabak und Tabakrauch als ätiologischer Faktor des Carcinoms. *Zeitschrift Für Krebsforschung*. <https://doi.org/10.1007/BF01636077>

- Liguori, I., Russo, G., Curcio, F., Bulli, G., Aran, L., Della-Morte, D., Gargiulo, G., Testa, G., Cacciatore, F., Bonaduce, D., & Abete, P.** (2018). Oxidative stress, aging, and diseases. In *Clinical Interventions in Aging*. <https://doi.org/10.2147/CIA.S158513>
- Lineweaver, H., & Burk, D.** (1934). The Determination of Enzyme Dissociation Constants. *Journal of the American Chemical Society*, 56(3), 658–666. <https://doi.org/10.1021/ja01318a036>
- Liochev, S. I.** (2013). Reactive oxygen species and the free radical theory of aging. *Free Radic Biol Med*, 60, 1–4. <https://doi.org/10.1016/j.freeradbiomed.2013.02.011>
- Liu, Z., Ren, Z., Zhang, J., Chuang, C. C., Kandaswamy, E., Zhou, T., & Zuo, L.** (2018). Role of ROS and nutritional antioxidants in human diseases. In *Frontiers in Physiology*. <https://doi.org/10.3389/fphys.2018.00477>
- Luciani, S., Martini, N., & Santi, R.** (1971). Effects of carboxyatractyloside a structural analogue of atractyloside on mitochondrial oxidative phosphorylation. *Life Sciences. Pt. 2: Biochemistry, General and Molecular Biology*, 10(17), 961–968. [https://doi.org/10.1016/0024-3205\(71\)90099-3](https://doi.org/10.1016/0024-3205(71)90099-3)
- Ma, Q.** (2013). Role of Nrf2 in oxidative stress and toxicity. In *Annual Review of Pharmacology and Toxicology*. <https://doi.org/10.1146/annurev-pharmtox-011112-140320>
- Maddatu, J., Anderson-Baucum, E., & Evans-Molina, C.** (2017a). Smoking and the Risk of Type 2 Diabetes. *Translational Research : The Journal of Laboratory and Clinical Medicine*, 184, 101. <https://doi.org/10.1016/J.TRSL.2017.02.004>

Maddatu, J., Anderson-Baucum, E., & Evans-Molina, C. (2017b). Smoking and the Risk of Type 2 Diabetes. *Translational Research : The Journal of Laboratory and Clinical Medicine*, 184, 101. <https://doi.org/10.1016/J.TRSL.2017.02.004>

Maddatu, J., Anderson-Baucum, E., & Evans-Molina, C. (2017c). Smoking and the Risk of Type 2 Diabetes. *Translational Research : The Journal of Laboratory and Clinical Medicine*, 184, 101. <https://doi.org/10.1016/J.TRSL.2017.02.004>

Maltais, F., LeBlanc, P., Whittom, F., Simard, C., Marquis, K., Bélanger, M., Breton, M. J., & Jobin, J. (2000). Oxidative enzyme activities of the vastus lateralis muscle and the functional status in patients with COPD. *Thorax*. <https://doi.org/10.1136/thorax.55.10.848>

Mannino, D. M., & Buist, A. S. (2007). Global burden of COPD: risk factors, prevalence, and future trends. In *Lancet*. [https://doi.org/10.1016/S0140-6736\(07\)61380-4](https://doi.org/10.1016/S0140-6736(07)61380-4)

Mao, G. D., & Poznansky, M. J. (1992). Electron spin resonance study on the permeability of superoxide radicals in lipid bilayers and biological membranes. *FEBS Letters*. [https://doi.org/10.1016/0014-5793\(92\)80675-7](https://doi.org/10.1016/0014-5793(92)80675-7)

Marques, E. A., Elbejjani, M., Frank-Wilson, A. W., Gudnason, V., Sigurdsson, G., Lang, T. F., Jonsson, P. V., Sigurdsson, S., Aspelund, T., Siggeirsdottir, K., Launer, L., Eiriksdottir, G., Harris, T. B., EA, M., M, E., AW, F.-W., V, G., G, S., TF, L., ... TB, H. (2020). Cigarette Smoking Is Associated With Lower Quadriceps Cross-sectional Area and Attenuation in Older Adults. *Nicotine & Tobacco Research : Official Journal of the Society for Research on Nicotine and Tobacco*, 22(6), 935–941. <https://doi.org/10.1093/ntr/ntz081>

Martinou, J. C., Desagher, S., & Antonsson, B. (2000). Cytochrome c release from mitochondria: all or nothing. *Nature Cell Biology*, 2(3). <https://doi.org/10.1038/35004069>

McCommis, K. S., & Finck, B. N. (2015). Mitochondrial pyruvate transport: a historical perspective and future research directions. *The Biochemical Journal*, 466(3), 443.

<https://doi.org/10.1042/BJ20141171>

McKeough, Z. J., Alison, J. A., Bye, P. T. P., Trenell, M. I., Sachinwalla, T., Thompson, C. H., & Kemp, G. J. (2006). Exercise capacity and quadriceps muscle metabolism following training in subjects with COPD. *Respiratory Medicine*.

<https://doi.org/10.1016/j.rmed.2006.01.017>

Mendelson, J. H., Sholar, M. B., Mutschler, N. H., Jaszyna-Gasior, M., Goletiani, N. v., Siegel, A. J., & Mello, N. K. (2003). Effects of intravenous cocaine and cigarette smoking on luteinizing hormone, testosterone, and prolactin in men. *Journal of Pharmacology and Experimental Therapeutics*, 307(1), 339–348. <https://doi.org/10.1124/jpet.103.052928>

Messner, B., & Bernhard, D. (2014). Smoking and cardiovascular disease: Mechanisms of endothelial dysfunction and early atherogenesis. In *Arteriosclerosis, Thrombosis, and Vascular Biology*. <https://doi.org/10.1161/ATVBAHA.113.300156>

Meyer, A., Charles, A. L., Zoll, J., Guillot, M., Lejay, A., Singh, F., Schlagowski, A. I., Isner-Horobeti, M. E., Pista, C., Charloux, A., & Geny, B. (2014). Cryopreservation with dimethyl sulfoxide prevents accurate analysis of skinned skeletal muscle fibers mitochondrial respiration. *Biochimie*, 100(1), 227–233. <https://doi.org/10.1016/j.biochi.2014.01.014>

Meyer, A., Zoll, J., Charles, A. L., Charloux, A., de Blay, F., Diemunsch, P., Sibilia, J., Piquard, F., & Geny, B. (2013). Skeletal muscle mitochondrial dysfunction during chronic obstructive pulmonary disease: Central actor and therapeutic target. In *Experimental Physiology*. <https://doi.org/10.1113/expphysiol.2012.069468>

- Meyer, J. N., Leung, M. C. K., Rooney, J. P., Sendoel, A., Hengartner, M. O., Kisby, G. E., & Bess, A. S.** (2013). Mitochondria as a target of environmental toxicants. In *Toxicological Sciences*. <https://doi.org/10.1093/toxsci/kft102>
- Minicucci, M. F., Azevedo, P. S., Polegato, B. F., Paiva, S. A. R., & Zornoff, L. A. M.** (2012). Cardiac remodeling induced by smoking: concepts, relevance, and potential mechanisms. *Inflammation & Allergy Drug Targets*, 11(6), 442–447. <https://doi.org/10.2174/187152812803589958>
- Mitchell, P.** (1961). Coupling of phosphorylation to electron and hydrogen transfer by a chemiosmotic type of mechanism. *Nature*. <https://doi.org/10.1038/191144a0>
- Montes De Oca, M., Loeb, E., Torres, S. H., De Sanctis, J., Hernández, N., & Tálamo, C.** (2008a). Peripheral muscle alterations in non-COPD smokers. *Chest*. <https://doi.org/10.1378/chest.07-1592>
- Montes De Oca, M., Loeb, E., Torres, S. H., De Sanctis, J., Hernández, N., & Tálamo, C.** (2008b). Peripheral muscle alterations in non-COPD smokers. *Chest*, 133(1), 13–18. <https://doi.org/10.1378/chest.07-1592>
- Morse, C. I., Pritchard, L. J., Wüst, R. C. I., Jones, D. A., & Degens, H.** (2008). Carbon monoxide inhalation reduces skeletal muscle fatigue resistance. *Acta Physiologica (Oxford, England)*, 192(3), 397–401. <https://doi.org/10.1111/J.1748-1716.2007.01757.X>
- Morton, A. R., & Holmik, E. V.** (1985). The effects of cigarette smoking on maximal oxygen consumption and selected physiological responses of elite team sportsmen. *European Journal of Applied Physiology and Occupational Physiology*, 53(4), 348–352. <https://doi.org/10.1007/BF00422852>

Moylan, J. S., & Reid, M. B. (2007). Oxidative stress, chronic disease, and muscle wasting. In *Muscle and Nerve*. <https://doi.org/10.1002/mus.20743>

Muggeo, V. (2008). *Segmented: An R Package to Fit Regression Models With Broken-Line Relationships.* R News.

https://www.researchgate.net/publication/234092680_Segmented_An_R_Package_to_Fit_R_Regression_Models_With_Broken-Line_Relationships

Muller, F. L., Liu, Y., & Van Remmen, H. (2004). Complex III releases superoxide to both sides of the inner mitochondrial membrane. *Journal of Biological Chemistry*. <https://doi.org/10.1074/jbc.M407715200>

Münzel, T., Hahad, O., Kuntic, M., Keaney, J. F., Deanfield, J. E., & Daiber, A. (2020). Effects of tobacco cigarettes, e-cigarettes, and waterpipe smoking on endothelial function and clinical outcomes. *European Heart Journal*, 41(41), 4057–4070. <https://doi.org/10.1093/EURHEARTJ/EHAA460>

Murphy, M. P. (2009). How mitochondria produce reactive oxygen species. In *Biochemical Journal*. <https://doi.org/10.1042/BJ20081386>

Muscat, J. E., Harris, R. E., Haley, N. J., & Wynder, E. L. (1991a). *Cigarette smoking and plasma cholesterol*. 121, 141–147. [https://doi.org/10.1016/0002-8703\(91\)90967-M](https://doi.org/10.1016/0002-8703(91)90967-M)

Muscat, J. E., Harris, R. E., Haley, N. J., & Wynder, E. L. (1991b). Cigarette smoking and plasma cholesterol. *American Heart Journal*, 121(1), 141–147. [https://doi.org/10.1016/0002-8703\(91\)90967-M](https://doi.org/10.1016/0002-8703(91)90967-M)

Nadruz, W., Claggett, B., Gonçalves, A., Querejeta-Roca, G., Fernandes-Silva, M. M., Shah, A. M., Cheng, S., Tanaka, H., Heiss, G., Kitzman, D. W., & Solomon, S. D. (2016).

Smoking and Cardiac Structure and Function in the Elderly: The ARIC Study (Atherosclerosis Risk in Communities). *Circulation. Cardiovascular Imaging*, 9(9).
<https://doi.org/10.1161/CIRCIMAGING.116.004950>

Naimi, A. I., Bourbeau, J., Perrault, H., Baril, J., Wright-Paradis, C., Rossi, A., Taivassalo, T., Sheel, A. W., Rabøl, R., Dela, F., & Boushel, R. (2011). Altered mitochondrial regulation in quadriceps muscles of patients with COPD. *Clinical Physiology and Functional Imaging*. <https://doi.org/10.1111/j.1475-097X.2010.00988.x>

Naserzadeh, P., Hosseini, M.-J., Arbabi, S., & Pourahmad, J. (2015). A Comparison of Toxicity Mechanisms of Cigarette Smoke on Isolated Mitochondria Obtained from Rat Liver and Skin. *Iranian Journal of Pharmaceutical Research : IJPR*, 14(1), 271.

Naserzadeh, P., & Pourahmad, J. (2013). Toxicity mechanisms of Cigarette Smoke on Eye and Kidney using Isolated Mitochondria. *Iranian Journal of Pharmaceutical Sciences*, 9(3), 55–62.

Neese, R. A., Benowitz, N. L., Hoh, R., Faix, D., LaBua, A., Pun, K., & Hellerstein, M. K. (1994). Metabolic interactions between surplus dietary energy intake and cigarette smoking or its cessation. *American Journal of Physiology - Endocrinology and Metabolism*, 267(6 30-6). <https://doi.org/10.1152/AJPENDO.1994.267.6.E1023>

Nemmar, A., Raza, H., Subramaniyan, D., Yasin, J., John, A., Ali, B. H., & Kazzam, E. E. (2013). Short-Term Systemic Effects of Nose-Only Cigarette Smoke Exposure in Mice: Role of Oxidative Stress. *Cellular Physiology and Biochemistry*, 31(1), 15–24.
<https://doi.org/10.1159/000343345>

- Neves, C. D. C., Lacerda, A. C. R., Lage, V. K. S., Lima, L. P., Tossige-Gomes, R., Fonseca, S. F., Rocha-Vieira, E., Teixeira, M. M., & Mendonça, V. A.** (2016). Oxidative stress and skeletal muscle dysfunction are present in healthy smokers. *Brazilian Journal of Medical and Biological Research*. <https://doi.org/10.1590/1414-431X20165512>
- Nogueira, L., Trisko, B. M., Lima-Rosa, F. L., Jackson, J., Lund-Palau, H., Yamaguchi, M., & Breen, E. C.** (2018). Cigarette smoke directly impairs skeletal muscle function through capillary regression and altered myofibre calcium kinetics in mice. *Journal of Physiology*, 596(14), 2901–2916. <https://doi.org/10.1113/JP275888>
- Nulton-Persson, A. C., & Szweda, L. I.** (2001). Modulation of mitochondrial function by hydrogen peroxide. *The Journal of Biological Chemistry*, 276(26), 23357–23361. <https://doi.org/10.1074/JBC.M100320200>
- Nyberg, A., Saey, D., & Maltais, F.** (2015). Why and how limb muscle mass and function should be measured in patients with chronic obstructive pulmonary disease. In *Annals of the American Thoracic Society*. <https://doi.org/10.1513/AnnalsATS.201505-278PS>
- Ojuka, E., Andrew, B., Bezuidenhout, N., George, S., Maarman, G., Madlala, H. P., Mendham, A., & Osiki, P. O.** (2016). Measurement of β-oxidation capacity of biological samples by respirometry: a review of principles and substrates. *American Journal of Physiology-Endocrinology and Metabolism*, 310(9), E715–E723. <https://doi.org/10.1152/ajpendo.00475.2015>
- Oliver-Rodríguez, J. C., & Wang, X. T.** (2015). Non-parametric three-way mixed ANOVA with aligned rank tests. *British Journal of Mathematical and Statistical Psychology*, 68(1), 23–42. <https://doi.org/10.1111/bmsp.12031>

- Örlander, J., Kiessling, K. -H, & Larsson, L.** (1979). Skeletal muscle metabolism, morphology and function in sedentary smokers and nonsmokers. *Acta Physiologica Scandinavica*. <https://doi.org/10.1111/j.1748-1716.1979.tb06440.x>
- Orosz, Z., Csiszar, A., Labinskyy, N., Smith, K., Kaminski, P. M., Ferdinandy, P., Wolin, M. S., Rivera, A., & Ungvari, Z.** (2007). Cigarette smoke-induced proinflammatory alterations in the endothelial phenotype: Role of NAD(P)H oxidase activation. *American Journal of Physiology - Heart and Circulatory Physiology*, 292(1), 130–139. <https://doi.org/10.1152/ajpheart.00599.2006>
- Pan, A., Wang, Y., Talaei, M., Hu, F. B., & Wu, T.** (2015). Relation of active, passive, and quitting smoking with incident type 2 diabetes: a systematic review and meta-analysis. *The Lancet. Diabetes & Endocrinology*, 3(12), 958–967. [https://doi.org/10.1016/S2213-8587\(15\)00316-2](https://doi.org/10.1016/S2213-8587(15)00316-2)
- Pande, S. V.** (1975). A mitochondrial carnitine acylcarnitine translocase system. *Proceedings of the National Academy of Sciences of the United States of America*, 72(3), 883. <https://doi.org/10.1073/PNAS.72.3.883>
- Papathanasiou, G., Georgakopoulos, D., Georgoudis, G., Spyropoulos, P., Perrea, D., & Evangelou, A.** (2007a). Effects of chronic smoking on exercise tolerance and on heart rate-systolic blood pressure product in young healthy adults. *European Journal of Preventive Cardiology*, 14(5), 646–652. <https://doi.org/10.1097/HJR.0b013e3280ecfe2c>
- Papathanasiou, G., Georgakopoulos, D., Georgoudis, G., Spyropoulos, P., Perrea, D., & Evangelou, A.** (2007b). Effects of chronic smoking on exercise tolerance and on heart rate-

systolic blood pressure product in young healthy adults. *European Journal of Preventive Cardiology*. <https://doi.org/10.1097/HJR.0b013e3280ecfe2c>

Park, S. H., Kwon, O. S., Park, S. Y., Weavil, J. C., Andtbacka, R. H. I., Hyngstrom, J. R., Reese, V., & Richardson, R. S. (2018). Vascular mitochondrial respiratory function: The impact of advancing age. *American Journal of Physiology - Heart and Circulatory Physiology*. <https://doi.org/10.1152/ajpheart.00324.2018>

Park, S. H. S. Y., Kwon, O. S., Park, S. H. S. Y., Weavil, J. C., Andtbacka, R. H. I., Hyngstrom, J. R., Reese, V., & Richardson, R. S. (2018). Vascular mitochondrial respiratory function: The impact of advancing age. *American Journal of Physiology - Heart and Circulatory Physiology*, 315(6), H1660–H1669.

<https://doi.org/10.1152/ajpheart.00324.2018>

Park, S. Y., Gifford, J. R., Andtbacka, R. H. I., Trinity, J. D., Hyngstrom, J. R., Garten, R. S., Diakos, N. A., Ives, S. J., Dela, F., Larsen, S., Drakos, S., & Richardson, R. S. (2014).

Cardiac, skeletal, and smooth muscle mitochondrial respiration: Are all mitochondria created equal? *American Journal of Physiology - Heart and Circulatory Physiology*.

<https://doi.org/10.1152/ajpheart.00227.2014>

Park, S. Y., Rossman, M. J., Gifford, J. R., Bharath, L. P., Bauersachs, J., Richardson, R. S., Abel, E. D., Symons, J. D., & Riehle, C. (2016). Exercise training improves vascular mitochondrial function. In *American Journal of Physiology - Heart and Circulatory Physiology*. <https://doi.org/10.1152/ajpheart.00751.2015>

Patel, S. P., Gamboa, J. L., McMullen, C. A., Rabchevsky, A., & Andrade, F. H. (2009). Lower respiratory capacity in extraocular muscle mitochondria: evidence for intrinsic differences in

mitochondrial composition and function. *Investigative Ophthalmology & Visual Science*, 50(1), 180–186. <https://doi.org/10.1167/IOVS.08-1911>

Pebay-Peyroula, E., Dahout-Gonzalez, C., Kahn, R., Trézéguit, V., Lauquin, G. J. M., & Brandolin, G. (2003). Structure of mitochondrial ADP/ATP carrier in complex with carboxyatractyloside. *Nature* 2003 426:6962, 426(6962), 39–44. <https://doi.org/10.1038/nature02056>

Peluffo, G., Calcerrada, P., Piacenza, L., Pizzano, N., & Radi, R. (2009). Superoxide-mediated inactivation of nitric oxide and peroxynitrite formation by tobacco smoke in vascular endothelium: studies in cultured cells and smokers. *American Journal of Physiology - Heart and Circulatory Physiology*, 296(6), H1781. <https://doi.org/10.1152/AJPHEART.00930.2008>

Pérez-Rial, S., Barreiro, E., Fernández-Aceñero, M. J., Fernández-Valle, M. E., González-Mangado, N., & Pece-Barba, G. (2020). Early detection of skeletal muscle bioenergetic deficit by magnetic resonance spectroscopy in cigarette smoke-exposed mice. *PLoS ONE*. <https://doi.org/10.1371/journal.pone.0234606>

Perkins, K. A., Epstein, L. H., Marks, B. L., Stiller, R. L., & Jacob, R. G. (1989). The effect of nicotine on energy expenditure during light physical activity. *The New England Journal of Medicine*, 320(14), 898–903. <https://doi.org/10.1056/NEJM198904063201404>

Perkins, K. A., Epstein, L. H., Stiller, R. L., Sexton, J. E., Fernstrom, M. H., Jacob, R. G., & Solberg, R. (1990). Metabolic effects of nicotine after consumption of a meal in smokers and nonsmokers. *The American Journal of Clinical Nutrition*, 52(2), 228–233. <https://doi.org/10.1093/AJCN/52.2.228>

Perry, C. G. R., Kane, D. A., Herbst, E. A. F., Mukai, K., Lark, D. S., Wright, D. C.,

Heigenhauser, G. J. F., Neufer, P. D., Spriet, L. L., & Holloway, G. P. (2012).

Mitochondrial creatine kinase activity and phosphate shuttling are acutely regulated by exercise in human skeletal muscle. *The Journal of Physiology*, 590(Pt 21), 5475.

<https://doi.org/10.1113/JPHYSIOL.2012.234682>

Perry, C. G. R., Kane, D. A., Lanza, I. R., & Neufer, D. P. (2013). Methods for Assessing

Mitochondrial Function in Diabetes. *Diabetes*, 62, 1041–1053. <https://doi.org/10.2337/db12-1219>

Perry, C. G. R., Kane, D. A., Lin, C. Te, Kozy, R., Cathey, B. L., Lark, D. S., Kane, C. L., Brophy, P. M., Gavin, T. P., Anderson, E. J., & Neufer, P. D. (2011). Inhibiting myosin-ATPase reveals a dynamic range of mitochondrial respiratory control in skeletal muscle.

Biochemical Journal, 437(2). <https://doi.org/10.1042/BJ20110366>

Pesta, D., & Gnaiger, E. (2012). High-resolution respirometry: OXPHOS protocols for human

cells and permeabilized fibers from small biopsies of human muscle. *Methods in Molecular Biology*. https://doi.org/10.1007/978-1-61779-382-0_3

Pettersen, J. C., & Cohen, S. D. (1993). The effects of cyanide on brain mitochondrial

cytochrome oxidase and respiratory activities. *Journal of Applied Toxicology*.

<https://doi.org/10.1002/jat.2550130104>

Picard, M., Ritchie, D., Wright, K. J., Romestaing, C., Thomas, M. M., Rowan, S. L.,

Taivassalo, T., & Hepple, R. T. (2010). Mitochondrial functional impairment with aging is exaggerated in isolated mitochondria compared to permeabilized myofibers. *Aging Cell*, 9(6),

1032–1046. <https://doi.org/10.1111/j.1474-9726.2010.00628.x>

Picard, M., Taivassalo, T., Gouspillou, G., & Hepple, R. T. (2011). Mitochondria: isolation, structure and function. *The Journal of Physiology*, 589(Pt 18), 4413.

<https://doi.org/10.1113/JPHYSIOL.2011.212712>

Poole, D. C., Behnke, B. J., & Musch, T. I. (2020). The role of vascular function on exercise capacity in health and disease. In *Journal of Physiology*. <https://doi.org/10.1113/JP278931>

Poredoš, P., Orehek, M., & Tratnik, E. (1999). Smoking is associated with dose-related increase of intima-media thickness and endothelial dysfunction. *Angiology*.
<https://doi.org/10.1177/000331979905000304>

Powell, J. T. (1998). Vascular damage from smoking: disease mechanisms at the arterial wall. In *Vascular Medicine* (Vol. 3).

Pryor, W., Stone, K., Zang, L., & Bermúdez, E. (1998). Fractionation of aqueous cigarette tar extracts: Fractions that contain the tar radical cause DNA damage. *Chemical Research in Toxicology*. <https://doi.org/10.1021/tx970159y>

Puente-Maestu, L., Pérez-Parra, J., Godoy, R., Moreno, N., Tejedor, A., González-Aragoneses, F., Bravo, J. L., Alvarez, F. V., Camano, S., & Agustí, A. (2009). Abnormal mitochondrial function in locomotor and respiratory muscles of COPD patients. *European Respiratory Journal*. <https://doi.org/10.1183/09031936.00112408>

Putti, R., Sica, R., Migliaccio, V., & Lionetti, L. (2015). Diet impact on Mitochondrial Bioenergetics and Dynamics. *Frontiers in Physiology*, 6(MAR), 109.
<https://doi.org/10.3389/FPHYS.2015.00109/BIBTEX>

Qin, W., Khuchua, Z., Boero, J., Payne, R. M., & Strauss, A. W. (1999). Oxidative Myocytes of Heart and Skeletal Muscle Express Abundant Sarcomeric Mitochondrial Creatine Kinase.

The Histochemical Journal 1999 31:6, 31(6), 357–365.

<https://doi.org/10.1023/A:1003748108062>

Raij, L., DeMaster, E. G., & Jaimes, E. A. (2001). Cigarette smoke-induced endothelium dysfunction: Role of superoxide anion. *Journal of Hypertension*.
<https://doi.org/10.1097/00004872-200105000-00009>

Raza, H., John, A., & Nemmar, A. (2013). Short-Term Effects of Nose-Only Cigarette Smoke Exposure on Glutathione Redox Homeostasis, Cytochrome P450 1A1/2 and Respiratory Enzyme Activities in Mice Tissues. *Cell Physiol Biochem*, 31, 683–692.
<https://doi.org/10.1159/000350087>

Redza-Dutordoir, M., & Averill-Bates, D. A. (2016). Activation of apoptosis signalling pathways by reactive oxygen species. In *Biochimica et Biophysica Acta - Molecular Cell Research*. <https://doi.org/10.1016/j.bbamcr.2016.09.012>

Rezayat, A. A., Moghadam, M. D., Nour, M. G., Shirazinia, M., Ghodsi, H., Zahmatkesh, M. R. R., Noghabi, M. T., Hoseini, B., & Rezayat, K. A. (2018). Association between smoking and non-alcoholic fatty liver disease: A systematic review and meta-analysis. *SAGE Open Medicine*, 6, 205031211774522. <https://doi.org/10.1177/2050312117745223>

Richardson, R. S., Leek, B. T., Gavin, T. P., Haseler, L. J., Mudaliar, S. R., Henry, R., Mathieu-Costello, O., & Wagner, P. D. (2004). Reduced mechanical efficiency in chronic obstructive pulmonary disease but normal peak VO₂ with small muscle mass exercise. *Am J Respir Crit Care Med*, 169(1), 89–96. <https://doi.org/10.1164/rccm.200305-627OC>

Robb, E. L., Hall, A. R., Prime, T. A., Eaton, S., Szibor, M., Visconti, C., James, A. M., & Murphy, M. P. (2018). Control of mitochondrial superoxide production by reverse electron

transport at complex I. *Journal of Biological Chemistry*.

<https://doi.org/10.1074/jbc.RA118.003647>

Robison, P., Sussan, T. E., Chen, H., Biswal, S., Schneider, M. F., & Hernández-Ochoa, E.

O. (2017). Impaired calcium signaling in muscle fibers from intercostal and foot skeletal muscle in a cigarette smoke-induced mouse model of COPD. *Muscle & Nerve*, 56(2), 282–291. <https://doi.org/10.1002/MUS.25466>

Rodgman, A., & Green, C. (2016). Toxic Chemicals in Cigarette Mainstream Smoke - Hazard

and Hoopla. *Beiträge Zur Tabakforschung International/Contributions to Tobacco Research*.

<https://doi.org/10.2478/cttr-2013-0764>

Rodriguez-Miguel, P., Gregg, J., Seigler, N., Bass, L., Thomas, J., Pollock, J. S., Sullivan,

J. C., Dillard, T. A., & Harris, R. A. (2018). Acute Tetrahydrobiopterin Improves Endothelial Function in Patients With COPD. *Chest*.

<https://doi.org/10.1016/j.chest.2018.04.028>

Roe, N. D., & Ren, J. (2012). Nitric oxide synthase uncoupling: A therapeutic target in

cardiovascular diseases. In *Vascular Pharmacology*.

<https://doi.org/10.1016/j.vph.2012.02.004>

Russell, A. P., Foletta, V. C., Snow, R. J., & Wadley, G. D. (2014). Skeletal muscle

mitochondria: A major player in exercise, health and disease. In *Biochimica et Biophysica*

Acta - General Subjects. <https://doi.org/10.1016/j.bbagen.2013.11.016>

Ruzicka, F. J., & Beinert, H. (1977). A new iron-sulfur flavoprotein of the respiratory chain. A

component of the fatty acid beta oxidation pathway. *Journal of Biological Chemistry*,

252(23), 8440–8445. [https://doi.org/10.1016/S0021-9258\(19\)75238-7](https://doi.org/10.1016/S0021-9258(19)75238-7)

- Sadaka, A. S., Faisal, A., Khalil, Y. M., Mourad, S. M., Zidan, M. H., Polkey, M. I., & Hopkinson, N. S.** (2021). Reduced skeletal muscle endurance and ventilatory efficiency during exercise in adult smokers without airflow obstruction. *Journal of Applied Physiology*, *japplphysiol.00762.2020*. <https://doi.org/10.1152/japplphysiol.00762.2020>
- Sakata, R., McGale, P., Grant, E. J., Ozasa, K., Peto, R., & Darby, S. C.** (2012). Impact of smoking on mortality and life expectancy in Japanese smokers: A prospective cohort study. *BMJ (Online)*. <https://doi.org/10.1136/bmj.e7093>
- Saks, V. A., Guzun, R., Timohhina, N., Tepp, K., Varikmaa, M., Monge, C., Beraud, N., Kaambre, T., Kuznetsov, A., Kadaja, L., Eimre, M., & Seppet, E.** (2010). Structure-function relationships in feedback regulation of energy fluxes in vivo in health and disease: mitochondrial interactosome. *Biochimica et Biophysica Acta*, *1797*(6–7), 678–697. <https://doi.org/10.1016/J.BBABI0.2010.01.011>
- Saks, V. A., Khuchua, Z. A., Vasilyeva, E. v., Belikova, O. Y., & Kuznetsov, A. v.** (1994). Metabolic compartmentation and substrate channelling in muscle cells. Role of coupled creatine kinases in in vivo regulation of cellular respiration--a synthesis. *Molecular and Cellular Biochemistry*, *133–134*(1), 155–192. <https://doi.org/10.1007/BF01267954>
- Saks, V., Belikova, Y. O., & Kuznetsov, A. v.** (1991). In vivo regulation of mitochondrial respiration in cardiomyocytes: specific restrictions for intracellular diffusion of ADP. *Biochimica et Biophysica Acta*, *1074*(2), 302–311. [https://doi.org/10.1016/0304-4165\(91\)90168-G](https://doi.org/10.1016/0304-4165(91)90168-G)
- Sanders, K. A., Delker, D. A., Huecksteadt, T., Beck, E., Wuren, T., Chen, Y., Zhang, Y., Hazel, M. W., & Hoidal, J. R.** (2019). RAGE is a Critical Mediator of Pulmonary Oxidative

Stress, Alveolar Macrophage Activation and Emphysema in Response to Cigarette Smoke.

Scientific Reports. <https://doi.org/10.1038/s41598-018-36163-z>

Satoh, M., Fujimoto, S., Haruna, Y., Arakawa, S., Horike, H., Komai, N., Sasaki, T.,

Tsujioka, K., Makino, H., & Kashihara, N. (2005). NAD(P)H oxidase and uncoupled nitric oxide synthase are major sources of glomerular superoxide in rats with experimental diabetic nephropathy. *American Journal of Physiology - Renal Physiology*. <https://doi.org/10.1152/ajprenal.00221.2004>

Scialò, F., Fernández-Ayala, D. J., & Sanz, A. (2017). Role of mitochondrial reverse electron

transport in ROS signaling: Potential roles in health and disease. In *Frontiers in Physiology*.

<https://doi.org/10.3389/fphys.2017.00428>

Seymour, J. M. M., Spruit, M. A. A., Hopkinson, N. S. S., Nataneck, S. A. A., Man, W. D.-C.

D. C., Jackson, A., Gosker, H. R. R., Schols, A. M. W. J. M. W. J., Moxham, J., Polkey, M. I. I., & Wouters, E. F. M. F. M. (2010). The prevalence of quadriceps weakness in COPD and the relationship with disease severity. *European Respiratory Journal*, 36(1), 81–88. <https://doi.org/10.1183/09031936.00104909>

Shally, A., & McDonagh, B. (2020). The redox environment and mitochondrial dysfunction in

age-related skeletal muscle atrophy. *Biogerontology*, 21(4), 461–473.

<https://doi.org/10.1007/S10522-020-09879-7>

Sharanya, A., Ciano, M., Withana, S., Kemp, P. R., Polkey, M. I., & Sathyapala, S. A. (2019).

Sex differences in COPD-related quadriceps muscle dysfunction and fibre abnormalities.

Chronic Respiratory Disease, 16. <https://doi.org/10.1177/1479973119843650>

- Shields, G. S., Coissi, G. S., Jimenez-Royo, P., Gambarota, G., Dimber, R., Hopkinson, N. S., Matthews, P. M., Brown, A. P., & Polkey, M. I.** (2015). Bioenergetics and intermuscular fat in chronic obstructive pulmonary disease-associated quadriceps weakness. *Muscle and Nerve*. <https://doi.org/10.1002/mus.24289>
- Siasos, G., Tsigkou, V., Kokkou, E., Oikonomou, E., Vavuranakis, M., Vlachopoulos, C., Verveniotis, A., Limperi, M., Genimata, V., Papavassiliou, A. G., Stefanadis, C., & Tousoulis, D.** (2014). Smoking and atherosclerosis: mechanisms of disease and new therapeutic approaches. *Current Medicinal Chemistry*, 21(34), 3936–3948. <https://doi.org/10.2174/092986732134141015161539>
- Sinha-Hikim, I., Friedman, T. C., Shin, C. S., Lee, D., Ivey, R., & Sinha-Hikim, A. P.** (2014). Nicotine in combination with a high-fat diet causes intramyocellular mitochondrial abnormalities in male mice. *Endocrinology*, 155(3), 865–872. <https://doi.org/10.1210/EN.2013-1795>
- Skladal, D., Sperl, W., Schranzhofer, R., Krismer, M., Gnaiger, E., Margreiter, R., & Gellerich, F. N.** (1994). Preservation of mitochondrial functions in human skeletal muscle during storage in high energy preservation solution (HEPS). *What Is Controlling Life?: 50 Years After Erwin Schrödinger's What Is Life?*, 3, 286.
- Sørheim, I. C., Johannessen, A., Gulsvik, A., Bakke, P. S., Silverman, E. K., & DeMeo, D. L.** (2010). Gender differences in COPD: Are women more susceptible to smoking effects than men? *Thorax*. <https://doi.org/10.1136/thx.2009.122002>
- Steffl, M., Bohannon, R. W., Petr, M., Kohlikova, E., & Holmerova, I.** (2015). Relation between cigarette smoking and sarcopenia: Meta-analysis. *Physiological Research*.

- Strzelak, A., Ratajczak, A., Adamiec, A., & Feleszko, W.** (2018). Tobacco Smoke Induces and Alters Immune Responses in the Lung Triggering Inflammation, Allergy, Asthma and Other Lung Diseases: A Mechanistic Review. *International Journal of Environmental Research and Public Health*, 15(5). <https://doi.org/10.3390/IJERPH15051033>
- Stucki, J. W.** (1980). The Optimal Efficiency and the Economic Degrees of Coupling of Oxidative Phosphorylation. *European Journal of Biochemistry*, 109(1), 269–283. <https://doi.org/10.1111/j.1432-1033.1980.tb04792.x>
- Sun, K., Liu, J., & Ning, G.** (2012). Active Smoking and Risk of Metabolic Syndrome: A Meta-analysis of Prospective Studies. *PLOS ONE*, 7(10), e47791. <https://doi.org/10.1371/JOURNAL.PONE.0047791>
- Tang, K., Wagner, P. D., & Breen, E. C.** (2010). TNF- α -mediated reduction in PGC-1 α may impair skeletal muscle function after cigarette smoke exposure. *Journal of Cellular Physiology*. <https://doi.org/10.1002/jcp.21955>
- Telenga, E. D., Hoffmann, R. F., T'Kindt, R., Hoonhorst, S. J. M., Willemse, B. W. M., Van Oosterhout, A. J. M., Heijink, I. H., Van Den Berge, M., Jorge, L., Sandra, P., Postma, D. S., Sandra, K., & Ten Hacken, N. H. T.** (2014). Untargeted lipidomic analysis in chronic obstructive pulmonary disease. Uncovering sphingolipids. *American Journal of Respiratory and Critical Care Medicine*, 190(2), 155–164. <https://doi.org/10.1164/RCCM.201312-2210OC>
- Terry, J. G., Hartley, K. G., Steffen, L. M., Nair, S., Alman, A. C., Wellons, M. F., Jacobs, D. R., Tindle, H. A., & Carr, J. J.** (2020). Association of smoking with abdominal adipose deposition and muscle composition in Coronary Artery Risk Development in Young Adults

(CARDIA) participants at mid-life: A population-based cohort study. *PLOS Medicine*, 17(7), e1003223. <https://doi.org/10.1371/JOURNAL.PMED.1003223>

Thatcher, M. O., Tippetts, T. S., Nelson, M. B., Swensen, A. C., Winden, D. R., Hansen, M. E., Anderson, M. C., Johnson, I. E., Porter, J. P., Reynolds, P. R., & Bikman, B. T. (2014). Ceramides mediate cigarette smoke-induced metabolic disruption in mice. *American Journal of Physiology - Endocrinology and Metabolism*. <https://doi.org/10.1152/ajpendo.00258.2014>

Tippetts, T. S., Winden, D. R., Swensen, A. C., Nelson, M. B., Thatcher, M. O., Saito, R. R., Condie, T. B., Simmons, K. J., Judd, A. M., Reynolds, P. R., & Bikman, B. T. (2014). Cigarette smoke increases cardiomyocyte ceramide accumulation and inhibits mitochondrial respiration. *BMC Cardiovascular Disorders*, 14(1). <https://doi.org/10.1186/1471-2261-14-165>

Tong, E. K., & Glantz, S. A. (2007). Tobacco industry efforts undermining evidence linking secondhand smoke with cardiovascular disease. *Circulation*, 116(16), 1845–1854. <https://doi.org/10.1161/CIRCULATIONAHA.107.715888>

Ueda, S., Matsuoka, H., Miyazaki, H., Usui, M., Okuda, S., & Imaizumi, T. (2000). Tetrahydrobiopterin restores endothelial function in long-term smokers. *Journal of the American College of Cardiology*. [https://doi.org/10.1016/S0735-1097\(99\)00523-9](https://doi.org/10.1016/S0735-1097(99)00523-9)

Ungvari, Z., Sonntag, W. E., & Csizsar, A. (2010). Mitochondria and aging in the vascular system. In *Journal of Molecular Medicine* (Vol. 88, Issue 10, pp. 1021–1027). Springer. <https://doi.org/10.1007/s00109-010-0667-5>

United States Department of Health and Human Services. (2014). The Health Consequences of Smoking - 50 Years of Progress. In *The Health Consequences of Smoking—50 Years of Progress: A Report of the Surgeon General*.

Vaart, H. van der, Postma, D. S., Timens, W., & Hacken, N. H. T. Ten. (2004). Acute effects of cigarette smoke on inflammation and oxidative stress: a review. *Thorax*, 59(8), 713–721.
<https://doi.org/10.1136/THX.2003.012468>

Van Den Borst, B., Koster, A., Yu, B., Gosker, H. R., Meibohm, B., Bauer, D. C., Kritchevsky, S. B., Liu, Y., Newman, A. B., Harris, T. B., & Schols, A. M. W. J. (2011). Is age-related decline in lean mass and physical function accelerated by obstructive lung disease or smoking? *Thorax*. <https://doi.org/10.1136/thoraxjnl-2011-200010>

van der Toorn, M., Rezayat, D., Kauffman, H. F., Bakker, S. J. L., Gans, R. O. B., Koëter, G. H., Choi, A. M. K., van Oosterhout, A. J. M., & Slebos, D. J. (2009). Lipid-soluble components in cigarette smoke induce mitochondrial production of reactive oxygen species in lung epithelial cells. *American Journal of Physiology - Lung Cellular and Molecular Physiology*. <https://doi.org/10.1152/ajplung.90461.2008>

van der Toorn, M., Slebos, D. J., de Bruin, H. G., Leuvenink, H. G., Bakker, S. J. L., Gans, R. O. B., Koëter, G. H., van Oosterhout, A. J. M., & Kauffman, H. F. (2007). Cigarette smoke-induced blockade of the mitochondrial respiratory chain switches lung epithelial cell apoptosis into necrosis. *American Journal of Physiology - Lung Cellular and Molecular Physiology*. <https://doi.org/10.1152/ajplung.00291.2006>

Vanderthommen, M., Duteil, S., Wary, C., Raynaud, J. S., Leroy-Willig, A., Crielaard, J. M., & Carlier, P. G. (2003). A comparison of voluntary and electrically induced contractions by

interleaved ¹H- and ³¹P-NMRS in humans. *Journal of Applied Physiology*, 94(3), 1012–1024. <https://doi.org/10.1152/japplphysiol.00887.2001>

Vanhatalo, A., Jones, A. M., Blackwell, J. R., Winyard, P. G., & Fulford, J. (2014). Dietary nitrate accelerates postexercise muscle metabolic recovery and O₂ delivery in hypoxia. *Journal of Applied Physiology*, 117(12), 1460–1470. <https://doi.org/10.1152/japplphysiol.00096.2014>

Veksler, V. I., Kuznetsov, A. V., Anflous, K., Mateo, P., Van Deursen, J., Wieringa, B., & Ventura-Clapier, R. (1995). Muscle creatine kinase-deficient mice. II. Cardiac and skeletal muscles exhibit tissue-specific adaptation of the mitochondrial function. *Journal of Biological Chemistry*, 270(34), 19921–19929. <https://doi.org/10.1074/jbc.270.34.19921>

Vignais, P. V., Douce, R., Lauquin, G. J. M., & Vignais, P. M. (1976). Binding of radioactively labeled carboxyatractyloside, atracyloside and bongkrekic acid to the ADP translocator of potato mitochondria. *Biochimica et Biophysica Acta*, 440(3), 688–696. [https://doi.org/10.1016/0005-2728\(76\)90051-7](https://doi.org/10.1016/0005-2728(76)90051-7)

Vinnakota, K. C., Dash, R. K., & Beard, D. A. (2011). Stimulatory effects of calcium on respiration and NAD(P)H synthesis in intact rat heart mitochondria utilizing physiological substrates cannot explain respiratory control in vivo. *Journal of Biological Chemistry*, 286(35). <https://doi.org/10.1074/jbc.M111.242529>

Wallimann, T., Tokarska-Schlattner, M., & Schlattner, U. (2011). The creatine kinase system and pleiotropic effects of creatine. *Amino Acids*, 40(5), 1271. <https://doi.org/10.1007/S00726-011-0877-3>

Wallimann, T., Wyss, M., Brdiczka, D., Nicolay, K., & Eppenberger, H. M. (1992).

Intracellular compartmentation, structure and function of creatine kinase isoenzymes in tissues with high and fluctuating energy demands: the “phosphocreatine circuit” for cellular energy homeostasis. *The Biochemical Journal*, 281 (Pt 1)(Pt 1), 21–40.
<https://doi.org/10.1042/BJ2810021>

Watt, M. J., Barnett, A. C., Bruce, C. R., Schenk, S., Horowitz, J. F., & Hoy, A. J. (2012).

Regulation of plasma ceramide levels with fatty acid oversupply: evidence that the liver detects and secretes de novo synthesised ceramide. *Diabetologia*, 55(10), 2741–2746.
<https://doi.org/10.1007/S00125-012-2649-3>

Webb, R. C. (2003). Smooth muscle contraction and relaxation. *American Journal of Physiology - Advances in Physiology Education*. <https://doi.org/10.1152/advan.00025.2003>

Weseler, A. R., & Bast, A. (2010). Oxidative stress and vascular function: Implications for pharmacologic treatments. In *Current Hypertension Reports*. <https://doi.org/10.1007/s11906-010-0103-9>

Whitton, F., Jobin, J., Simard, P. M., Leblanc, P., Simard, C., Bernard, S., Belleau, R., & Maltais, F. (1998). Histochemical and morphological characteristics of the vastus lateralis muscle in patients with chronic obstructive pulmonary disease. *Medicine and Science in Sports and Exercise*. <https://doi.org/10.1097/00005768-199810000-00001>

Wisniewski, E., Gellerich, F. N., & Kunz, W. S. (1995). Distribution of Flux Control among the Enzymes of Mitochondrial Oxidative Phosphorylation in Calcium-activated Saponin-skinned Rat Musculus Soleus Fibers. *European Journal of Biochemistry*, 230(2), 549–554.
<https://doi.org/10.1111/J.1432-1033.1995.0549H.X>

Wobbrock, J. O., Findlater, L., Gergle, D., & Higgins, J. J. (2011). The Aligned Rank Transform for nonparametric factorial analyses using only ANOVA procedures. *Conference on Human Factors in Computing Systems - Proceedings*, 143–146. <https://doi.org/10.1145/1978942.1978963>

Wollenman, L. C., Vander Ploeg, M. R., Miller, M. L., Zhang, Y., & Bazil, J. N. (2017). The effect of respiration buffer composition on mitochondrial metabolism and function. *PLoS ONE*, 12(11). <https://doi.org/10.1371/journal.pone.0187523>

Wu, K., Luan, G., Xu, Y., Shen, S., Qian, S., Zhu, Z., Zhang, X., Yin, S., & Ye, J. (2020). Cigarette smoke extract increases mitochondrial membrane permeability through activation of adenine nucleotide translocator (ANT) in lung epithelial cells. *Biochemical and Biophysical Research Communications*. <https://doi.org/10.1016/j.bbrc.2020.02.160>

Wüst, R. C. I., Morse, C. I., Haan, A., Rittweger, J., Jones, D. A., & Degens, H. (2008). Skeletal muscle properties and fatigue resistance in relation to smoking history. *European Journal of Applied Physiology*, 104(1), 103–110. <https://doi.org/10.1007/s00421-008-0792-9>

Yamashita, S. ichi, & Kanki, T. (2018). Mitochondrial Bioenergetics - Methods and Protocols. In *Methods in Molecular Biology* (Vol. 1782).

Zhang, X., & Gao, F. (2021). Exercise improves vascular health: Role of mitochondria. *Free Radical Biology and Medicine*, 177, 347–359. <https://doi.org/10.1016/j.freeradbiomed.2021.11.002>

Zhao, J., & Hopke, P. K. (2012). Concentration of reactive oxygen species (ROS) in mainstream and sidestream cigarette smoke. *Aerosol Science and Technology*. <https://doi.org/10.1080/02786826.2011.617795>

- Zhivotovsky, B., Galluzzi, L., Kepp, O., & Kroemer, G.** (2009). Adenine nucleotide translocase: a component of the phylogenetically conserved cell death machinery. *Cell Death & Differentiation* 2009 16:11, 16(11), 1419–1425. <https://doi.org/10.1038/cdd.2009.118>
- Zurlo, F., Larson, K., Bogardus, C., & Ravussin, E.** (1990). Skeletal muscle metabolism is a major determinant of resting energy expenditure. *J Clin Invest*, 86(5), 1423–1427. <https://doi.org/10.1172/JCI114857>